Development of an Integrated Robotic Polishing System

By

Eugène Benoit Florent KALT

A Doctoral Thesis

Submitted in partial fulfilment of the requirements for the award of Doctor of Philosophy of Loughborough University

August 2016

I would like to dedicate my work to

Jean-Batiste-Eugène KALT

Docteur en médicine de la Faculté de Paris (Kalt, 1886)

"The only source of knowledge is experience."
Albert Einstein
-Physicist

Abstract

This thesis presents research carried out as part of a project undertaken in fulfilment of the requirements of Loughborough University for the award of Philosophical Doctorate. The main focus of this research is to investigate and develop an appropriate level of automation to the existing manual finishing operations of small metallic components to achieve required surface quality and to remove superficial defects.

In the manufacturing industries, polishing processes play a vital role in the development of high precision products, to give a desired surface finish, remove defects, break sharp edges, extend the working life cycle, and meet mechanical specification. The polishing operation is generally done at the final stage of the manufacturing process and can represent up to a third of the production time. Despite the growth automated technology in industry, polishing processes are still mainly carried out manually, due to the complexity and constraints of the process.

Manual polishing involves a highly qualified worker polishing the workpiece by hand. These processes are very labour intensive, highly skill dependent, costly, error-prone, environmentally hazardous due to abrasive dust, and - in some cases - inefficient with long process times. In addition, the quality of the finishing is dependent on the training, experience, fatigue, physical ability, and expertise of the operator.

Therefore, industries are seeking alternative solutions to be implemented within their current processes. These solutions are mainly aimed at replacing the human operator to improve the health and safety of their workforce and improve their competitiveness. Some automated solutions have already been proposed to assist or replace manual polishing processes. These solutions provide limited capabilities for specific processes or components, and a lack of flexibility and dexterity. One of the reasons for their lack of success is identified as neglecting the study and implementing the manual operations.

This research initially hypothesised that for an effective development, an automated polishing system should be designed based on the manual polishing operations. Therefore, a successful implementation of an automated polishing system requires a thorough understanding of the polishing process and their operational parameters.

This study began by collaborating with an industrial polishing company. The research was focused on polishing complex small components, similar to the parts typically used in the aerospace industry. The high level business processes of the polishing company were capture through several visits to the site. The low level operational parameters and the

understanding of the manual operations were also captured through development of a devices that was used by the expert operators. A number of sensors were embedded to the device to facilitate recording the manual operations. For instance, the device captured the force applied by the operator (avg. 10 N) and the cycle time (e.g. 1 pass every 5 sec.). The capture data was then interpreted to manual techniques and polishing approaches that were used in developing a proof-of-concept Integrated Robotic Polishing System (IRPS). The IRPS was tested successfully through several laboratory based experiments by expert operators. The experiment results proved the capability of the proposed system in polishing a variety of part profiles, without pre-existing geometrical information about the parts.

One of the main contributions made by this research is to propose a novel approach for automated polishing operations. The development of an integrated robotic polishing system, based on the research findings, uses a set of smart sensors and a force-position-by-increment control algorithm, and transpose the way that skilled workers carry out polishing processes.

Acknowledgements

Firstly, I would like to express my sincere gratitude to my supervisors, Dr R.P. Monfared and Prof M.R Jackson, for their continuous support through my PhD study, for their patience, motivation, and immense knowledge. Their guidance helped me throughout the research and writing of this thesis.

My sincere thanks also go to the EPSRC Centre for Innovative Manufacturing in Intelligent Automation, who provided me with the opportunity to join their team and work on such a challenging project.

Many thanks also to the Wolfson School of Mechanical and Manufacturing Engineering of Loughborough University for funding this research.

I also would like to thank my fellow PhD students, the research staff, and technicians, for their technical and moral support, the stimulating discussions, and helping me through the research project and outreach projects during the last three years.

Moreover, I would like to thank the East-Midland based SME for welcoming me to their company. This collaborative work provided us with an interesting insight into the standard operation procedure of finishing processes and the current challenges in industry today.

Finally, I would like to thank my family and friends for additional moral support and pushing me to become a better person.

Content

List of Figure

List of Table

Glossary

AE	Acoustic Emission sensor
AMPS	Automated Polishing System
AR	Augmented reality
Blending Contact	Contact between the abrasive grain and the surface
CAD	Computer Aided Design
CAM	Computer Aided Manufacturing
Cartesian	Coordinate system in XYZ (mm) and ABC (deg.) axes
CCD	Charged Coupled Device
CMM	Coordinate Measuring Machine
CNC	Computer Numerical Control
data point (unit)	Number of point collected with a unit of 1 per point
DoF	Degree of Freedom
Dust cover	Protect the multi-axial force and torque sensor from dust
Dynamic behaviour of force and torque sensors	Gravity and inertia effect on force and torque readings
Features	Scratches, pits, burn marks, machining marks, cracks, burr, and shiny spots
Feed rate	Cutting speed in material removal processes
Fixture	Device enabling the capture of manual polishing parameters through a set of sensor
FTS	Multi-Axial Force and Torque Sensor
Fx, Fy, Fz	Force output in x, y, z axes
GUI	Graphical User Interface
HMD	Head Mounted Display
HTA	Hierarchical Task Analysis
Hz	Hertz
IMU	Inertial Measurement Unit
Increment	Input value for force-position control
IRPS	Integrated Robotic Polishing System
Joint Angle	Robot joint angle in each degree of freedom (deg.)

Keep the flow	Term used professional polisher is industry which designate the action of keeping a constant movement and force through the operation.
MoCap	Motion Capture
MRR	Material Removal Rate
MSD	Musculoskeletal Diseases
NetBox	Used by the multi-axial force and torque sensor to convert and stream data in real-time
P## grit	Average number of grain per mm^2
Pattern A	Simple Pressure technique applied at specific location onto the surface
Pattern B	Linear Translation technique are used remove defects and burr at the edge of the part
Pattern C	Surface Profiling technique are used for removing a uniform layer of material along the surface
PLM	Platform Lean Management
PPE	Personal protective equipment
PTC	Passive tool control
PSD	Position sensing detector
Rework	process where batches are finished again by the same operator until passing quality control
Root-rad	Finishing operation of the root -radius of a complex industrial part
RT-RPS	Real-Time Robotic Polishing System
SIMTech	Singapore Institute of Manufacturing Technology
SME	Small and Medium Enterprise
SOP	Standard Operating Procedure
tp	Duration of 1 polishing action
Trailing/leading edges	Fine edges of an industrial part
Tx, Ty, Tz	Torque output in x, y, z axis
User Interface	Software developed by the author for the design of the IRPS
UWB	Ultra-Wideband Ranging
Vibration white finger disease	MSD generated from long exposure to high level of vibration, effects include decrease of tactile feeling, and nom and tingling feeling in the hand
VR	Virtual Reality
VTS	Vulcan Tactile System
Waviness	Term used in metrology that designate the overall shape of a surface

Chapter 1 Towards an Integrated Robotic Polishing System

In the manufacturing industry, mechanical finishing plays a vital role in the development of a product's surface quality and final geometry (Dickman, 2007). Mechanical finishing typically includes deburring, grinding, polishing, buffing, and final visual inspection of a workpiece. These processes are usually performed at the final stage of the manufacturing process of a component or product and may represent up to a third of production time in some industries (Liang Liao and Fengfeng Xi, 2005).

One of the main reasons for polishing is to improve surface finish by removing minimal amounts of material; this is done in order to smooth a particular surface until obtaining the desired surface finish (i.e. roughness or aesthetic aspect) without affecting the geometry of the workpiece (Besari et al., 2010; Dickman, 2007; Liang Liao and Fengfeng Xi, 2005).

Mechanical polishing as a common polishing process refers to the removal of a layer of material by means of abrasive tools to reduce the surface roughness to the desired level (i.e. roughness average or Ra). These processes are usually performed progressively - starting from high abrasive grit, such as in grinding, to fine abrasive grit, used in polishing or buffing operations - until the desired smoothness is achieved. The smoothing of surfaces generally involves removing scratches, machining marks, pits, and other defects or features to obtain a uniform roughness evenly distributed throughout the workpiece (Besari et al., 2010; Liang Liao and Fengfeng Xi, 2005).

The polishing processes are very important and widely used in the aeronautical industry; whether it is to meet dimensional and geometrical tolerances, mechanical specifications such as friction, or to meet the desired visual aspect. For example, hydraulic turbines produce electricity by converting water flow into kinetic energy in electric generators (Khakpour and Birglenl, 2014). The main factor that affects the efficiency of these hydraulic turbines is the friction between the water and the turbine blades. The level of friction will depend on the quality of the surface finish. Thus, decreasing the surface roughness of the turbine blade will significantly decrease the friction loss and increase the

efficiency of the turbine. Therefore, additional processes such as grinding and polishing are required after initial machining processes (Varghese et al., 2015). In addition, some polishing processes can improve the service life of a component.

Due to the recent economic growth, industries with polishing as part of their core processes have had difficulties recruiting and training sufficient numbers of highly skilled manual workers to meet their requirement. In addition, as is the case for many other manual operations, the process specifications and skill requirements are rarely documented and may be lost when manual workers move away from businesses. These are some of the reasons for the recent demand for alternative solutions for manual polishing.

Automated polishing is a potential solution that can improve the working environment and improve flexibility and repeatability in resource management. Despite the wide-spread use of automated solutions, manual operation is still extensively used in polishing processes in various industries. Manual polishing is a laborious task requiring a long period of training, often within an unhealthy environment. For example, in the grinding operation of heavy turbine blades, operators are subject to severe injuries due to chronic exposure to vibration (e.g. white finger disease), noise and dust. Furthermore, the quality and time of operations typically vary from job to job based on the operators' skill level. Nonetheless, the operators have the advantage of being able to adapt quickly to changes and learn from their mistakes. For example, human operators can adjust their polishing technique in real-time based on visual and tactile feedback (see Chapter 4).

Some automated solutions have already been proposed to assist or replace human operators in such unhealthy environment. For instance, mass polishing, such as barrel deburring by Harper Surface Finishing Systems Inc. (Davidson, 2001), or robotic grinding by KUKA (KUKA Gmb, 2014), provide limited solutions for specific processes or components. However, these solutions typically lack the flexibility and dexterity that human operators offer. Some of the polishing skills that are particularly challenging to automate include rapid reasoning and decision-making based on visual inspections, and fast adjustment of the polishing patterns, e.g. in response to a defect on the surface.

To develop a robust automated polishing system, it is essential to incorporate human skills into the automated systems. Therefore, it is necessary to understand and capture these manual skills to be able to build the automated system on that basis.

Following a review on the current automated polishing systems (see Section 2.2), it was found that the manual skills have largely been neglected when designing such automated systems. To the author's knowledge, no automated solutions have yet been developed to understand human skill in this domain of the industry, nor how to implement them within an automated polishing system. This is a factor contributing in the lack of robust automated polishing systems used in industries as part of their production systems.

The initial research reviews led to the following research hypothesis:

A robust automated polishing system should be built based on the understanding and adoption of manual processes and operators' skills.

Therefore, it was envisaged that these investigations should lead to the development and implementation of an automated system; following the comprehensive understanding and assessment of both manual processes and operators' skills (Besari et al., 2010).

The research hypothesis was examined in a SME based in the East-Midlands which specialises in the polishing and finishing of high-value components, such as turbine blades from the aerospace industry (see Chapter 4). Based on prior experience with various automation suppliers, the company showed strong reluctance in replacing human operators with automated systems due to the danger of losing workers' undocumented experience and knowledge of polishing processes. This was in spite of their serious problem with recruiting and maintaining their workforce.

The proposed research hypothesis was also supported by the experts in this company and it was envisaged that this research on developing an automated polishing system should be initiated by the capturing of human skills.

1.1 Research Gap

Polishing operations are core processes in many industries and are mainly performed manually. This is often due to the complexity of operations and the highly demanding set of skills required. Businesses in this domain of industry have recognised that they are heavily reliant on individuals' skills and personal knowledge on polishing processes, and are therefore seeking automated solutions. While automated solutions should improve the general health and wellbeing of operators (by removing them for a hazardous environment), they should also improve efficiency by optimising quality, repeatability, and speed of processes.

Despite a number of existing research and industrial work in the domain of automated polishing systems, such systems have not yet been successfully implemented in industry. The reason may be the focus on achieving product specification through automated polishing, rather than on (or in addition to) understanding and incorporating the existing polishing processes.

The identified research gap targeted for this research study is to understand and capture manual polishing processes and build an automated process upon the lessons learned from manual processes.

To date, no other research or industrial initiatives are reported to have taken this approach and it is anticipated that this approach can potentially advance the state of the art within this domain of research.

Towards this end, the development of an Integrated Robotic Polishing System based on the capture and analysis of manual polishing processes has been proposed in this research.

1.2 Research Aims

This project aims to develop and test an integrated robotic polishing system based on the capture and understanding of manual polishing processes, using existing technologies and processes.

1.3 Research Objectives

It was envisaged that capturing and analysing the operator technique(s) will give insight into how the polishing tasks are completed. By analysing the captured data, a robotic polishing system could reproduce the polishing processes originally carried out by human operators. The initial research objectives are defined below and illustrated in Figure 1.1:

- Obj.1: Review the existing technologies, industrial and research work.
- Obj.2: Identify the specification of polishing processes in industry, such as production/process specification and needs. This is to establish links between manual processes, automated systems, and the required product specification.
- Obj.3: Develop a fixture to capture manual polishing operation.
- Obj.4: Understand and interpret manual processes and human skills.
- Obj.5: Develop and test a proof of concept automated robotic polishing system based on manual processes and human skills.

The above objectives also aim to investigate the applicability of automation within highly flexible and dexterous manual processes, and to propose a novel solution for our industrial collaborator.
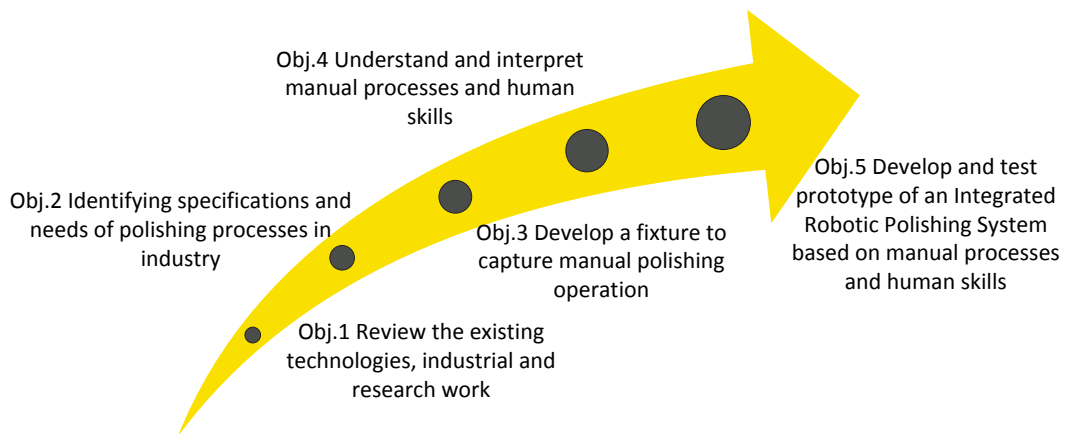
Figure 1.1: Research objectives

The proposed solution should be focused on the development of a novel intelligent system capable of capturing system changes in real-time using a range of automated devices, such as 2D/3D machine vision, laser stripe, and multi-axial force and torque sensors. The potential intelligence embedded into the proposed system was tested for complicated manual operations, such as surface defect removal from small components.

To meet Objectives 2 and 3, this research work began with multiple visits to a SME polishing company to understand the whole manufacturing process of polishing and the needs for automation. A fixture was designed to capture and interpret data from manual

operations. Finally, the captured knowledge was analysed and implemented into the proposed automated system.

1.4   Research Scope

To define a manageable research goal within the given timeframe, the scope of this research is defined as follows. The research focused on small, complex, metallic components such as those commonly used in the aerospace industry. This was considered to be a suitable sector of industry due to collaboration with relevant industrial partners, expected demand for such systems in the future, and the laboratory capability available to this project.

The research was further narrowed down to capturing and understanding manual processes and operators' preferences and techniques, saving a complete human factor study for future follow-up research projects.

This project concentrated further on the removal of machining marks and improving the surface roughness in polishing operations. This includes the removal of scratches and other surface defects, but excludes the real-time monitoring of the overall dimension and geometry of the workpiece.

The system developed in this research would include a robotic arm with an end effector to hold the workpiece, and a series of instruments (e.g. 2D vision, laser stripes, force torque sensor, motion sensor, etc.) to measure and control both defects on the surface and the polishing path in real time, as illustrated in Figure 1.2. It is also expected that control over other parameters such as the rotation speed of the abrasive tool, tool wear, or monitor vibration should also have an impact on the overall system. However, the impact of these parameters is considered to be beyond the scope of this research.
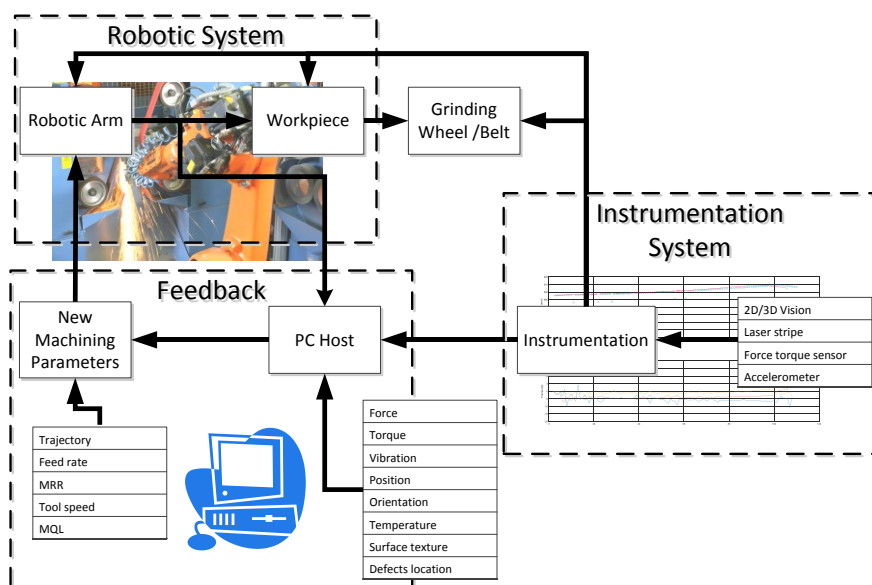
Figure 1.2: Novel automated polishing system

1.5 Thesis Outline

Chapter 2: Literature Review & Background Research

This chapter focuses on setting the scene for the project and understanding the challenges and needs for automation in mechanical polishing processes. This chapter also describes the importance of human skills in industry and the technology for capture of manual operation and human movements.

Chapter 3: Research Approach

This chapter shows the methodology used in this research. Speculative systems using both fully automated and semi-automated technology are also presented.

Chapter 4: Industrial Application

This chapter illustrates the collaborative work carried out in the second year with an SME specialised in finishing of mechanical components. The work carried out includes a study of their current process for potential automation. The collaboration also includes an understanding of the general approaches and philosophy in use during standard operating procedures and the possible automated solutions for the company to implement.

Chapter 5: Enable the Capture of Manual Polishing Parameters

The chapter focuses on the development of a fixture to capture the forces and movements of a human operator. The design process of the fixture is included in this chapter. Selection and testing of various sensors to capture data is also described. Finally, the chapter presents a calibration experiment with the fixture to understand the collected data during a simulation of manual polishing operation.

Chapter 6: Capturing Manual Polishing Parameters

This chapter presents the study of the capture of manual polishing parameters collected from skilled human operators using the developed fixture. The analysis of the approaches used by the operators is also described.

Chapter 7: Development of an Integrated Robotic Polishing System

This chapter focuses on the development of the novel automated polishing system based on the capture and understanding of the manual operation. This chapter first presents the polishing parameters captured in Chapter 6 and discusses how they can be translated within an automated system. The design of robotic cell and equipment used for the automated cell is also presented. Lastly, the development of the intelligent automated polishing system is presented and tested.

Chapter 8: Discussion

This chapter focuses on discussing the results and findings of the research. This chapter includes what was learned from human operators through the literature review, case study,

and data captured. This chapter also reports what tools and systems were developed during the research (including outcomes and shortcomings). Business aspects for automated polishing are also discussed.

Chapter 9: Conclusion

This chapter summarises the work carried out and the findings of this research. In addition, the achievements, contribution to knowledge, and publications are reported. Finally, the project limitations and future work are also discussed.

Chapter 2 Literature Fully Review and Background Research

Current automated solutions use either robotic arms, computer numerical control (CNC), or mass finishing machining to polish workpieces. Much research has already been carried out using these technologies. The main issues of these solutions are: the control over the polishing force; the geometry of the workpiece; the machining time and associated cost; poor or no real-time feedback during the machining; poor or no real-time adaptation; and the lack of understanding and interest in manual processes.

These parameters are still under investigation in both research and industry. However, research has focused mainly on a specific component, such as turbine blade or moulds, without a real understanding of the manual polishing processes. Moreover, these studies focused on few of the technical aspects of automation, such as workpiece geometry, the contact force between the part and abrasive tool, or integration of commercial technologies to develop an automated solution.

A background research has been carried out. The literature review described in this chapter focus on mechanical polishing (Sections 2.2 to 2.5), and capture of human operation (Section 2.6). The literature review presented in this chapter was carried out to set the scene, understand key challenges, introduce concepts in relation to the research, and narrow the area of study to define the scope.

2.1   Background Review

2.1.1   Mechanical polishing

Mechanical polishing technologies and techniques are reviewed in Sections 2.2 to 2.5. This is to establish the state-of-art for current technology and research; and to define challenges

and gaps for the research. This section also points out the lack of areas studied, as well as the advantages and disadvantages of each system studied or developed. The technologies reviewed in this research are limited to mass finishing, robotic arms, and Computer Numerical Control (CNC), as these systems are commonly used in industry today.

2.1.2   Capture Human Operation

The capture of human operation is another important factor. This is carried out in order to understand how manual polishing processes are carried out by human operators and what influence the environment may have on the task or the human operator. The literature review is limited to a basic understanding of biomechanics (capture of force and motion) and human factors (decision-making), as it has been undertaken from a manufacturing engineering point of view.

2.2   Mechanical Polishing Fundamentals

2.2.1   General Definition

Within manufacturing industry (such as aeronautical and energy), finishing processes plays a vital role in the development of product's surface quality and final geometry. Mechanical finishing typically includes deburring, grinding, polishing, buffing, and final visual inspection of a workpiece. These processes are usually performed at the final stage of the manufacturing process of a component or product and may represent up to a third of production time in some industries (Besari et al., 2010; Liang Liao and Fengfeng Xi, 2005).

In general, metal workpieces may fit dimensionally into a final assembly as machined or perform their function, but they may not last. Therefore, additional processes such as grinding and polishing are required after initial machining processes (Varghese et al., 2015). These processes are critical to give the desired surface finish, remove defects, break sharp edges, extend the life cycle, and meet design specification of a component (Dickman, 2007; Kenton, 2009).

Mechanical finishing processes refers to all operations that alter the surface by physical means (Dickman, 2007). This may include enhancing the visual aspect or removing excess material (Guyson, 2013). These operations are essential to the manufacture of high-quality products, but are labour intensive and time-consuming (Ahn et al., 2002). In addition, these processes are usually performed progressively, starting from high abrasive grit, such as in grinding, to finer abrasive grit, used in polishing or buffing operations, until the desired surface roughness is achieved.

Moreover, some industries with polishing as part of their processes may have had some difficulties recruiting and training sufficient numbers of highly skilled workers to meet demand. In addition, as is the case for many other manual operations, the process

specifications of polishing and skill requirement are rarely documented or may be lost when manual workers move away from businesses. These are some of the reasons for the recent demand for alternative solutions for polishing processes.

Factors to consider when investing in polishing equipment are the limitations of the part size and shape, the batch size, and consistency and repeatability (Kenton, 2008). The abrasive used and the finishing characteristics desired, in relation to the equipment or method used, are shown in Table 2.1 and 2.2.

In addition, it is advises, that industries and researchers should be aware of all alternatives as all systems presented in Table 2.1 have advantages and disadvantages (Kenton, 2008). Hence the selection of the equipment or system would depend mostly on how the function of the part, or on the environment in which it is been used. Therefore, choosing the right finishing process would not only meet the surface finish required but also could significantly reduce the production cost (Huang et al., 2002).

Table 2.1: Common material removal systems (Kenton, 2008)

Common material removal systems		
Abrasive blasting	Abrasive wheel and belt	Wheel blasting
Cryogenic blasting	Water jet	Wet blasting
Abrasive extrusion	Ultrasonic	Thermal
Chemical	Mass finishing	Spindle/Drag
Turbo-abrasive	Orbital	Magnetic

2.2.1.1   Polishing

Polishing of high-value components, such as moulds or dies, consumes a large amount of resources and time. Polishing processes are very important and widely used, whether it is to meet mechanical properties, design specifications; or to meet the desire visual aspect (Khakpour and Birglenl, 2014). The main reason for polishing is to improve the quality of the surface finish by removing minimal amounts of material and to smooth a particular surface until obtaining the desired surface finish (i.e. roughness or aesthetic aspect) without affecting the geometry of the workpiece (Besari et al., 2010; Dickman, 2007; Liang Liao and Fengfeng Xi, 2005), as illustrated in Figure 2.1.

Smoothing of surfaces generally involves removing scratches, machining marks, pits, and other defects or features to obtain a uniform surface roughness evenly distributed throughout the part surface.

Figure 2.1: Example of an aeronautical workpiece before (left) and after (right) finishing process

The term mechanical polishing refers to an abrasive operation that follows grinding and precedes buffing. The definition of polishing, which is not to be confused with buffing, is the surface enhancement by means of metal removal. In brief, polishing reduces the surface roughness to the desired level, which leads to a better surface quality.

Within the range of finishing equipment listed in Table 2.1 and Table 2.2, there are three main techniques used in industry today, as seen below:

• *__Manual Polishing__*: A process involving a trained operator using handheld tools or abrasive belts or wheels. A polishing wheel is usually used to remove excess material after machining or casting. The buffing wheel will determine the final surface texture, e.g. mirror or bright surfaces. Manual polishing is constrained by the experience and judgment of the operator, which may influence the quality of the surface finish, finishing time, accuracy, form and geometry.

• *__Mass Finishing:__* An automated technology more and more in popular in industry. Originally used for polishing and deburring operations of large batches of small parts, it is starting to be investigated for higher value components. Mass finishing techniques include machines such as vibratory bowl or centrifugal bowl finishers. However, they still require an experienced operator to choose the right media, compound, and finishing time.

• *__Computer Numerical Control (CNC):__* CNC technology (i.e. centreless grinder) is already available for grinding or polishing. However, this type of technology is still expensive. On the other hand, more and more work is currently being carried out to use CNC milling technology for surface finishing operation, primarily to reduce the cost of using such equipment.

• *__Robotic arm with end effector:__* As in manual operation, the robotic arm would control the position of either the workpiece or the tool. This technology aims to imitate the work of a human operator while achieving a better consistency in quality of surface finish and in minimum time. It is also being introduced to remove humans from laborious and hazardous work environments, hence improving the health and safety. However, the more complex the task, the more difficult it is to integrate and the more expensive the solution will be.

Table 2.2: Non-official classification for finishing equipment (Kenton, 2009)**.**

Classification	Description
Type 0	This system is for manual hand working of parts only. Energy is directed downward in a back and forward motion or circular pattern with an abrasive medium. The greater the downward force, the greater the abrasion.
Type 1	This system is used on relatively flat materials where force is directed downwards and parallel to the material being worked, via a wheel, disc, or belt; creating a horizontal wiping action to smooth surface features.
Type 2	This system is used primarily for surface preparation for thickness coating. This uses the abrasive blast method where the energy force is transmitted to solid particles, which are directed perpendicular (or at a slight angle downward) to the workpiece. This results in a rough textured surface finish.
Type 3	This system is used in mass finishing type equipment. This uses abrasive particles or media in a random combination or mixed energy forces or patterns that occur in all directions relative to the part. The results produced are modified blended surfaces and uniformly worked parts.
Type 4	This system, used in the plating industry, is primarily an electrical current directed through a liquid medium-type energy force system. The results produced are both surface and sub-surface molecular changes to parts.
Type 5	This system is an air-based, high-temperature heat method. This is a very selective material removal system that works primarily on surface irregularities or burrs. The results of this process vaporise and melt thin surface protrusions.

2.2.1.2 Buffing

Buffing is the processing of a metal surface to give a specific or desired finish, ranging from semi-bright to mirror-bright or high lustre, using a soft cotton mop or wheel. There are four basic forms of buffing: satin finishing, cut-down buffing, cut-and-cut-down buffing, and lustre buffing (Dickman, 2007).

The rotation of the buffing wheel on the workpiece removes peaks and consequently reduces the average roughness (Zhang and Lim, 2002). The effect of the buffing wheel may vary depending on the finishing time needed and the job requirements. The tool properties should include good wear resistance, good impact strength, good fracture toughness, low friction, good corrosion resistance and lubricant wettability (Zhang and Lim, 2002).

2.2.2   Mechanical Forces, MRR and Other Parameter

2.2.2.1   *General Parameters*

As with all material removal systems, in mechanical polishing, there are factors of energy (i.e. movement, speed, or velocity), resistance (i.e. pressure, friction, compression, or contact) and physical setup (i.e. tool type, grinder type, grain size, and polishing pressure). These parameters are important for both surface finishing quality and machining speed (Liang Liao and Fengfeng Xi, 2005; Liao et al., 2008).

The key to polishing operations is to maintain a constant contact stress (or force) between the abrasive tool and the workpiece surface throughout the process. It is the contact stress that will determine the quality of the surface polished, and not the cutting force (or force exerted on the tool) (Liao et al., 2008). However, as the surface quality improves, it becomes correspondingly more difficult to further polish the surface of the workpiece (Kenton, 2008). In addition, during polishing operations, the tool wear increases which leads to a reduction in the polishing performance (i.e. quality, time, MRR) (Ahn et al., 2002). The worn tool must be replaced before the tool wear becomes severe; however, in some cases, a worn grinding belt may be used for polishing operations (Capone et al., 1960).

In general, adequate polishing parameters - such as constant contact force - will facilitate the removal of marks, improve surface quality, avoid under or over polishing and reduce the tool wear and finishing time - and hence, cost (Guiot et al., 2011).

2.2.2.2   *Contact Stress Model*

The contact stress or force represents the mechanical interaction between the tool and the workpiece. This includes the size of the contact area, the contact stress, and the friction force (Ahn et al., 2002; Besari et al., 2010; Liang Liao and Fengfeng Xi, 2005; Liao et al., 2008). Based on A. Roswell's model, the force applied by the tool can be determined for any given geometry under a constant contact stress (Liang Liao and Fengfeng Xi, 2005; Roswell, 2004). Two levels of contact model can be defined: micro contact modelling and macro contact modelling. Micro contact model concerns the micro-depth of cut of the grains of the abrasive tool, and macro contact modelling is based on the Hertzian contact theory.

In the Hertzian model, the contact between the tool and workpieces is represented as two discs pressed together, and is assumed to be elastic (as illustrated in Figure 2.2). The point of contact occurs when both discs are touching, and become an elliptical surface when the force increases.
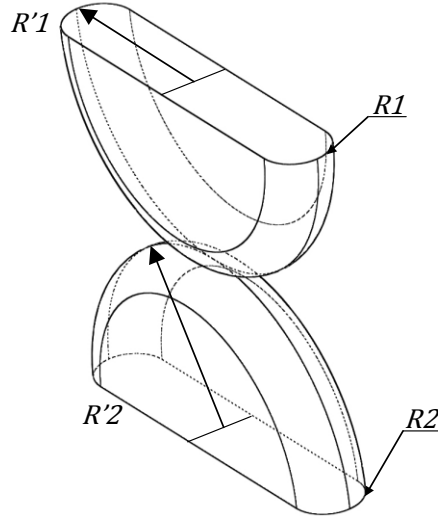
Figure 2.2: Two Curved Bodies Pressed Together

In the Hertzian model, the force should be perpendicular to the plane of the contact surface (Liang Liao and Fengfeng Xi, 2005) and the contact area is assumed to be elliptical (Liao et al., 2008). The constant force in polishing changes the geometry of a curved part, while the constant stress polishing does not. Equations 2.1 to 2.3 can be used to calculate the contact stress, where P_m is the stress at the contact surface, F is the variation in applied force necessary for constant contact, and T_f is the friction torque, resulting from the frictional force between the polishing tool and workpiece.

$$P_m = \frac{2b}{3E(k')\Delta}$$

Eq.(2.1)

$$F = \frac{9\pi\ E^2\ (k')\Delta^2\ P_m^3}{4k}$$

Eq.(2.2)

$$T_f = \frac{\mu_k P_m}{3}\int_0^{2g}(a^2cos^2\ e + b^2sin^2e)^{3/2}de$$
$$= \frac{1}{3}\mu_k P_m\pi(a^3 + b^3)$$

Eq.(2.3)

2.2.2.3   *Material Removal Rate*

MRR can be defined as the amount of abrasives that cut the metal per unit area (Ahn et al., 2002; Besari et al., 2010). As for the contact stress, the material removal rate (MRR) is an important factor in any material removal process. The MRR value is dependent mainly on the contact force between the tool and the workpiece, the belt speed, and the feed rate in the tangential direction (Huang et al., 2002)..

According to Weng-Jong Lin et al. (Wen-Jong Lin et al., 2004), typical MRR of a grinding belt highly decreases from the first operation. Therefore, a constant MRR is required for optimum polishing operation. This decrease in MRR is due to abrasive wear of the belt, but this may be compensated for by increasing the belt speed and decreasing the workpiece feed rate. In general, rough polishing operation will demand a large MRR and a slower feed rate; whereas in fine polishing, if the feed rate is too slow, it may cause excessive metal removal which may damage the workpiece (Ahn et al., 2002). Typically, MMR increases with the increase of the contact force and the belt speed, with a decreased feed rate (Huang et al., 2002). Higher pressure will cause deeper cutting depth, hence a higher MRR. However, high MRR might result in burning marks on the workpiece, due to over-cut.

Preston's model (see Equation 2.4, below), which was developed for glass polishing, is still used today to determine MRR in abrasive processes:

$$MRR = \frac{dz}{dt} = K \times P \times V$$

<div align="right">Eq.(2.4)</div>

Where P is the average pressure of contact, V is the relative velocity of the tool/part relative, and K is the Preston coefficient (which is determined experimentally and depends on parameters, such as part material, abrasive, and lubrication) (Guiot et al., 2011). The Preston coefficient can be calculated using Equation 2.5.

$$K(t) = K_0 . w(t)$$

<div align="right">Eq.(2.5)</div>

2.2.2.4 Tool Wear

Typically, the tool wear is significant in grinding processes due to the hardness of the material. Axinte (Axinte et al., 2009) studied the wear of abrasive tools during polishing. The authors took the following factors into consideration: the density of the abrasive grains left on the tool surface; the capability of the tool to remove the milling marks; and the surface finish produced. They found that the grit embedded into the machined surface, using abrasive machining could result in a reduction of fatigued performance.

During their experiment, Huang (Huang et al., 2002) found a high tool wear after the first workpiece and a decrease in MRR after three. This shows the intertwining relationship between MRR and tool wear, as demonstrated in Section 2.2.2.3.

2.2.2.5   Force Control

As previously stated, the contact force in polishing processes must be kept constant. Therefore, force control is particularly important to avoid over- or under-cuts, as the material removal rate should be uniform along the surface to achieve the desired profile and surface finish (Huang et al., 2002). This is even more critical for parts with a complex

profile (i.e. high curvature surface); in cases where a part's surface geometry varies, the constant tool force will generate a high contact stress under a small contact area, leading to over polishing (Liao et al., 2008). Alternatively, a small contact stress under a large contact area (e.g. low curvature surface), can lead to under-polishing. Therefore, the contact force should be changed to avoid over-or-under-cut (Liao et al., 2008). Additionally, a misalignment of the part on the polishing tool, such as a tilt, can result in displacements and increase the tool wear (Beaucamp et al., 2011).

In passive force control or passive tool control (PTC), the MRR is dependent on the contact force between the tool and the workpiece, the belt speed and the feed rate in the tangential direction. Spring systems may be used to adjust the contact force in PTC. The sensitivity of the contact force to profile variation may be adjusted by changing the spring stiffness and the pre-load, which also reduces the vibration generated during machining (Huang et al., 2002).

2.3   State of the Art

This section presents the common methods used today for mechanical polishing. Even with the growth of automated systems such as robotics, Computer Numerical Control, or mass finishing, manual operation is still widely in use. Some other existing technologies are shown in Table 2.1, but the following methods are the main processes of mechanical finishing used in industry and in research laboratories.

2.3.1   Manual Polishing

Typically, polishing is a highly skilled manufacturing process with many constraints and interactions with the environment (Besari et al., 2010). These processes have largely been carried out manually. Manual polishing operation is: very labour intensive; highly skill dependent; costly; prone to errors; environmentally hazardous due to abrasive dust; and, in some cases, inefficient with long process times. The quality of the finishing will depend (Wen-Jong Lin et al., 2004) on the level of training, experience, fatigue, and expertise of the operator. In addition, these operations require exceptional skill that can only be taught by experienced operators (Tsai et al., 2005).

The working environment is an crucial factor to account for in the challenge of automation (Huang et al., 2003; Wen-Jong Lin et al., 2004). The dust, noise, and vibration produced by the polishing process are detrimental to human health (Tsai et al., 2005). The Health and Safety Executive (HSE) suggests that operators wear a set of personal protective equipment (PPE) including goggles, earplugs, safety shoes and to take regular breaks as long-term exposure to vibration can create severe injuries (Health Safety Executive, 2000, 1999).

Despite all of this, manual operation is still the best method for polishing processes. This is due to the skill and experience of the operator to perform high quality of surface finish in the minimum amount of time. Manual polishing processes are difficult to automate because they require quick adaptation to the changing surface as well as tool wear, which only a skilled operator can monitor using their own visual and tactile feedback.

Figure 2.3: Example of an industrial part being polished by a skilled worker

2.3.2   Robotic End-Effector

Industrial robots are commonly used for simple, repetitive tasks (Chen et al., 2000). Machining applications have been mostly restricted to - and proved to be an economic solution for - deburring, chamfering and finishing of workpieces that possess a constant geometry (Chen et al., 2000; Huang et al., 2002). Robotic machining has certain advantages over conventional CNC machining, such as high flexibility, good repeatability, capability of integration with peripherals such as sensors and external actuators, and lower cost.

Therefore robotic polishing may be a good alternative for automation processes (Chen et al., 2000). However, current technologies are not stiff enough to handle heavy machining dynamics, such as some milling or grinding processes (Huang et al., 2002).

Automated polishing process using robots is generally done with the assumption that the workpiece has either no defect or all defects are considered as uniform onto the surface (Akbari and Higuchi, 2002). Moreover, robot programs are generally inflexible (as in CNC's). Hence all workpieces receive the same treatment (e.g. time, force, tool strategy) (Besari et al., 2010).

To help the automated system to meet (Huang et al., 2003; Wen-Jong Lin et al., 2004) the rigidity, dexterity and repeatability requirements - as well as the adaptability and capability of a human operator - a mechatronic system (i.e. robot embedded with a set of sensors) must be developed around these variables to meet requirements and overcome the challenges. This approach may require a set of tools to reconstruct workpiece profiles, control the robot motion, and/or adjust tools in real-time for optimum operation (Akbari and Higuchi, 2002; Chotiprayanakul et al., 2012; Huang et al., 2003; Wen-Jong Lin et al., 2004).

In the majority of the autonomous systems, the force data obtained during polishing is used as the main output (Akbari and Higuchi, 2002) so that the contact force and the tool angle can be adjusted in real-time for optimum operation. In addition, studying the relationship between the number of passes and the resultant surface finish may also help to reach optimal polishing conditions.

Typically, the process should start with an abrasive tool with a larger grain size and gradually go down to a smaller tool (Tsai et al., 2005). Moreover, the polishing path should distribute the force evenly on the surface, leaving no over-or-under polished area. Furthermore, the polishing path should pass through the same point in as many directions as possible although, if this is done repeatedly, this may cause a recess on the surface.

2.3.3   Computer Numerical Control

As the industry progresses from hand to machine operations, Computer Numerical Control (CNC) equipment continues to make great improvements in speed and precision (Davidson, 2005). Since high-speed machining (HSM) was introduced, the necessity of polishing has been reduced (Ahn et al., 2002). Traditional CNC machines have dramatically modified the organisation of manufacturers, by reducing manufacturing cycle times and increasing quality of products. However, they may not fully replace finishing operations (Guiot et al., 2011).

In automated applications, CNCs can be a good alternative to the robotic arms (Chen et al., 2000). The main advantage of CNCs is the repeatability and precision of the machine movement (Guiot et al., 2011). This has led to higher component accuracies while lowering machining time, and therefore lower costs, except for critical components such as rotating discs or blades, where the requirements are difficult to meet (Besari et al., 2010; Kenton, 2009).

Commercial solutions, such as centerless machines, are already available for grinding and heavy polishing. However, more and more work is being carried out towards using CNC milling for polishing or finishing operations. This approach consists of using either tools similar to those used in manual polishing (abrasive discs mounted on a deformable carrier) or custom polishing tools (abrasive cylinder or cone attached to a metallic shaft) (Axinte et al., 2009; Beaucamp et al., 2011; Guiot et al., 2011). The polishing tool is pressed against the surface of the part, with no attempt to actively control the Z position of the tool (therefore, actively controlled with a CNC machine tool). CNCs do not provide force feedback control, but the polishing force can be managed with the length of the tool.

One solution to control of the contact force is to use a separate force device, which generates a tool force independent of the motion. The force control of the tool can be decoupled from the motion control. Since the force device is directly mounted onto the tool, the delay in the force generation is reduced. In practice, the tool compliance of a CNC can be implemented either passively or actively (Liao et al., 2008). However, if the part is slightly misaligned with the tool, the tool may gouge the part, leaving unwanted cutting marks on the surfaces, or the tool could break. In addition, a human operator is still needed to load and unload the machine, programme it, insert the tools, and monitor the process (Kenton, 2009).

On the other hand, in CNCs the machining path and strategies for polishing are often issued from experiment (Guiot et al., 2011). Lubrication can be performed in both dry (chilled air) and wet (MQL), which reduce the heat transferred to avoid premature tool wear and improve the quality of surface finish (Axinte et al., 2009).

It can be concluded that the use of CNCs for polishing may be beneficial in terms of precision and repeatability. However, these technologies do not provide enough flexibility for polishing processes compare to manual or robotic.

2.3.4   Mass Finishing

The most common means of surface finishing in industry is via mass finishing systems. Common surface finishing operations require: deburring; descaling; surface smoothing; edge-breaking; radius formation; removal of surface contaminants from heat treatment and other processes; bright finishing; and pre-plate or coating surface preparation (Benjarungroj et al., 2011; Kenton, 2009).

Mass finishing technology was initially used for the finishing of small parts (such as coins) in large batches. Mass finishing processes starts by loading the workpieces and media together into the mass finishing machine; then the movement of the machine causes media to finish the workpieces.

In current practice, an experienced operator first selects the appropriate type of media for the workpieces to be processed, as illustrated is Figure 2.4. For instance, coned shaped media would perform well for small radius or holes. This decision is based on the type of liquid compound and the polishing time required (Cariapa et al., 2008). During the finishing operation, the workpieces are periodically visually inspected manually by the operator, and the process is stopped when the desired surface condition is achieved. Successful implementation of mass finishing processes and the quality of the surface finish will depend on the type of mass finishing machine, the material and geometry of the media, the liquid compound, the material and geometry of the workpiece, and finishing time (Kenton, 2009).
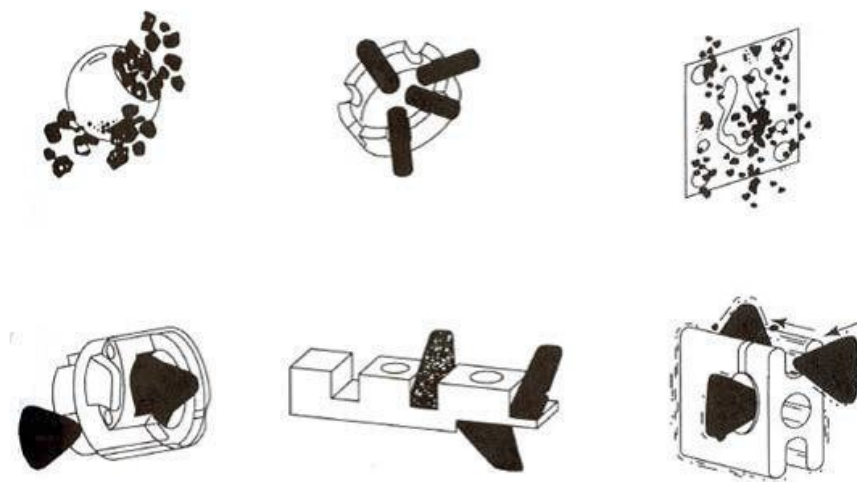

Figure 2.4: Examples of cutting action in mass finishing (Gillespie, 2007)

The composition and geometry of a media determines whether it is a cutting or finishing type of media (see Figure 2.4), and thus affect the quality of the surface finish. Common shapes of media include pyramids, cones, cylinders, and spheres (Cariapa et al., 2008).

Most media are abrasive tools that modify the workpiece surfaces by levelling down the surface irregularities or removing small amounts of material from the surface and edge. The liquid compound solution acts as the chemical inhibitor on workpiece surfaces to inhibit corrosion, reduce friction, cool the workload, and remove soils from the bowl. Another benefit of mass finishing is that all materials are work-hardened to some extent and make the surface denser (Kenton, 2009). Therefore, part life and performance is improved.

As presented above, mass finishing is a great alternative for finishing operation of large batches of small parts. Due to its successful implementation, industries currently are investigating the mass finishing of larger parts.

2.3.5   Abrasive Blasting System

Abrasive blasting (or sandblasting) is another finishing process, where abrasive particles are propelled at high speed from a blast machine, using the power of compressed air (Cym Materiales, 2013; Hansel, 2002). Material is removed from the workpiece surface due to the impact of abrasive particles that cut into the surface. This forms tiny peaks and valleys that are controlled by: the size, type and hardness of the abrasive; the air pressure; and the distance and angle of the nozzle to the surface. Abrasive blasting is commonly used for mechanical cleaning, shot peening to alter mechanical properties (e.g. increasing the fatigue resistance of the material), and preparing surfaces for additional operations (i.e. painting or coating) (Cym Materiales, 2013).

The quality of the process is determined by the effectiveness and performance of the whole system (Hansel, 2002), as well as the experience of the operator. However, a large portion of blasting operations can be automated. Automated processes can improve manual operation (Guyson, 2013) and aid workers during laborious or hazardous task, such as stripping off rust and paint (Chotiprayanakul et al., 2012).

Abrasive blasting systems are composed of: a blast machine; nozzles; spray gun (pneumatic or electrical); air compressor; abrasive (type and size); recovery and cleaning of abrasives; dust extractor; part movement and support system; and controls and instrumentation.

Typically, the air compressor, blast machine and abrasive constitute the three main components of the system. The compressor must produce sufficient air pressure and volume to convey the abrasive sand from the machine to the surface. This is important as the result of the finishing is dependent on how efficiently air moves from the compressor to the surface.

The size, type, shape and number of nozzles used are determined by the production rate and the aspect desired. The diameter of the nozzle orifice will determine the amount of work done and the amount of air and abrasive used per hours. Typically, a good control of the spray may save substantial amounts of compressed air and abrasive while lowering the risk of injuries.

The last major component in abrasive blasting system is the abrasive (Guyson, 2013). The abrasive type will produce the desired finish on the surface. Abrasive blasting can improve the appearance of a part by removing stains, residue, corrosion, scratches and tool marks to provide a uniform appearance. After the abrasive hits the part, it falls into the collection hopper under the machine (Cym Materiales, 2013). Recirculation and cleaning of the abrasive shot is required to maintain a consistent cleaning operation.

As described above, abrasive blasting systems may be a good alternative for polishing processes. This method has the advantage of being able to be used by a human operator or mounted onto a robotic arm. The criteria used to select the type of abrasive blasting system depends on the size and shape of the parts, the condition of the surface to be cleaned, the final surface finish specification, and the overall process required.

2.4 Automated Challenges

Many industries already benefit from the advancements in multi-axis machining to produce parts to very precise tolerances and specifications. Up to a third of manufacturing time is allocated to finishing processes. Therefore the industry is strongly motivated to automate such processes to drive down the high costs associated with utilising hand tools and to remove manual workers from health hazard exposures, whilst keeping the same of level quality or better (Axinte et al., 2009; Kenton, 2009; Wen-Jong Lin et al., 2004).

Industrial robots have been widely used to perform well-defined, repetitive tasks in carefully controlled environments, but fully autonomous operation of the robot may not be cost-effective (Chotiprayanakul et al., 2012). The cost of the technical challenge is an important factor - even if belt grinding is cheap and widely used, fully automated equipment can be expensive (Wen-Jong Lin et al., 2004). The production requirements dictate the level of automation. Tele-operation by means of a haptic device can provide a useful and practical solution in such situations (Chotiprayanakul et al., 2012). It is also essential to ensure that the jobs left over for human operators are within their capabilities and make the best use of human skills and knowledge in combination with the technology available (C. Siemieniuch and Sinclair, 1995). As a result, the possible automated system cannot only rely on the teach-and-play or programming (Chen et al., 2000).

The successful implementation of an automated polishing system requires a thorough study of the polishing process (Besari et al., 2010). In the past, much research has been carried out to investigate automated polishing systems. According to M.J. Tsai (Tsai et al., 2005), an exact and clear measurement of the polishing parameters should be carried out. The new automated system should then use the current measured surface roughness of the workpiece and the targeted roughness to find the optimal polishing parameters.

The main challenge in polishing is to maintain a constant polishing force. Controlling this variable in an automated polishing process is difficult (Liang Liao and Fengfeng Xi, 2005). Due to friction between the tool and the part, the tool speed will be affected when the tool pressure is changed. The contact stress model is usually introduced based on a Hertzian contact model, relating the tool pressure to the contact stress of the contact area on the part

and to the friction torque resulting from the tool pressure to the tool speed (Liang Liao and Fengfeng Xi, 2005; Wen-Jong Lin et al., 2004).

However, the polishing force does not guarantee a constant contact stress between the polishing tool and the part being polished, and it is this contact stress that determines the quality of the polished part. According to Liao (Liang Liao and Fengfeng Xi, 2005), if the contact stress is too high the part will be over polished; if the polishing tool speed varies, polishing will be non-uniform.

Experiments in research laboratories and in industry have shown that the cost-reduction benefit is the main driving force behind the initial process implementation (Davidson, 2005; Liang Liao and Fengfeng Xi, 2005; Wen-Jong Lin et al., 2004). To this end, a concerted effort has been made to implement a robotic system to provide more consistent work quality which is less prone to error (see Section 2.5). However according to Besari et al. (Besari et al., 2010), automated systems will never fully replace the need for manual operation.

Nevertheless, the overall results of the different research would encourage further developments in robotic polishing applications.

2.5   Related Work

2.5.1   Research Application

The Singapore Institute of Manufacturing Technology (SIMTech) and Nanyang University have worked on an automated solution for grinding and polishing for the refurbishment of turbine blades. In industry, the repair and grinding operations of turbine blade are currently carried out manually by skilled operators. When damaged, the turbine blade is repaired, as it was found to be cheaper than producing a new part. The refurbishment process of turbine blades starts by an operator manually filling gaps and cracks on the surface, and then grinding and polishing the whole surface, to restore its original geometry.

Between 1999 and 2004, these researchers developed two solutions: SMART Robotic System (Huang et al., 2003) and a Self-compensated Closed Loop Real-Time Robotic Polishing System (RT-RPS) (Wen-Jong Lin et al., 2004) . Both solutions include various tools developed in-house (Chen et al., 2004, 2000, 1999; Gong et al., 2000; Huang et al., 2003, 2002; Ng et al., 2004; Wen-Jong Lin et al., 2004). These systems begin the process by measuring the surface of the workpiece (as it is covered with brazing material). The measured geometry is then compared and matched to various templates. These templates include a particular set of parameters. Finally, the polishing and grinding operations are carried out through various abrasive belts, using the parameters selected previously.
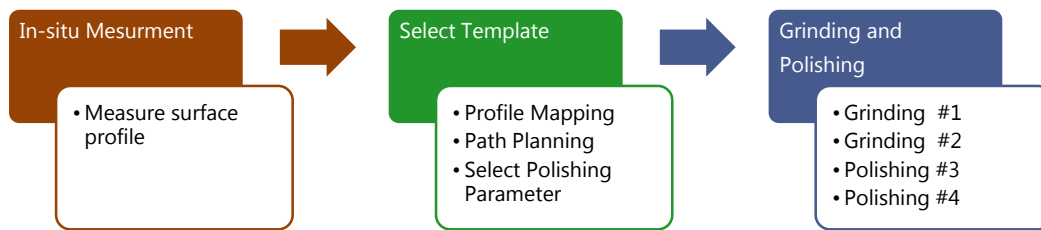
Figure 2.5: Grinding and polishing process of turbine blade refurbishment

Based on the literature, these authors have done a complete research (to date) of the grinding and polishing operations of complex components. This includes the development of several systems and tools, which needed to be done as each workpiece has unique defects (e.g. brazing material, cracks, and marks). However, it is somewhat regrettable that the set of parameters created for each part is based on a template and not created based on the defects. Finally, it is also regrettable that each part is not assessed at the end of the process.

M.J. Tsai (Tsai et al., 2005) developed a software (GUI) for automated polishing system (AMPS) for the polishing operation of mould. Their system aimed to adjust the path of the robot depending on the geometry of the workpiece and the grain size of the polishing tool. The software developed by the authors may be sufficient for the polishing operations of a curved surface. However, this system still relies on the skill and experience of a human operator to enter the correct inputs.

Liao et al. (Liao et al., 2008; Roswell, 2004) have developed a system and model for automated polishing and deburring using a dual-purpose compliant tool head. The authors investigated and developed a mathematical model to compute and control the contact stress generated during polishing (see Section 2.2). Their system is designed like a CNC, where the system follows a pre-planned path (e.g. g-code). However, the position of the tool is adjusted through a pressure sensor and pneumatic actuator to keep the contact stress constant. This solution may be sufficient for small parts and optimum contact stress (through the compliant tool head). However, further work should be considered in the measurement and assessment of the part before and after the process. Finally, this solution may not be cost effective for industry, as it includes in-house tool development and costly commercial solution.

C. Tournier (Pessoles and Tournier, 2009) and D.A. Axinte (Axinte et al., 2009) have investigated the capability of traditional CNC machines (i.e. 5-axes CNC milling) to carry out polishing operations for gas turbine engines (Axinte et al., 2009) and plastic injection moulds (Pessoles and Tournier, 2009). As mentioned in Section 2.3, in these studies, CNC machine tools have shown good precision and repeatability when following a pre-planned path, with good surface finish as well. However, some problems with abrasive tool wear were observed (i.e. needing to change tool after each workpiece).

Okamoto (Ito and Morishige, 2009; Okamoto and Morishige, 2012) focused on developing an automated system to remove milling marks from a metal workpiece using visual inspection. In this system, a 2D image of the workpiece surface is captured between each pass in order to assess whether more passes are needed for the required surface quality. The system includes a grinding disc and a CCD camera mounted onto a 6DoF robotic arm.

Despite the benefits of using 2D vision for polishing processes, their current approach requires a long polishing time in relation to the required surface quality: 45 passes were required in order to remove all machining marks on the workpiece surface. It was regrettable, however, that the author did not controlled the force applied to the surface but instead switched polishing passes between a horizontal and a vertical path.

J.H. Ahn (Ahn et al., 2002, 2001) developed an intelligent robotic polishing system for sculpted die using an acoustic emission sensor (AE). Traditionally, tactile feedback of skilled operators is translated into force feedback systems for automation using force and torque sensors. However, the authors argued that the tactile feedback of the operator can be translated into a mechatronic system via an AE sensor. In their developed system, the adjustment of the polishing parameters is captured by the AE sensor to monitor the polishing operation in real-time. However, this only applies to the tool wear. The intelligent system, based on the level of noise (AE sensor), decides when to change and select a more appropriate abrasive tool to carry out the operation. Each abrasive integrates a specific set of parameters to use for the robotic system.

T. Sasaki (Sasaki et al., 1992, 1991a, 1991b) have investigated some of the habits of skilled polishers for the development of an automated grinding solution. However, their study is limited to the habits of skill workers operating conventional horizontal grinders and comparing these results to a CNC grinding machine. The authors found that the automated system was twice as fast but provided the same quality of surface finish as a manual operator. However, it was noted that some key parameters (such as force, speed, or operator decision) are missing from this study. Therefore, a more detailed study of the manual polishing operation should be carried out.

H. Du (Du et al., 2015) have developed a robotic polishing method and system for the polishing operation of curved titanium alloy workpieces. Their system uses a robotic arm to follow a pre-planned path generated from CAM (computer aided manufacturing). The force and position compliance is done through a flexible end-effector embedding a multi-axial force and torque sensor, servo and support motor, and sand paper. The position-based force control is generated from the force and torque output, which is then converted into a vector to calculate the new vector position.

H. Du's method (Du et al., 2015) has shown good results during their experiments. However, it is regrettable that the flexibility of their system comes from the tool and not the workpiece (as is the case for a human operator). Unfortunately, their study of manual operation was limited to the capture of the force necessary to polish such workpieces; their study does not include a full understanding of the force and torque sensor behaviour, and the robotic path was based on CAM generated from a g-code (CNC).

2.5.2   Industrial Applications

Industrial companies have already introduced automated technologies such as CNC grinding, robotic polishing, or mass finishing. However, the implementation and use of these automated systems remain difficult. The following section presents some alternative automated solutions available for finishing processes.

PoliMATIC (Fraunhofer, 2013) is a European project carried out by Fraunhofer and various industrial partners for robotic polishing of free-formed mould and dies. Their system includes a CAD/CAM package, force control and in-situ metrology.

AESCULAP (KUKA Gmb, 2014), a company specialising in medical equipment, has introduced partial automation within their processes in collaboration with KUKA Gmb. They wanted to optimise their process by shortening the production time and reducing cost. The automated system is composed of two robots (one for grinding and polishing and one for buffing) working on the finishing of a single component. Aside from some in situ measurement, the system repeats the same action and takes 6 minutes to finish one part, whereas a skilled operator can work faster.

ARCOS systems (Arcos, 2013) is a machine tool manufacturer that provides industrial solutions and services for various companies. Their solutions include a complete automated cell with robotic arms, grinding-polishing-buffing stations, and a vision system to assess the workpiece.

SHL Automatiserungstechnik (SHL-Automatisierungstechnik, 2015) is another machine tool manufacturer that supplies surface finishing equipment. They also propose an automated cell solution, albeit without in-situ measurement.

RJH Finisher (RJH, 2014) is yet another supplier for the finishing industry. One of their products is a semi-automated grinding station, primarily used for deburring batches of workpieces, which is operated by skilled operators.

VULCAN Europe (Vulcan Engineering, 2015) has also worked on a semi-automated grinding system called VTS, Vulcan tactile system. The robotic system is operated by a skilled worker to assist the grinding process of large foundry components with a haptic feedback device.

While these systems (RJH, 2014; Vulcan Engineering, 2015) could reduce the risk of injuries, they may not be cost effective and are still heavily reliant on the operator's skill and experience.

2.6 Human Processes

Software engineering techniques such as CAD or product leam management (PLM) (Annarumma et al., 2008; Chang and Wang, 2007; Määttä, 2007) platforms are used to analyse the manual operation procedure and to obtain the task specifications for the development of automatic solutions.

Ergonomists and manufacturing engineers collect data from various processes to organise the whole production., particularly when manual jobs are the central element of planning and control the supply chain (C. Siemieniuch and Sinclair, 1995). For example, in assembly, time recording facilitates surveys and analyses the process (Schenk et al., 2011). In addition, mechanical or electronic sensors may be used to record and determine the distribution time for each task in order to reduce the labour.

2.6.1   Human Factor

Within manufacture, human force is still the most important component of the competitiveness of a company, through the employee's presence, knowledge, and skills applied every day. The increase in investment in new technologies (such as automation) is increasing the pressure for the use and return on capital of these assets. These new technologies will also change the ratio of capital and labour based on the critical skills to use these new tools. Without good training of employees, companies may lack the necessary skills to use these new technologies, which would consequently reduce their competitiveness (C. Siemieniuch and Sinclair, 1995).

Humans have some particular qualities. They can learn and make decisions from little information or errors, and innovate; overall, they can control and adapt to unexpected changes (C. Siemieniuch and Sinclair, 1995). This makes them more effective and more flexible to the production of higher-quality goods and to changes in processes. This is why trained, skilled operators produce a high quality of surface finish in a short amount of time, regardless of the type of workpiece (Hansel, 2002).

However, manual finishing processes are still laborious and can increase the health and safety risk to the operators. For these reasons, industries should provide sufficient training and personal protective equipment (PPE) (Hansel, 2002).

This is why the importance of knowledge and skills of a trained operator helps to create and maintain competitiveness (C. Siemieniuch and Sinclair, 1995). To achieve this, industries must be able to model their enterprise in order to explore different arrangements of skills and competencies, to structure themselves, to grow in size and to stay competitive (C. Siemieniuch and Sinclair, 1995).

In general, human factor decisions are left to designers using guidelines and standards. However, present guidelines and standards are too general. Therefore, there is a need to

develop tools and methodologies that can easily be implemented in industry. The fundamental principle of human factors is that it should be based on a user-centred design that allows input from an expert at all stages of the design and build process (C. Siemieniuch and Sinclair, 1995).

The work environment is specific to the task carried out and its production rate. In manual polishing, the normal work area should be within the limits of a comfortable reachable movement (or near boundary). The design of a polishing cell, from an ergonomics point of view, can effectively enhance the productivity through the interaction between various components (e.g. the task required, production rate). Whether the operator is sitting or standing does not affect the operator's reachable envelope. It is the task requirements that will affect the size of the working area. Specific jobs that require strength, speed or accuracy will place different constraints on the parameters of the work area, regardless of posture. Therefore the preferred boundary (standing or sitting) is driven by the specific demands of the task itself (Nur and Dawal, 2010).

In most industrial working cells, operators perform manual tasks that involve repetitive motions and loading. This may result in muscle fatigue, repetitive strain injuries, musculoskeletal injuries and musculoskeletal disorders (or MSD) due to the repetitive muscle strain of the task (Ma et al., 2008; Nur and Dawal, 2010). Muscle fatigue is defined as the point at which the muscle is no longer able to sustain the required force to complete the task. The overexertion of muscle force and muscle fatigue can induce acute pain and chronic pain in the human body.

MSD is still a serious health problem; according to L. Ma (Ma et al., 2008) almost half of industrial workers are suffering from it. Work related MSD has been found to be associated with several factors such as force, posture, movement, vibration and anxiety. Force and fatigue are important factors, as they are dependent on the workers performance (Ma et al., 2008). The intensity, repetitiveness and duration of the external load should also be considered. Individual factors, like gender, age, and weight and so on should be considered as well (Ma et al., 2008).

MSDs are caused by an overexertion of muscle force or frequent high muscle load pain in muscles and other tissues of the human body (Ma et al., 2008). The feeling of the fatigue is due to personal factors (i.e. muscle mass), the force exerted on the muscle over time, and the external loads (Ma et al., 2008). Even with a task requiring a light exertion (Nur and Dawal, 2010), the maximum external force needed changes over time due to the external loads. The larger the force used by the operator is, the faster they feel fatigue, and the longer the force is maintained, more tired they will be (Ma et al., 2008).

Other factors, such as standing position, can cause fatigue, exhaustion and lower back pain if maintained for a long period. Excessive reaching can also increase force and torque around a joint, which may increase the risk of injury (Nur and Dawal, 2010).

As presented above, humans are an important factor in the company and process level. Despite the introduction of new technology, the human workforce is still the best advantage of industries in term of competitiveness and quality of service. Humans have some great advantages, such as flexibility and adaptability, but some tasks may impact them severely (e.g. MSD). New technologies are primarily introduced to ease the process and increase

competitiveness. However, the implementation of these new tools may fail due to the lack of proper training or insufficient planning.

2.6.2   Capture Motions

Recording posture and movement is important in ergonomics, as it allows researchers to study a task and the resultant effects (i.e. injury, performance) (Dutta, 2012; Welch, 2002). Operator motion is usually captured during a specific task using motion tracking systems (Ma et al., 2008; Welch, 2002). The captured data are then evaluated so that the muscle fatigue or the complexity of a task is computed.

Typical ergonomic evaluations of a manual task are carried out in the field. The manual task is often captured through cameras and other equipment. To complete the capture and analysis of the task (i.e. posture of the worker), additional tools (such as virtual reality or virtual human) may be used to evaluate the human performance, such as postures, movements, stresses and strains (Schlette and Rossmann, 2009). This is because most of the manual handling jobs are implemented in the process dynamic (Ma et al., 2008).

The evaluation of the task procedure can give ergonomists more detailed information, which can improve the quality of work, reduce delays, improve the working conditions and decrease MSD risks (Ma et al., 2008; C. Siemieniuch and Sinclair, 1995).

To capture the manual skill of the operator in polishing, the method chosen should be compliant to the task as many parameters can affect the finishing result (Tsai et al., 2005). Modern motion capture technology poses a wide range of techniques, possibilities and applications. These technologies are based on different principles, exhibiting different performance characteristics, designs and applications (Welch, 2002).

Motion sensors are often used in computer graphics systems for five primary purposes: view control (to provide position and orientation control of a virtual camera); navigation (help users navigate through a virtual environment); manipulation (user manipulate virtual objects in 3D environment); instrument tracking (match virtual computer graphics representations with their physical counterparts, i.e. computer-aided surgery or mechanical assembly); and avatar animation (moving animated characters through full body motion capture) (Welch, 2002).

However, today's systems are not accurate enough or suited for field work or detection of MSD risks to particular muscles (Dutta, 2012; Ma et al., 2008). L. Ma (Ma et al., 2008) states that the main issue of current commercial technology is their non-consistency, where in some cases, the results of a task may differ depending on the technology used (Ma et al., 2008).

According to G. Welch and E. Foxlin (Welch, 2002), there is no technology today that is likely to emerge or overcome the current problems in motion capture. Therefore the key to choosing the right technology is to recognise the different needs of the application and meet those needs with one or more technologies (Welch, 2002). Following this idea, L. Ma (Ma et al., 2008) mentioned that, as no technology is currently suitable for tracking full-body

motion and finger motion at the same time, in order to capture all necessary information of the worker's operation, the integration of different sensors is then necessary (Ma et al., 2008).

2.6.2.1   *Motion Sensor Characteristics*

The main requirements and characteristics for adequate motion trackers are that they should be tiny, self-contained, complete, accurate, fast, immune to occlusion, robust, tenacious, wireless, and cheap (Welch, 2002). However, current technology fails at least seven of these ten characteristics (Welch, 2002). In Table 2.2, some recommendations have been made based on the characteristic shown above (Ma et al., 2008; Welch, 2002).

Table 2.2: Primary requirements for motion sensors (Ma et al., 2008; Welch, 2002)

Characteristic	Requirement
Small	Size of an 8-pin DIP (dual in-line package) or even a transistor
Self-contained	No other parts to be mounted in the environment or on the user
Complete	Tracking all six degrees of freedom (position and orientation)
Accurate	Resolution better than 1 mm in position and 0.1 degrees in orientation
Fast	Running at 1,000 Hz with latency less than 1 ms.
Immune to occlusions	Needing no clear line of sight to anything else and other obstacle in the environment
Tenacious	Tracking its target, no matter how far or fast it goes
Wireless and Good autonomy	Running without wires for three years on a coin-size battery
Cheap	Less than $1 each in quantity
Update Rate	From 24/25 Hz for real-time visualisation of the motion
Robustness	Tracking should be stable and prevent influences from the environment.
Data Transferring	High transfer of data is necessary to ensure real-time measurement

In general, for full-body motion tracking of a human using tools or interacting with virtual objects, the accuracy should be as high as possible. For example, in industrial applications, the accuracy should be within 1 mm in position and 0.1 degrees in orientation, but for other applications, such as character animation, biometrics, or recording general moves, accuracy is not very critical (Ma et al., 2008).

Transferring the data from tracking devices is another problem. There is real-time (online) and non real-time (offline) tracking. In general, tracking data can be saved and processed for further simulation (Ma et al., 2008).

2.6.2.2 *Motion Sensor Types*

As there is a large number of technologies for motion tracking systems that can sense and interpret electromagnetic fields or waves, acoustic waves, or physical forces, these systems most often estimate data from electrical measurements of mechanical, inertial, acoustic, magnetic, optical, or radio frequency. Each approach has advantages and limitations, such as physical medium or measurement limitations imposed by the devices that arise in a specific application (Welch, 2002).

Inertial Sensor Unit

An inertial measurement unit (IMU) uses micro-electro-mechanical sensors to determine motion and orientation. The components of translation and rotation of motion are measured through a 3-axial accelerometer, gyroscope and magnetic field. A PC host calculates and reconstructs the motion sequence (Welch, 2002).

One advantage of these systems is their independence from a reference system (unlike in GPS, cameras or ultrasonic systems). They can be attached directly to a moving object or human limb. They are small in size (Schenk et al., 2011) and completely self-contained, so they have no line-of-sight (Welch, 2002). They also have very low latency, can be measured at relatively high rates, and the measured velocity and acceleration can generally be used to predict the future position. However, their main weakness is the drift: if one of the accelerometers has a bias error, the output (or computed) position would diverge from the true position.

The applications of these systems have been proven to be very valuable when combined with one or more other sensing technologies (such as optical sensing or radio-wave) (Welch, 2002), for ergonomic or manufacturing operations (Schenk et al., 2011).

Mechanical Sensing

Mechanical sensors use physical links between the target and the environment. The basic approach includes series of two or more rigid mechanical pieces interconnected with electromechanical transducers. Then the position of the object can be estimated with respect to its environment (from one end to the opposite end). The most common usage of mechanical sensing today is in articulated haptic devices. These devices need to know the tip position to apply appropriate forces. This approach can provide very precise and accurate estimation of the position for a single target in a small range of motion (Welch, 2002).

Acoustic Sensing

Acoustic systems or acoustic emission systems (AE) use sound waves, operating on the time of flight of an ultrasonic pulse from its transition to the sensing. To measure the absolute distance, it is crucial to know the starting distance and then keep track of the number of accumulated cycles (Welch, 2002). The reason why this method only works for acoustic sensors is that the sound is travelling slowly, which creates a time difference between the arrival of the direct path pulse and the first reflection.

The advantage of acoustic sensors is their integration into motion tracking systems, which helps to reduce error, although their accuracy would depend on the size of the active surface area (e.g. larger the surface is, larger the range). However, the main concern of acoustic sensors is the effect of multipath reflections, because walls and objects in a room will reflect acoustic signals, which can create noise or bias in a measurement (this is why acoustic sensors are not popular). Hopefully, building a hybrid system that combines acoustic sensors with an inertial sensor is possible (Welch, 2002).

Optical Sensing

Optical sensing relies on measurements of reflected or emitted light. These systems work with two components: light sources and optical sensors. The light sources can be either a passive object that reflects the light or an active device that is generating light. There are two types of optical system: Position Sensing Detector (PSD) and charge-coupled device (CCD).

PSDs use semiconductor devices to indicate the position of the centroid of the light reaching the sensor. These sensors also offer a measurement based on the total light reaching the device, like a photo sensor. Hence the system can use the controlled light source to distinguish the target from the ambient light (Welch, 2002).

CCD systems use an array of pixel sensors that convert light energy into an electrical charge over a short time to produce a sampled image (Welch, 2002). The result is that image-forming devices are typically limited to relatively few measurements per unit of time when compared to the simpler analogue optical PSD (Welch, 2002).

The capture of 1D or 2D images typically offers more constraints on an estimation of poses, such as the extractions of shapes, shading, or motion of multiple image features (Welch, 2002). In addition, the processing of these images may be computationally heavy (Welch, 2002).

Radio and Microwave sensing

Radio and microwave systems are electromagnetic wave-based tracking techniques. They are mainly used in navigation systems, such as radar systems. However, as they become

more precise, smaller and cheaper, there could be some application for human motion tracking. They can also provide a greater range than other quasi-static magnetic fields sensors (Welch, 2002).

In addition, radio waves are a suitable alternative to acoustic systems for outdoor tracking as they are unaffected by wind or air temperature, though they are rapidly attenuated in water. Most of these systems operate on the principle of time-of-flight. As in acoustic systems, radio waves signals are vulnerable to distortion for indoor application, due to reflections. Various signal-processing strategies can improve the resolution (Welch, 2002).

However, sensors such as Ultra-Wideband Ranging (UWB) have the advantage of reducing the risk of interference with other systems, because of their very low-level background noise. Therefore, they have the ability to find indoor applications. In addition, UWB sensors can achieve a resolution as small as few millimetres as they are radio frequency based motion trackers (Welch, 2002).

Magnetic Sensing

Magnetic systems are a common method for tracking graphics interaction. They measure the local magnetic field vector using three orthogonally oriented magnetic sensors to estimate the position and orientation of the sensor unit with respect to the source unit. The position resolution in the radial direction from the source to the sensor will depend on the magnetic field strength; in other words, the separation distance from the source. The three advantages of magnetic sensors for human tracking are their size (small enough to be worn), no line-of-sight (magnetic fields pass right through the human body), and tracking of multiple sensors (e.g. one sensor attached per joint) (Welch, 2002).

2.6.2.3   *Motion Sensor Technology Application*

Head tracking for interactive graphics is the biggest challenge in motion tracking application. This is because humans have a lifetime of experience in perceiving our environment and interacting with physical objects (Welch, 2002). As a result, fooling the human senses can prove to be extremely challenging, requiring high accuracy and resolution, and low latency (Welch, 2002).

The main application of motion tracking can be found in virtual reality games (VR), flight or vehicle simulators. In these applications, a person is seated or standing in a pod at an arcade, wearing fully immersive gear. This allows the user to looks around and interact inside of a virtual world (Welch, 2002). These applications are seen as easier from a motion tracking perspective, as they do not require a large tracking area, high accuracy, or tracking of large numbers of objects (Welch, 2002).

Magnetic trackers are popular (and with good reason), as they can perform well at very close range, and they are cheaper and easier to use than other elaborate trackers (Welch, 2002). However, in applications in which the user does not have move around much, a

3DOF orientation tracker can suffice (Welch, 2002). Moreover, magnetic trackers may result in latency and distortion if in a metallic environment. Therefore, optical or inertial approaches are often preferred in these applications (Welch, 2002).

The following section presents some of the current applications of motion tracking technology.

Virtual Reality

In virtual reality (VR), a person's view of the real world is integrated into a virtual world. General requirements for VR are no nausea during simulation and the visual content of the simulation should be updated in real-time. Simulation of a worker's operation in the virtual environment can provide a visualisation to the worker performing the task and the interactions between the worker and virtual objects (Ma et al., 2008). Virtual reality systems in ergonomic studies are typically taken to generate virtual working environments, which can interact with the work with haptic interfaces and optical motion capture systems (Ma et al., 2008).

For example, in a virtual environment, an operator can have the same spatial feelings as working in the field. In addition, this virtual environment can be a copy of the current environment that the operator is working or it can equally be a new or redesigned area including new virtual objects (fixed or movable), working stations and machine tools (Ma et al., 2008; Welch, 2002).

Augmented Reality

The basic idea behind augmented reality (AR) is to use special equipment (such as HMD) to add 3D computer graphics to a person's view of the real world so that the virtual objects appear to coexist with physical objects (Welch, 2002). Compared with immersive VR, AR applications are typically sensitive to static and dynamic tracking errors, such as virtual objects that appear in the wrong location or are obvious when compared to static physical objects (Welch, 2002).

Full-Body Motion Capture

While VR and AR applications typically require precise position and orientation for a single target, full body motion capture requires a large number of targets (i.e. markers, sensors, or reference points). For example, in applications such as character animation, the position of the user's head is required through numerous markers. (Welch, 2002).

Virtual Production

Virtual Production is used for the planning of modern production lines (Schlette and Rossmann, 2009). It allows an easier evaluation of designs and scheduling schemes in order to provide an optimum layout and control for the final decision (Schlette and Rossmann, 2009). Virtual production was originally developed to provide tools for the programming and simulation of automated systems, such as industrial robots (Schlette and Rossmann, 2009). Thus, these simulations focused on technical elements of the process, while neglecting human factors, even for modern production lines that have working stations where materials and workpieces are handled, manipulated or monitored by hand (Schlette and Rossmann, 2009). However, virtual production has the advantage of providing in-depth concepts and technical validation through the simulation of the technical components in the production line (Schlette and Rossmann, 2009).

Haptic Feedback

Haptic feedback systems are used provide the user with the feeling of touching or grasping virtual objects. To simulate the user's feelings, the haptic feedback systems should include a high rate of interaction with the virtual objects so that the detected force feedbacks are calculated in real-time (Ma et al., 2008).

Virtual Human

Virtual humans represent the operators during the task. The representation of the human is then mapped into a virtual environment. The use of motion tracking data and the virtual environment can assist the worker to complete the task and can give the observer or assessor an overview of the worker's operation and performance (Ma et al., 2008). The virtual human allows a modelling of the skeleton and muscles to compute the force and dynamic of each muscle (Ma et al., 2008). The virtual human can be modelled from the worker or a database, but it is still necessary to adjust the model according to tracking data for each person, as mapping errors may be created (Ma et al., 2008).

2.6.3   Related Work

2.6.3.1   Example 1: Novice vs. Expert

S.N Min (Min et al., 2011) have worked on the effects of the presence and height of handrails in construction work, where back pain occurs most frequently. This will result in poor stability (of balance) of the worker, making them more vulnerable to accidents in the workplace. The authors concluded that the effects between the floor height and the level of

anxiety were higher for a novice at first floor, while the floor level did not affected experts. They also found that higher floor caused higher stiffness on back muscle for both the novice and experts. However, the novices were more affected than the experts, by higher stiffness. When more back muscles are used to help to maintain stability, this may lead to the worker becoming tired more easily, and possibly back pain due to the increased pressure on the spine (Min et al., 2011).

The result of their experiment shows that both experts and novices have higher psychological and physiological anxiety when the risk of falling down is increased. However, novices showed higher psychological and physiological anxiety than experts. Therefore, novices may be more exposed to higher risk in work delay or injuries, due to the increasing of psychological and physiological factor (e.g. anxiety) (Min et al., 2011).

On the other hand, it is recommended to carry out a complete safety education, management, supervision, work hour adjustment, enforcement of work in pairs, and train novices when assigned to a job with a high risk of incidents (Min et al., 2011).

2.6.3.2   *Example 2: Capture Worker's Posture*

Liang MA developed a framework, where a worker's operation needs are tracked and digitalised so that the positions of the worker's limbs are known, as well as tracking detailed motion, such as finger movements and overall posture (Ma et al., 2008). The authors claim to have re-designed the current techniques for ergonomic and biomechanical analysis to be suitable for computer analysis (Ma et al., 2008).

Three hardware systems were used to build a prototype to design the framework: virtual simulation system, motion capture system and haptic interfaces. The virtual simulation system consists of a graphic simulation module and display module computer graphic station (with a projection system) (Ma et al., 2008). The motion capture system was used to collect the real working data, such as capturing the operator movement (Ma et al., 2008). Markers are attached to each key joint of the human body. The evaluation module then assessed the different aspects of manual handling work based on different criteria (Ma et al., 2008).

In their framework, personal factors and external load history were also considered to evaluate the muscle fatigue. It can be easily used and integrated into simulation software for real-time evaluation, especially for dynamic working processes (Ma et al., 2008).

2.6.3.3   *Example 3: Design of a Virtual Human for Ergonomic Assessment*

In Christian Schlette and Jugen Rossmann's research, the Virtual Human consists of standard kinematic chains that are arranged and coupled to each other to approximate the degrees of freedom of the human body (Schlette and Rossmann, 2009). Through the simulation and animation of their Virtual Human, the analysis of the ergonomic conditions of a manual task at the workplace can be carried out (Schlette and Rossmann, 2009).

The Virtual Human presented by C. Schlette and J. Rossmann covers an approach to program, control and supervise anthropomorphic kinematics as a multi-agent system (MAS), where the each agent manages the motion of kinematic chains representing the limbs and the torso of the human body (Schlette and Rossmann, 2009).

2.6.3.4 Example 4: Evaluation of 3D sensor for Ergonomic Studies

Tilak Dutta (Dutta, 2012) evaluated the Microsoft Kinect as a portable 3-D motion capture system for ergonomic assessment. The Kinect's limitations can be minimised simply by using markers of appropriate size made from appropriate materials. The point of interest on the subject's body should be aligned with the centre of the coloured disc. Two Kinect sensors with orthogonal views can be integrated into the same system with minimal interference to the resulting depth image (Dutta, 2012).

Chapter 3 Research Approach

3.1 Introduction

Polishing processes can represent up to a third of the manufacturing time in some industries (Besari et al., 2010). Despite automated solutions developed in both the research domain (Section 2.5.1) and in industry (Section 2.5.2), there is still a need for further research. Solutions have mainly been aimed at replacing the entire polishing process and typically focus on specific components, such as turbine blades or mould dies.

It was concluded that existing solutions do not sufficiently study, capture or address the manual processes, nor the way the current processes are being carried out (see Sections 2 and 4). Consequently, there is a lack of trust among some businesses in using advanced technologies, such as robotics, to handle polishing processes. For these reasons, it was concluded that the design and implementation of an automated polishing system should be based on a thorough understanding of manual operations. This is the main hypothesis in this research. Learning from human and from manual processes is crucial in the development and integration of an automated system which has the right level of deployment of advanced technologies.

The research approach taken to investigate the hypothesis comprises: a) observation and experimentation with real industrial cases; b) understanding and capture of the process variables during multiple visits to the sites, and implementing an innovative device to extract quantitative data; c) performing further in-house experiments in a controlled environment; and finally d) developing and testing an automated polishing system based on the lesson learned from manual processes.

In this chapter, the selection of the research methodology is explained, followed by a proposed solution to tackle the capture of current manual processes, operation variables, the impact of human operators on the processes, and the new automated solution.

3.2 Research Methodology

There are many ways to conduct research, but only few ways to describe it. For example, research can be defined as a process to find answers to a problem (Hughes, 2005). Most research in engineering focuses on identifying output/outcomes, such as mechanical failure, by reducing plausible causes or using a set of variables (Borrego et al., 2009; Kowalczyk, 2015).

Several research approaches such as qualitative, quantitative, or mixed method could be used. However, the applications of these methods may differ by researcher and subject (e.g. social science or engineering) (Bryman, 2003).

Quantitative, qualitative and mixed research methodologies can be distinguished by how the research findings are collected and analysed. For example, quantitative research uses numbers and qualitative research uses a more descriptive style, and mixed research is somewhere in between (Borrego et al., 2009; Hughes, 2005; Kowalczyk, 2015)

In quantitative methods, figures and numerical values are used to test the research hypothesis and make predictions. This has the advantage of using statistical equations and formulas to ensure the precision of the results and find relationships not just with observations. By focusing on specific parameters and variables, this the scope is restricted to what is relevant. Also, bias introduced from the researcher's point of view and opinion is removed with the analysis of numbers (Kowalczyk, 2015). The other advantage of quantitative methods is that the research findings can be replicated with a larger sample size, to generalise the findings (Borrego et al., 2009).

In quantitative methods, data typically includes surveys, instruments, or statistical tools for analysis (Borrego et al., 2009). Data may also include interviews (if structured and analysed as quantitative) and non-numerical answer (if collected and categorised as numerical findings). The type of data collected will depend mainly on the hypothesis and research question. However, numerical data could be falsely presented and seen as facts and not as data (Hughes, 2005). Qualitative methods focus on the collection and analysis of textual data, such as surveys, interviews, focus groups, and observations, in which the study is carried out for events or a small group of persons or individuals. This method may be beneficial when the study focuses on depth rather than breadth. The main idea of qualitative method is to give a general picture or idea of what the researcher is seeing. However, it may create bias or subjectivity towards a researcher's point of view (Kowalczyk, 2015). In addition, statistical tools are difficult to use in this method as it is difficult to quantify the data collected. The research hypothesis or question typically questions what is occurring, why it occurs, and how it affects other phenomena While numbers may be used, most often the answers to these question require general or contextual descriptions (Borrego et al., 2009).

The decision of the methodology or approach for the research used will depend on the type of data collected or the stage in the research process (Borrego et al., 2009). Quantitative methods can be seen as more direct with results, and easier to be analysed and interpreted. However, qualitative methods are more open and responsive to the subject. Both types are correct and helpful and are not exclusive as it is possible to use both approaches in the same study (Hughes, 2005).

Mixed research methods are often described as the third research method after qualitative and quantitative. Creswell defined 'mixed methods' as a method involving the collection and data analysis of both qualitative and quantitative data in the same study. In addition, the data are collected concurrently or sequentially, giving priority to the integration of data at one or more stages of the research process (Borrego et al., 2009).

The mixed research method could also include an "Action Research" method. Action research is explained as "learning by doing" (Brydon-Miller et al., 2003). It is a problem-solving method using repetitive activities or manipulating variables to compare and reflect on the results before and after some experiments. It is considered a mixed approach because both quantitative and qualitative methods could be used to reflect the result of experiments. These may include many methods, such as case studies, lab experiments, interviews and surveys.

In this research approach, a combination of quantitative and qualitative methods were used to assist the cross-validation of data from multiple sources, as shown in Table 3.1. These sources include diagrams, case studies, action research, numerical data from instruments, observations, discussions and interviews with experts, and background research.

Table 3.1: Quantitative and qualitative methods used in this research

Quantitative Research	Qualitative Research
Diagrams	Expert Observation & Opinion
Case Study	Pictures and Videos
Action research (mainly quantitative)	Interviews and Discussions
Instruments	Background research & Literature Review

In the following section of this chapter, the research approach taken in this study is explained. Various research methods selected for different stages of this study are also identified.

3.3   Proposed Research Approach

The research aim and objectives are specified in Chapter 1. The main research hypothesis of this study was also described earlier in relation to the understanding and capture of manual polishing operations and, on that basis, developing an automated polishing system. To achieve these aims, a collaboration with an industrial company was initially established to facilitate elicitation of data for manual operations and industrial requirements. The manual processes were replicated within the research laboratory environment to continue extensive experiments and ultimately develop an intelligent automated polishing system.

Figure 3.1 illustrates the research approach taken in this study for the development of an Integrated Robotic Polishing System (IRPS) proposed by the author. This research is limited to the removal of material and defects for finishing processes (research scope) in manual operation and fully automated systems (proposed solution).

At stage 1 of this research, as shown in Figure 3.1, a study of manual polishing process was carried out in industry and in the research laboratory. Visits at a Small and Medium-sized Enterprise (SME) based in the East Midlands, were carried out to learn about manual polishing processes and to identify the potential need for automation. This collaboration included the collection of data through videos and interviews of skilled polishing experts at different stages of the process for three industrial parts (low, medium, and high batch volume). The process sequence is captured through videos, discussion and observation - in addition to business diagrams - to assess the current production rate and capabilities.

Further knowledge elicitation was carried out regarding the understanding of the manual polishing operations through design, build, and implementation of a special-purpose fixture used by skilled polishers (explained in Chapter 5). The fixture comprises a set of sensors to capture the forces and movements of a skilled human operator during manual polishing operations. A benchmark experiment was also carried out to evaluate and select the sensing technologies required to be integrated within the fixture.
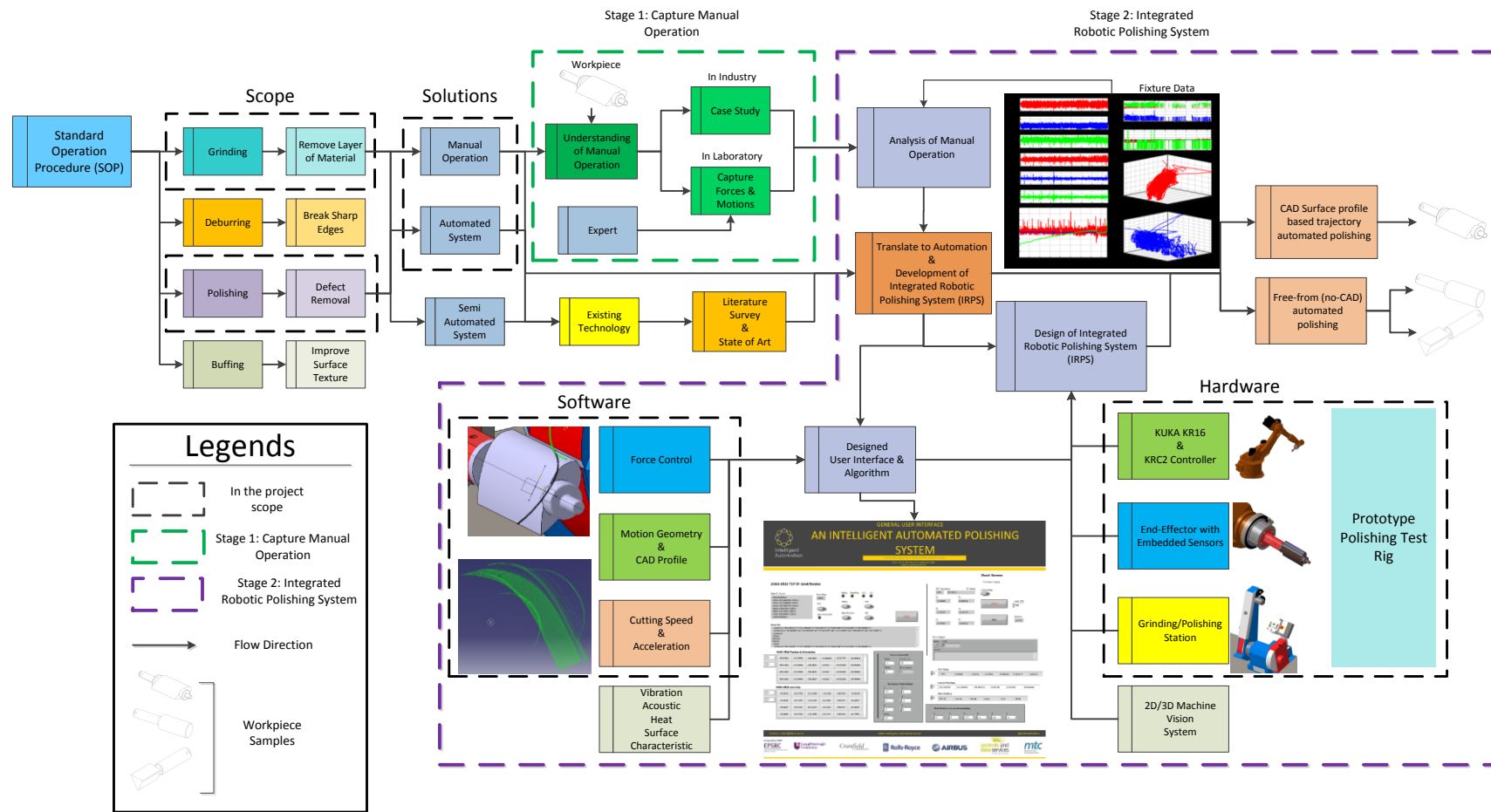
Figure 3.1: Research methodology diagram

In the experiments with the fixture (described in Chapter 6), the techniques and approaches of skilled operators are captured for the standard polishing operation procedure of industrial parts. The system variables initially deemed to be necessary to capture were:

- Operators' hand movements: Position and orientation of workpiece, the force applied during polishing, and speed used when removing a layer of material or defects.
- Polishing parameters: Monitoring forces, torques, vibration, and acceleration/feed rate.
- Workpiece geometries: Measuring profile and surface geometry of parts, locating and measuring defects and assessing the surface quality and texture before-during-after operations

Further system variables were identified such as vibration, temperature, and noise, but were decided to be considered for future research.

At stage 2 of this research, data collected at stage 1 are analysed and interpreted, leading to development of a proof of concept test rig and user interface for the proposed Integrated Robotic Polishing System. First the data collected with the fixture are analysed offline to identify patterns in the different techniques used by skilled operator. These data are also cross-referenced with data captured within industry. These data are then translated and implemented in a test rig for the development of the IRPS. The test rig is built from commercially available technologies (further discussed in Chapter 7).

The IRPS would be composed of robotic arm (KUKA KR16), to manipulate the workpiece using a predetermined tool path (from CAD/CAM software). A set of sensors, such as a multi-axial force and torque sensor, and 2D/3D machine vision system, would also be included within the robotic system to monitor and control the machining parameters. Finally, the polishing operation would be carried out on a dual-grinding and polishing station.

A user interface and algorithm was built for the test rigs using the aforementioned equipment. The multi-axial force and torque sensor would monitor and change the force applied to the workpiece surface. The robot motion would be based on the operator motion or CAD geometry of the profile to polish. However, in the current approach, the need for CAD should be eliminated, as the end-effector would follow the workpiece profile through the multi-axial force and torque sensor output. The feed rate and cutting speed would also be controlled by the multi-axial force and torque sensor or the accelerometer. The feed rate of the robotic arm should be changed based on the defect or feature to remove, for an optimal polishing process.

Machine vision is required for a fully-automated system to detect and locate the potential defects on the workpiece surface and assess the texture quality, as illustrated in Figure 3.1. For instance, a laser scanner may be used to measure the size of the defects, and evaluate the geometry of the workpiece profile. The measurement of the surface quality may be done in between each polishing pass or more frequently. These data would then be used to change the machining parameters, such as feed rate and trajectory. This would aim to

achieve a better surface quality in less time with the same flexibility as manual polishing. However, machine vision is beyond the scope of this research.

Other machining parameters such as the rotation speed of the abrasive tool, abrasive tool wear, vibration, noise, heat, and pass frequency are also beyond the scope of this research, but may be considered for further research.

The Integrated Robotic Polishing System developed (Chapter 7) was tested in multiple experiments. The experiments initially include imitating the way currently operators follow the profile of the workpiece, by following the CAD geometry, and finally real-time change in trajectory based on data received from the multi-axial force and torque sensor collected data in real-time. Further experiments would be carried out on free-form workpieces, with parts of unknown geometrical profile. This is to eliminate the necessity for CAD model data by following the profile of the workpiece based on the multi-axial force and torque sensor output. The second set of experiments also included multiple geometries (e.g. cylindrical and triangular) as a proof of concept for the IRPS.

3.4   Research Structure

This research is divided into two main stages with a comprehensive literature review to support each one, as illustrated in Figure 3.2. In stage 1, Chapters 4 to 6 of this thesis describe the collaboration with skilled operators, in both industry and local laboratory, and the development of a fixture to enable capture of the process variables. At stage 2, the development of the Integrated Robotic Polishing System (IRPS) is reported in Chapter 7 with detailed discussion on the development of the proof of concept test rig.
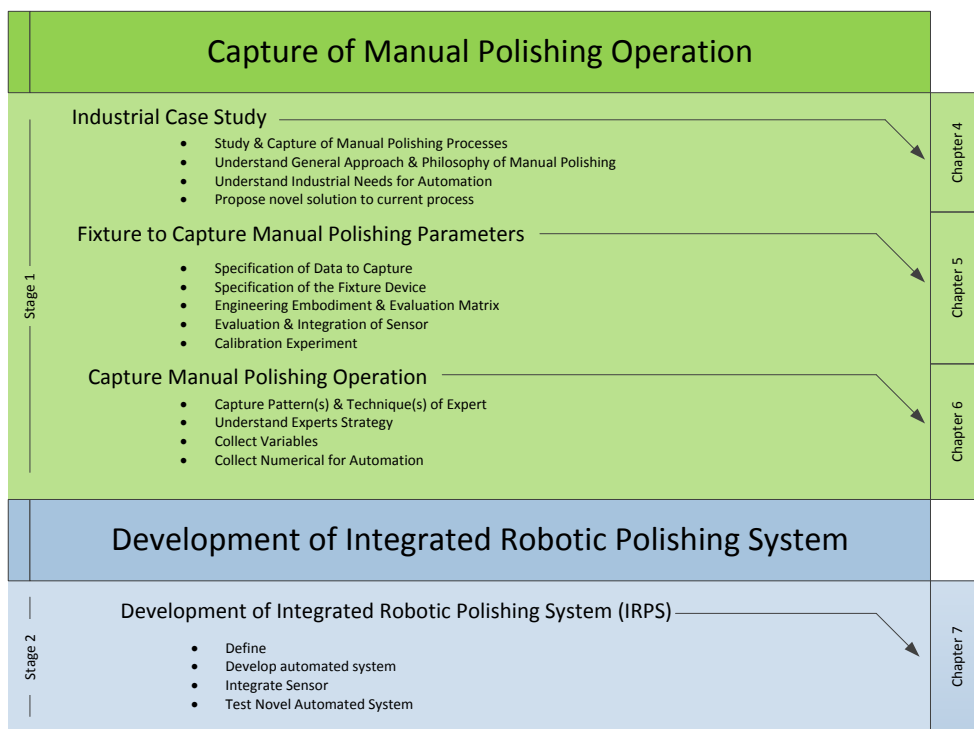
Figure 3.2: Structure of thesis

Chapter 4 Industrial Case Studies

4.1 Industrial Collaboration

As explained in Chapter 3, the first stage of the capturing and understanding of manual polishing operations was done in collaboration with an industrial partner. The company is a Small and Medium-sized Enterprise based in the East-Midlands (UK), which provides a wide range of finishing services for major companies, mainly in the aerospace and power generation industries. The company claims to be the leading company in finishing processes for aerofoil blades in terms of quality and service. Their current turnover is £1 million per year and they estimate this to grow to £4 million in the next few years.

The company specialises in manual finishing processes, but is looking to re-introduce automated technology within their processes. This company has tried to implement automated solutions in the past with unsatisfactory results. Automation was intended to achieve the projected production volume and to reduce their heavy reliance on skilled operators and training programmes.

According to the company, their automated system failed because it was not as fast and flexible as their skilled operators. For example, the system was not able to inspect the quality of the polishing surface and adapt the process parameters as quickly as their operators. Additionally, the specifications of the parts (e.g. form, geometry, size, defects, etc.) were too complex for the system. Hence, the company is not willing to fully eliminate their skilled workers through automation.

The following case study discussed in this chapter is a collaborative work between the company and this research, to analyse and support incremental implementation of a new automated solution, and to increase productivity and improve working environment for the current workforce. This collaboration also aims to provide a better understanding of manual polishing operation and finishing processes as a whole, and to define industrial need for automation, proposing novel solutions to improve the current process and to capture parameters and variables for the development of the proposed IRPS (see Chapters 3 and 7).

This collaboration included the collection of data through videos and interviews of skilled polishing experts at different stages of the process for three industrial parts (see Figure 4.1). The process sequences were captured through video, discussion and observation, and illustrated through a number of business diagrams to assess the current production processes, rate and capabilities.

Figure 4.1: Graphical representation of industrial parts under study (drawn by the author)

4.2 Current Processes and Environment

Figure 4.2 illustrates part of the company's layout of the workshop. This includes six sections: 1) A visual inspection cell where all batches are inspected manually at each stage of the finishing process by four operators 2) a main workshop where various parts (e.g. turbine blades, variable vanes, snubber blades) are finished manually by skilled operators using abrasive tools such as belts, wheels and mops 3)   an area for mass finishing for the deburring and cleaning of small components (automated barrelling has replaced abrasive blast finishing) 4) a small area for grinding and deburring of gas flow vents, where workers use hand-powered tools 5) a metrology area with two CMMs for the measurement of the gas flow vents, and finally 6) a grinding area for large and heavy components (i.e. steam blades).
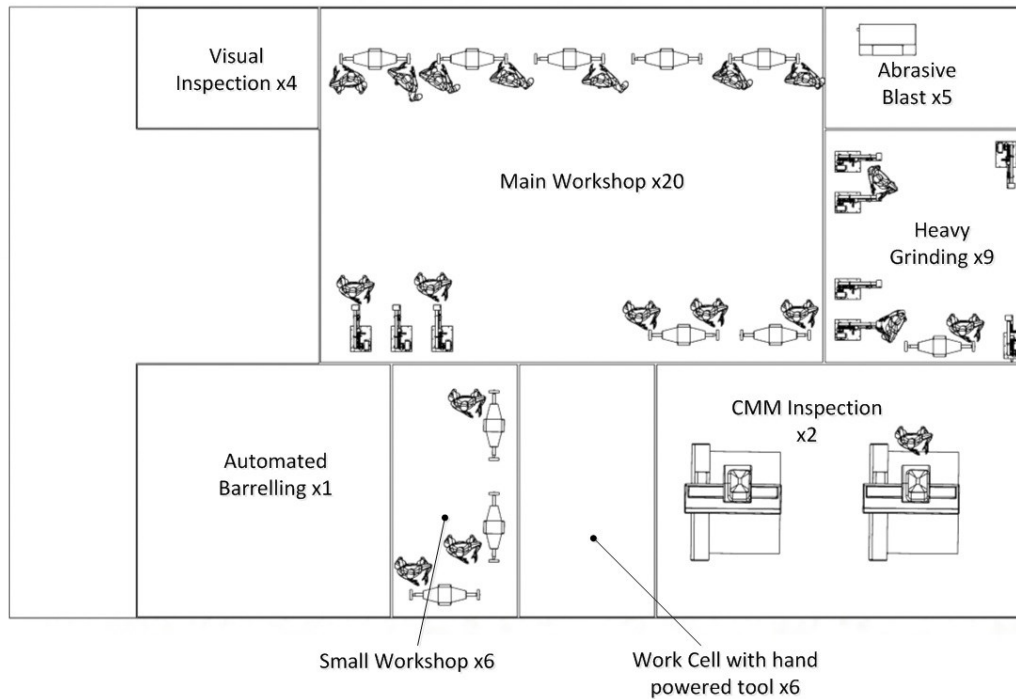
Figure 4.2: Company workshop floor layout (drawn by the author)

All operators are multi-skilled and flexible to adapt with the workload. For example, some operators may change task depending on the volume and demand. The production rate for each operator may go up to 2000 parts per shift. Also, the training of a new operator may take from several weeks to several months. The training typically requires the workshop manager over watching a new employee until being able to perform the task autonomously. The shift pattern varies based on production demand and could extend to 3 shifts if necessary.

From their current processes, the company believes that the grinding operation of large components is their main problem, as the vibration produced during the operation is severely affecting the operators. Many operators suffer from vibration white finger or related muscular skeleton disorders (MSD) after 2 years of work. Consequently, the operator must be moved to a different part of the finishing process, due to the loss of dexterity and sensation in the operator's hands. To comply with health and safety regulations, each operator is required to take frequent breaks, which clearly has a significant impact on the company's productivity.

The shop floor workers are paid per part, and they mainly comprise independent contractors with flexible shift patterns. A typical shift starts at 6.00 am and finishes at 2.30 pm with regular breaks. However, the work in their current process is not sequential, as each operator mainly works on one component (carrying out the whole finishing process or focusing at a specific stage). Also, the re-work of parts (marked by an operator from the visual inspection) is carried out by the same operator. Depending on demand, some operators may work on multiple types of parts or processes.

The company uses the same approach and standard operating procedure (e.g. rough grinding then fine polishing) for all of their finishing processes. Therefore, the variation in workpieces (such as size and geometry) does not significantly affect the production time and cost.

The production rate per operator depends on the component to finish and the skill level. Each part has a different batch size and number of required tasks. Therefore, each operator is paid differently. For example, the operators working on medium sized compressor blades are paid £5.00 per part, while the operators carrying out the root radius operation of small turbine blades are paid only £0.50 per part. The production rate of small blades is from 180 to 240 per day depending on the operator, while operators working on double snubber blades produce 24 parts per day on average. In total, the company finishes approximately 1500 to 2000 parts a day from all ranges and types.

The company is working primarily with aerospace and power industries, which provides 75% of the workload. As their main client validates the standard operation procedure for their components, and allows a limit of up to 8% of scrap for each batch. In 2012, the SME's highly skilled operators had a 2% rate of part rejection. However, their client may sometimes not inform them of the percentage of part rejected from batches. Therefore, the lack of communication between them and their client prevented more precise data and follow-up on the quality of service provided.

According to the quality manager, the minimum number of operators needed in each area are: two on centrifugal barrelling; five on the plate form preparation; four on flush-cosmetics after centrifugal barrelling; six to eight on root radius; six on the variable vane all over polish; and two on medium compressor blades.

4.3   Manual Finishing Processes – The Case Study

Components 1, 2, and 3[1] are the three main workpieces finished by the company. Due to their geometrical complexity and low, medium and large batch volumes respectively, these parts were selected for the research case study. The following sections are presenting the current processes for these three components. To capture the current process, it was essential to be on the workshop floor and document the process. The documentation of each process includes SOP (Standard Operating Procedure), HTA (Hierarchical Task Analysis), activity diagrams, videos and pictures, and discussion with different employees. Full documentation could not be provided by the company, which resulted in some data missing in the planning and SOP of the processes. However, a general understanding could be extrapolated from the collected data.

---

[1] The name of the industrial components had to be removed due to confidentiality.

4.3.1   Component 1

According to the SME, component 1 (Figure 4.3) is their most difficult workpiece to finish. This is due to its complex geometry which has a spiral concave and convex surface with two concave wings on each side. Two specialised operators carry out the entire finishing process.
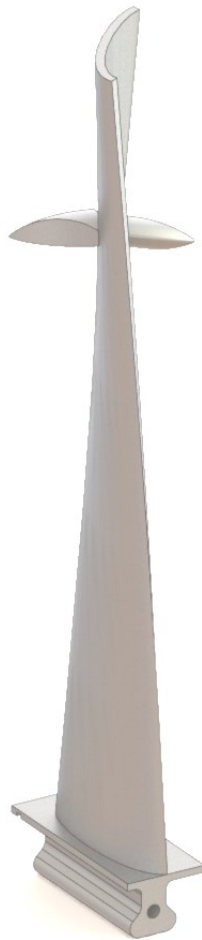
Figure 4.3: Geometrical representation of component 1 (drawn by the author)
Due to the commercial sensitivity of the case study, the actual parts are not shown

Figures 4.4 to 4.7 illustrate the complete finishing process captured during multiple visits. It is important to note that the complete SOP could not be provided. Therefore, the SOP illustrated by Figure 4.4 is based on the data collected below and shown in Figures 4.5 to 4.7.

Two operators at the company finish 48 pieces a day (24 each), from first grinding to final polishing, whereas an operator at their main client would only produce 20 a week. It takes 10 minutes on average to finish one part. The entire finishing process must be completed before all parts are inspected in the visual inspection cell. On average, 80% of the parts need re-work because of defects and marks left by the operators. Therefore, every batch

will have to go back and forth between the workshop and the visual inspection cell a number of times. This may be due to human error, complexity of the task, the volume of production, and the time spent per part.
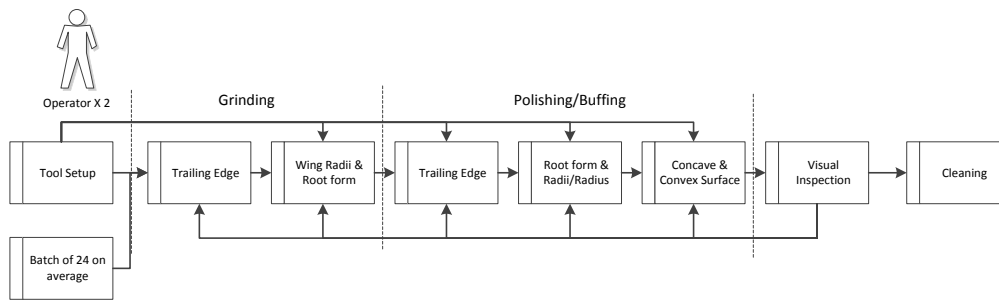
Figure 4.4: Component 1 standard operation procedure (drawn by the author)

From the HTA, it is noted that each workpiece is completed in 18 stages. In each stage, the operator is focusing on a different part of the process (e.g. trailing edges or root radii). At each stage, the finishing tool is changed, for instance from a high grit grinding disk to a soft mop. Each grinding disk is reshaped manually by the operator. By doing this, the operator modifies the disk geometry to fit the profile or geometry of the workpiece (e.g. a wing section). Moreover, most of the finishing tools are made and reconditioned in-house. The reconditioning of each tool is done by applying a layer of one of three types of abrasive grain and leaving them to bake in an oven overnight.

Figure 4.5 to Figure 4.7 illustrate the complete finishing process captured for this component. The operators start the finishing process by the grinding operation of the leading edge and trailing edge of the blade, the radii of the wing, and the concave/convex section around the wings. This initial stage of the finishing process focuses on and around the wings, and on and around root radius, as they are the most delicate sections of the workpiece.

After focusing around the wings, the operators grind and polish the various radius, root-forms, small edges, and wings of the workpiece. Then, the operators continue to polish the wing sections and radii/radius and around these sections, with a set of abrasive disks and mops.

The root form and radii are then mopped with a buffing wheel or mop disk with polishing paste to improve the surface aspect quality. The concave and convex surfaces are then mopped with the trailing edges. It was noted that the grinding and first polishing operations of the concave and convex surfaces of the part are carried out incrementally from the previous operations (i.e. trailing edge or wing section).

Lastly, the operators apply a final polishing to some geometrical features (e.g. radius, root form, around wings, trailing and leading edge). Before sending the entire batch to visual inspection, the operators must clean all parts using a spray compound and a cloth.

In the visual inspection cell, each part is inspected manually by a skilled worker. They inspect the parts for marks and defects and assess the quality of the surface aspect. When a defect is found (e.g. pitting, scratches, or flats), the part is marked for re-work. The re-work

process is done by the same operator, who will polish the part again but only where it is marked. It is interesting to note that every operator has their own work "signature", where the defects and marks left are consistent and recognisable.

No difference in the finishing procedure was noted between each operator. Moreover, each step was carried out with precision and each operator followed the shape of the surface or feature that was finished, while applying a constant force (which could not be measured at this stage of the research).

The following activity diagrams, which have been generated by the author (Figures 4.5 to 4.7) are illustrating the finishing procedure of component 1 described above.
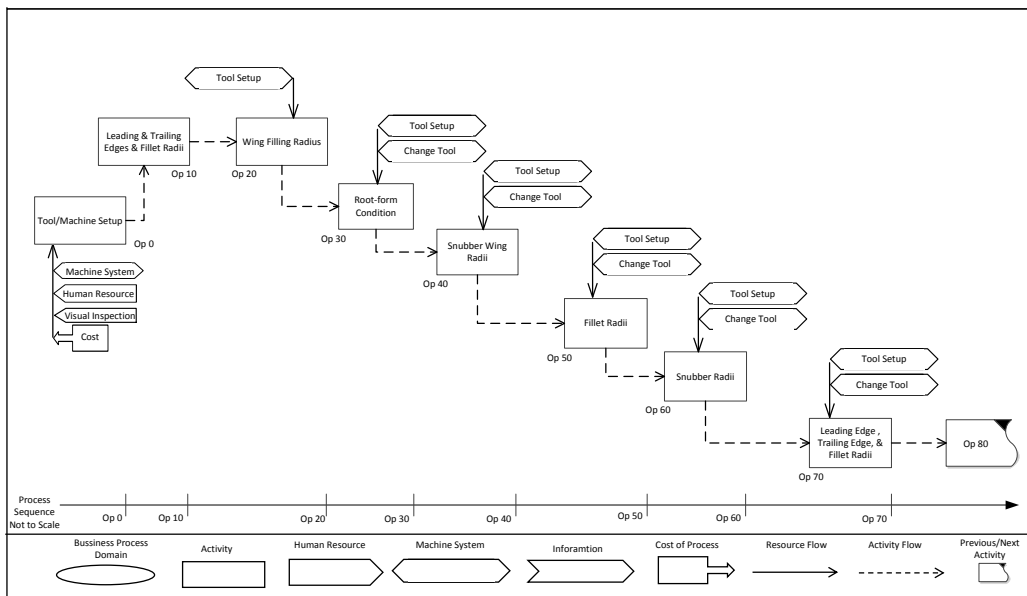
Figure 4.5: Component 1 process diagram 1 of 3 (drawn by the author)
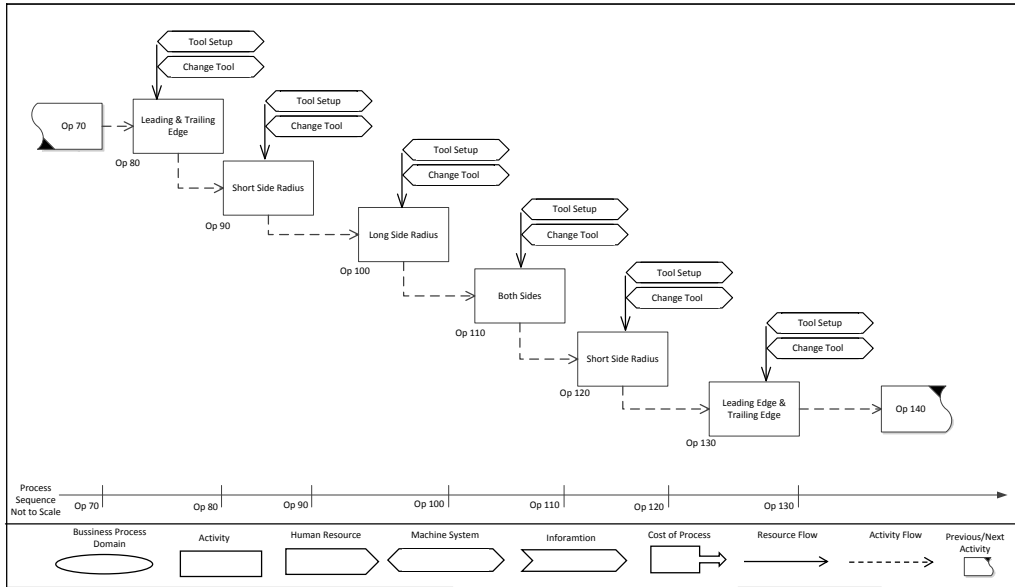
Figure 4.6: Component 1 process diagram 2 of 3 (drawn by the author)
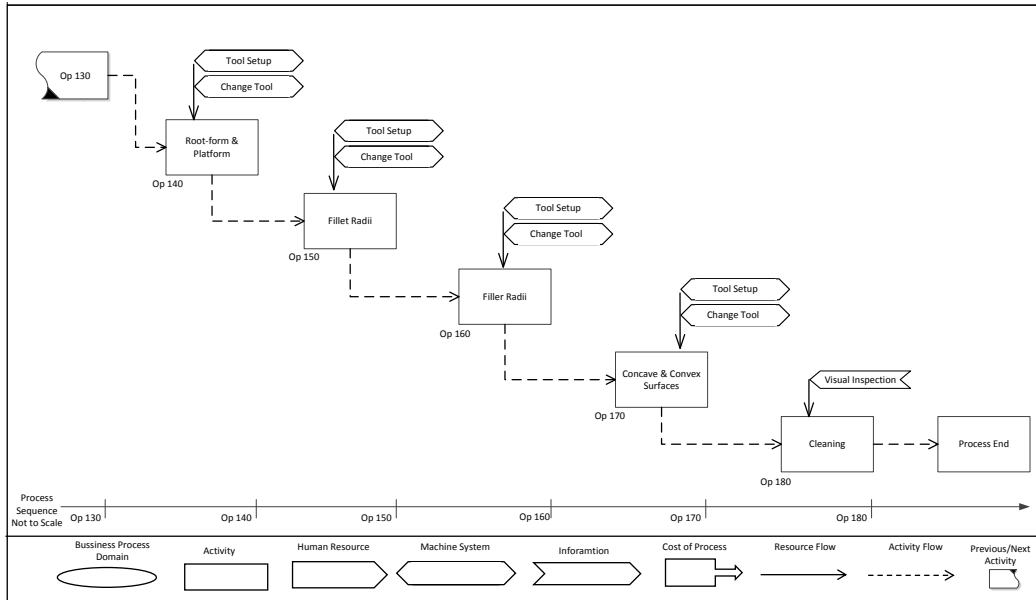
Figure 4.7: Component 1 process diagram 3 of 3 (drawn by the author)

4.3.2 Component 2

The component 2 (Figure 4.8) is the second part considered in this case study with a fully-manual finishing process. The part comes with studs placed at the closed ends, and features concave and convex surfaces on the blade. The company is currently able to produce 500 to 600 of these components per week. Figure 4.9 and Figure 4.10 present the detailed process required to finish component 2, developed as part of this research.
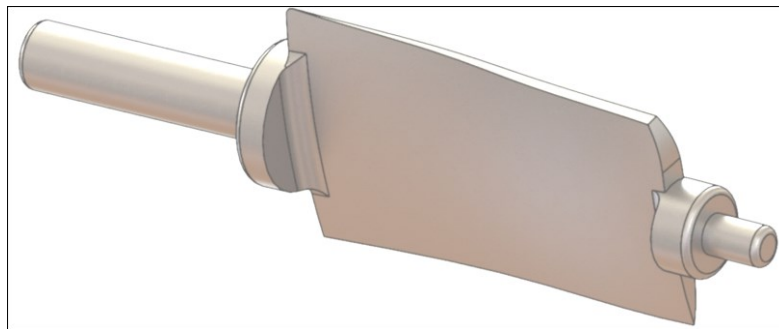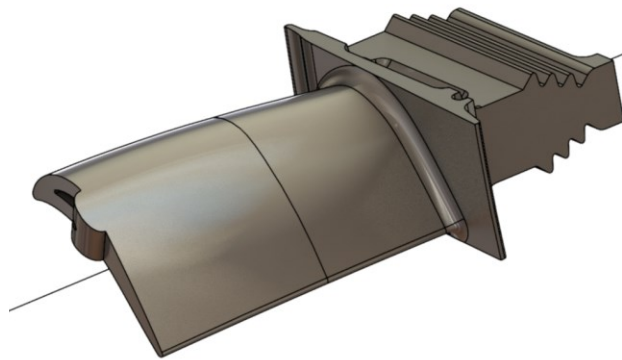

Figure 4.8: Geometrical representation of component 2 (drawn by the author)
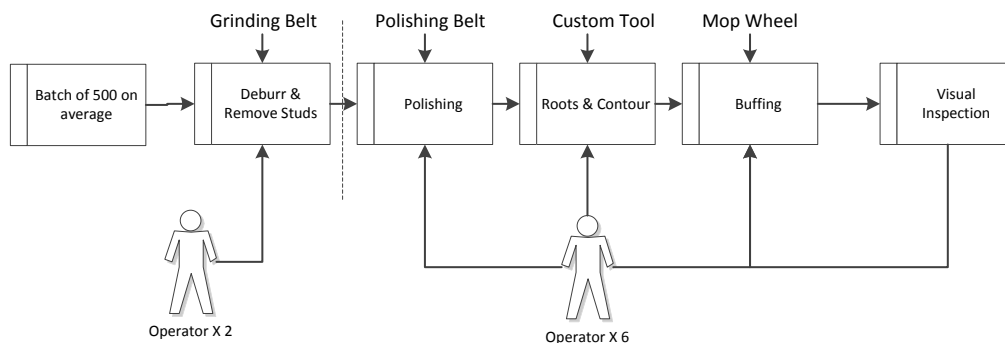
Figure 4.9: Standard operation procedure of component 2 (drawn by the author)

From Figure 4.9 to Figure 4.10 and the data captured, the finishing operation procedure for the component 2 can be described as follows.

Two operators start by performing the deburring and removal of studs on the edges of the blade. It was noted that the grinding belt used for this operation must be changed every 20 parts. Each part takes an average of 37 seconds to be finished at this stage of the process. Studs and burrs are usually removed in one pass, which requires a high force.
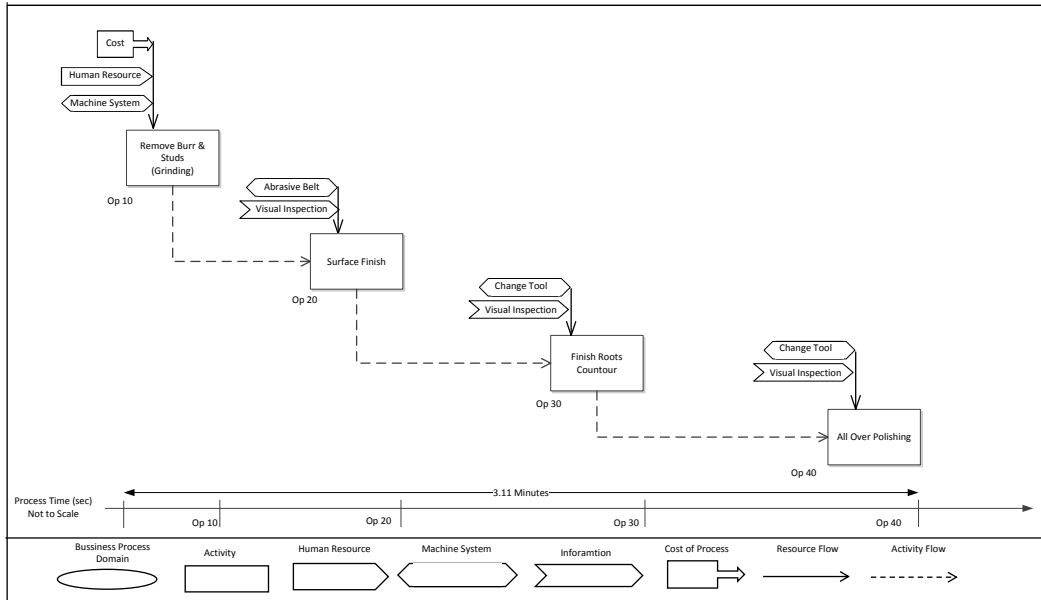
Figure 4.10: Component 2 process diagram (drawn by the author)

The principal health issue with this stage of the finishing process is that the force applied by the operator - and the vibration generated to remove such a large layer of material (5 mm) in a single pass - can cause serious harm, such as vibration white finger disease.

The parts are then sent for further finishing operation in the small workshop (see Figure 4.2). Five to six people carry out the rest of the finishing process; each operator can produce from 75 to 120 pieces per day, depending on skill and experience.

An abrasive belt is first used to polish the concave and convex surfaces of the part. This operation takes 60 second per part on average. Then another operator uses a custom abrasive tool to polish the roots and contours. This operation typically takes an average of 14 seconds. The final finishing operation of the concave and convex surface is carried out into two stages. A first rough polishing is applied followed by a finer polishing. Each stage takes 30 seconds on average. The whole process, including the change and calibration of the abrasive tool, takes 3.11 minutes on average.

Finally, the parts are passed through to the visual inspection cell. In case of re-work, the parts are returned to the operators for further finishing.

4.3.3   Component 3

The final component considered in this case study is component 3. The finishing process is composed of manual finishing, automated finishing through mass finishing, CMM measurement, and additional machining operation(s) by the company's clients. On average, 40,000 to 45,000 parts are finished monthly by the SME. It is interesting to note that, since the introduction of mass finishing technology (e.g. automated barrelling) in their processes, the volume of production has doubled for this workpiece. Due to the volume of production, this component arrives at the company's workshop in batches of 540 and they complete between 1200 to 1500 parts a day.

Figure 4.11: Geometrical representation of component 3 (drawn by the author)
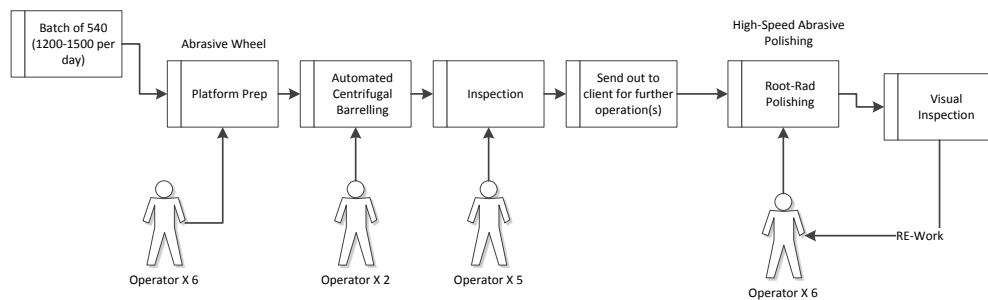
Figure 4.12: Standard operation procedure for component 3 (drawn by the author)

The finishing process starts with the polishing of platform and roots (platform prep), where six operators each produce 180 to 240 parts a day on average. The main requirement of the root operation is to polish the root and the aerofoil without exceeding 2 mm above the radius. To complete this operation, two different tools are needed for one part. The operators must change tool every 15 parts.

The second stage of the process is to send the parts to the automated barrelling cell for cleaning, de-burring, and improvement of the surface roughness and texture. The main advantage of mass finishing process is that; it is able to polish 540 parts in a single cycle of 3 hours. Two operators work on the centrifugal barrelling machine and another five inspect each part and mark them for rework if necessary.

The final stage of the finishing process is the cosmetic polishing. The cosmetic polishing is only carried out after automated barrelling and before being sent back to their client for further machining operation. Cosmetic polishing consists of polishing the aerofoil and the roots on a high-speed polishing machine. The operations take 14 and 17 seconds respectively. An operator produces 250 parts a day on average.

Further root-rad and aerofoil polishing is carried out after receiving the batch back from their client. On average, these processes take 30 seconds for the root-rad and 48 seconds for the aerofoil.

The complete manual process of component 3 takes 4.32 minutes per part, including the change and setup of each finishing tool.

Finally, the parts are sent to the visual inspection cell. On average, it takes 10 seconds per part to be inspected by one operator (team of six) and the volume scrap for re-work is around 50%-60%.
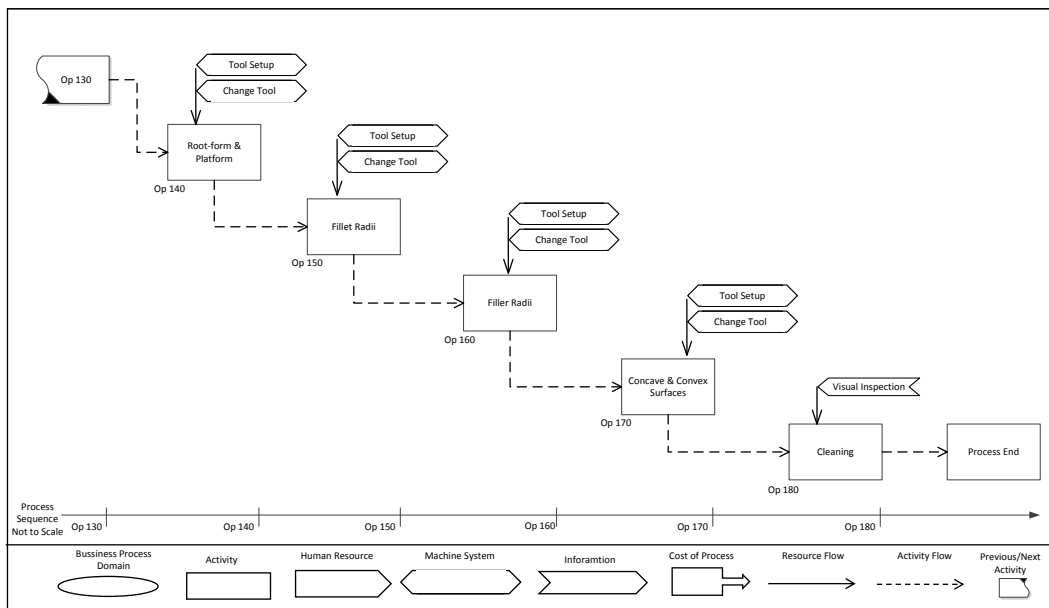
Figure 4.13: Component 3 process diagram (drawn by the author)
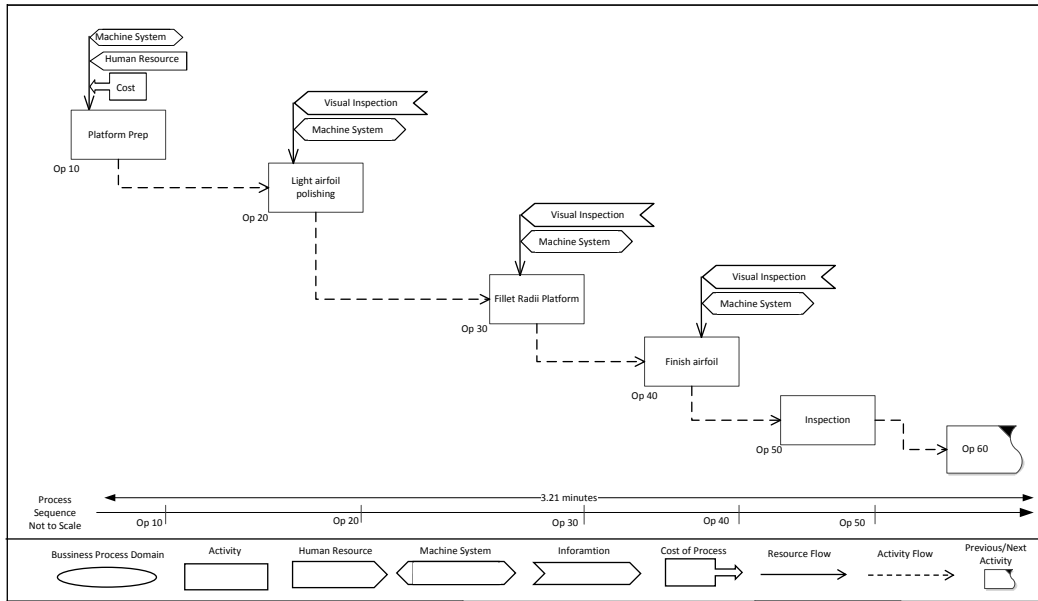
Figure 4.14: Component 3 process diagram (drawn by the author)

4.4 Analysis of the Current Processes

4.4.1 Common and unique aspects of the finishing processes

This collaboration has provided useful information for the capture of manual polishing processes, and a better understanding of entire finishing processes in industry.

The captured processes from this company showed a number of similarities in finishing operations for all three parts under study. The sequence of each process starts with a coarse grinding or polishing and ends with a finer polishing or buffing. Some of the common aspects of the finishing processes are identified as trailing edges, leading edges, root-rad, radii, radius, and convex and concave surfaces.

Based on the observations and data analysis, it was also noted that every process includes multiple small operations using a specific tool (commercial or custom-built) with a short tool life, multiple visual inspections, and re-work (depending on the workpiece).

In addition to the current processes, some of the approaches and habits of the operators were captured. For example, during training, a new operator is told to "keep the flow". This means that the operator needs to follow the profile of the part until the surface quality is satisfactory or all defects are removed. Also, some of the operators leave their own 'signature' marks or defects on the workpiece. However, all operators are flexible and can work on multiple components or processes.

The principle issues found during the visits and following the analysis of the data collected are 1) the health and safety, as some operations can severely injure the operator, and 2) the tooling cost, arising from custom-built tools, short abrasive wear and multiple tools for multiple operations.

To date, the current processes meet the required volume of production. However, mass finishing technology, such as automated barrelling, has proven to be an effective solution to enable the company to cope with the current demand. Nevertheless, the projected increase in production volume in the next few years is the main drive for the company management team to seek alternative automated solutions to increase productivity while improving the working environment for the workforce.

4.4.2   Potential Automated Solutions

Following the completion of the data capture at the collaborator's site, an intense data analysis, and business feasibility study were carried out to design, formulate and optimise new finishing cells using both automated and manual polishing operations. Different automated solutions were investigated and draft proposals were discussed with the industrial partners.

The main criteria when proposing an automation polishing system should include: a) taking advantage of similarity of processes between main parts (i.e. components 2 and 3) to improve productivity; b) improving the working environment for the workforce by assigning heavy, dangerous, and repetitive tasks to the automated system (i.e. robots); and c) maintain the skilled labour for more delicate and complicated processes, to preserve the know-how and skill set of the manual operators and reduce the initial automation investment cost.

Initially, both commercial and research-based solutions available at the time were studied, as summarised below.

Commercial Solutions 1: RJH Finishing WALLABY Rise & Fall Grinder

At one end of the automated technology spectrum, RJH Finishing has developed a system (WALLABY Rise & Fall Grinder (RJH, 2014) that integrates an abrasive belt and a 2-axis table (*x-y*) for grinding and deburring operations. The system can be programmed by an operator or operated manually. Additionally, a jig or fixture may be mounted on the table to add more degrees of freedom. According to the manufacturer, their system is able to remove heavy burrs from multiple workpieces in a single pass.

Figure 4.15 illustrates the WALLABY Rise and Fall Grinder system operated by a skilled worker to remove heavy burrs on multiple parts (mounted on a fixture). Five parts are attached to a jig, which is mounted onto the 2-axis table. The operator can programme or manually move the table to remove the burrs.

For a more cost-effective solution, a similar system could be developed for the SME. It was proposed that the system could use jigs or fixtures to mount one or several parts, such as variable vanes. Then an operator may manually or automatically operate the system to remove heavy burrs, studs or any thick layer of material.

It was envisioned that such a system could potentially improve the health and safety issues in the company, however, it would not have improved the productivity to the level that meets the future increased demand.

Figure 4.15: RJH Finishing WALLABY Rise & Fall Grinder

Commercial Solutions 2: Vulcan Europe VTS Machine

At the other end of the automated technology spectrum, suppliers of teleoperation systems - such as Vulcan Engineering (Vulcan Engineering, 2015), offer a remotely controlled robotic grinding and polishing systems with or without haptic feedback. The process would still require manual operators to perform the tasks; however, there will be no direct contact between the parts and the operators.

A number of commercial solutions for teleoperation systems (such as robot controlled manually or human-robot collaboration) and feedback systems already exist (Chotiprayanakul et al., 2012; Nagata et al., 2001; Nakajima et al., 2004) Vulcan Engineering has developed a semi-automated system using robotic and haptic feedback technology for deburring and the grinding of heavy foundry components (Vulcan Engineering, 2015). This system integrates technologies developed by Vulcan Engineering, KUKA GmbH, and Force Dimension using a haptic feedback controller and a robotic arm offering three operational modes. Mode 1 is a fully manually-controlled system including real-time force feedbacks to control all parameters of movements for maximum material removal. Mode 2 is a semi-automated option where the operator has programmed it manually. This mode is mainly used for grinding operations over local areas and the system will perform the task until the routine is completed. Mode 3 is fully automated, using referenced located positions for repeated operation.

The investigated system, as shown in Figure 4.16, includes a robotic cell (KUKA 6 DoF robotic arm) with a haptic feedback controller (Omega 3DoF), a standard joystick, a cabin

for the operator, and software to monitor and calibrate the system. The manufacturer estimates the cost of such a solution to be between £460,000 and £830,000. The VTS machine system is primarily used for the heavy grinding and deburring operation of large foundry components.

Figure 4.16 illustrates the VTS Machine system in use by a skilled operator for heavy deburring and grinding operation of a large foundry component. As part of the feasibility study, this solution was identified as unsuitable and not cost-effective for the SME due to its significant initial investment cost and the immaturity of the haptic technology for a robust industrial production.

Figure 4.16: VTS Machine

Research Solution – Haptic feedback polishing system

Haptic feedback devices have recently been introduced to several fields, from medical (e.g. delicate surgical operations) to general customer devices (e.g. video games, mobile phones, etc.). However, industrial and machining applications are still mainly carried out in research laboratories. Some solutions have shown the use of such technology for the grinding of very large components (e.g. boat shell, heavy foundry) as described above.

Significant research is carried out by various research groups to improve the responsiveness of the haptic system to enable its integration with manufacturing systems such as polishing devices. A benchmark study (Harders et al., 2006) has been carried out indicating the strength and weakness of this technology in different application domains. In brief, it advises that if high force feedback is required, high precision would be sacrificed and the device would be stiffer and have a higher friction and inertia value. Vice versa, if delicate and precise movements are required, a low friction and low inertia device should be chosen.

It was suggested in this research that a haptic mechanism could potentially be developed upon the existing commercial systems to be customised for polishing small components at

the company. However, to improve the performance of such a system, a set of smart sensors would be required to process the feedback signals in near real-time. Figure 4.17 illustrates a proposed haptic feedback polishing system that may be developed for grinding and polishing operations of industrial components, similar to the work carried out by the company. This solution would include a robotic arm (to hold the part) and a haptic feedback controller operated by a skilled worker.

For example, such a system could assist operators in removing heavy marks or a thick layer of material in grinding operations of components 1 and 2: the skilled operator would receive force or vibration feedback at a level that does not risk long term injury. In addition, it could be also imagined that the system would help the operator's decision-making through the haptic feedback controller or virtual environment.

The key benefits of such a system would be to improve the health and safety of the operators and to reduce training time.
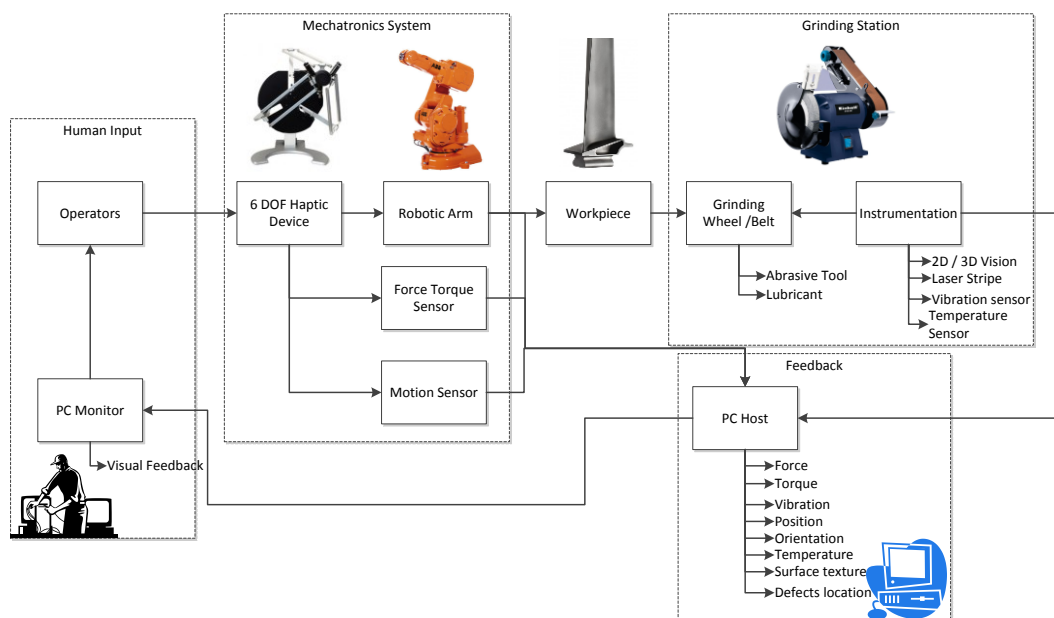
Figure 4.17: Diagram of semi-automated solution for research project

Research Solution – IRPS

The second research-based solution developed in this project and proposed to the industrial partner is the development of the IRPS (Integrated Robotic Polishing System) presented in Chapter 7.

In brief, by adopting this solution, the polishing processes would be divided into manual (for extremely fast and delicate processes) and automated processes using a controlled robotic grinding and polishing system based on current manual operations.

The proposed flexible cell, illustrated in Figure 4.18, would integrate a robotic cell to carry out laborious or challenging tasks such as root-rad or heavy grinding of two components (2 and 3). Manual operation would be reserved for more complex and skilled tasks, such as cosmetic polishing or removal of light defects, and would still be carried out manually by the company's skilled workers.

Automated Finishing Area

Abrasive Belt 1

Robotic Arm

Abrasive Belt 2

Material Removal – Machining marks removal – all over polishing – defects removal

Inspection Cell

Locate Defects – assess quality of surface – Marking for Re-work

Final Inspection & Shipping

Manual Finishing Area

Bench Grinder 3

Bench Grinder 4

Bench Grinder 5

Defects removal – fine polishing – radii – re-work

Mass Finishing

De-burring – De-scaling – Cleaning – Fine Polishing

Figure 4.18: Example of finishing process using automated technology within current process

In addition, the company would continue to use the automated barrelling machine to clean, deburr, de-flash, and improve the surface aspect of multiple components. An inspection cell, using manual visual inspection and automated inspection, could also be used to assess each workpiece individually, before further finishing, re-work, or shipping to clients.

The layout of the flexible finishing cell would include:

- Robotic cell, for the grinding and rough polishing operation.
- Mass finishing, for deburring, cleaning, de-scaling, and fine polishing.
- Inspection cell, for the automated defects inspection of the robotic cell, and manual visual inspection of each batch.
- Manual Finishing, to carry out further finishing operation and re-work.

Benefits of such a system would be to reduce the whole finishing time, reduce the workload of the manual process, increase productivity, improve health and safety, and increase capacity for the future business expansion.

However, such a system requires research on the development of a robotic system that interacts with the workpiece and the polishing tool in real-time and reconfigures its trajectory and the cutting parameters based on the techniques learned from manual operations. This constitutes the main objective of this project and will be discussed in the following chapters.

Chapter 5 Enabling Capture of Manual Polishing Parameters

As described in Section 2.6, software engineering techniques such as CAD or PLM platforms (Annarumma et al., 2008; Chang and Wang, 2007; Määttä, 2007) are used to analyse the manual operation procedure in order to obtain the task specifications for the development of an automatic solution. Ergonomists and manufacturing engineers collect data from various processes to organize the full production. In particular, manual jobs are a central element of planning and control the supply chain (C. E. Siemieniuch and Sinclair, 1995). For example, in addition to surveys, mechanical or electronic sensors could be used for a clear analysis of the manufacturing process (Schenk et al., 2011).

To the author's knowledge, the collection of data from skilled operators in manual polishing processes, considered in this research, has not been done before. As mentioned in the research hypothesis (Section 1.1), it is important to understand how the manual process is carried out to influence the development of the novel automated polishing system. For this purpose, a fixture was developed to enable the capture of data and knowledge from skilled operators, such as individual techniques and polishing habits, patterns, forces and torques, speed, feed rate, and various other parameters that were outside the scope of this research.

In this chapter, the development, testing, and calibration of the fixture are presented.

5.1   Specifications

Standard polishing operations of industrial parts are mainly carried out manually by skilled workers. In standard operating procedure (see Chapter 4), the operator holds the workpiece and pushes it against an abrasive belt or wheel to remove defects or improve the surface texture (as shown in Figures 5.1 and 5.2). The quality of the surface finish and the polishing time may vary from operator to operator and from job to job.
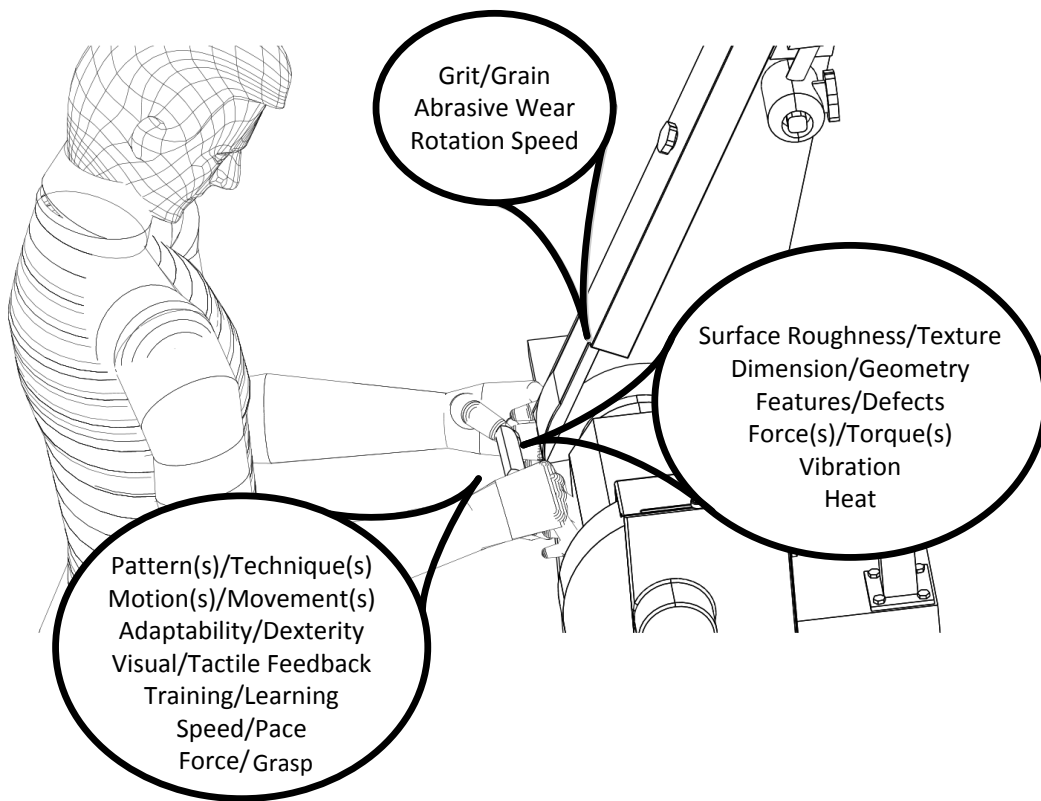
Figure 5.1: Parameters and variables involved in manual polishing processes
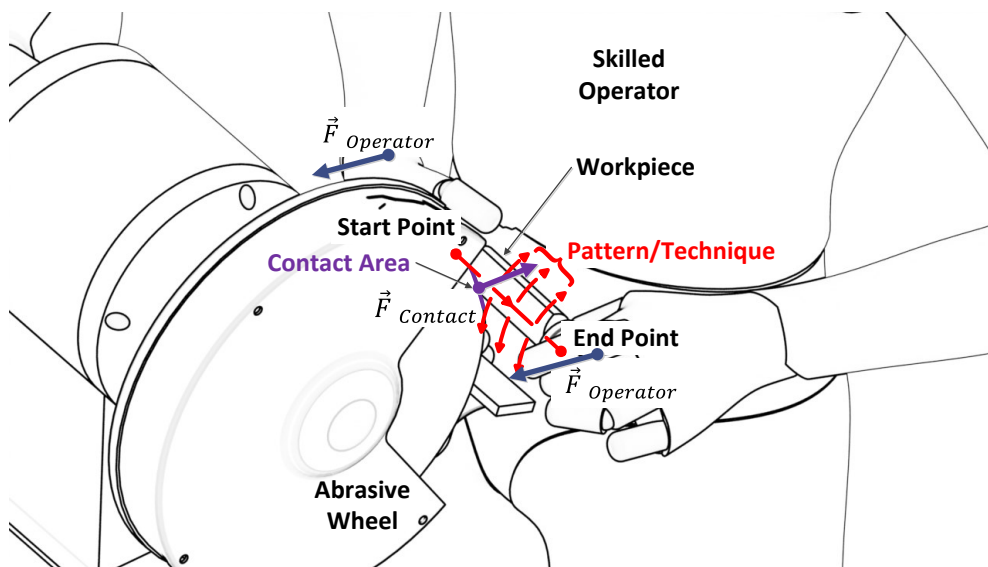
Figure 5.2: Parameters under study

The quality of the process is monitored visually by the operator, often after each or several passes (depending on the operator), to locate any remaining defects or assess the surface quality. The operator adjusts machining parameters accordingly in real-time through visual inspection and tactile feedback. This approach is repeated by the operator until the quality is satisfactory.

As illustrated in Figures 5.1 to 5.3, manual polishing processes involve a great number of parameters and variables. Some of the variables include: the contact force between the part and abrasive tool used to remove defects or layer of material; the motion speed of each polishing action; the machining path or operator movement; and the assessment of the quality and geometry of the part. Other variables such as vibration, heat, noise, abrasive wear, and hand grasp may be considered but are beyond the scope of this research.

In addition to the machining parameters and operation variables, the other objectives of this experiment are to answer the following questions:

☞ *What are the operator techniques or unwritten rules of manual operation?*

For instance, in Standard Operating Procedure (see Chapter 4), skilled operators follow the profile or form of the part (i.e. keep the flow). This is to avoid altering the part geometry and dimension, only modifying the surface texture. Skilled operators may also apply more force or carry out the operation longer in order to remove defects or improve surface aspect.

☞ *What variables should be identified?*

The reason for the capture of manual polishing parameters was to identify key variables and to answer the following questions:

- ✓ How many passes are carried out before the assessment of the workpiece surface?
- ✓ Do all operators follow the same pattern or approach?
- ✓ Is more force required when removing a defect, or are more passes?
- ✓ What is the polishing time per part?
- ✓ Does the speed or feed rate have an impact on removal of a defect?
- ✓ How do operators cope with the tangential force created by the rotation of the wheel?

Currently, the capture of the operator technique(s) in this research is limited to the general approach (i.e. patterns and techniques) and force used during the manual polishing operation of an industrial component. To enable this, a series of sensors were embedded into the fixture, as described in the following section.

5.2 Sensor Integration

A set of sensors were embedded into the fixture. The fixture also comprised a sample workpiece for the operator to polish as according to standard operating procedure. The measurement devices embedded within the fixture and the main parameters captured are illustrated in Figure 5.3 and are described below:

A. Force and torque generated from the polishing operation were captured using a multi-axial force torque sensor (Shunk Gamma (Automation, 2013)). The sensor was able to output three forces (Fx, Fy, Fz) and three torques (Tx, Ty, Tz) in real-time.

B. The operator's movements and patterns were captured using a Vicon motion capture system (Fern'ndez-Baena et al., 2012). Reflective markers were placed on the fixture to be tracked by two cameras placed around the experiment environment. The pattern output would provide information about the operator's motions and would then be used as trajectory on the robotic arm.

C. The inertial measurement unit, IMU - Xsens MTw (Xsens, 2013) monitored the orientation of the fixture (through the gyroscope and magnetometer), the vibrations generated during contact with the abrasive belt, and the speed used by the operators (through the accelerometer).
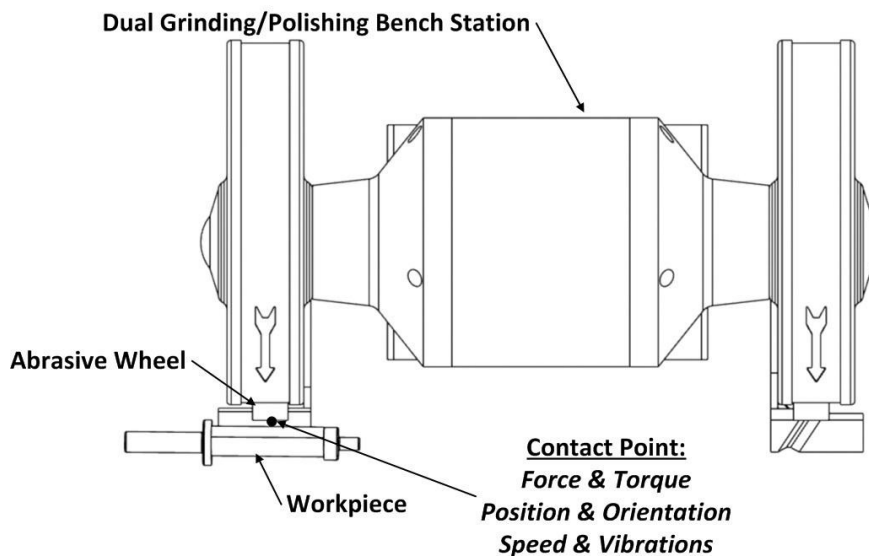
Figure 5.3: Parameter to capture with the fixture in manual operation

The polishing time was also accurately recorded to enable the cross referencing between the quantitative data (e.g. fixture and sensors) and qualitative data (e.g. videos and interviews) collected in Chapters 4 and 6 respectively. The matching of data from the three sensors should facilitate the analysis of data. Furthermore, fixture calibration was required to define a comparison benchmark used for different experiments. Sensors calibration and benchmarking is described in Section 5.3 and the fixture calibration is presented in Section 5.4.

5.3   Sensor Calibration Experiment

A set of systematic experiments was carried out to provide a reliable reference point for the various measurement sensors mounted on the fixture. These experiments provided a benchmark to interpret the sensory data in the context of manual polishing operations. One set of experiments focused on the calibration of the multi-axial force and torque sensor, and the second set on benchmarking and selection of motion sensor(s).

A more comprehensive description of these experiments may be found in Appendix A. However, a brief presentation of the known values of forces, torques, motions, and speed – both generated by the sensors and applied to the fixture - is described in this section. Some of the polishing parameters, such as feed rate, were also calibrated by combining data (i.e. measure motion speed and time).

5.3.1   Multi-Axial Force and Torque Sensor Calibration Experiments

Figure 5.4 illustrates the set of calibration experiments for the multi-axial force and torque sensor through single and multi-axial forces.

In the first experiment tested the precision of the sensor under a single axis force and using different sampling rates. The minimum and maximum errors recorded with the sensor were 0.02N and 0.06N respectively. This represented less than 5% error for any sample rate, which is an acceptable accuracy for this test.

In the second experiment, a multi-axial force (and the resultant torques) was applied to the sensor. As expected, the combination forces (*Fx*, *Fy*, and *Fz)* remained unchanged; however, the torque values were linked to the distance between the load contact point and the sensor (see Figure 5.4).
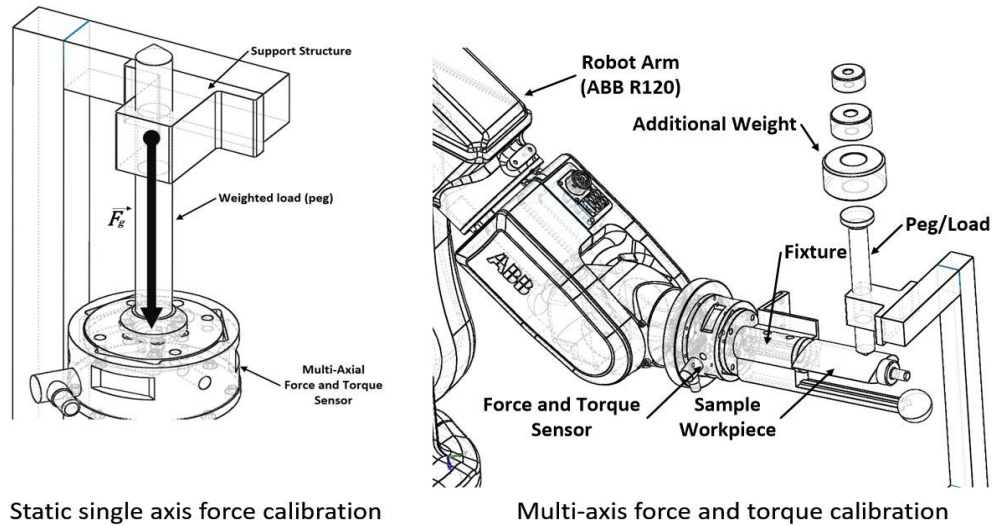
Figure 5.4: Pre-calibration process for the force and torque sensor

Further details on these two sets of calibration experiments with the multi-axial force and torque sensor are given in Appendix A.1.

5.3.2 Motion Sensors Benchmark and Calibration Experiments

The following section focuses on motion capture technology. These experiments aimed to demonstrate the capabilities of selected technologies to track the operator's movements with the fixture. At the end of these experiments, the motion capture system shown to be best-suited to this task was selected.

As for the multi-axial force and torque sensor, further description and analysis of the following experiments can be found in Appendix A.2.

5.3.2.1 *Inertial Measurement Unit (Xsens MTw)*

Figure 5.5 illustrates the benchmark experiment for the Inertial Measurement Unit (IMU). The aim of this experiment was to evaluate the capability and reliability of the Xsens MTw IMU sensor (Xsens, n.d.) to track human movement within a small workspace (such as in manual polishing) and investigate the processing of acceleration data into position data, using different algorithms.

The conventional method (El-fatatry, 2003.; Fischer et al., 2013; Glanzer et al., 2009; Hang et al., 2012; Jones, 1979; Khan, 2013; Ramaswamy, 2011; Rogers, 2003; Roviaire and Nasseh, 2009; Slifka, 2004; Welch, 1995; Zhang et al., 2012) uses a double integration approach to calculate positional data from acceleration, as illustrated in Figure 5.5. In this experiment, a known path was drawn on paper and the sensor was moved along the path repeatedly to calibrate the accuracy of the sensor.

The results indicated that this sensor could reliably provide inertial data, such as acceleration and gyroscopic data. Therefore, speed can be calculated based on the time recorded. However, the sensor was not able to meet the requirements for the positional accuracy (double integration of acceleration). This was probably due to the small workspace and movements, such as the one used in manual polishing processes.

Further details on the sensor calibration experiment is given in Appendix A.2.
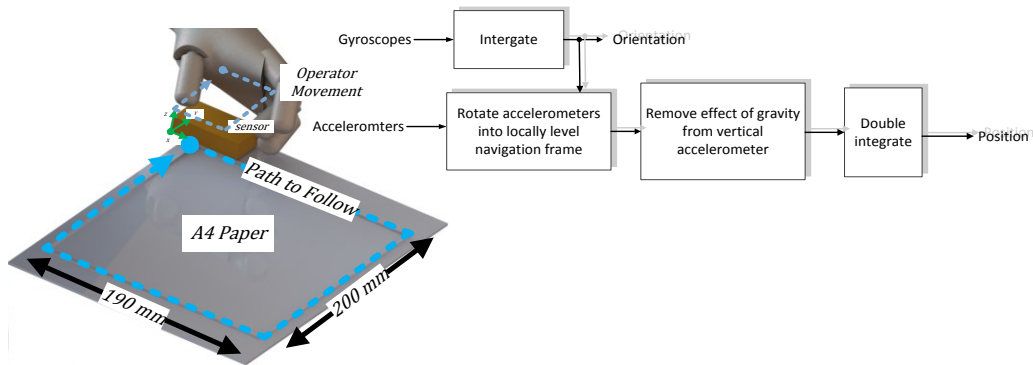
Figure 5.5: Benchmark and sensor calibration experiment for the IMU sensor

5.3.2.2 *Motion Controller (Leap Motion)*

Figure 5.6 illustrates the benchmark experiment with a commercial motion controller (Leap Motion). This experiment focuses on the assessment, and the capability of the sensor to track hands or fingers in 3D space and small environments was evaluated.

As for the inertial measurement unit, the motion controller tracked the operator movement when following a rectangular path, as illustrated in Figure 5.6. A set of experiments was carried out with three different sensor configurations. Overall, the sensor did not provide adequate results for this experiment, despite having shown good capabilities in other applications (Adhikarla et al., 2014; Bassily et al., 2014; Hsu et al., 2014; Huang et al., 2014; Mohandes et al., 2014; Wang et al., 2014). However, the sensor was adequate at tracking gesture when in a horizontal position.

Further details on the sensor calibration experiment with the motion controller is given in Appendix A.2.
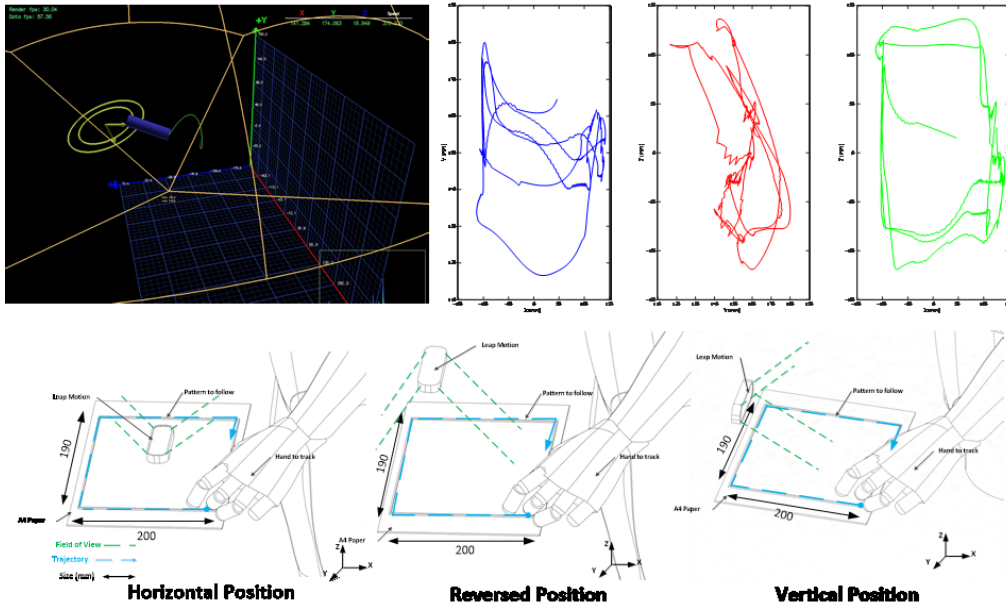
Figure 5.6: Benchmark and sensor calibration experiment for Leap Motion

5.3.2.3   3D Motion Capture System (Vicon)

Figure 5.7 illustrates the benchmark and calibration experiment with a 3D motion capture system (Vicon motion capture system or Vicon MoCap) (Pfister et al., 2014). Two set of experiments were carried out to 1) assess the positional accuracy, and 2) evaluate sensor integration and capability to capture human movements.

Initially, the markers were mounted on a robot end-effector to assess the positional accuracy of the sensor. The minimum and maximum positional difference found between the sensor and robot reading were 0.1 and 0.5 mm respectively. The positional accuracy identified in this experiment was considered acceptable for this project.

In the second experiment, the markers were mounted on an operator's hand while moving along a known path as for prior experiments with the IMU and motion controller. The data provided by the sensor clearly shows the path drawn by the operator's hands. Also, based on the experiment's elapsed time, the pattern of movements can be clearly identified.

Further details on the sensor calibration experiment with the Vicon MoCap is given in Appendix A.2.
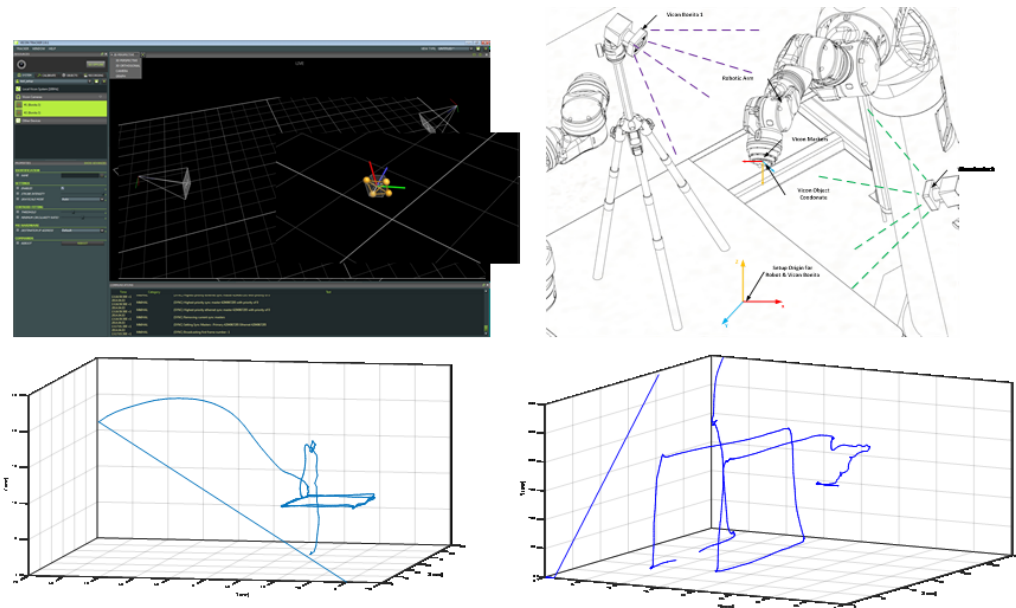
Figure 5.7: Benchmark and sensor calibration experiment for Vicon 3D Motion Capture System

5.3.3   Benchmark and Calibration Results for the Sensors

The benchmark and sensor calibration experiments were carried out to evaluate the precision of each sensor, and to choose a set of sensors to be integrated within the fixture. Several sensors evaluated showed suitable results; whereas others - such as Leap Motion - did not provide acceptable performance.

From the results observed, a fixture was planned in order to integrate: the multi-axial force and torque sensor (Shunk Gamma) to measure forces and torques; the motion capture system (Vicon) to track the motion of the operator; and the inertial measurement unit (Xsens MTw) to measure speed and vibration during the process.

Further details on this section is given in Appendix A.2.

5.4   Fixture Design

5.4.1   Design Layout and Engineering Embodiment

To accommodate all three sensors required (multi-axial force and torque sensor, IMU, and Vicon MoCap) to enable the capture of data and variables for manual polishing, a specific fixture design was developed. In addition to embedding all of the sensors into one device, the fixture had to be light and comfortable as it would be used by a human operator, and mechanically resistant to polishing operation to endure various forces during the experiments, and to protect the sensors.

Multiple fixture designs were developed and tested through an engineering embodiment process. An evaluation matrix was produced to select the most suitable design based on design specification requirements. Table 5.1 shows a summary of criteria used for each concept and their evaluation. A comprehensive description for the fixture design is described in Appendix C.

Table 5.1: Evaluation Matrix for Fixture designs

Design	001	002	003	004	005	006	007	008
Datum	Yes	No	No	No	No	No	No	No
spec.								
Ergonomic	*Datum*	-	=	---	--	=	+	+++
Weight		--	-	++	+++	=	+	---
Num. Component	2	1	2	1	1	3	1	1
Num. Sensors	2	2	2	2	2	2	2	3
Assembly	*Datum*	=	+	+++	++	++	+++	+++
Manipulations		-	=	---	---	=	++	+++
Volume of Material	*Datum*	+	+	++	+++	=	--	--
Aesthetic		=	=	=	-	+	++	++
Size		=	=	+++	+++	=	=	=
Portability	*Datum*	=	=	+	+	=	+	+
Capture of data		=	=	--	--	=	++	+++
Σ=		4	6	1	0	7	1	1
Σ+		1	1	10	12	3	12	14
Σ-		4	1	8	8	0	2	2
Σ+ : higher than datum, Σ= : same as datum, Σ- :lower than datum								

Figure 5.8 illustrates the partial evolution of the different concepts and designs for the fixture. Due to the design restrictions, based on the criteria shown above and the sensor specifications, the fixture designed was refined (from design 001 to 008).

Furthermore, the physical design and selected material were considered carefully to reduce the weight of the fixture and improve mechanical properties. After some testing, further ergonomic and mechanical changes were made to the fixture, as presented in Section 5.4.2 and Appendix C.
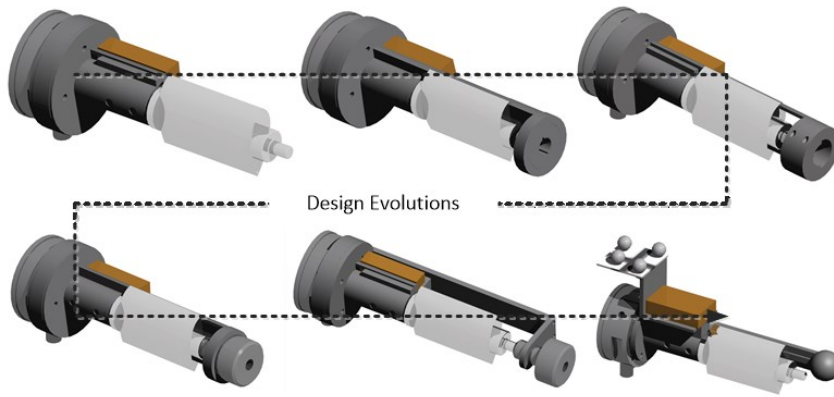
Figure 5.8: Progressive design steps of the fixture

5.4.2 Mechanical Strength Investigation

Initial testing of Design 008 of the fixture revealed a number of mechanical strength issues. A new design for the fixture was developed based on improving the mechanical strength. The strength of the fixture was calculated against deflection. Figure 5.9 illustrates a partial view of the investigation and improvements made to the fixture. For the purpose of simplifying build and calculations, the investigation focused on the deflection of two perpendicular cantilever beams using Euler-Bernoulli theory (Bauchau and Craig, 2009; Beléndez et al., 2002; Euler, 2013; Feynman et al., 2011, 1963; Georgiades et al., 2013; Will, 2012).

The maximum force applied to the fixture was determined in the calibration stage to be about 100N. This value was used in the design of the fixture to ensure the necessary mechanical stability. Further details on the calculation and the Euler-Bernoulli investigation are described in Appendix C.3.

L-Shaped Cantilever Beam

Beam A

Beam B

Maximum Deflection:

$$\delta = \frac{F.L^3}{3EI}$$

Where δ is the maximum deflection (m), F is the force applied on the beam (N), L is the beam length (m), E is the material young modulus (Nm), and I is the beam cross section (m^4).

Calculation of displacement x-y direction :

$$\delta ab = \delta a \times cos\theta_a + \delta b \times sin\theta_b$$

Where δab is the total displacement calculated for the fixture.
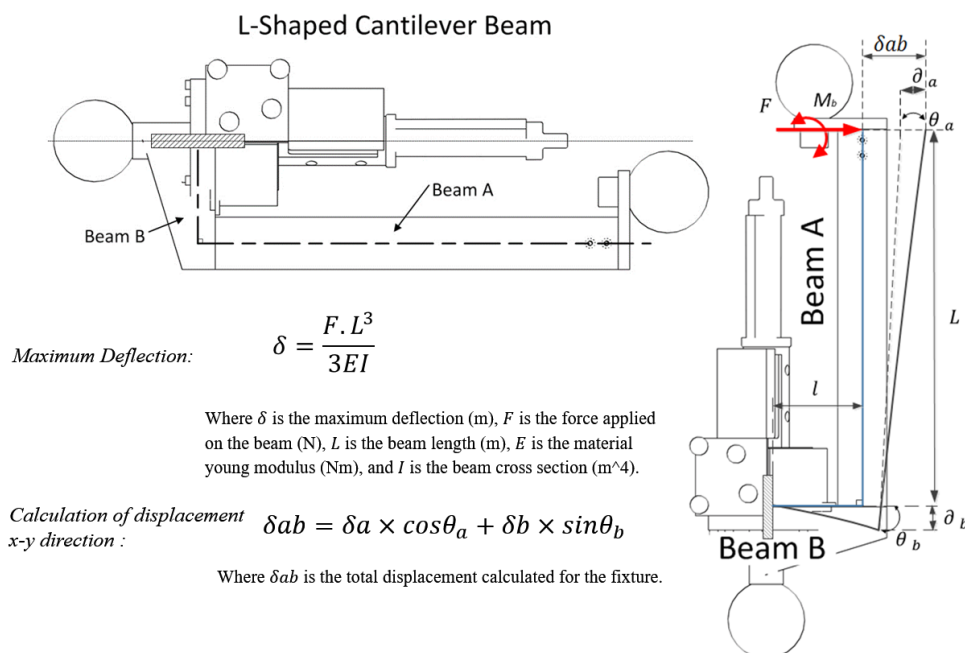
Figure 5.9: Investigation of the fixture deflection

5.4.3   Final Design

Figure 5.10 illustrates the final design of the fixture. This design was found to be ergonomic while accommodating all three sensors. In addition to the Euler-Bernoulli calculations, some additional dimensional adjustments were made to meet British Standards and machinability requirements. Moreover, it was find by the author and the operator (through first test and simulation before calibration experiments) that the total weight of the fixture including the sensors was acceptable. The ergonomic design was also find acceptable, therefore, the fixture would not affect the operators' techniques during the experiments. Further details on the final fixture design are in Appendix C.5.
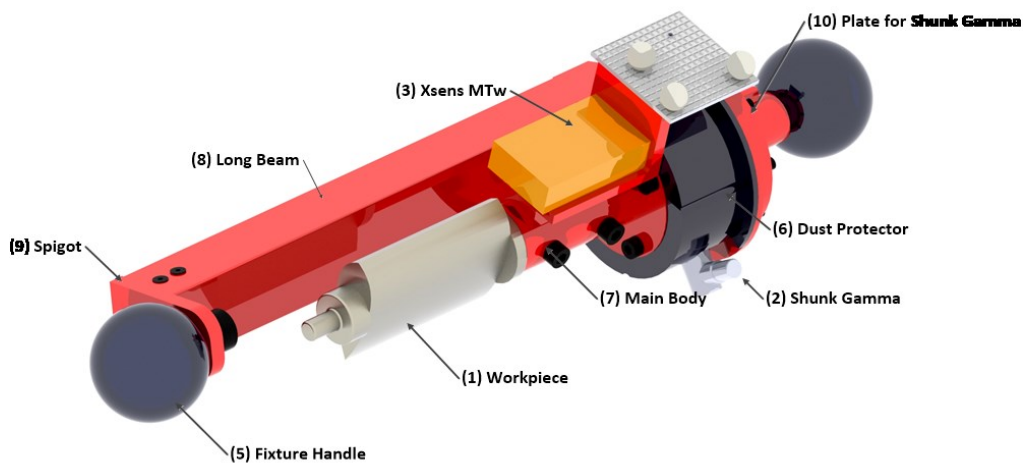
Figure 5.10: Final fixture design with embedded sensors

5.5   Fixture Calibration

A set of calibration experiments was carried out for the fixture. The aim of these experiments was to collect and integrate data from all sensors. The first experiment was carried out to synchronise data from the sensors for data analysis. The second calibration experiment was an initial investigation of force gravity compensation. Further investigation is developed in Chapter 7. The third and last set of calibration experiments was to collect and interpret the data from the fixture and sensors for manual polishing operation using known techniques. Further description of all calibration experiments are described in Appendix B.

5.5.1   Calibration Experiment 1: Data Synchronisation

Due to the setup and specification of the sensors (e.g. sample rate), the decision was made to synchronise the three sensors' data offline to simplify the analysis process. The sensors

were triggered manually and individually for this experiment, and therefore a small time delay between the different sensors was created.

In this experiment, the Vicon MoCap was triggered first, then the inertial measurement unit and force and torque sensor were calibrated and triggered. A time delay of 20 seconds was implemented to allow internal initiation processes for the IMU and the multi-axial force and torque sensor.

Figure 5.11 illustrates sample data collected during the fixture calibration experiment. A synchronisation line indicates the reference point for data comparisons for each sensor at a specific moment of the experiment. Further detail on the synchronisation of data is given in Appendix B.1.
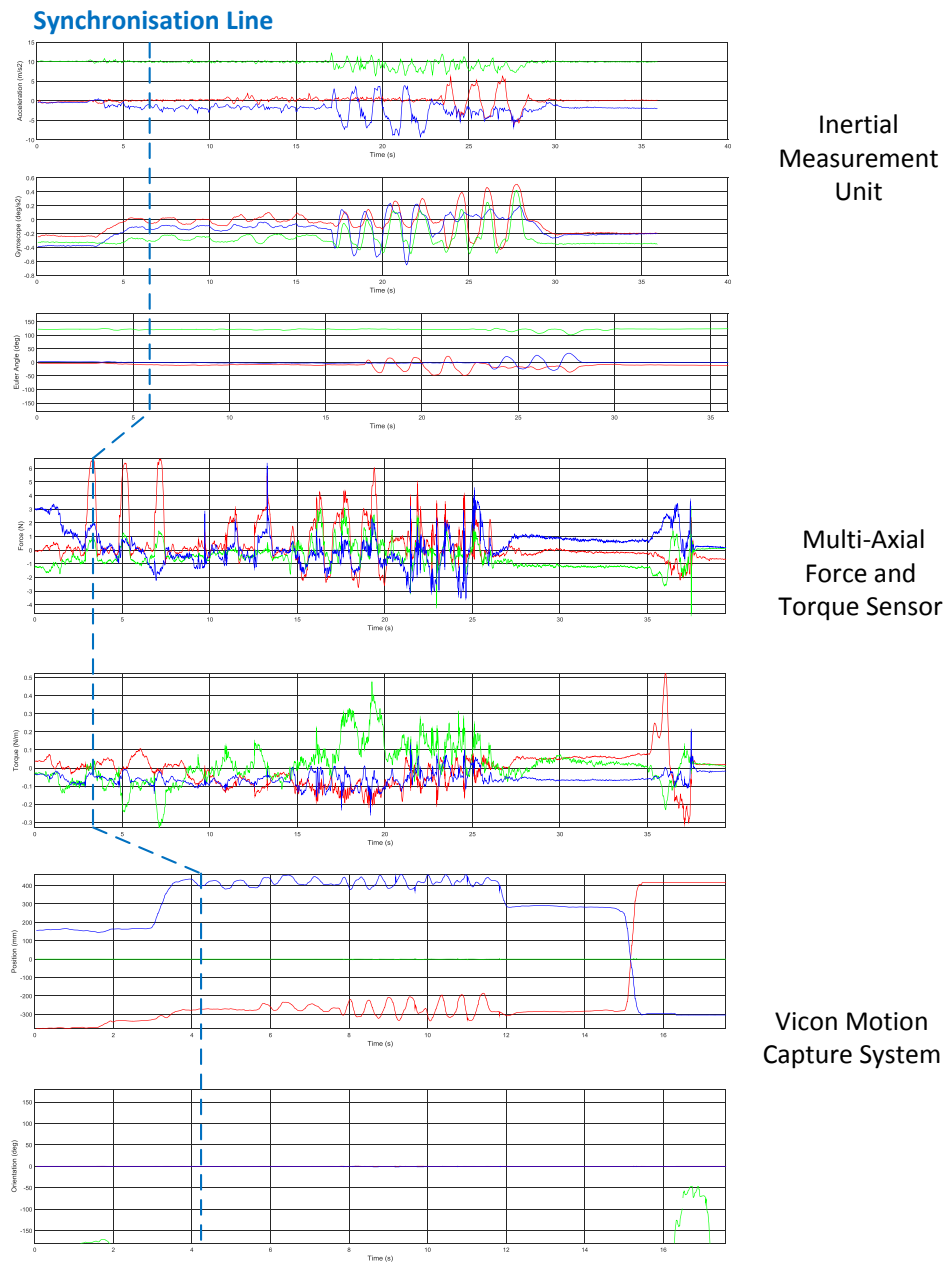
Figure 5.11: Data synchronization between three sensors

5.5.2 Calibration Experiment 2: First Investigation of Force Gravity Compensation

Initial tests with the fixture showed inertial data (e.g. acceleration and Euler-orientation) from the multi-axial force and torque sensor under operator movement (change in position and orientation), without any external force applied to the sensor.

The aim of this calibration experiment was to determine the value of the forces and torques measured at different orientations of the fixture. A combination of the data from the inertial measurement unit and the multi-axial force and torque sensor was used as a validation method to confirm the precision required for angular forces applied by the operator movement, as illustrated in Figure 5.12.

The results of this experiment indicated a relation between the IMU output (e.g. acceleration and Euler-orientation angles) and the force readings (multi-axial force and torque sensor output) in 3 axes. The maximum force output observed was 15 N for a rotation of over 90 degrees. Any forces generated under 45 degrees were too small to be relevant. Therefore, it was concluded that the inertia output should, in addition to capturing speed and vibration, be used to compensate forces output due to the operator movements.

Further information on this experiment and the force gravity compensation investigation are described in Appendix B.2 and Chapter 7.
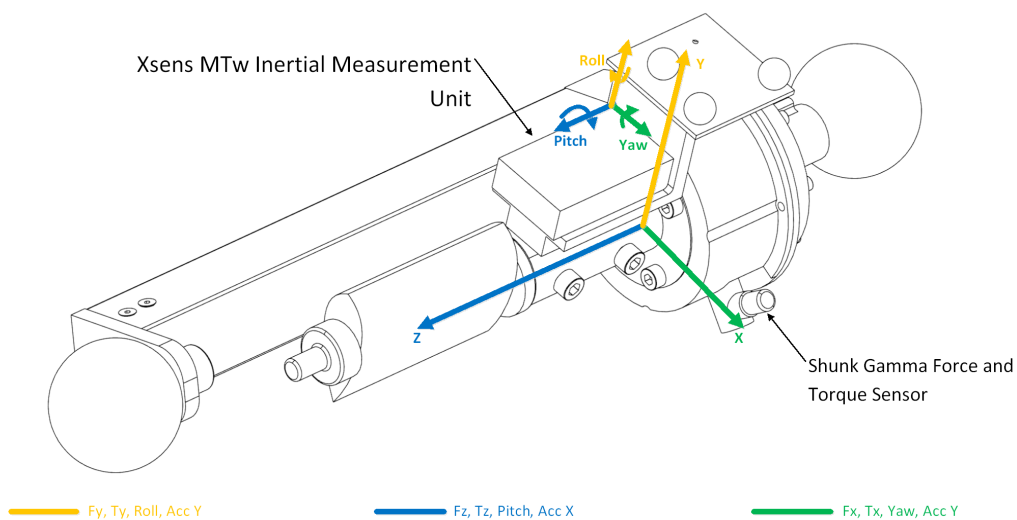
Figure 5.12: Fixture with force and torque and inertial measurement unit

5.5.3   Calibration Experiment 3: Interpreting Data Output

These calibration experiments were aimed at capturing and understanding data output during the manual polishing operation of a sample workpiece. In addition to capturing data from the different sensors, this calibration experiment was used to validate the capture and analysis procedure, and interpret the data provided by the fixture.

Three polishing techniques were used in this experiment, based on prior knowledge and observation of skilled operators as discussed in Chapter 4. The techniques included a simple pressure (used to remove defects at a specific location), a linear translation (used for trailing and leading edges) and surface profiling (used for overall finishing). These techniques were selected as they are widely used during standard operating procedure of the manual polishing process.

Figure 5.13 illustrates the setup and parameters captured by the fixture during this experiment. The operator's task was to carry out the polishing operation with the fixture using the different techniques described above.

The experiment was carried out with a traditional linisher belt, two Vicon MoCap cameras at each side to record the operator's movements, and the fixture recording accelerations, vibrations, forces and torques.
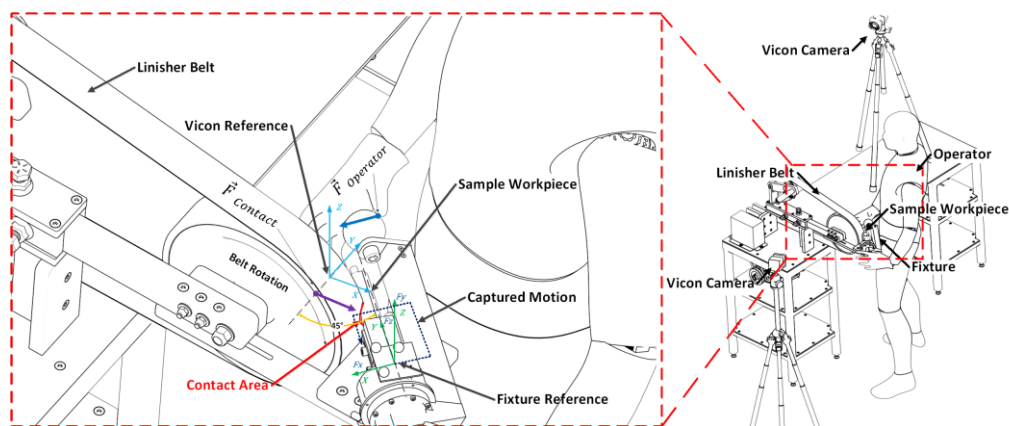
Figure 5.13: Setup for calibration experiment

In this calibration experiment, the operator carried out four iterations. In the first iteration, the operator used all three techniques (simple pressure, linear translation, and surface profiling). This was used to identify multiple techniques within the same operation. In the second iteration, the operator applied a single pressure of the sample workpiece against the abrasive belt for 1 second each at three different locations (chosen in the length of the part to include the effects of torque). In the third iteration, the operator executed a horizontal movement (linear translation) starting from one side of the workpiece to the other (from left to right, and right to left, repeated three times). Finally, in the fourth iteration, the operator followed the profile of workpiece, as it is a technique commonly used by skilled workers in industry.

5.5.3.1 Iteration 1: Technique and Pattern Identification

This iteration focused on identifying several techniques that may be used by skilled operators (see Chapter 6). The operator was tasked with using three techniques (simple pressure, linear translation, and surface profiling). Figure 5.14 illustrates the result of the pattern identification iteration. The change of pattern and technique was clearly observed.

The operator started the experiment by applying a static pressure to different locations on the surface (Simple Pressure - Pattern A), then moved the fixture horizontally while keeping the contact between the surface and the abrasive belt constant and perpendicular (Linear Translation - Pattern B). Finally, the operator followed the profile of the workpiece (Surface Profiling - Pattern C).

Further detail on Iteration 1 is described in Appendix B.3.
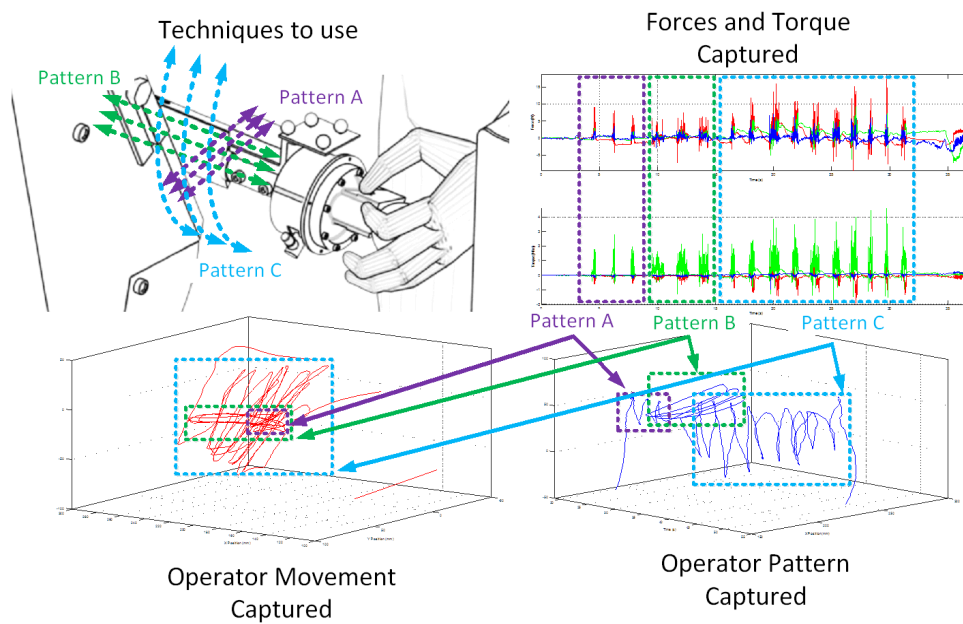
Figure 5.14: Iteration 1 – Technique and Pattern Identification

5.5.3.2 Iteration 2: Simple Pressure Technique

This iteration focused on a simple pressure technique applied at different locations on the workpiece surface. The operator's task was to apply a simple pressure against the abrasive belt for 1 second before changing location on the surface.

Figure 5.15 illustrates the results of this iteration. From the data collected, it can be observed that the operator applied a pressure at four different locations on the surface (A1 to A4). The data collected by the multi-axial force and torque sensor shows data around Fx and Ty, which represent the force applied by the operator and the change in torque at different areas on the surface respectively.

Further details on Iteration 2 is described in Appendix B.3.
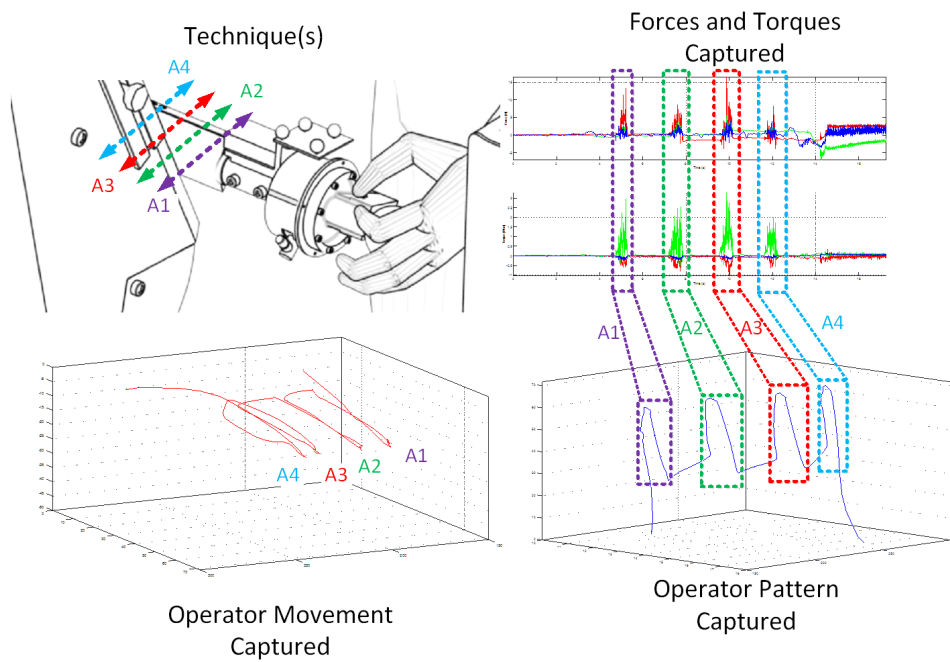
Figure 5.15: Iteration 2 – Simple Pressure Technique

5.5.3.3   Iteration 3: Linear Translation

Iteration 3 focused on the application of a constant force while moving the fixture horizontally (Linear Translation). This technique is commonly used in industry for polishing or deburring the trailing or leading edges of a workpiece. The operator's task was to polish the workpiece surface by applying a constant pressure to the surface and moving the fixture horizontally, from one end to the other in both directions.

Figure 5.16 illustrates the results of this iteration. From the data collected it can be observed that, when the operator moved the fixture in one direction while maintaining a constant force, the data showed a clear change in the direction of motion. For example, the data output from the multi-axial force and torque sensor shows readings in the *Fx*, *Fz*, and *Ty* axis. *Fx* and *Fz* output was due to the contact with the abrasive tool and the movement of the operator respectively. Torque along the *Ty* axis was generated from the contact with the abrasive tool, as in Iteration 2.

Iteration 3 is further detailed in Appendix B.3.
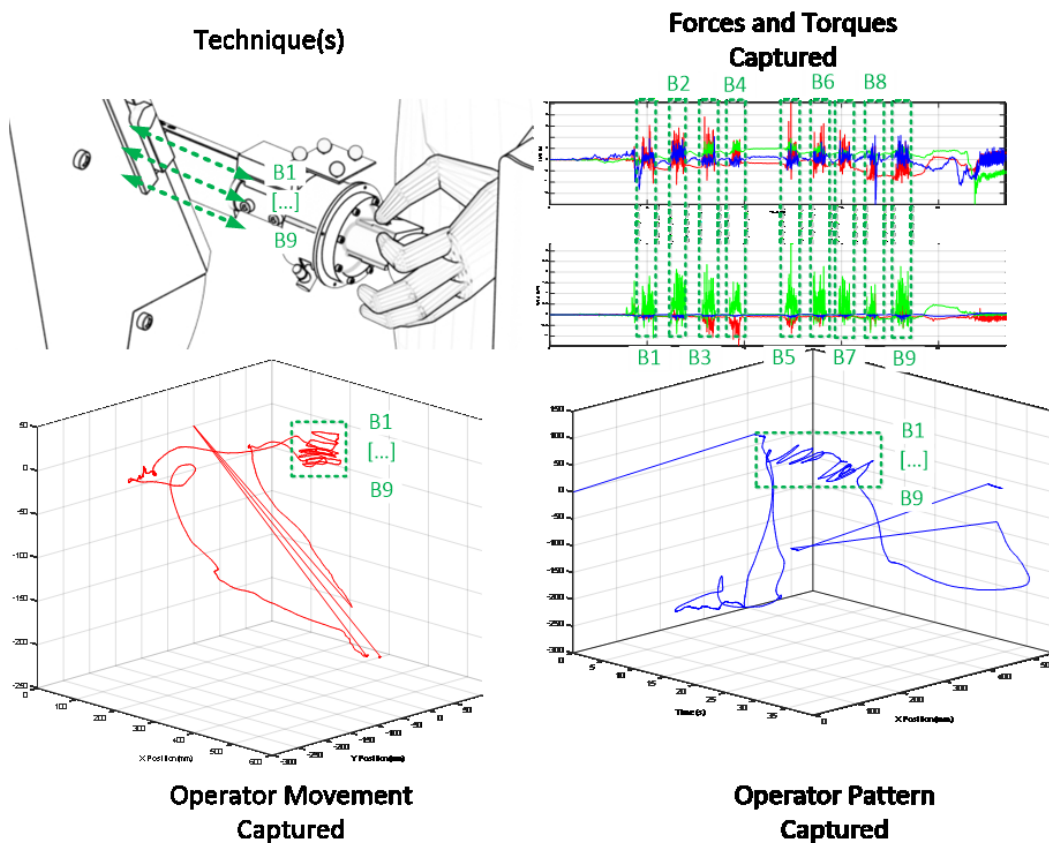
Figure 5.16: Iteration 3 – Linear Translation

5.5.3.4 Iteration 4: Surface Profiling

Iteration 4 focused on removing a layer of material while following the profile of the workpiece surface, without modifying the geometry of the part. The operator's task was to polish the whole surface of the sample workpiece by following the profile of the surface.

Figure 5.17 illustrates the results of this iteration. From the data collected, it can be observed that operator movement matches the waviness[2] of the workpiece surface. This indicates that the operator followed the profile of the surface without affecting its geometry.

The multi-axial force and torque sensor showed readings for Fx, Fy, Fz, Tx, and Ty. Due to the complexity of the operator movement, a distribution of the contact force was observed along the x-y-axes. As described in Calibration Experiment 2 (see Section 5.5.2), complex movements have an impact on the force and torque reading due to the inertia and orientation of the fixture. Therefore, the contact force is distributed along Fx-Fy and Tx-Ty axes. Finally, Fz readings were generated form the horizontal movement of the operator, as in Iteration 3.
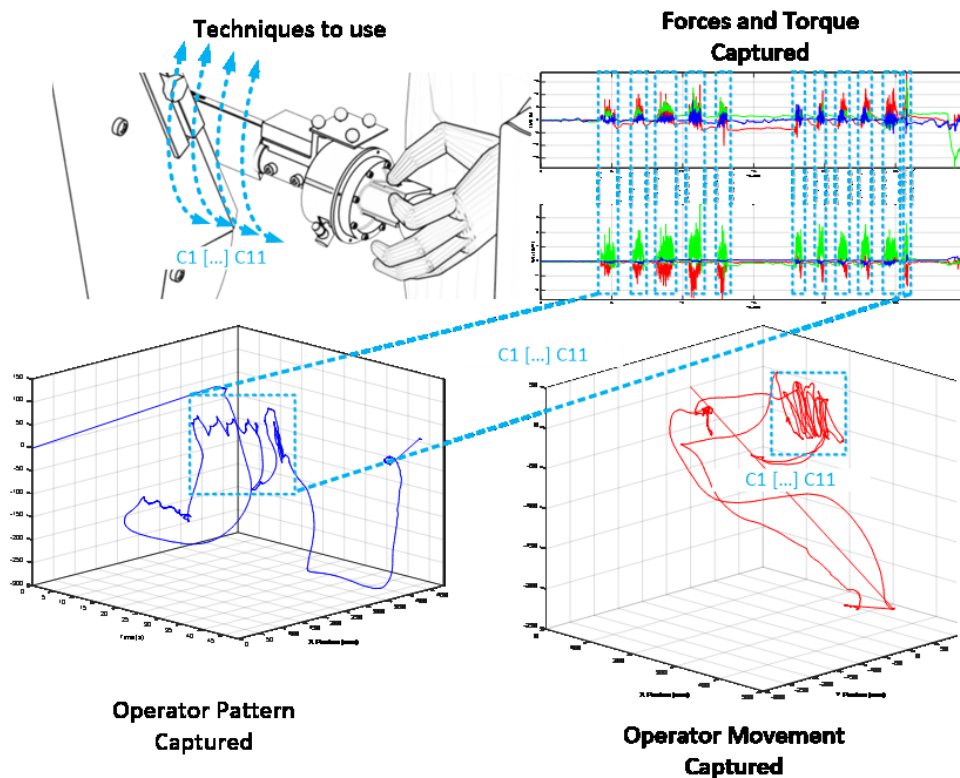
Figure 5.17: Iteration 4 – Surface Profiling

---

[2] In metrology, waviness is the measurement of the more widely spaced component of surface texture. It is a broader view of roughness because it is more strictly defined as "the irregularities whose spacing is greater than the roughness sampling length".

5.5.4 Analysis and Discussion

The aims of these calibration experiments were 1) to capture and synchronise data from different sensors, 2) correlate force and torque readings with inertia, and 3) validate the capture and analysis procedure for manual polishing operation.

Overall, the experimental procedure (including fixture and sensors) gave good results in capturing and interpreting manual polishing operations. The data captured showed the patterns and forces used by the operator during each technique. This would aid the understanding of how manual polishing operation is carried out by skilled operators, which is described in the following chapter. Matching data from various sensors triggered at different times was a difficult task, and could be a potential source of error for further experiments. However, cross-referencing and synchronising of the data was successful offline by searching for similar patterns in data.

In addition, the gravity and inertia effect of the operator's movements on the readings from the multi-axial force and torque sensor was investigated. Further information on this is described in Appendix B.2 and Chapter 7.

5.6 Conclusion on Capturing Process

In this chapter, the development of a device enabling the capture of manual polishing parameters was described. The fixture device is embedded with a multi-axial force and torque sensor, an inertial measurement unit, and a 3D professional motion capture system.

The multi-axial force and torque sensor was used to measure forces and torques involved during manual polishing operation. The inertial measurement unit was used to obtain the speed (or feed rate) and vibration. Finally, the 3D motion capture system captured the movements and patterns of the operator.

A set of calibration experiments was carried out with each sensor. These experiments aimed to calibrate each sensor individually. A benchmark experiment was also carried out for the section of the motion sensor.

Finally, a set of experiments was carried to calibrate the fixture with the sensors. The experiments showed good capabilities for the fixture and the sensors to capture force, speed, and motion data, and to carry out the analysis for capturing and interpreting patterns and techniques of skilled human operator.

The key objective of the calibration experiments was to identify and to understand the data output from the fixture. The techniques used in Calibration Experiment 3 (simple pressure, horizontal movement, and surface profiling) were chosen as references for the capture of manual polishing parameters experiment (see Chapter 6), as these techniques are commonly used by the skilled operators in industry (see Chapter 4).

Further details on the development and testing of the fixture are described in Appendix A to C.

Chapter 6 Capture of Manual Polishing Parameters

In this chapter, the capture and analysis of the manual polishing parameters are described. To capture all necessary parameters, three experiments with two different skilled operators were designed and carried out. This was due to the difficulty in finding qualified polisher for the experiment. However, the sample size was found to be reasonable to capture the overall process, as the primary objectives of these experiments were to provide a better understanding of the manual polishing process, and to capture parameters used by skilled operators for the development of the automated system, described in the next chapter.

This chapter is divided into six sections. The first section reports the setup and the procedure followed in each experiment. The second section presents the capture of data for grinding operation. In the third and fourth sections, the capture of data when removing heavy (coarse polishing) and light defects (final polishing) respectively are explained. Finally, the data collected are analysed in the following section and some recommendation for automation are summarised in the final section.

Figure 6.1 illustrates use of the polishing fixture by a skilled operator. Further detailed information on the capture and analysis of manual polishing parameters is presented in Appendices C to E.
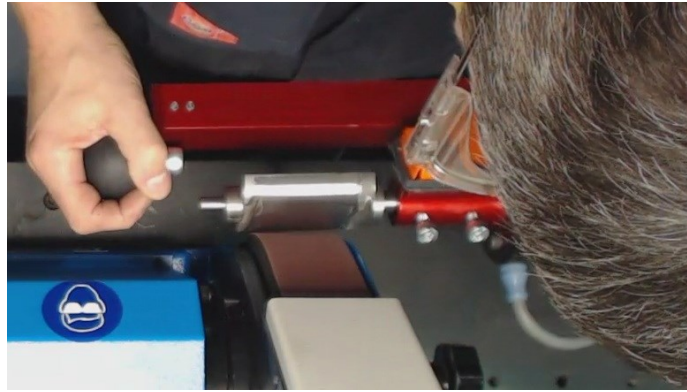
Figure 6.1: Skilled operator polishing the sample part with the fixture (see video on the attached CD)

6.1   Setup and Procedure

The series of experiments reported in this chapter were carried out within the research laboratory on a test rig designed for manual and automated polishing processes. Figure 6.2 illustrates the experimental setup for the capture of manual polishing parameters from highly skilled operators. The test rig is equipped with a dual-linisher station (RJH Fallow) with an aluminium oxide abrasive belt (P240 grit), a soft cotton mop, and a variable rotation speed controller. Each experiment was captured through a Vicon MoCap system (with two cameras mounted on a frame) and the fixture embedding sensors, to capture the operator's motions and forces during manual polishing operation.

As stated in Chapter 5, the designed fixture is equipped with: the multi-axial force and torque sensor (to capture forces and torques); inertial measurement unit (to capture speed and vibration); and markers for the Vicon MoCap (to capture position and orientation of the fixture). In the following set of experiments (see Sections 6.2 to 6.4), two highly skilled operators were tasked with carrying out grinding and polishing operations on a small metallic sample workpiece. The workpiece is similar to an industrial component used in aerospace, as seen in Section 4.3. Three sets of experiments were carried out as follows:

➢ Experiment 1 (Section 6.2) captures the techniques and parameters used by the operator for grinding operation. The objective of this experiment was to capture and cross-reference the data with the techniques observed in Section 5.5.

➢ Experiment 2 (Section 6.3) captures the techniques and parameters used by the operator for polishing operation. The objective of this experiment was to capture the parameters and techniques deployed by the operator for the removal of heavy grinding marks and the improvement of the surface finish.

➢ Experiment 3 (Section 6.4) demonstrates the techniques used by the operator for final polishing operation. The objective of this experiment was to capture the parameters and techniques used by the operator for the removal light defects in known locations and the improvement of the surface texture.

It should be noted that, in each experiment, the operators followed the sequence of the standard polishing process as practised in industry: grinding, coarse polishing, and fine polishing.

Finally, the data collected were analysed offline after each experiment. The analysis carried out elucidated the patterns and techniques used by each skilled operator. Moreover, the collected data were cross-referenced with interviews, videos, the results observed in the previous experiment (see Section 5.5) and in industrial visits (see Section 4.4). This provided a better understanding of the techniques, approaches and parameters used by skilled operators during manual polishing operation, for the development of the automated polishing system.
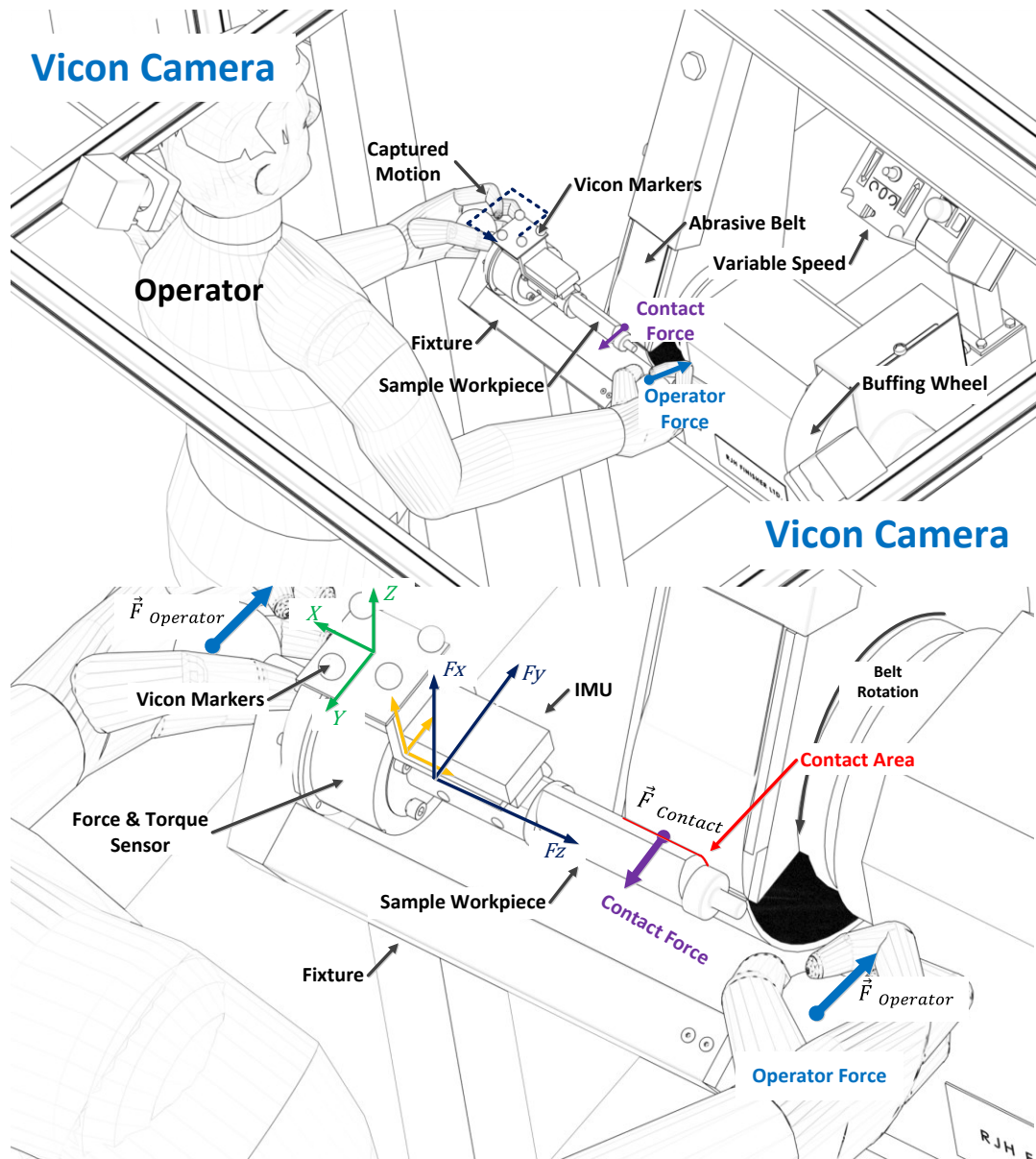
Figure 6.2: Setup diagram for capture of manual polishing operation

6.2   Experiment 1: Removing a Thick Layer

In industry, the first step of finishing processes is the grinding and deburring operation of the workpiece. This experiment was carried out to help with cross-referencing and interpreting the operator's habits during manual polishing operation. In this experiment, the operator had the task to remove a thick layer of material from the whole surface of the sample workpiece using the fixture. The objective of this process is to remove machining marks lefts after the milling operation. The data captured in this experiment was compared to the data captured in Section 5.5 to identify each technique and pattern used by the operator.

A workpiece was mounted on the fixture and the operator completed the task in 1 min 10 s. Figure 6.3 shows a summary of the data captured during this experiment. Patterns B and C (linear translation and surface profiling respectively – Section 5.5.3) were mainly identified as techniques used by the operator. It was also found that the operator started the experiment by following the profile of the surface (Pattern C). During this stage, the operator removed a layer of material from the whole surface in several passes. Then the operator focused on the trailing edge of the part using a linear movement (Pattern C) with a small inclination of the fixture. Finally, the operator focused at specific areas on the workpiece surface (using Pattern A and C) but inspected the workpiece more frequently.

From the experiment discussed above, the operator followed a similar process sequence as observed previously and discussed in Section 4.4. The operator sequence started with grinding the whole surface in one or few passes (rough grinding), followed by polishing of the trailing edge (specific feature), and finished by grinding the surface at specific location only (re-work). Finally, it was noted that, during the first part of the process sequence, the operator grinds and inspects the surface frequently, but in the last sequence of the process, the inspection was carried out after each pass.

Inertial Measurement Unit

Vicon MoCap

Multi-Axial Force and Torque Sensor

Trailing Edge Pattern
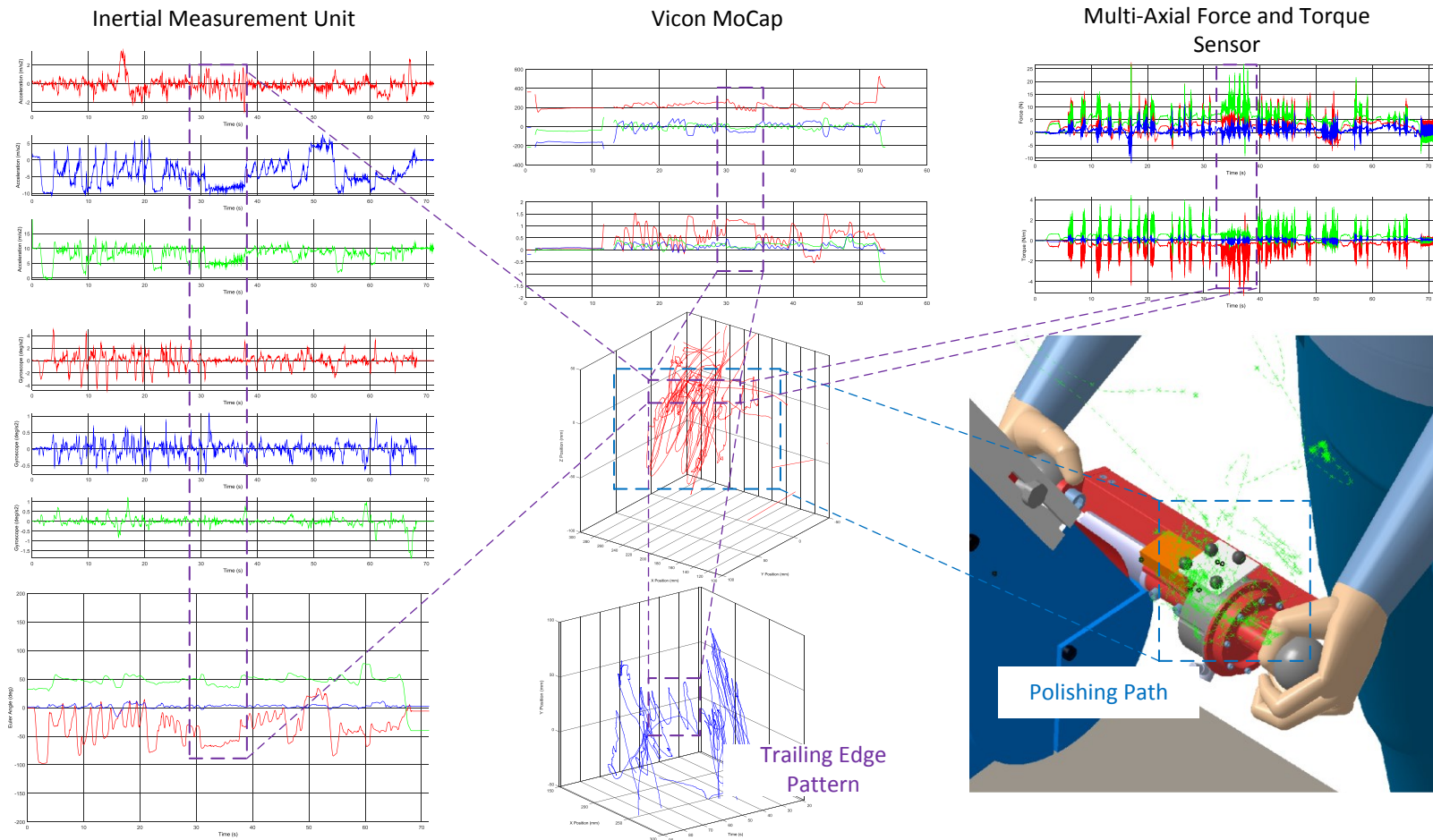
Polishing Path

Figure 6.3: Data collected in Experiment 1: Removing a Thick Layer

6.3   Experiment 2: Removing Machining Marks

In industry, it is not unusual to have heavy machining marks left on the surface after grinding or rough polishing operation. Removing such marks is part of the standard polishing operation in many processes, including those carried out by our industrial partner.

In this experiment, the operator had the task of removing heavy grinding marks and to improving the surface aesthetic of the workpiece. This is typically carried out by using different grades of polishing wheel. The data captured focused on the techniques deployed by a skilled operator to remove such features and improve the quality of the surface finish. The operator patterns and techniques were expected to be similar to Experiment 1 but with different values for parameters. Finally, the collected data were compared to the calibration experiment (see Section 5.5), as in Experiment 1.

Based on the captured quantitative data and the qualitative data (e.g. video and discussion), it was observed that the operator followed the same process sequence as in the previous experiment. With respect to the SOP, the operator polished the whole surface in order to remove all defects in few passes. The operator polished the surface slowly (decrease in feed rate) to remove more material and therefore the defects. The operator removed most of the defects in 2 passes before inspecting the surface. The operator was able to remove all of the defects in a few passes in 1 min 43 s. As with the previous experiment, the trailing edge was polished once the defects were removed. The rest of the sequence was focused on improving the surface quality of the workpiece.

Using the same approach as in Experiment 1, the operator used Pattern C to remove defects and improve the surface aspect, and used Pattern B for the trailing edge. Discussion with the operator also revealed that each polishing action (or pass) should be performed twice. According to the operator, moving the workpiece against the grain of the abrasive belt allows the operator to remove material whereas moving back allows the operator to rectify the pass marks and straighten the edges.

Overall, the captured data indicate that the operator's force and movement remained constant during the experiment. However, the speed varied to adjust the feed rate. It was also observed, and confirmed by the operator, that a change of pace (or speed, feed rate) is necessary during the operation, depending on the surface feature or volume of material to remove. This change of speed is crucial as it allows the operator to remove features and defects without affecting the geometry and dimension of the workpiece. Finally, it was observed that during the polishing of the trailing edges a lower force was applied by the operator. The polishing force was reduced to avoid damaging the part or causing severe injuries to the operator.
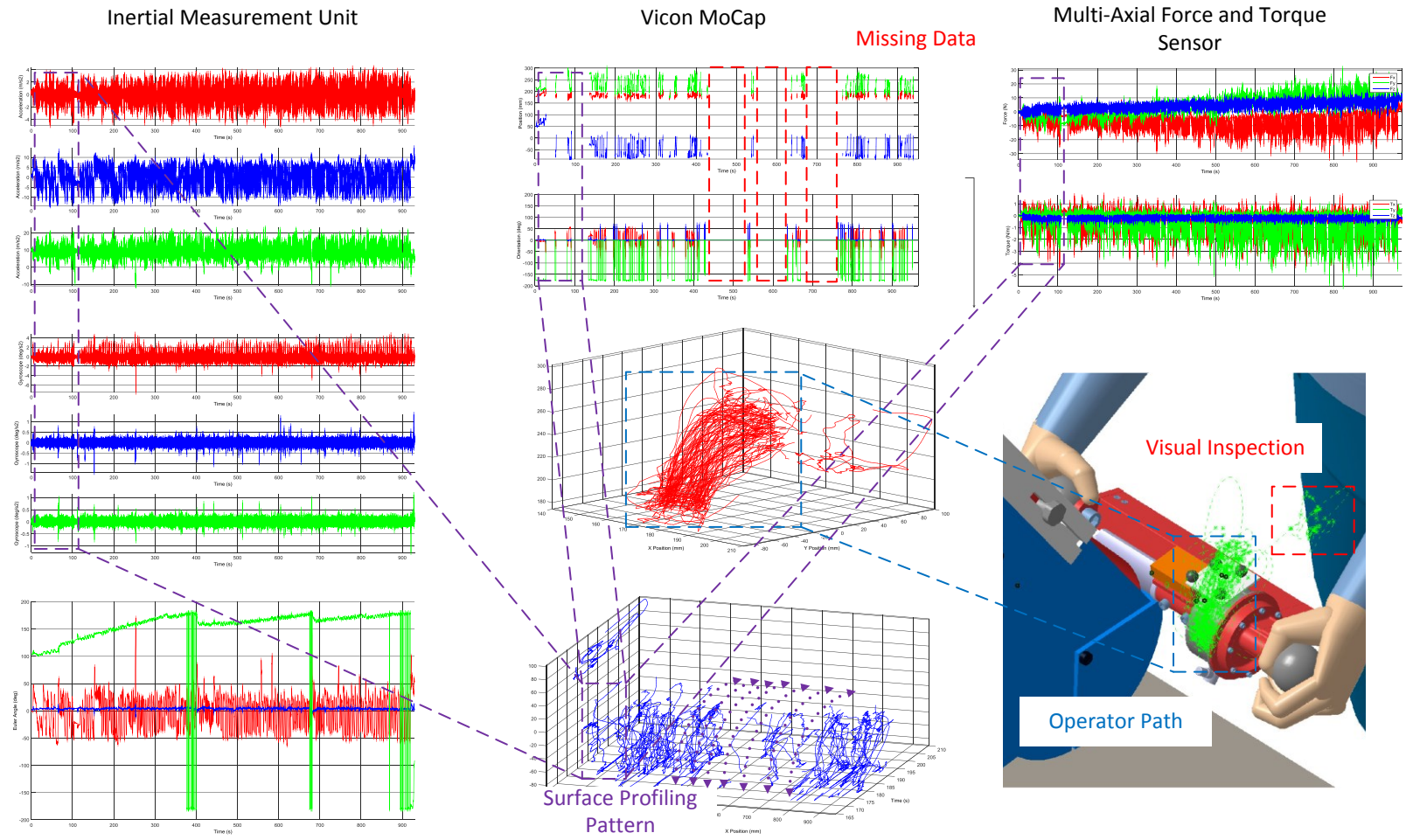
Figure 6.4: Data collected in Experiment 2: Removing Machining Marks

6.4   Experiment 3: Removing Defects

It can be observed that re-work of some parts is a common practice in many polishing companies, including at the partner's site. This is typically due to the under-skin defects in raw material delivered to the company or, more commonly, due to operator error leading to light surface defects remaining on the parts and failing the quality control inspection. At our industrial partner's site, it was observed that up to 50-60% of component 2 (see Section 4.3.2) in some batches needed re-work.

In this experiment, the operator had the task of removing light defects (localised on the surface) and improving the surface aesthetic until satisfactory. This experiment aimed to capture the techniques deployed by the operator when removing light defects at specific locations and improving the surface texture. Prior to this experiment, the defects were intentionally applied to the surface at known coordinates.

As in the previous experiments, the operator followed a similar approach and sequence. The operator identified the defects visually and removed them progressively by following the profile of the part (Pattern C – surface profiling). All defects, except those at the top part of the surface, were removed within the first 2 minutes of the experiment. While improving the surface aesthetic, the operator removed the remaining defects (in 3 min 16 s). As in the previous experiments, the operator polished the trailing edges after removing the defects. Moreover, the surface inspection was carried out after each or several (up to 5) passes. It was observed that the operator was more cautious with the feed rate and the material removal rate and carried out visual inspection more frequently. In other words, the operator waited to complete the task before inspecting the surface visually and carrying out more passes. It was also observed that the polishing area for a specific defect was expanded as little as possible to minimise the process time while maintaining a consistent surface quality.

Overall, the operator's speed was faster than the previous experiments. This was to remove the light defects and improve the surface aesthetic without altering the dimension and geometry of the workpiece. In addition, inspection and assessment of the surface was carried out more frequently than in the other experiments, due to the nature of the job (i.e. removing localised defects).

However, it was observed that, due to the operator's attention to detail, the polishing speed alternated between slow (to remove more material) and fast (to remove defects without altering the surface), resulting in a long polishing time (15 minutes).
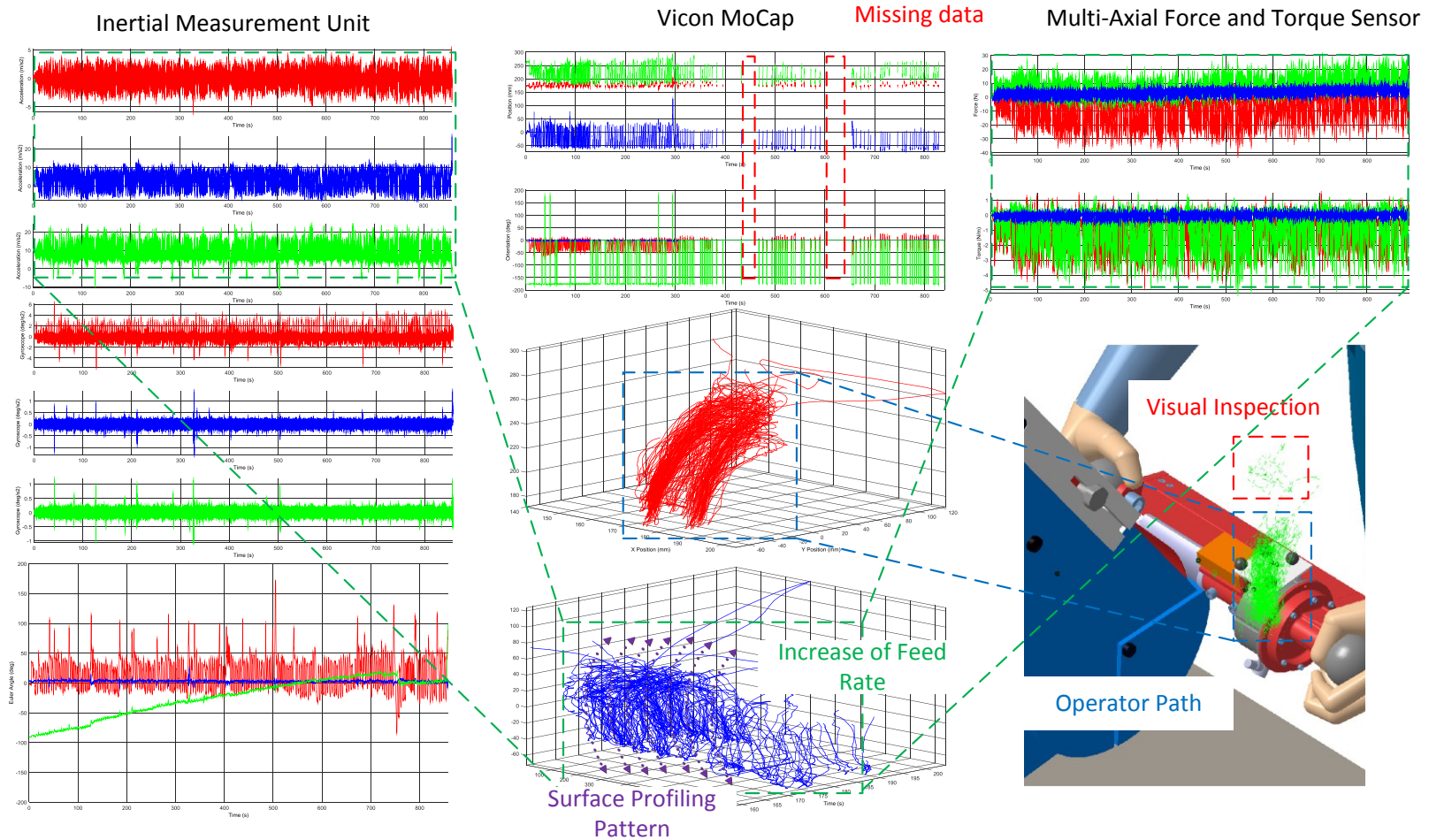
Figure 6.5: Data collected for Experiment 3: Removing Defects

6.5   Data Analysis

Based on the standard operation procedure for manual polishing, it was observed that operators are required to follow the profile of the workpiece surface while keeping a constant force (i.e. "keep the flow") and frequently inspect the quality of the surface visually. This procedure is repeated by the operator until the quality of the workpiece is satisfactory. The polishing process and the operator's patterns and techniques during manual polishing were captured with the fixture (quantitative data) and videos and discussions (qualitative data).

Overall, the data captured with the fixture support the interview and discussion with both skilled operators and with the information collected during the site visit in industry.

In the following sections, the data collected during each experiment are analysed and discussed.

6.5.1   Sensor Performance

It was confirmed in Section 5.6 that the fixture and the set of sensors performed well when capturing manual polishing parameters and variables during the calibration phase. Similar performance was observed during the experiments described in this chapter. In this section, the performance of the sensors during the three experiments are discussed.

The multi-axial force and torque sensor measured the force and torque involved during the operation. However, the data output of the sensor also included inertia and gravity effect due to the mass of the fixture and movement of the operator (avg. 5-10N in each axis). Moreover, the sensor was able to provide the timing (and length) of each polishing action. Therefore, the operator speed could also be computed.

As in the calibration experiment (Section 5.6), the initial measurement unit was able to capture acceleration, gyroscopic data, magnetic fields, and Euler-angle orientation in 3-axes. The accelerometer provided the speed, the direction and pattern of the movement, and the vibration generated at each polishing action. The gyroscope indicated the change in orientation of the fixture, which was used in tandem with the Vicon MoCap.

Finally, the Vicon MoCap system captured the path followed by each operator. The data captured showed similarity with the surface geometry of the sample workpiece, which indicated that both operators mainly followed the profile of the surface. However, due to the setup of the experiment and the complexity of movement captured, the Vicon MoCap system was not able to perform as well as expected (resulting in some missing data and plot holes). Therefore, the orientation data captured with the IMU was used to complete the analysis of the operator movement.

The results are illustrated in Figures 6.3 to 6.5 and more detailed information regarding the performance of each sensor is given in Appendix F.

6.5.2   Operator Polishing Patterns

The process parameters and operation variables which were captured during the experiments with the two skilled operators are summarised in Table 6.1. The first operator (Operator 1) is a qualified machinist, polisher, and welder, with the second operator (Operator 2) also being a qualified machinist.

From the data collected, it was learned that the operators continuously follow the profile of the part while keeping a constant force against the abrasive tool. The direction of contact between the workpiece and the abrasive tool must be kept perpendicular during the operation; the operators were able to maintain this variable at a constant value. It was noted that, in order to keep the contact force constant and perpendicular, the operators compensate for torque and vibrations with their hands (tactile feedback).

The process sequences used in Experiments 1 to 3 were similar for both operators. Each operator started the experiment by removing the defects or marks in a few passes, before focusing on the improvement of the surface texture. It was also observed that the operators polished the entire surface area and then focused at specific or localised area(s) to polish only where it is required. In addition, it was noted that the visual inspection was done frequently but not necessarily after each pass. The operators also heavily relied on their vision to assess the quality of the part, and their tactile senses (such as touch) to monitor the operation in real-time, such as monitoring the blending contact.

Adjustments made to the process by each operator was done by changing the speed of movement (and in some cases, force) which changes the material removal rate without affecting the surface texture. This allowed the operator to remove more defects or improve the surface aesthetic without affecting the dimension or geometry of the workpiece. Although the contact between the workpiece and the abrasive tool must be kept perpendicular, some specific features or areas on the workpiece surface are difficult to reach (i.e. the lower corner); both operators had to change the fixture orientation in order to eliminate this particular feature that was difficult to reach.

The main differences between each operator were that Operator 1 followed the same pattern and kept the same parameters (i.e. keep the flow – constant force and movement), but changed the speed (feed rate) until the surface quality was satisfactory. The movement of each pass was also carried out in both directions, once downwards to remove a layer of material or defect and once upwards to correct the pass or straighten the edge. Meanwhile, Operator 2 also followed the profile of the part, but a change of speed, force, and movement was observed, in order to change the material removal rate at specific locations.

The main findings of these experiments are illustrated in Figure 6.6, and are summarised in Table 6.1. In brief, the operators follow the same pattern (i.e. force and motion) but apply a longer contact (t_p) at the start of the operation and then speed up the pace. This method allows the operator to remove most of the defects at the start of the operation and then improve the surface quality where required, without over-or-under polishing the surface.

When developing the automated system, these parameters and techniques are to be translated by following the profile of the part with the robot, while controlling the force and feed rate depending on the defects to remove. More discussion on the subject of automation is given in Section 6.6.
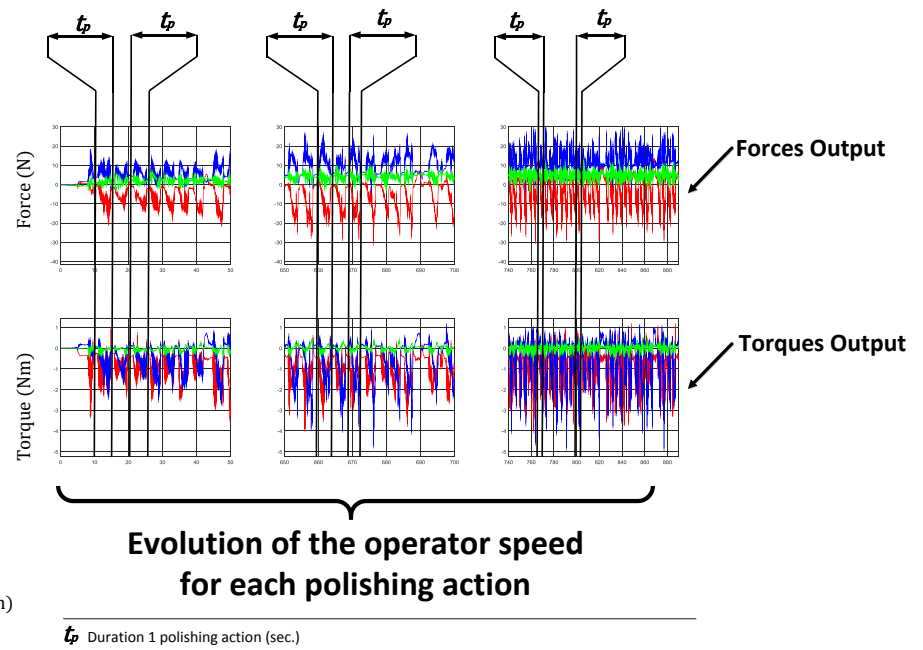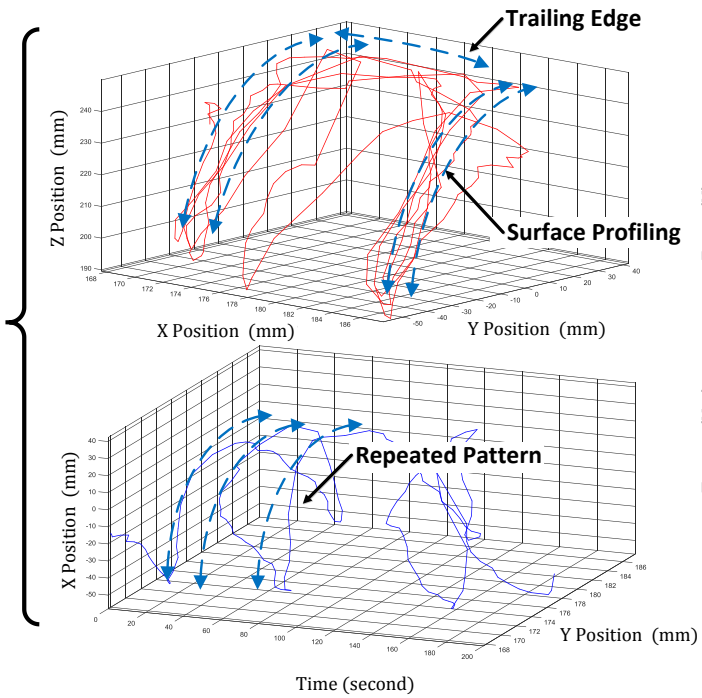
Figure 6.6: General polishing approach used by skilled operator

Table 6.1: Operators technique captured with fixture and discussion

Parameters	Operator 1	Operator 2
Path	Mainly follows the curve of the part and changes movements for trailing edge and radii. Contact between the part and the belt is kept perpendicular at all times.	Mainly follows the curve of the part and changes movements for trailing edge and radii. Changes position and orientation of the part depending on the type and location of the features to remove.
Force	The contact force is kept constant during the entire operation.	Changes the contact force depending on the volume of material to remove.
Torque Vibration	Torques and vibrations are compensated for by the operator's hand, to keep contact perpendicular to the abrasive belt.	
Speed	The speed is changed depending on the type of defect or the operation to carry out. A slower speed will increase the MRR to remove heavy features (i.e. grinding and first polishing operation). A faster speed will decrease MRR to increase the quality of the surface texture without over-polishing the part (i.e. final polishing and buffing operation).	
Visual feedback	First assessment of the surface is done at the beginning of the operation Further inspections at specific locations are done frequently (i.e. the surface to polish or the location of features). This helps the operator to focus only where the defects are located. Inspection is mainly done after each pass but also can be done after several passes depending on the type of defect. Visual feedback is also used to control the blending contact of the part against the abrasive tool during the operation (indicating where the part is being polished).	
Auditory feedback	Auditory feedback can indicate how much force is applied to the part and the level of degradation of the tool. However, auditory feedback for the operator is not important as the mandatory wear of ear plugs (PPE) reduces its effectiveness and they rely more heavily on vision/touch.	
Tactile Feedback	In standard operation, vibration is generated when the part makes contact with the abrasive belt. This allows the operator to know how much force is applied to the part and compensate for the torque generated from the vibration to keep a perpendicular contact.	
General Approaches	a. Polishing of the whole surface in a few passes at the beginning of the operation. b. Assessment of the quality of the surface frequently. c. Focusing at the specific area where features are located. d. Repeating b) and c) until the quality of the part is satisfactory.	
Individual Pattern	Changes the speed depending on the type and location of the features. Each pass is bidirectional, where one movement is done downwards (to remove a layer of material), followed by one movement upwards (to correct the pass). The heavy defects are removed after 5 passes. The rest of the operation was focused on the improvement of the quality of the surface.*	Changes speed, force, and position depending on the type and location of the features. Started by polishing the whole surface, then focused on complex geometrical features (e.g. radii, trailing edge), and finally focused at specific area (re-work)
Experiment Duration	Remove heavy defects: > 2min Improvement of the surface aspect: 14 min*	First polishing: 30 sec. Trailing edges: 7 sec. Re-work: 30 sec.

*note that in real industrial conditions with batches, the duration would be reduced (i.e. 1 min per part)

6.5.3 Material Removal Rate (MRR)

In addition to the data captured with the fixture, the profile of the polished surface was measured. The measurement of the surface profile was carried out using a laboratory custom-built blue laser scanner. The point cloud of data collected may help to determine the material removal rate (MRR) of the operators. Figure 6.7 shows the surface aspect of the sample workpiece before and after Experiment 2 (see Section 6.3).
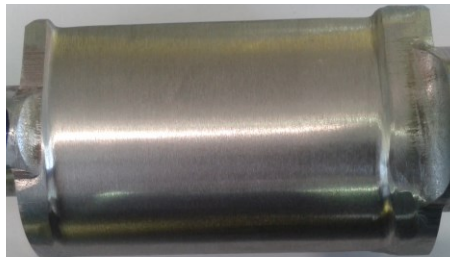
Figure 6.7: Surface texture before and after polishing

The 3D point cloud of the surface measured with the blue laser scanner (see Figure 6.8) shows the layer of material removed during the experiment. Using CAD software and data processing, the volume of material removed by the operator, was measured by comparing the measured surface to the original CAD file.
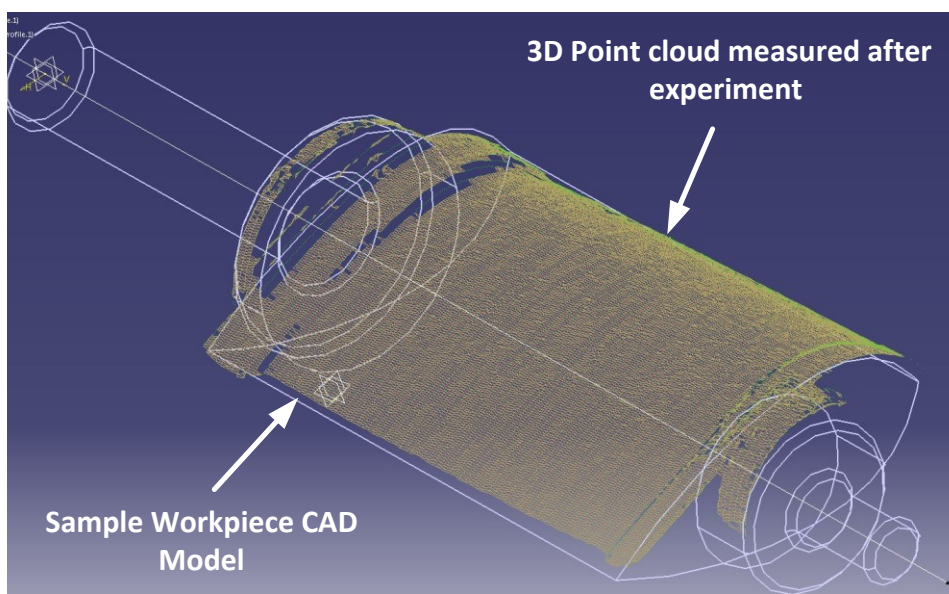
Figure 6.8: MRR measurement using 3D point cloud and CAD model

From the data shown in Figures 6.7 and 6.8, it can be observed that the operator removed a significant layer of material (over 2.5 mm) from the whole surface during Experiment 2. The operator was instructed to only remove the heavy grinding marks and to improve the surface roughness (Ra) until the quality of the surface was satisfactory.

Due to the operator's attention to detail, the polishing the sample workpiece took 15 min, including 2 min to remove the defects and 13 min to increase the surface quality. However, Operator 1 assures the author that in the normal industrial environment, less time would have been spent per workpiece (e.g. 1 min), such as with Operator 2. Therefore, less material would have been removed. Nonetheless, this does not affect the understanding of the manual polishing process as carried out by Operator 1. Moreover, it indicates that the operators adjust their polishing technique for each part through experimenting on sample parts.

6.5.4 Analysis of Polishing Action Frequency

The polishing process by each operator was completed in several passes. The number of passes and the frequency of their occurrence can vary between operators. It was found that the frequency of each polishing set changed as the operator understood the process better through tactile and visual sensing and adjusts the polishing parameters accordingly. It was also identified that the length of each polishing action changed depending on the action to carry out. In the example shown in Figure 6.9, it can be observed that the operator completes a pass in 5 s at the start of the operation but then speeds up to 3 s per pass at the end of the experiment.

Figure 6.9 illustrates the forces and torques measured in Experiment 2. It was mentioned earlier that, in addition to the force and torque output, each polishing action can be monitored through the multi-axial force and torque sensor. Based on the duration of each polishing action, the operator's speed can be calculated.
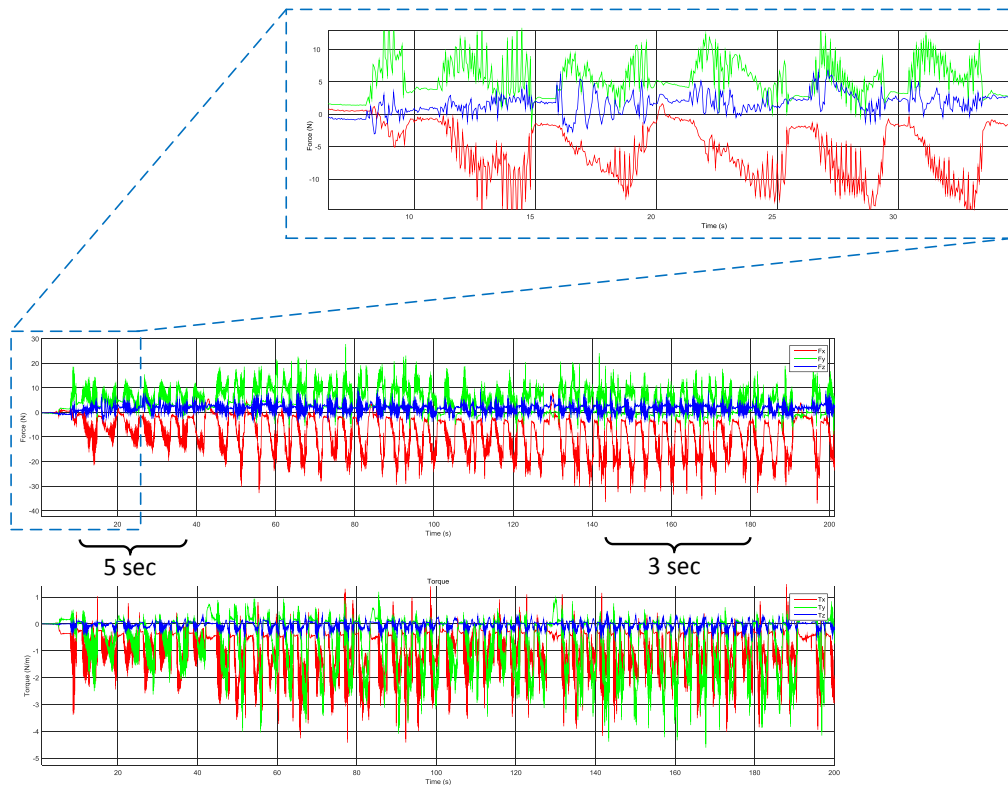
Figure 6.9: Example of the frequency of the polishing action

6.6 Preliminary Recommendations for Automation

The capture of parameters and variables for manual polishing operations was carried out in this chapter. Overall, the data collected supported the interviews and discussions with the operators, as well as the general approach and philosophy used in standard operation procedure (see Section 2.2 and Section 4.4).

In automation, these captured parameters should be translated by having a system that can follow the profile of the workpiece surface while controlling the force and feed rate depending on the defects to remove. Moreover, the automated polishing system should follow the same approach as the human operator (see Table 6.1). Therefore, the novel integrated robotic polishing system developed in this research should:

1. Follow (and control) the geometry of the workpiece being polished.
2. Identify and locate the defects on the surface, using 2D/3D vision technology.
3. Adapt the feed rate in real-time, depending on the location and type of defects.
4. Keep a constant force and perpendicular contact between the part and the abrasive tool, using force control.
5. Focus the polishing operation at specific area(s) only where required and not simply the whole surface.

Further details on recommendations for automation are given in the next chapter.

Chapter 7 Integrated Robotic Polishing System

This chapter describes the development of the proposed Integrated Robotic Polishing System (IRPS) based on the understanding of captured manual polishing processes. Initially in Section 7.1, the operator's patterns and parameters deployed in manual polishing are analysed and recommendations for automation are discussed. Sections 7.2 to 7.3 present the development of the test rig and user interface for the IRPS. Finally, the tests of the IRPS are discussed in Sections 7.4 and 7.7.

7.1 Translating Manual Polishing Parameters for an Automation System

Currently, there are a number of robotic polishing prototypes developed by various industrial and research groups. It was discussed, in Chapters 1 and 2, that the main success of existing systems has been in polishing of simple parts, and no system is currently deployed at industrial production level for more complicated components.

A large amount of these automated systems typically use a robotic arm that follows a trajectory based on parts' CAD model. In addition, a constant force feedback is received from the point of contact with the abrasive tool that enables adjusting the trajectory based on the force threshold predefined for the system.

However, in manufacturing of high-value components, the schematics and engineering documents are often not available to the finishing suppliers due to information sensitivity (see Chapter 4), and therefore the robotic polishing has to be pre-programmed based on individual components. This has proved to be impractical and time-consuming at industrial level.

In addition, it was experienced that the current automation technology available in the market cannot compete with the human operation in term of speed and flexibility (see Chapter 4). This was especially noticed when in-process control quality is carried out by operators. For instance, when our industrial partner tested an automated robotic system

within their processes, their system failed because it could not match the flexibly and speed of their skilled workers, in term of rapid reasoning, decision making, and fast adjustment.

In this research, the captured parameters and variables discussed in Chapter 6 were translated and used to develop a similar mechatronic-based polishing system, referred to as IRPS (Integrated Robotic Polishing System) in this research. Some of the lessons learned from manual operation were considered essential for the design of the automated polishing system. Nonetheless, it was also understood that some of the techniques used by the operators are deployed due to limitations of humans' dexterity and control, to accurately adjust process parameters and variables such as motion, orientation, force and torque.

The main findings from capturing manual polishing operations indicates a number of critical design consideration for the development of the proposed integrated robotic polishing system (IRPS). These are summarised below and in Table 7.1.

Three polishing patterns were identified in manual polishing operations (see Chapters 4 and 6). The first pattern captured was Pattern A - constant pressure. In this technique the operator applies a static pressure at a specific location onto the surface. This is used to remove specific features from the surface of a part. The second pattern captured was Pattern B - linear translation, where the operator applies a constant force while moving horizontally. This technique is often used to deburr the trailing and leading edged. Lastly, the third pattern captured was Pattern C - surface profiling, where the operator was following the geometry of the surface. This was used to remove a uniform layer of material along the surface.

For polishing parts with complex surface curvatures, it was clear that skilled operators tend to follow the profile of the workpiece surface while keeping a constant force with a perpendicular contact angle to the abrasive tool. In addition, this perpendicular contact angle minimises torques applied to the surface and therefore makes the part handling easier and more stable. Moreover, skilled operators simply and continuously detect and rectify misalignment of the contact angle (e.g. torque compensation), while maintaining a normal contact point. These techniques allow the operator to remove the defects and improve the surface finish without affecting the part geometry.

Furthermore, it was observed that in addition to surface profiling, operators polish thin features of the parts, such as the trailing or leading edge, using a linear movement (Pattern B). This technique allows the operator to deburr or straighten the edges, and to remove material or features that would not be removed with surface profiling (Pattern C). It was observed that this approach is used due to the complexity of the geometry and the limitation of the operators' dexterity and their control over the polishing parameters. For instance, it was observed that in polishing of thin or sharp edges, this would require finer motor skills and a more accurate force control by the operator to avoid damaging the part or getting injured.

To compensate the need for such high level of accuracy, operators change their polishing pattern (from Pattern C to B). However, it was envisaged that a robotic arm would be able to remove a layer of material on the whole surface in one pass, without the need for changing the patterns. This could be achieved by providing sufficient sensory feedback along the surface profile.

Hence, a gradual decrease of the machining speed should be embedded to the automation system when approaching the trailing and leading edges of the component. This should be based on continuously monitoring the polishing force and not following the pre-existing data such as CAD/CAM which, as explained earlier, may not be available.

By further analysing the experiments' results, it was understood that polishing force (and its associated torques) is an important variable that operators tend to monitor and keep constant. The reason is that the large magnitude of the tactile sensing feedback generated by the force is easily detected and controlled by the operator. The torques generated during the polishing process are also tend to be compensated by the operator, through maintaining them in one direction by adjusting the blending contact with the abrasive tool. It was envisaged that in automation a multi-axial force and torque sensor could be used to ensure that the contact force is uniform and perpendicular to the abrasive tool.

The speed or feed rate was also analysed and was identified as an important parameter for the manual operators. Skilled operators would often change their speed depending on the type of feature or surface. Therefore, to vary the volume of material to remove (or MRR), operators tend to maintain a constant polishing force and vary speed or feed rate for optimal polishing. For example, in order to remove a defect, the operator decreases their speed to remove more material. Conversely, to avoid altering the surface aspect, the operator's speed increases.

It was envisaged that a similar approach can be adopted for the automated system. For instance, during a rework process to remove surface defects, the material removal rate would be increased in the region where the defect is located. This could be achieved by increasing contact force or by reducing feed rate.

It was also observed that vibrations are also accounted for by the operators. Vibrations is generated when the part is in contact with the abrasive tool while the operator compensate the torque with their hand to keep the workpiece in perpendicular angel to the tool. Vibrations are mainly used by the operator as an indication for the magnitude of polishing force and pace used through tactile feedback. However, vibrations may cause damage to the surface quality or faster tool wear. Therefore, additional sensors are still required to replicate the tactile feedback that operators receive from vibrations. On the other hand, the stiffness of robot arms should negate the undesirable impact of vibration on surface quality (Ilangovan et al., 2016). Replicating vibration feedback in automated system is beyond the scope of this research.

In addition to the tactile feedback, skilled operators also use visual and auditory feedback to monitor and adjust polishing parameters in real-time. Auditory feedback could be used by skilled operators to identify tool wear, excessive amount of machining force, and change in material. However, auditory feedback can be difficult due to the mandatory use of personal protective equipment (PPE). Therefore, the auditory feedback is excluded from this research.

It was observed that visual feedback is extensively used by manual polishers to assess the quality of the polished surface, locate potential defects between polishing passes, and monitor the blending process. Machine vision technology can be deployed as part of the IRPS to replicate the visual feedback in a similar way. However, the speed of such feedback

is expected to be much lower than those generated by a human. On the other hand, this could be compensated by the need for less rework due to the consistency of the automated system.

Hence, it was decided that similarly to the manual polishing process, the speed of the operation with an automated system could be better and more accurately controlled than the polishing force. In an automated defect removal process, varying force and feed rate would require integration of a vision system (to identify the location of the defects) and a multi-axial force and torque sensor (to measure the force) to the robot. However, varying only the feed rate may eliminate the need for the force control feedback, and therefore improves the overall efficiency of the system.

While human operator adjusts process parameters in real-time, this could be a major design issue when polishing complex curvatures using a robotic arm. It can be assumed that the speed of data exchange can hinder the polishing performance, therefore the automated system may fall behind (as discussed with the industrial partner who failed to implement a prototype automated system). Therefore, it was concluded that an automated system requires an additional feedback loop to vary the process speed through feed rate in accordance with the system performance. This would allow collecting and applying all sensory data in real-time.

In general, it is suggested that the overall polishing strategy used by skilled operators could also be implemented within a robotic arm equipped with the necessary sensors. A number of techniques used by skilled operators such as constant contact force, change of feed rate, assessing the surface quality visually, torque compensation, and using specific patterns, can be supported by a mechatronic polishing system. Some of the individual habits and techniques that change from one operator to another, which depends on their skill level, experience, and capability and dexterity to maintained that level of skill are not included within the scope of this research.

As part of the general conclusions from the site and laboratory observations, it was also observed that while most skilled operators are capable of maintaining the same level of skills, number of errors increases by the duration of polishing processes, therefore affecting the number of re-works. This is clearly due to the fatigue that occurs frequently in such laborious processes. This highlights one of the main advantage of automated systems over manual polishing process. Interpretation of manual polishing processes to the automated one is summarised in Table 7.1.

Table 7.1: Translation of manual polishing into an automated system

Parameters	Manual Procedure	Automated System
Path	Follow profile of the part and uses different movements for more complex features	Pre-programmed routine(s) or sub-routine(s) for each geometry and feature to remove via CAD/CAM or teach pendant.
Contact Force and Torque	Contact force kept constant during the entire operation. Tactile feedback provided through operator's hands. No additional torque should be involved due to constant contact force and perpendicular contact to the abrasive belt	Force control using force and torque sensor. The robot will adapt its position and orientation based on the FT data to keep 1) constant contact force, and 2) perpendicular contact
Vibration	Compensated by operators' hand to keep perpendicular contact	Robot stiffness should be enough against the level of vibration expected. Alternatively, design damping system for grippers can be considered.
Speed	Change speed depending on the type and location of the defect.	Change feed rate of the programmed routine or sub-routine.
Visual feedback	a. Assess surface quality b. Monitor process during blending contact	a. 2D vision to identify and locate defects. Laser scanner to measure the surface roughness and measure surface profile. Helios system to measure defects. b. Can be done through force/position control
Auditory feedback	Indicates to the operator the amount of force applied and the level of degradation of the tool.	Use of AE sensor to monitor tool wear and control force. However, may not be necessary if multi-axial force and torque sensor is already used.
Tactile feedback	Allows the operator to know how much force is applied on the part.	Use of force control.
Operation strategy	1. Inspect and locate features 2. Polish at specific area where defect is located (use different techniques if needed) 3. Repeat until surface texture is satisfactory	Follow operator strategy using vision system and pre-planned program modifications for defects. Force control would be used keep a constant and perpendicular force during the whole operation. Feed rate would be changed based on the surface feature. Finally, the process would be carried out until the surface texture is satisfactory.

7.2   Automated Polishing Cell

The automated polishing cell is a test rig developed within the research laboratory, as part of this research for manual and automated polishing experiments. The test rig includes a KUKA KR16 industrial robot, a KRC2 controller, a commercial multi-axial force and torque sensor (Shunk Gamma) and dual-finishing station (RJH Fallow). The test rig is enclosed with clear glass panelling to protect the user from the dust and noise whilst enabling them to monitor the operation from outside.

In addition, a set of software applications and a user interface were developed by the author to integrate the robot control system to a set of sensors deployed for the IRPS. Furthermore, a new control algorithms have been invented to embed the lessons learned from manual polishing operations to the automated system. Further information on the user interface is presented in Section 7.3.

The developed fixture, explained in Chapter 5, was partially used and mounted onto the robot end-effector as an adaptor. This adaptor embedded with a multi-axial force and torque sensor, the sample workpiece for polishing, and the dust cover. The Vicon MoCap and IMU sensors were not implemented in the rig, as the robot controller can provide position and orientation data, as well as feed rate and speed.
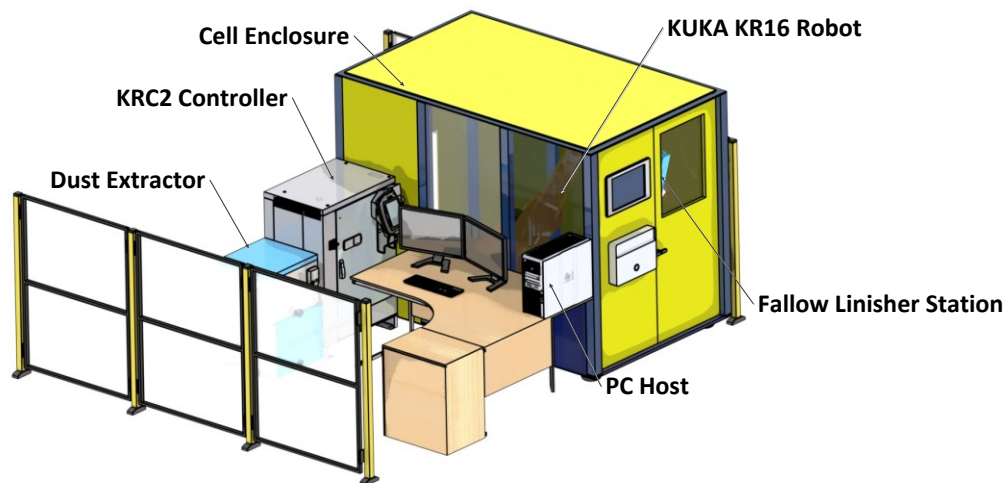
Figure 7.1: Developed cell for the intelligent automated polishing system

7.3 Integrated Robotic Polishing System (IRPS)

The proposed IRPS is a proof-of-concept automated polishing cell designed and built as part of this research based on the manual polishing parameters and operators' skills identified by this research. The following sections summarise the development of this system.

7.3.1 System Description

The main capabilities of the IRPS was aimed at achieving: a) tracking the geometry of a workpiece by manipulating the robot trajectory in real time, b) identifying and locating potential defects on the surface, c) adapting the process parameters such as changing the feed rate in real-time based on the type of defects while maintaining a constant perpendicular polishing forces using force control sensor, and d) manipulating the part orientation in relation with the abrasive tool to minimise the undesirable torques and forces. Figure 7.2 illustrates some of the operational parameters of the system.

The IRPS includes sets of commercial and laboratory built hardware and software, as illustrated by Figure 7.3. The system comprises of a 6 DoF KUKA robot and controller, a Shunk Gamma multi-axial force and torque sensor, and a dual-finishing station that are available commercially. Both multi-axial force and torque sensor and the robot arm are integrated via Ethernet through a custom built user interface developed by the author.

The multi-axial force and torque sensor is connected to a NetBox (Automation, 2013) allowing the streaming of data in real-time. The robot exchanges data using KUKA XML software via TCP/IP protocol. The KUKA XML allows to send and receive a string of data from and to the robot through the real time operating system.

A set of developed algorithms embedded in the user interface calculates the next position of the robot trajectory. The algorithms generate continuously the next point in the trajectory based on the sensory data and the conditions put in place by the developer. The data exchange is carried out once the robot has moved to its final position, i.e. the last point of the location send to the robot in a point-to-point programming method. While the robot moves to the instructed position, the algorithms generate the next positional point to be send to the robot. A point-to-point approach had to be use due to the limitation of KUKA XML.

The user interface was developed to integrate the different hardware and software solutions. As illustrated in Figure 7.3, the user interface is used to communicate with the robotic controller; collect force and torque data in real-time; locate defects through vision system (not physically implemented in this research); change feed rate and tool rotation speed; and implement strategy learned from manual polishing operation. Consequently, a new set of parameters including position and feed rate are sent to the robot controller. This is repeated until the quality of the part surface is satisfactory.

Further functionality could be simply added to the user interface to control the cutting speed of the abrasive tool. However, this facility was not available in the developed polishing cell.
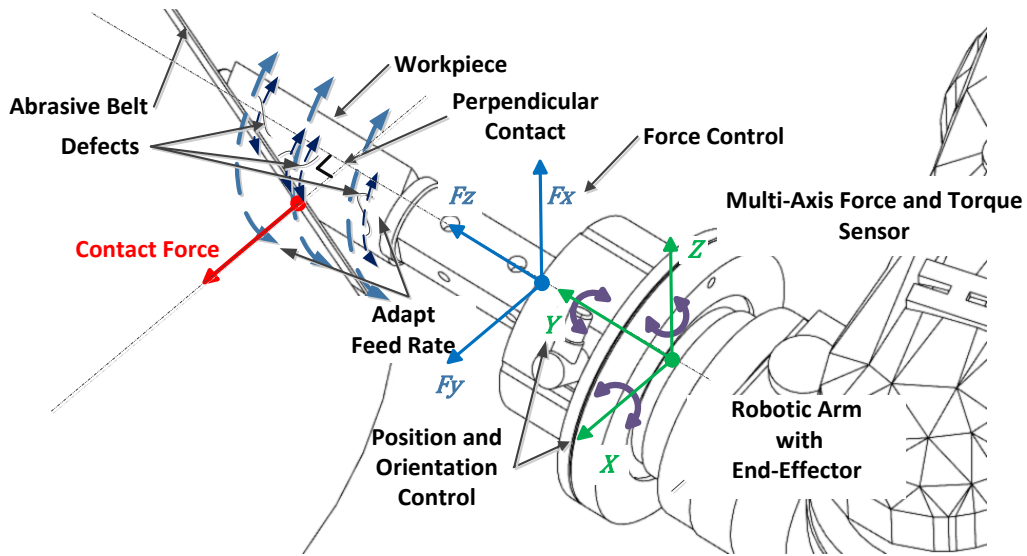
Figure 7.2: Integrated Robotic Polishing System diagram 1 of 2
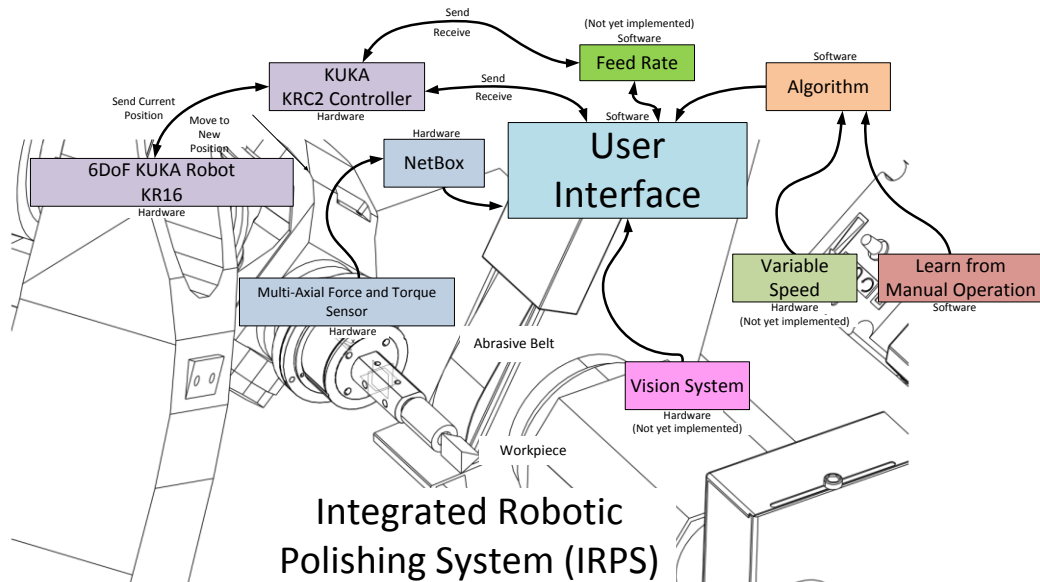
Figure 7.3: Integrated Robotic Polishing System diagram 2 of 2

7.3.2 User Interface

A graphical user interface (GUI) was designed and developed by the author to integrate and synchronise the multi-axial force and torque sensor with the robotic arm controller, collect data from both the sensors and end-effector, and calculate new incremental positions for the robot until the desired polishing force is reached. In addition, the user interface allows the user to input and control desired parameters, such as the polishing force thresholds and minimum positional increments.

The developed user interface, illustrated in Figure 7.4, shows the various interface components and the inputs/outputs data of the system. This includes: the position and orientation of the end-effector (in Cartesian and Joint axes); the multi-axial force and torque sensor data in real-time and at specific points; the desired user inputs (desired force and incremental position – i.e. operational conditions); and the calculation of the new position for the end-effector based on the data collected and the user input.
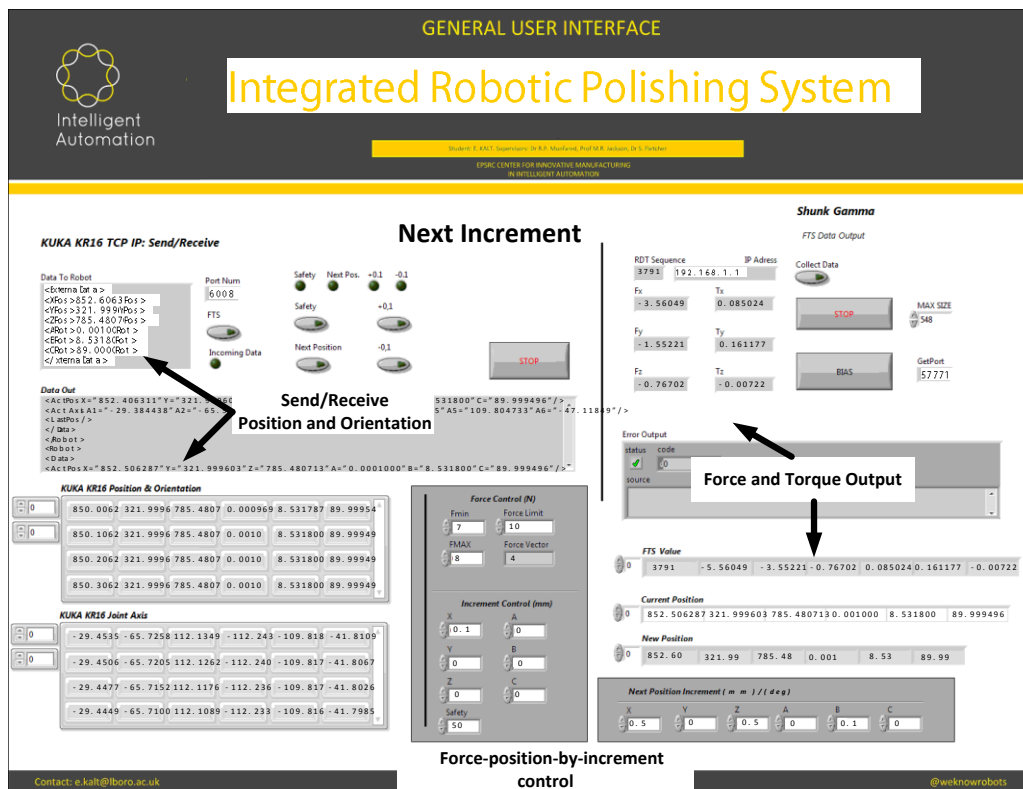
Figure 7.4: Graphical User Interface developed for the IRPS

Further details on the GUI are illustrated in Figures 7.5 to 7.8. Figure 7.5 illustrates the string of data received and send from and to the robot controller via TCP/IP protocol and KUKA XML.
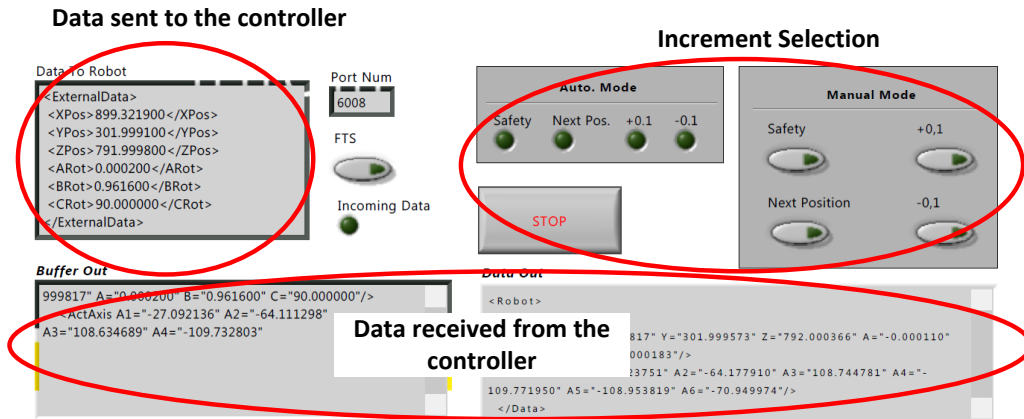
Figure 7.5: Send and receive data to/from robot

Figure 7.6 illustrates the string of data received from the robot controller stored into two arrays (one for the position and orientation data in Cartesian axis and one for in Joints angles). These data are then used to calculate a new positional value based on the force recorded, and for further data analysis carried out offline.
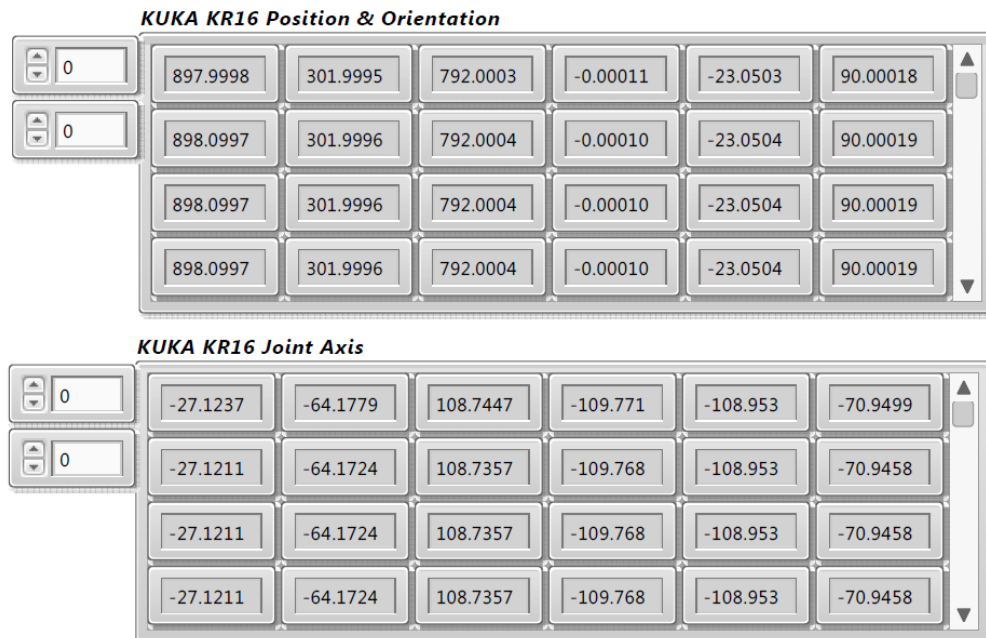
Figure 7.6: Robot positional data (Cartesian and joint Axis) into Array

Figure 7.7 shows a functional component of the user interface that enables real-time streaming of data from the multi-axial force and torque sensor. Force values are display in N (Newton) and torque values in Nm (Newton meter).
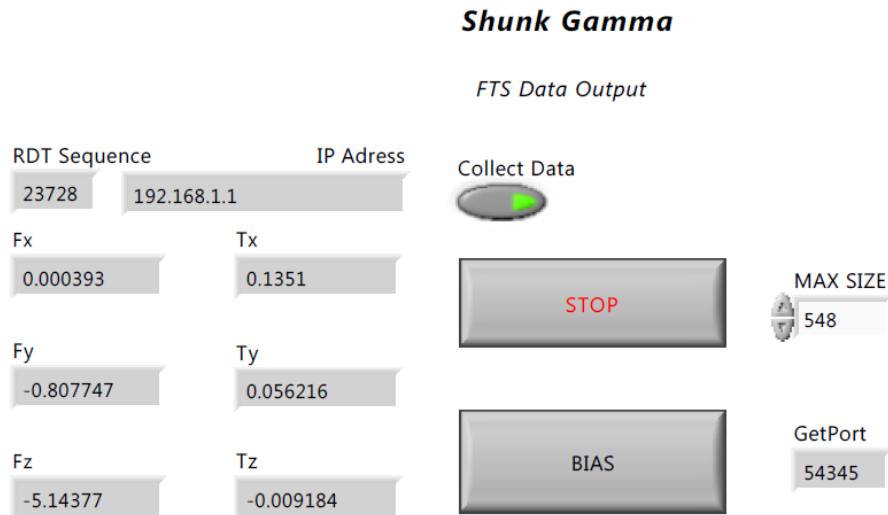
Figure 7.7: Stream force and torque data in real-time

Lastly, Figure 7.8 illustrates the main panel of the user interface for the IRPS. Figure 7.8(A) shows the user input for the desired polishing force and the incremental value for the end-effector to use (in a repeated loop until reaching the desired force). Figure 7.8(B) shows the second input panel for the user to configure based on the geometry of the surface. Finally, Figure 7.8(C) is presenting the calculation of the new *xyz* coordinate of the robot arm based on the force output and the current position of the end-effector.
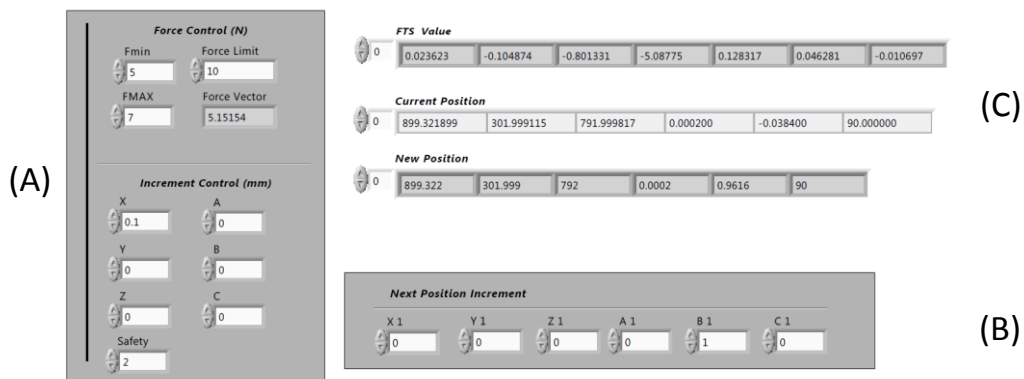
Figure 7.8: Force-position-by-increment panel

7.3.3   Algorithms to calculate the positional data

As part of the developed user interface, the data collected from the sensors are analysed in real time and the next positional data set is generated to define the subsequent coordination data that robot should increment to. A new force-position-by-increment algorithm was developed to calculate the next coordination data based on the sensory feedback, and the polishing strategy (e.g. functional conditions) interpreted from the manual operations.

Table 7.2 illustrates the different functions and tools developed for the force-position-by-increment algorithm. Functions 1 and 2 stream and convert data from the multi-axial force and torque sensor. Functions 3 and 4 convert the positional data (as a string) from the robot to one array for the position in Cartesian coordinates and one array for the value of the Joint axes respectively. Functions 5 to 8 are used for data manipulation before calculating a new incremental position for the robot. Finally, functions 9 and 10 are used for gravity compensation to remove the inertia and weight effect from the multi-axial force and torque output.

Table 7.2: Functions developed for the force-position-increment control algorithm

No.	Function	Description
1		Convert signal into force (N) and torque (Nm)
2		Stream and collect force and torque data in real time
3		Save string of data from the robot into an array and keep only the values for the joints axis
4		Save string of data from the robot into an array and keep only the values for Cartesian coordinates
5		Remove duplicates of position
6		Match string position
7		Remove previous position
8		Convert string value to a double integer value
9		Look up table for force gravity compensation
10		Compute current force value

As illustrated in Figure 7.9, the user interface receives coordination data from the robotic arm. These data are then stored into two arrays, one array for Cartesian and the other for Joint Axis coordinates. Once the end-effector position is received, the multi-axial force and torque sensor is triggered. Then the force and torque output is merged to the current position of the end-effector. Based on this information recieved, a new coordinate is calculated and then send back to the robot arm, as illustrated in Figures 7.9 and 7.10.
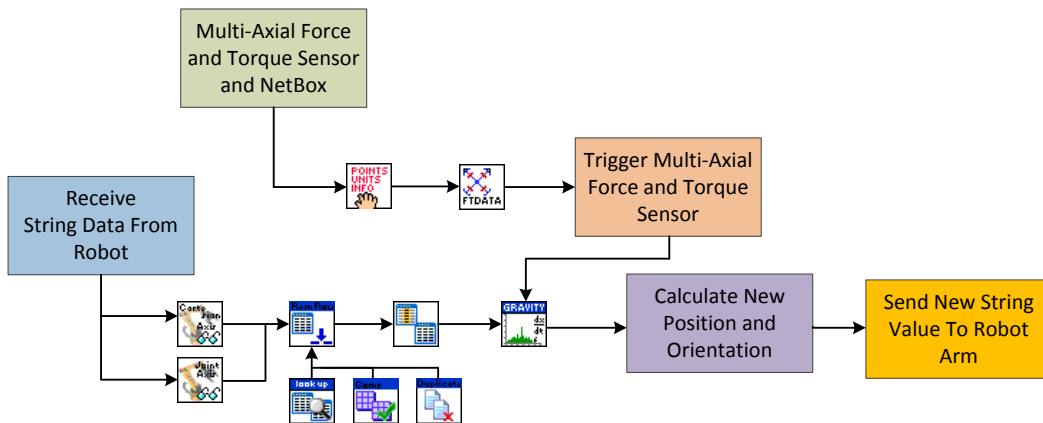
Figure 7.9: Block diagram of the developed algorithms for the IRPS

In this method, the force output of the multi-axial force and torque sensor is captured at each position of the robot end-effector. A new position is then calculated based on the force captured. For example, if the captured force is below the desired force limit, the robot would then move forward with an increment of 0.1 mm until reaching the desired contact force, as illustrated in Figure 7.10. In this manner, the polishing operation is uniform across the whole surface and the need for CAD data would be removed as the robot follows the surface based on the output force.
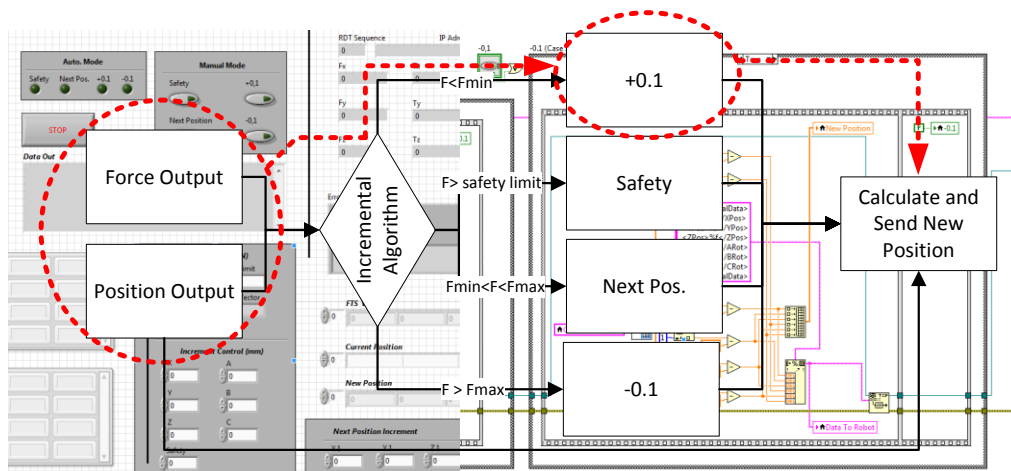
Figure 7.10: Example of the force-position-by-increment algorithm

7.3.4   Automated Polishing Experiments

Following the development of the IRPS cell, a set of experiment were designed to test the system and validate the design concept. Further three experiments were designed to test the applicability and the viability of the proposed system. The first three experiments with the hand held fixture were discussed in Chapter 6.

In Experiment 4, the multi-axial force and torque sensor was calibrated for the robotic system to ensure precision of the data received from the sensor.

In Experiment 5, a layer of material was removed from a curved surface of a part, based on the available CAD geometry of the workpiece. This experiment was carried out to test and calibrate the robot motions by eliminating some of the system variables, such as the real time trajectory adjustment. This experiment was to imitate the way that skilled operators follow the profile of the part, to assess the robot precision by comparing with the CAD data, and to determine the minimum amount of polishing force (i.e. force threshold) necessary to polish the part.

In Experiment 6, the IRPS was put into practice by polishing the surface of a spectrum of parts with various geometrical profiles, categorised from "easy" to "hard". Three different parts were considered: a cylindrical, curved and triangular part. No CAD information of the parts' profiles was made available to the system.

A cylindrical part that represented a simple profile for an automated system, locates at the easy side of the spectrum (see Figure 7.11). This profile is considered easy for the automated system because only one robot motion, i.e. rotation, has to be controlled to meet the profile. Nonetheless, this profile is probably one of the most difficult for manual operation, due to the insufficient positional control by skilled operators.
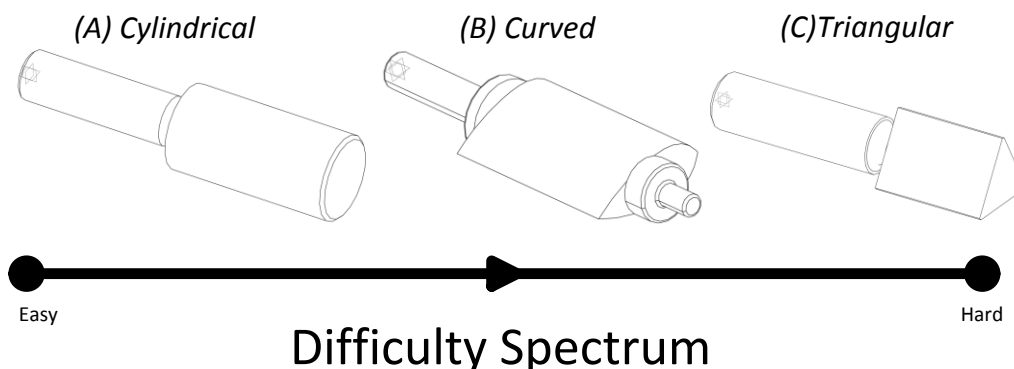
Figure 7.11: Difficulty spectrum for the part surface profiles

At the other side of the difficulty spectrum, a triangular part was tested. The polishing of the flat surfaces of this part represented one of the most difficult polishing operation using a robotic arm. For the purpose of this experiment, the triangular sample is polished in a similar way to the cylindrical or curved surface, as illustrated in Figure 7.12. Therefore, to polish the triangular surface, the IRPS would adjust the position along *x-axis* until the desired force is achieved. Then, it moves to the next point on the surface with a rotation in *y-axis* and a translation in *x-axis,* away from the polishing tool. The difficulty of this profile is due to the fact that, to maintain the flatness of the surface, the magnitude of the positional increments should be minimised and measured in three axes. In addition, the highest level of force control should be deployed to detect the slightest changes in the force, which in turn triggers trajectory adjustments.

Arguably, this profile could be considered the easiest form for manual polishing operations, as the operators could use a different polishing pattern (i.e. linear translation or flat movement – Patter B) to complete the part. However, the rationale for choosing this part is to test the applicability of the IRPS in an extreme case scenario – and by doing so, assessing the level of generality of the approach proposed.

It should be noted that the author is not recommending the proposed approach for polishing a flat surface profile. In a normal operation, the polishing of a flat surface is done without significant positional feedback, as the movement of the robot is linear.

Any curved profile, such as those used by the industrial partners (i.e. form B in figures 7.11 and 7.12) is expected to fall between the two ends of the difficulty spectrum, therefore the experiment was focused on the cylindrical and triangular profiles.
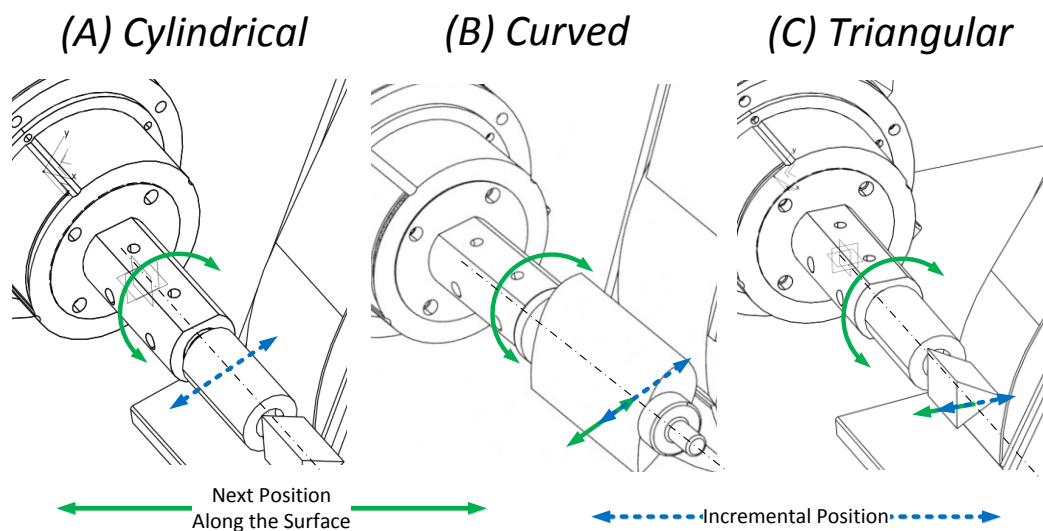
Figure 7.12: Automated polishing approach for various surfaces

7.4 Experiment 4: Multi-Axial Force and Torque Sensor Calibration

Prior to the IRPS polishing experiments, it was important to test and calibrate the multi-axial force and torque sensor. The main reason for this calibration experiment was to investigate, understand and accommodate into algorithms, the gravity and inertia effect observed in Section 5.5, intended for robotic application.

The literature review showed that the dynamic behaviour of force and torque sensors has rarely been investigated due to the complexity involved. In force control for robotics, the use of Jacobians of the robot kinematics is necessary (Villani and Federico, 2007). Using the Jacobian to compute the dynamic behaviour of the force and torque sensor may be accurate but can be challenging. Some researchers have explored different methods of gravity compensation, but there is still a need for further work. For example, L. Richter and R. Bruder (Richter and Bruder, 2013; Richter et al., 2012, 2010) developed a method based on acceleration and gravitational effects to compensate for force and torque error.

In their research, the authors assumed that the effect of the gravity ($\vec{g}$) was given by the weight of the force and torque sensor and the weight of the gripper attached at the end-effector. Therefore, the calibration of the multi-axial force and torque sensor was carried out with similar equations and methodology to L. Richter and R. Bruder (Richter and Bruder, 2013; Richter et al., 2012, 2010) , as illustrated in Figure 7.13. Further details on this investigation and experiment are given in Appendix I. The result of this calibrated was used to compensate the gravity within the force-position-by-increment algorithms.

$$F_g = \left({}^{E}\zeta_{FT} \right)^{-1} . \left({}^{R}\zeta_{E} \right)^{-1} . F_0$$

$$f_t = \frac{M_f}{l_c}$$

$$F_0 = \begin{pmatrix} F_x^0 \\ F_y^0 \\ F_z^0 \end{pmatrix} = \begin{pmatrix} 0 \\ 0 \\ -f \end{pmatrix}$$
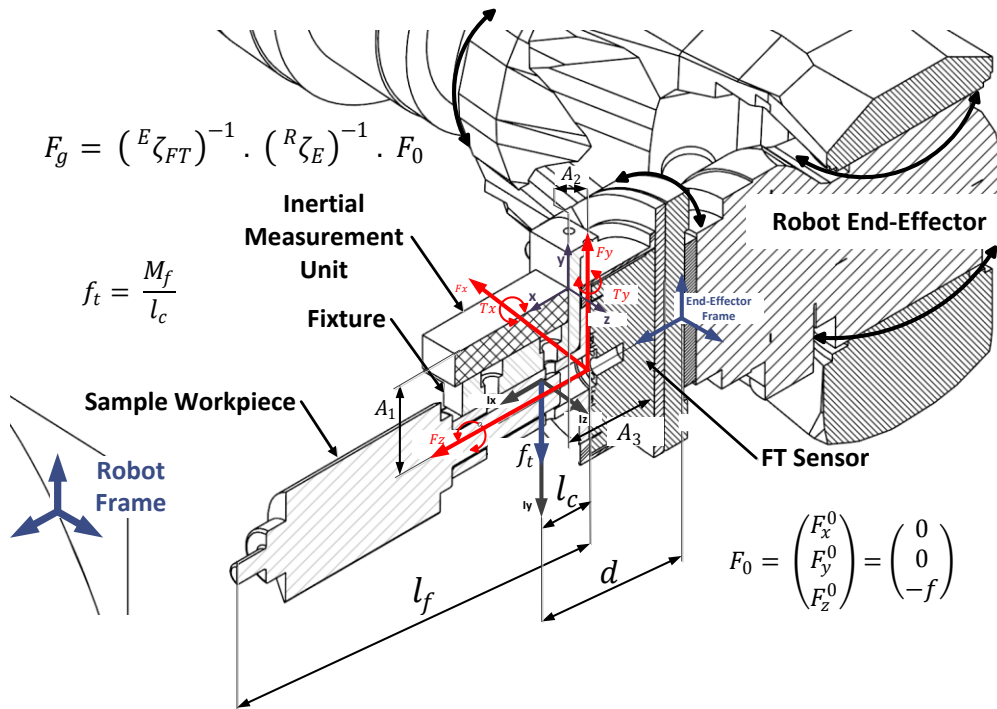
Figure 7.13: Force gravity investigation

7.5 Experiment 5: Surface Profile-Based Trajectory

This experiment focused on collecting force and torque data when following the profile of the workpiece. This was named Surface Profiling (Pattern C) and is found to be one of the main techniques used in manual polishing processes. The objective of this experiment was to compare the robot positional data with the CAD data and assess the ability of the robot to trace the part profile. In addition, in this experiment the nominal force threshold was determined.

The IRPS had the task to follow the profile of the workpiece (as illustrated in Figure 7.14) in the same way that the skilled operator carried out the operation with the fixture (see Chapter 6). A number of safety measures were also added to the algorithms, for example, "if the polishing force exceeded 10 N, the end-effector will retract to a safe position".

As the geometry and dimensions of the sample workpiece are known from the CAD model, it was possible to generate a tool path for the robotic arm from several points on the surface of the workpiece (shown in Figures 7.14).

Figure 7.15 presents part of the experiment's results. It can be observed in this diagram that the robot followed the profile of the workpiece with an adequate precision. In addition, the polishing force was successfully collected for each point of the surface profile in real time. Finally, the safety measure was tested successfully by intentionally increasing the force. The diagram in Figure 7.15 illustrates that the robotic arm has move to the safe position six times as the polishing force exceeded 10 N.
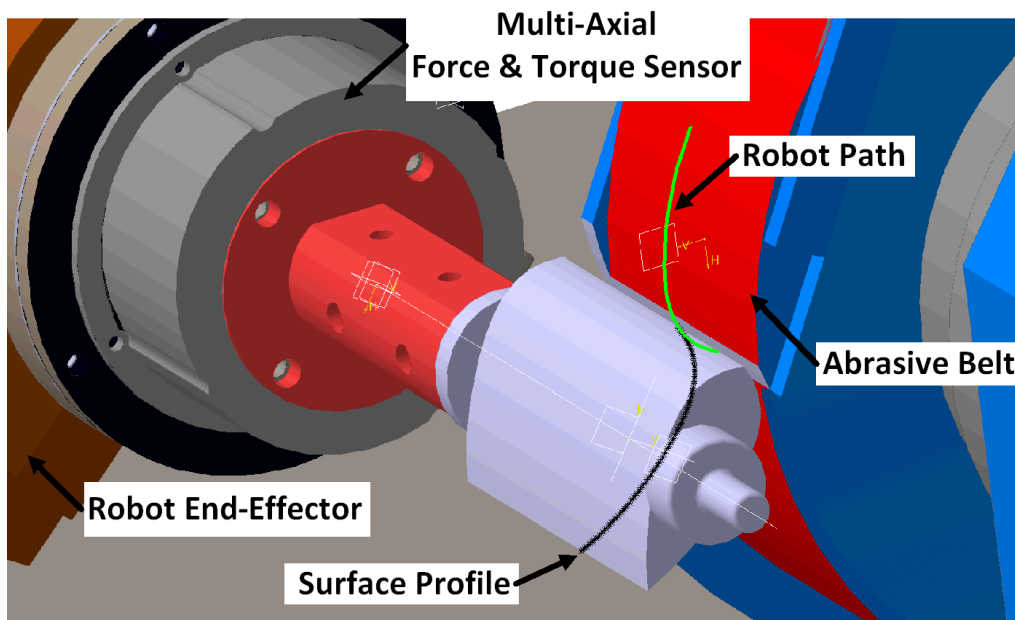
Figure 7.14: Diagram of the automated system following the profile of the sample
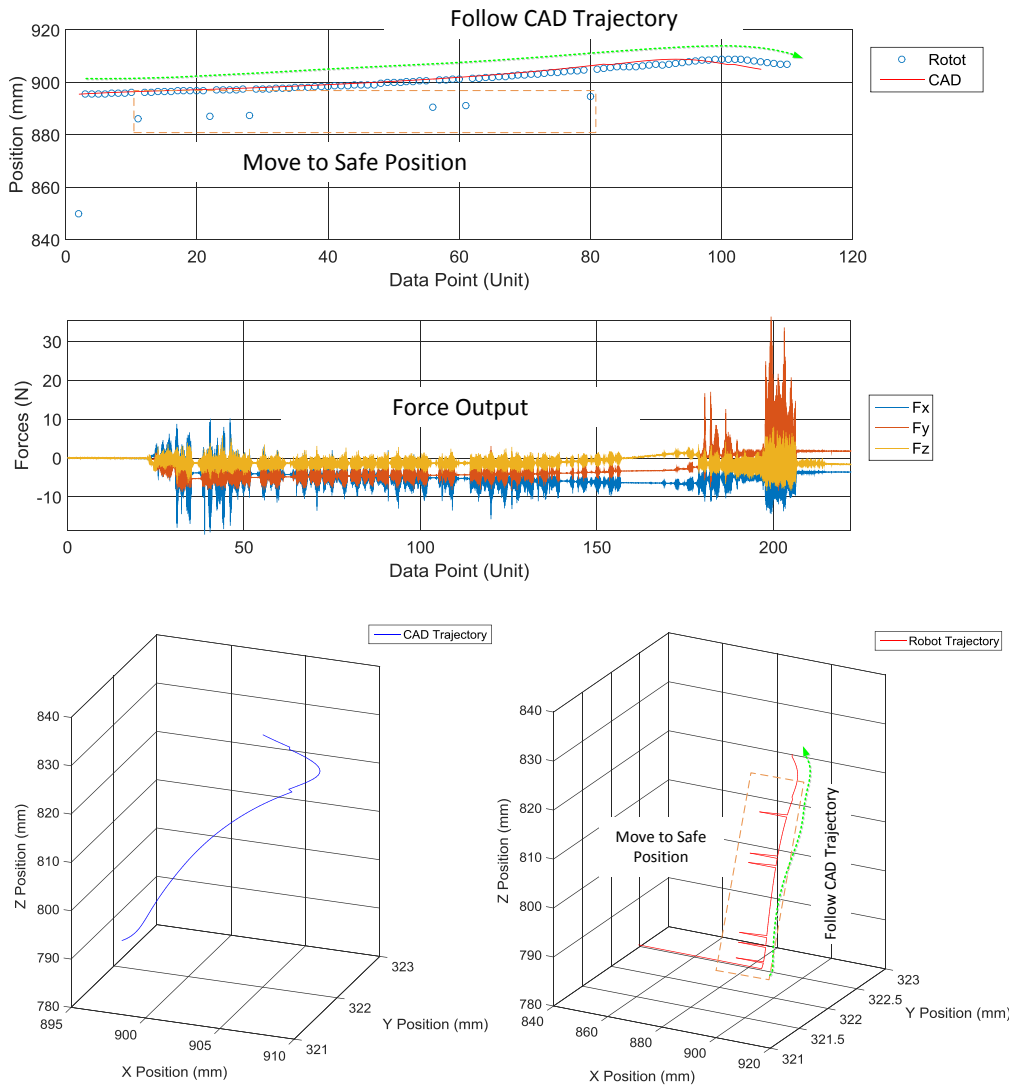
Figure 7.15: Force and path for surface profiling of a complex surface

7.6 Experiment 6: Free-Form Path Control

In the previous experiment, the part was polished based on the CAD geometry to simulate how human operators follow the geometry. However, the operator does not have CAD data or geometry data as part of their polishing processes. The ability of the operator to follow the profile of the surface is based on the tactile feedback from the force applied to the surface. The following experiments are aimed at polishing sample workpieces based on the polishing force and not the CAD geometry.

The "User" panel of the developed user interface tool is divided into several sections, as seen in Figures 7.4 to 7.8. The main section controls the polishing force, including the minimum and maximum force values that the user applies (in this case, the robot force thresholds), the limit value before the robot goes to a safety position, and the polishing force applied at the current position. The user chooses the increment value and axis (as well as the direction) of the robot to move until reaching the desired force. The user also chooses the next relative position to polish the surface. This is based on the fine motor skills of the human operator (often using their whole body) to follow the profile of the part via touch feedback.
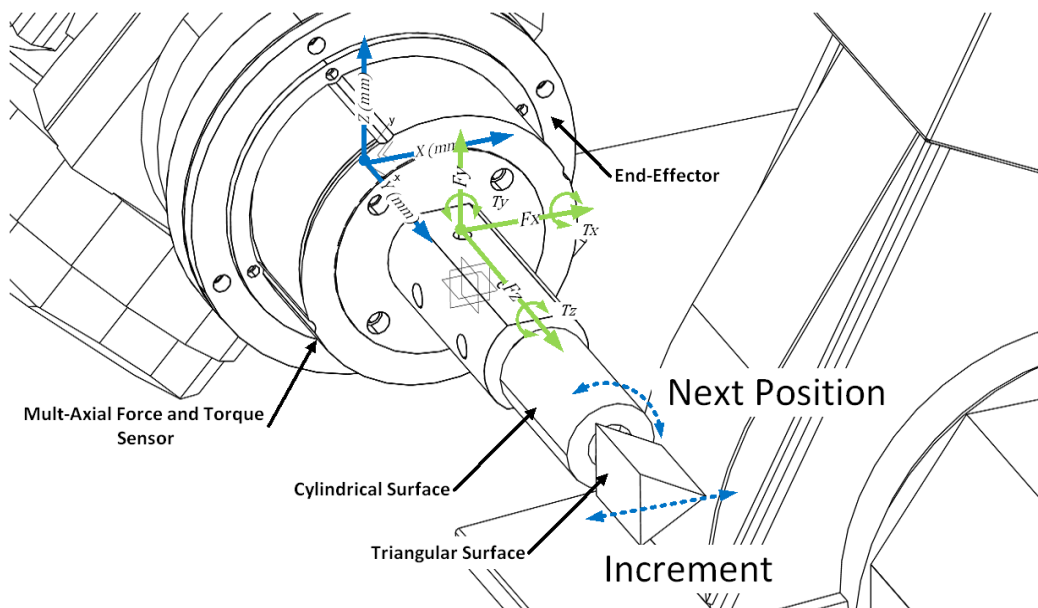
Figure 7.16: Free-form polishing for triangular and cylindrical surfaces

Figures 7.16 and 7.17 illustrates the polishing operation of two surfaces (cylindrical and triangular) with the IRPS and the force-position-by-increment algorithm. To polish a cylindrical or triangular surface without any CAD data, a general scenario was used where the user requires the robot to apply a force of 7.5±0.5 N to the surface (polishing force for robotic system was identified between 7 and 8 N in experiment 4). The algorithm adds or subtracts an incremental value of 0.1mm to/from the current position of the robotic arm until reaching the desired force (7.5±0.5 N). The algorithm then generates and sends the new set of data to the controller for the robot to move to its next position on the surface.

This would be repeated until the whole surface is polished. Figure 7.16 illustrates part of the actual workpiece polished in the IRPS cell.
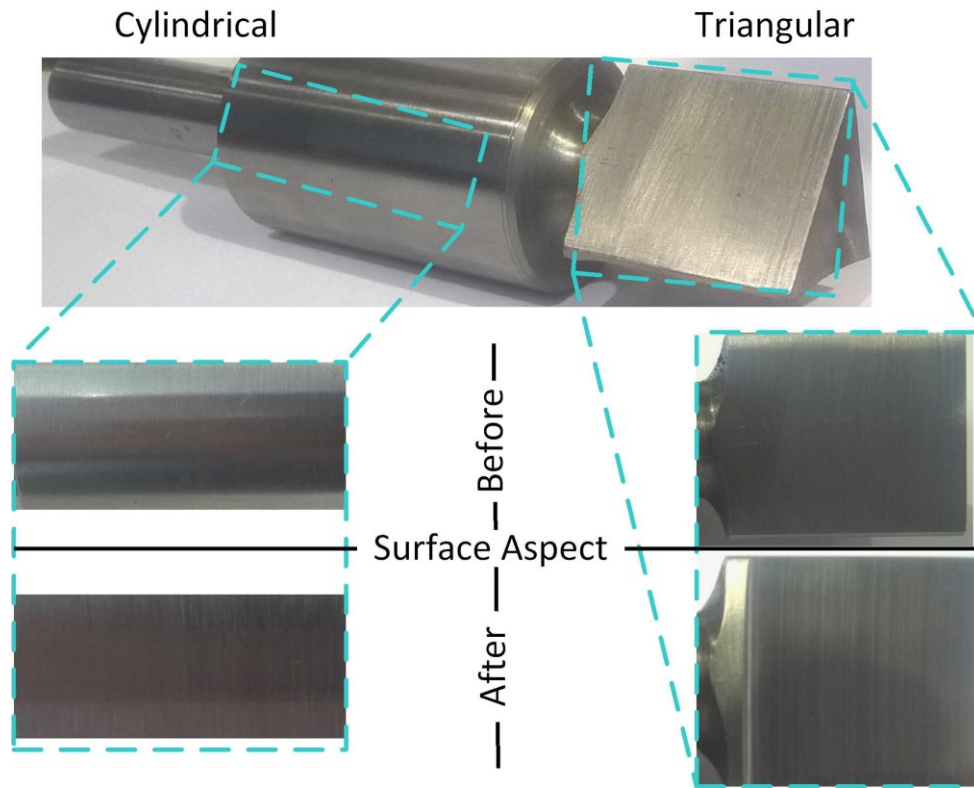
Figure 7.17: Quality of the surface finishing before and after polishing operation with the IRPS

7.6.1   Free-Form Polishing Operation of a Cylindrical Surface

The first test carried out with the developed Integrated Robotic Polishing System was focused on polishing of a cylindrical surface. Unlike human, the robot end-effector can control the position and orientation solely in one direction in order to keep the constant force on a cylindrical surface, where an operator would change position in *x* and *z-axis* (*Px* and *Pz*) and orientation in *y-axis* (*Ry*).

For this experiment, the user used a polishing force of 4.5±1.5 N to be applied on the surface with an incremental position of ±0.1 mm in the *x*-axis. If the polishing force reached or exceeded 10 N, the end-effector would move to a safe position (2 mm in *x*-axis). Once the desired force had been obtained at a point, the end-effector would move to the next relative position (1 mm in *B*-axis).

Figures 7.18 and 7.19 illustrate the position and orientation, and the forces and torques output, of the IRPS polishing a cylindrical surface. From the results, it can be observed that the position of the end-effector changed slightly (*x-axis*) to keep the force constant on the surface while moving in the *Ry*-axis to polish the surface.
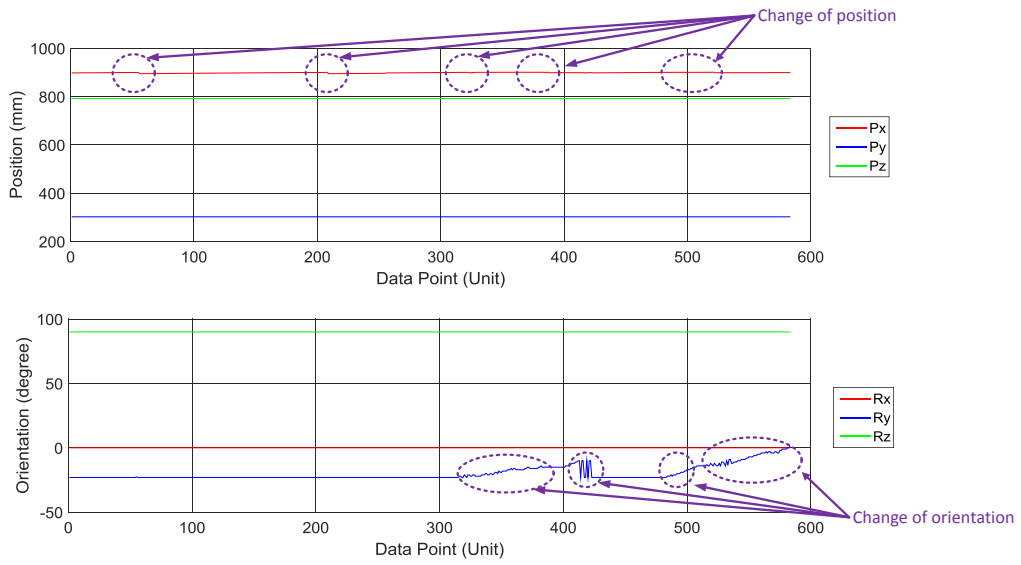
Figure 7.18: Cartesian position recorded for cylindrical surface
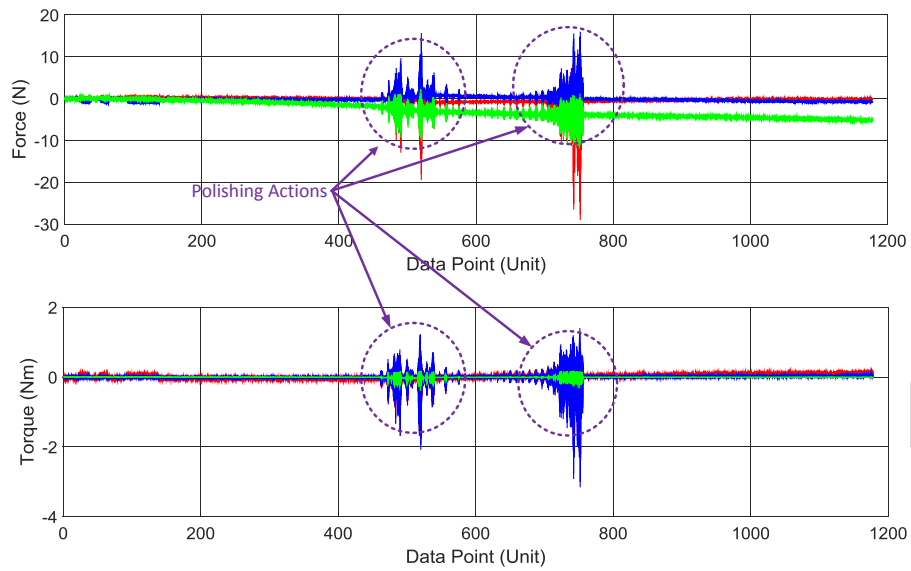
Figure 7.19: Forces and torques recorded for cylindrical surface

7.6.2 Free-Form Polishing Operation of a Triangular Surface

The second test carried out with the developed Integrated Robotic Polishing System was focused on the polishing of a triangular surface. Unlike the previous experiment, it was necessary for the robot end-effector to control the position and orientation in two directions (P*x* and *Ry*) in order to keep the force constant and to move to the next point on the surface.

For this experiment, the user used the same polishing force, position increment and safety limit as above for cylindrical polishing: a polishing force of 4.5±1.5 N was applied to the surface with increments of ±0.1 mm in the *x*-axis. If the polishing force reached or exceeded 10 N, the end-effector would move to a safe position (2 mm in *x-axis*). Once the desired force had been obtained at a point, the end-effector would move to the next relative position: polishing of triangular geometry requires biaxial movement (0.2 in *x-axis*, 0.2 in *B-axis*).

Figures 7.20 and 7.21 illustrate the position and orientation, and forces and torques output when polishing a triangular surface. From the results, it can be observed that the position of the end-effector remained somewhat constant (in *x-axis*) to keep a constant force polishing force, while moving backwards along *Px-axis* and rotating around the *Ry-axis* to polish the surface.
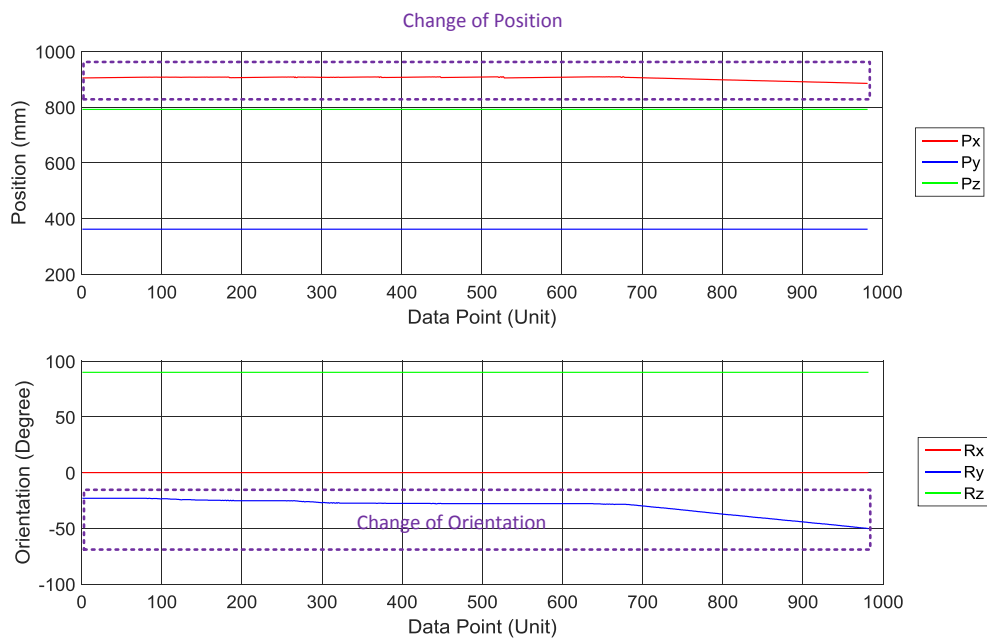
Figure 7.20: Cartesian position recorded for triangular surface
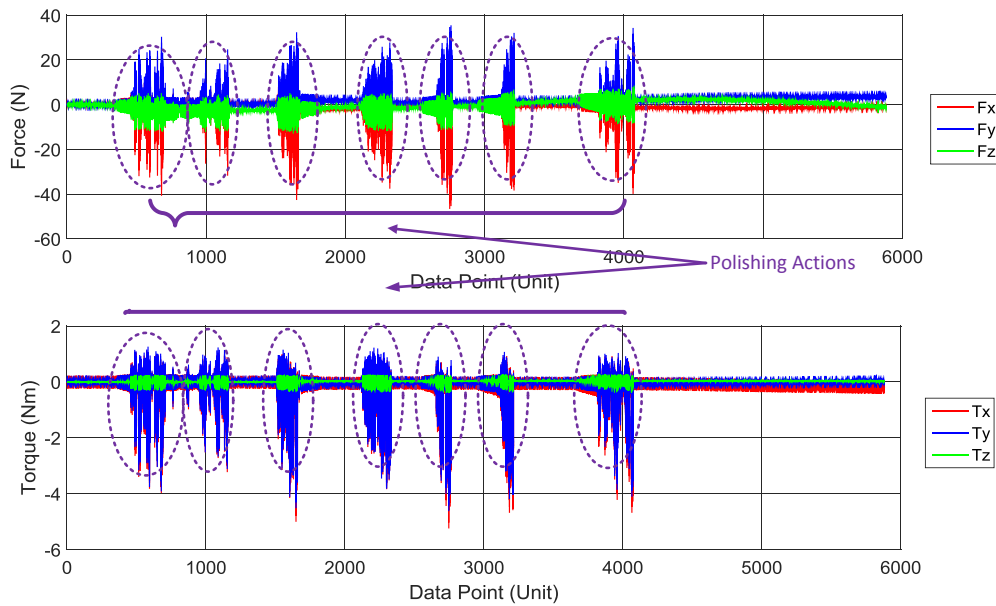
Figure 7.21: Forces and torques recorded for triangular surface

7.7   Results of the Experiments

Based on the data captured in previous experiments, it was decided to develop an automated system that would be able to provide a uniform surface removal by changing the feed rate depending on the type of defects at specific locations, as a skilled operator does. This would be achieved by using a machine vision technology to locate the defects and force control to apply a constant force while changing feed rate to modify the amount of material to remove.

Two sets of tests were carried out as part of the experiment 6 to test polishing capability of the IRPS. In the first test, the system had the task to remove a layer of material from a curved surface, while measuring the amount of polishing force required. The IRPS was able to follow the surface geometry from CAD data. However, it was observed that the surface finish was not uniform due to inadequate force control.

In the second test, it was decided to test the system without geometry data. During the experiment, two geometries were tested as they represent the two opposite end of a surface difficulty spectrum. The polishing of the cylindrical surface was easily carried by the IRPS. This process was deemed to be very challenging for manual operators. In this test, the end-effector moved along *x-axis* to keep a constant force while rotating around *y-axis*. The test with the triangular surface was slightly more complex due to the flat features. In these test, the end-effector moved along *x-axis* to keep a constant force while rotating around *y-axis* and moving backwards in *x-axis*, as to not damage the flat features of the triangular surface.

The test resulted in a slightly curved surface in the triangular shape. The reason is believed to be inadequate performance of the system, particularly manifested in the centre of the flat surface, where the maximum system performance is required to handle sensory and

-134-

generated data. However, the algorithm used to calculate the trajectory was proved to be correct and applicable to a wide range of part profile variety.

Chapter 8 Discussion

This chapter focuses on discussing the results and findings of the research. Section 8.1 presents the data collected from human operators. These data include the data collected in industry and research laboratory, and the detailed review of capturing human and polishing processes as covered in the literature review (see Chapter 2). Section 8.2 presents and discusses the integrated robotic polishing system developed in this research. Lastly, Section 8.3 presents and discusses the work undertaken with the industrial collaborator.

8.1   Learning from Human

The work reported in this research has provided a good understanding of the manual polishing processes. The data collected from qualitative study (e.g. observations and interviews) and quantitative experimentations (e.g. fixture design and experiments) provided insight into the approaches and techniques used by human operators during manual polishing processes. The qualitative results focused on the general techniques and strategies to use in manual polishing, while the quantitative results provided the variables and parameters (including a range of values for each one) for both manual and automated processes.

Despite the use of automated technologies, such as CNC or robots, polishing and finishing, processes are still widely carried out manually by skilled workers in industry; whether this is to remove defects, improve the surface texture, or meet the mechanical specifications. These processes are laborious and hazardous. However, humans have some unique qualities. They can learn, make decisions from little information and innovate; therefore, they can control and adapt quickly to changes. These factors make skilled operators more effective and flexible for the production of higher-quality polishing components and also in process changes. This is why trained, skilled operators produce a high quality of surface finish in short amounts of time - regardless of the complexity of the workpiece. Nonetheless, some of these techniques are found to be used by the operators due to the limitations of humans' dexterity and control, to accurately adjust process parameters and variables (e.g. fine motion, force, and torque).

From the experiments, it was evident that some of the techniques developed by the human operators were necessary to compensate the existing limitations of the manual processes in

the range and accuracy. Therefore, it was concluded that learning from human operator should not mean reproduce the exact manual processes in automation. Furthermore, some of these techniques would not affect the development of the IRPS.

In Chapter 4, analysis of a number of industrial components was reported and obtained from multiple visits. It was established that the process sequence for different components remained the same, despite their differences in size, geometry and batch volume sizes. Some of the similarities between the finishing processes are found to be trailing and leading edges, root-rad, radius, wings section and curved surface. Overall, the finishing process of an industrial component progresses from removal of large features and defects to improving the aesthetic aspect of the surface (e.g. from grinding to buffing).

As each process is similar, skill operators would often work on multiple components or processes making them flexible and highly versatile. During training, skilled operators are taught to "keep the flow", as described in Section 4.4. This allows the operators to follow the surface profile while applying force against the polishing tool. This approach eliminates the need for accurate geometrical and dimensional data (such CAD or schematics), while the force applied by the operator remains constant and perpendicular to the abrasive tool. The perpendicular contact is manually maintained by the operator, who compensates based on tactile feedback from the resultant torque and vibrations. Tactile feedback allows the operators to control the level of vibration, force, and torque generated during the operation. In addition to tactile feedback, visual feedback is intensively used by the operators to assess the part between passes (i.e. locate defects), and monitor the process in real-time.

During the industrial visits, it was also observed that some processes require multiple inspections and re-works. Despite the fact that the company provides a high quality of service and has a low volume of scrapes (less than 2%), each operator is leaving their own defects/marks, known as the machining "signature", on the workpiece, which is easily identifiable by the visual inspection team.

One of the main issues observed in industrial manual finishing process was the impact of the working environment on the workforce. For instance, the vibration generated form the grinding operations of large turbine blade induce severe injuries to the operators. According to the company, the operators start suffering from vibration white fingers syndrome after 2 years, forcing the company to move them to another process. To minimise the risk of severe injury, each operator must take regular breaks, which reduce the capacity by up to 30%.

As part of this research, a fixture embedded with smart sensors was developed to capture parameters and variables from a human operator and to understand how manual polishing operations are routinely carried out. During the experiments (see Chapters 5 and 6), the fixture device has shown good performance in collecting the desired data. In addition, it was demonstrated that the experiments could be replicated in industry or research laboratories for further study. The fixture data has been cross-referenced with observations and interviews with skilled operator in industry and in the research laboratory, to provide the variables and parameters to control during polishing. By recreating the industrial operations in the research laboratory, showed that the process sequence, parameters, and patterns observed from both operators were similar to what have been previously observed in industry.

Figure 8.1: Capture of manual polishing parameters with the fixture

In general, the polishing processes for the observed components should be carried out using a high grit abrasive tool to a lower grit one. Each step of the process should be carried out the same way and monitored constantly, until the surface finish is satisfactory. Moreover, it was found that the quality of the surface finish is primarily dependent on the polishing movement, the force applied to the surface, vibration and torque compensation, and the feed rate or speed, in both automated and manual operation.

Three polishing patterns were identified in manual polishing operations, as follow: simple pressure – Pattern A, linear movement – Pattern B, and surface profiling – Pattern C. In addition, these three patterns and techniques captured in industry and in the research laboratory do not change regardless the type of workpiece or feature to remove.

It was observed that skilled operators tend to follow the profile of the workpiece (e.g. surface profiling) while keeping a constant force with a perpendicular contact angle to the abrasive tool. The perpendicular contact angle is maintained by the operators to minimise the torque applied to the surface and therefore makes the part handling easier and more stable. Moreover, through tactile feedback the skilled operator can continuously detect and rectify the orientation of the part, while maintaining a constant contact force. In this manner, the operator is able to remove defects and improve the surface finish without altering the part geometry.

In addition to surface profiling, it was observed that the operators carry out the polishing operation of trailing and leading edges using a linear movement pattern while decreasing the polishing force. This technique allows the operator to deburr, straighten, and to remove material or features located at the edge of the part. However, it was concluded that, this technique is used due to the lack of dexterity, precision, and control over small movements and force changes. In addition, it was observed that this technique requires finer motor skills as the force and movement must be controlled precisely to avoid damaging the part or injuring the operator.

The analysis of the experimental results revealed that polishing force is an important parameter in manual polishing operations. The polishing force is continuously monitored by the operators through tactile feedback (e.g. level of vibration) who tries to keep it constant and perpendicular to the surface profile. As mentioned earlier, the operator

compensates polishing forces and the torques generated from the vibrations in contact with the abrasive tool by stabilising the part orientation, making it easier to handle and therefore to create a uniform surface finish. Data from the fixture shows that the operator was applying a constant force (avg. 10N – for the part used in this research) along the surface while keeping the surface perpendicular to the abrasive tool.

It was also stipulated that the reason that manual operators primarily tend to control and maintain the forces, rather than other parameters such as feed rate, is because of the magnitude of the force feedback (e.g. reaction forces, torques, and vibrations). This feedback enables better control by human operators due to the lack of control and accuracy for finer movements.

While the operators attempt to keep forces and their directions constant, they would often change the polishing pace or feed rate to achieve different MRR. For instance, in order to remove a defect, the operator would decrease their speed to remove more material (i.e. increasing the MRR), and avoid to alter the surface aspect. Therefore, to vary the volume of material to remove (or MRR), skilled operators tend to maintain a constant polishing force and vary speed or feed rate throughout the operation.

These findings were supported by the analysis of the fixture data and discussions with the operators. It was also observed that the frequency of each polishing action changes through the operation. For instance, in Experiment 3 the operator completed a pass every 5 s at the start of the experiment to remove the defects (therefore more material), before speeding up the pace (i.e. one pass every 3 s) to improve the surface finish.

8.2   Development of the IRPS

The results of the experiments carried out in industry and laboratory provided a good understanding of the techniques deployed by skilled worker in manual polishing processes. The data captured with the fixture were cross-referenced with the discussions and interviews, and observations carried out in industry and research laboratory. The quantitative data captured with the fixture matched the qualitative data captured through videos and discussions in industry and laboratory settings. In addition to the approaches deployed by the operators, some of the essential values, such as polishing forces and initial feed rates were specified through the experiments.

It was understood that an automated system will have advantages over the manual operations, such as finer control over movement and forces, and consistency of operations, and safety. However, it was also observed that in manual polishing skilled operators are faster and more flexible than existing automated system This was observed for several components with complex geometries studied. However, this is expected to be correct for any processes and components. Further analysis revealed that the need for range of sensors are needed to cover all operators' senses (i.e. visual and tactile). Although it may be argued that the core technology required already exist, but the performance necessary for industrial applications have yet to be implemented.

Therefore, it was concluded that the IRPS should not necessarily operate identical to the way human operators perform. For instance, skill operators tend to change their approach, such as patterns and force, when polishing a thin edge of a part. This is typically based on tactile and visual feedbacks received, such as vibration and noises. However, the stiffness of robot arms would negate the undesirable impact of torque and vibration, therefore can provide a smooth and constant polishing parameters. Moreover, a set of sensor within the automated system can provide tactile and visual feedbacks to change and control the process variables.

However, it can be argued that while skilled operators are able to adjust the process parameters in real-time (e.g. reasoning, decision making), the speed of data exchange in an automated system could hinder the system performance as such the system would fall behind. On the other hand, additional sensors and feedback loops can provide a better control over the process parameters, reducing the need for rework, therefore machining time. Therefore, in the IRPS, additional measures were made to reduce the speed of the operations to enable capturing and processing the data within the available time (i.e. 1 sec.).

During several experiments with the fixture and the robot, it was observed that the multi-axial force and torque sensor behaves unexpectedly due to the mass attached to the robot arm (or fixture) and the kinematic of the movements (human's and robot's). Therefore, a calibration of the multi-axial force and torque sensor was carried out. A look-up table (generated from the calibration experiment - experiment 4) was used to remove the effect of the gravity on the force and torque outputs. A preliminary investigation, prior to the test, showed that the compensation for the gravity effect of the force and torque output should be done with a Jacobian (from a pure control point of view). However, it was found alternative to ensure the calibration of the sensors, and remove the effect of the gravity at each line of actual data received from the robot. The results of this calibration was then used for Experiment 5, hence the look-up table.

In this experiment, the impact of the resultant torques was also understood. Similar to the force control, the torque generated from the polishing force should also be controlled and minimized. The lack of torque control in this experiment resulted in an uneven surface quality, as it used CAD data. However, the experiment showed encouraging results for further testing with the IRPS.

Based on the results of Experiment 5 (as discussed in the previous chapter), the application of the IRPS concept was further tested and validated through polishing operation of a range of different surface profiles, without using CAD data. This was to mimic the way that skilled operators polish a part by following the surface profile based solely on the force feedback. However, in the case of polishing an unknown geometry, alternative solutions should be used for gravity compensation as the path is not pre-programmed.

During these tests, two geometries were investigated, cylindrical and triangular surface, as they represent the two opposite end of a surface difficulty spectrum. The polishing of the cylindrical surface was easily carried by the automated system. Due to the precision of the robot arm, the system polished the surface by rotating the part to remove a layer of material from the surface, while keeping a constant contact with the abrasive belt in *x-axis*. The test with the triangular surface was slightly more complex due to the flat features. In this test,

the end-effector had to keep a constant force (along *x-axis*), while moving to it next point on the surface by rotating around *y-axis* and moving backwards in *x-axis*.

During the test with the triangular part, it was also observed that a slight curved surface was formed, even with a very fine motion increments. It was concluded that the lack of speed in data exchange and inadequate inputs parameters resulted in underachieving performance of the system. However, the sensor integration and the developed algorithms were proved to be logically correct and applicable generically to a range of surface geometries.

Based on the results discussed above, the IRPS cell was able to remove a layer of material on both the cylindrical and triangular surface without altering their geometries. The results of these experiments also demonstrated the capabilities of the IRPS to keep a constant force of 4.5 ± 1.5 N along the surface while moving over a complex curvature. The IRPS was able to move with a small increment (±0.1 mm) until the contact force was reached. The quality of the surface finish at the end of the process was very good in the cylindrical part and satisfactory in the triangular part.

As a final note on the technical performance of the IRPS, the proposed system uses KUKA XML software as a standard way of transferring data from and to the robot. While KUKA XML is a very useful in providing the current position and orientation of the end-effector in both joint axis and Cartesian axis, it lacks in speed of data exchange. A latency of up to 1 second was observed causing a "jerky" motion in the robot arm, which could result in low surface quality. This is because the system can only do one task at a time, such as sending information, or reading information, or moving to a new coordinate.

However, there are other more efficient approaches to exchange data between robot and external sensors. These methods can potentially improve the efficiency of the data exchange process by communicating directly to the robot in real-time. Some of the existing packages developed by the robot manufacturers, such as RSI (robot sensor interface) could significantly facilitate the data exchange process (i.e. frequency 8 ms). In addition, with RSI no modification of the user interface would be required.

8.3   Business Aspect: Implementation of a Potential Industrial Solution

Although the business aspect of the automated polishing systems is not in the main focus of this research, it was necessary to investigate some of the related issues. The research problem was initiated by an industrial collaborator, whose current processes were used as an example for this research. The data extracted from this company has linked into a number of complementary research (e.g. capture human factor, business of automation), including this research. The author's contribution to the following business study was to propose alternative solutions (such as IRPS) in their practices, determine the level of automation required, and design a new site layout based on the application of the IRPS for automated polishing. This section summarises the author's proposal for the application of IRPS within the partners site.

In Chapter 4, collaboration with a local SME, was discussed. The company provides finishing services for various industries, such as aerospace, and currently meets its production targets using a large number of manual skilled workers. Each operator is responsible for the whole or partial finishing process for one or multiple components including production, tooling, re-working, and sometimes inspections. Each operator is paid based on the volume of batches produced per day. However, the company is expecting a growth in production volume, which they may not be able to accommodate within their current resources. Therefore, the company is seeking for alternative solutions, such as automation, to meet future demands.

As part of their business requirement, the automated system should be able to be integrated within their current processes without fully replacing their workforce, and should be able to perform as well as their manual operators in terms of quality. However, in terms of speed of production, the company is prepared to accommodate slower but more consistent automated solution.

Furthermore, the company has introduced automated solutions in the past. However, their system was not able to perform the polishing and inspection as well as their operators, and the part specifications were too complex for the automated system. This has led to a lack of faith in automation. Nonetheless, since the introduction of mass finishing technology to their process, the company has doubled the production of one of their components.

Following a number of visits, data for three main components were captured, as explained in Chapter 4. Each part represented a different part size and geometry (e.g. small, medium, and large), and volume of production (e.g. small, medium, and high). Similarities were found between each component, in term of process sequence and operator approach. Each component is finished, starting from a high grit abrasive to a finer grit (or soft mop), and specific features such as trailing edges or root radius are carried out separately. Each component is controlled individually by the visual inspection team and may be marked for rework. The rework is carried out by the same operator in the workshop floor, whom often leaves identifiable 'signature' marks or defects on the surface. Batches may go back and forth between the visual inspection cell and the workshop multiple times before meeting the finish requirements.

Based on an in-depth analysis of the data captured and the experiences gained from the tests using the IRPS cell, the company was proposed a flexible automated solution including manual and automated finishing operations. The business analysis based on the time and complexity of the processes (not discussed in this thesis) identified that a part of the processes which are common in all components can be cost effectively with automation. However, some of the other more complex processes that are unique to one specific components are not financially viable for automation. Therefore, a proposal was made to the partner to re-classify the process sequences and categorise the operations based on their level of complexity and their ability to be automated.

For instance, instead of completing the entire process of a part by one operator, it was suggested that all relatively simpler polishing operations, such as grinding and deburring, be carried out by an automated system and the skilled operators' time should be used only for polishing the complex features, such as aerofoil wings and radius. The author (with

support from the other researchers in the group) has proposed a new layout for the company.

This solution integrates automated and manual polishing operations of one or several types of components in one large polishing cell. Using this system, it could be envisaged that a robotic arm may carry out heavy grinding and deburring operations for each batch; as these processes are the most time-consuming, as well as being most prone to errors, reworks and risking injuries. Each component would then be inspected manually (or automatically) before going for further operation that would be carried out by one or several skilled operators.

By allowing the operator to focus on less laborious tasks, the risk of severe injury will be reduced, and the volume of production can be increased by the introduction of automated technology and improvement of the process sequences. This approach also guarantees maintaining the know-how and the expertise of the manual operators within the company, while reducing the reliance of the company on individuals.

The proposed flexible automated system was found to be viable for higher volume of production. It was concluded that the current production level would not met the financial criteria to implement the IRPS approach in this company. In addition, a major change in production strategy was proposed to ensure the time of the skilled operators are efficiently used for complex processes only. On the other hand, the concept of semi-automated polishing system (such as haptics and teleoperation) was also found promising for the future business development of the company.

Chapter 9 Conclusions

9.1 Research Overview

Polishing processes are critical in many industries as they are mainly performed manually at the end of manufacturing processes. Manual polishing processes are typically used due to the complexity of the operation and they are highly skills dependent. The growth of automated technology and the difficulties of recruiting and training sufficient personnel has forced some businesses, such as our industrial partner, to seek for alternatives solution. This was recognised by the industrial collaborator, who relies heavily on individuals' skills and personal knowledge, and are therefore investigating in alternative solutions. While these solutions should improve the health and safety of operators, they should also improve competitiveness by optimising quality, repeatability, and speed of processes.

Despite a number of existing research and industrial work in automated polishing, such systems have not yet been successfully implemented in industry. The reason may be that the focus of these work was to achieve product specification through automated polishing, without understanding and incorporating existing manual processes. This has led to an important factor contributing to the lack of robust automated polishing systems used in industries as part of their production systems.

Therefore, in this research, investigations were envisaged to contribute to the development and implementation of an automated polishing system – one which follows a comprehensive understanding and assessment of the manual processes and operators' skills. Based on the research objectives presented in Section 1.3, the IRPS system was proposed through: a review of existing technologies in industrial and research work; identification of the polishing processes specifications and needs; developing a framework to capture manual polishing operations; understanding and interpreting captured manual polishing parameters; and finally, developing and testing of an automated system based on manual process.

These objectives were achieved during the research. In addition to meet the research objectives, the research hypothesis (see Chapter 1) has been proven. Towards this end, the development of an Integrated Robotic Polishing System based on the capture and analysis of manual polishing processes has been proposed in this research. The proposed integrated robotic polishing system (IRPS) includes a multi-axial force and torque sensor and a robotic

arm to polish any given surface based solely on the force output, removing the need for CAD. In addition, a user interface was designed to input and monitor desired parameters. On the polishing operation of unknown surfaces, experiments demonstrated that the automated system was able to remove a uniform layer of material solely based on the force output.

9.2   Research Achievements

With the development of the Integrated Robotic Polishing System, the following was achieved in this research, which also meets the research objectives (see Section 1.3):

- A collaboration work with an industrial partner was carried out. This collaboration provided with a better understanding of the general finishing processes and approaches in use during standard manual polishing procedures. The collaboration included the study of the finishing processes for three industrial components. Lastly, this collaborative work provided a potential solution for the company to implement for these components.

- A fixture device to enable the capture of manual polishing parameters was developed in this research. The fixture is embedding a multi-axial force and torque sensor to enable the capture of the forces and torques during manual polishing operation. An inertial measurement unit and a 3D motion capture system were also used to capture movements and patterns of skilled human operators.

- Laboratory test with the fixture was successfully carried out. These experiments captured parameters and variables used by skilled operators during manual polishing operation of a small metallic workpiece (similar to ones used in industry).

- The data collected during industrial visits and research laboratory experiments were further analysed for automation. This analysis was carried out (see Section 7.1) to discuss how the manual process could be translated into automation and what variable(s) to focus on when developing an automated polishing system. The IRPS system was then developed based on these research findings.

- Finally, the IRPS concept was successfully tested for two geometrical surfaces (cylindrical and triangular). These geometries were chosen as they represent the two ends of the difficulty to polish spectrum for automated systems (where cylindrical is 'easy', and triangular, 'hard'). The cylindrical surface was easily polished by the IRPS. However, for the triangular shape, it was more difficult for the IRPS. On the other hand, the IRPS demonstrated good capabilities to polish any geometries solely based on the force output removing the need for CAD data or pre-planned path.

To support this research, several publications were successfully produced. The articles submitted and published in conferences and journals papers are as follows:

- E. Kalt, R.P Monfared, M.R. Jackson, "*An Intelligent Automated Polishing System*", 3rd Annual EPSRC Manufacturing the Future Conference, Glasgow, 2014.
- E. Kalt, R.P Monfared, M.R. Jackson, "*Development of an intelligent automated polishing system*", Proceedings of the 16th international conference of the european society for precision engineering and nanotechnology, Nottingham, 2016.
- E. Kalt, R.P Monfared, M.R. Jackson, "*Towards an automated polishing system – capturing manual polishing operations*", IJRET International Journal of Research in Engineering and Technology, 2016.
- E. Kalt, R.P. Monfared, M.R. Jackson, "*Development of an Integrated Robotic Polishing System (IRPS)*", International Journal of Advance Manufacturing Technology, 2016. (to be submitted).

9.3   Contribution to Knowledge

The development and integration of robotic polishing systems have been previously carried out by industries and other research groups. Nonetheless, none of these solutions meet the aims and objectives of this research. As mentioned in Chapter 1, to develop a robust automated polishing system, it was essential to incorporate human skills into the automated system. Therefore, it was necessary to understand and capture these manual skills to develop the IRPS system on that basis. The design of the IRPS system developed as a part of this research contributes considerably to the state-of-art of mechanical polishing processes, by introducing novel approaches, and improving the current methods. The contributions of this research include:

Further Knowledge on Manual Polishing Processes

Existing automated polishing systems do not consider the skill deployed by manual operators. The study and capture of manual polishing processes carried out in industry and laboratory provided complementary qualitative and quantitative information. This is one of the significant contributions of this research: providing a better understanding of skilled operators' techniques and providing appropriate variables for automation. The systematic analysis of the capture of manual polishing processes is provided with the key parameters and the appropriate level of technology to consider for the development of an automated polishing system.

Development and test of an Integrated Robotic Polishing System

The second significant contribution of this research was to propose a novel approach for automated polishing operations. The development of an integrated robotic polishing system, based on the research findings, uses a set of smart sensors and a force-position-by-increment control algorithm, and transpose the way that skilled workers carry out polishing

processes. The tests presented in Section 7.6 demonstrate the capabilities of the IRPS system to carry out automated polishing operations of two geometrical surfaces (cylindrical and triangular), solely based on the force output. This was to remove the need for CAD data - as this is not always available to companies specialised in finishing services.

Further to the contributions described above; the framework reported in this thesis provides a systematic approach to develop optimal level of automation required for the polishing process, as being investigated in this research. Furthermore, the effectiveness of this framework has been demonstrated though its application for the development of an automated polishing system based on the understanding and adoption of manual processes and operator's skills.

9.4   Research and Technological Limitations

During this research, the author became aware of the complexity of manual polishing processes and the level of skill and dexterity deployed by human operators. It was subsequently understood that automating such processes would be challenging. Even though the research objectives within the scope were met, however the following have not been achieved during the research, due to limited resources and time, or due to some technological limitation:

- A vision system to detect and locate potential defect on the part surface has not been implemented in this research. However, the IRPS was developed to be able to add sensors and control more polishing parameters without any modifications.

- Feed rate control has not been implemented due to the lack of machine vision. Complementary work with machine vision and RSI would enable the change of feed rate depending on the type of feature located onto the surface.

- Lack of tactile sensings, such as controlling the torque and vibration has been implemented. Controlling these variables can be carried out with the multi-axial force and torque sensor. In addition, this sensor required further work on force gravity compensation.

In addition, to what has been mentioned above, it is somewhat regrettable that a thorough study of manual operations has not been completed. Nevertheless, the research has provided the minimum and foundational information needed to develop the IRPS, and it was successfully developed and tested within the research laboratory.

9.5 Further Work

Due to the limited resources and time allocated to the research, this research could be continued further in a number of ways, as described below:

The work on the study and capture of manual polishing processes could be continued. For instance, further work towards human factor should be carried out. The human factor study may include ergonomic analysis of the task, cognitive (decision-making) analysis, or impact of vibration white finger on skilled operators. Further experiments with the fixture could be also carried within industry or research laboratory. For instance, to generalise the research findings, capturing more processes or more operators could be carried out.

Further development of the IRPS, attempting to control more polishing parameter, should also be carried out. For example, a vision system should be added to assess and locate potential defects on the surface. Work with KUKA RSI should also be carried out, allowing a better speed of data exchange between the robot and PC host. KUKA RSI should be able to transfer data in real-time (8 ms) for better polishing operation with the force-position-by-increment algorithm. In addition, RSI is able to change the feed rate depending on the type of feature detected by the vision system. Torque and vibration control could also be added to the IRPS. Acoustic emission sensors could be used to monitor the abrasive tool-wear, therefore the rotation speed of the abrasive tool could be controlled to improve cutting parameter and tool wear. A more thorough investigation into the multi-axial force and torque sensor behaviours for gravity compensation should also be carried out.

Finally, the IRPS could be tested and implemented within an industrial production line, as suggested in Chapter 4. This would demonstrate the performance and advantage of the IRPS over existing solution within an industrial environment.

List of Publications

TOWARDS AN AUTOMATED POLISHING SYSTEM - CAPTURING MANUAL POLISHING OPERATIONS

Eugene Kalt[1], Radmehr Monfared[2], Michael Jackson[3]

[1]Wolfson School of Mechanical, Electrical and Manufacturing Engineering, Loughborough University, UK
[2]Wolfson School of Mechanical, Electrical and Manufacturing Engineering, Loughborough University, UK
[3]EPSRC Centre for Innovative Manufacturing in Intelligent Automation, Loughborough University, UK

Abstract

Advancements in robotic and automation industries have influenced many manual manufacturing operations. With a great level of success, robots have taken over from man in many processes such as part manufacturing, transfer and assembly. However, in other traditionally manual operations such as polishing, automation has only partially been successful, typically limited to parts with simple geometry and low accuracy. Automated polishing systems using robots have been attempted already by a number of industrial and research groups; however, there are few examples of deploying such a system as a part of a routine production process in high-technology industries, such as aerospace. This is due to limitations in flexibility, speed of operation, and inspection processes, when compared with manual polishing processes. The need for automated polishing processes is discussed in this article and the problem with the existing system was explained to be a lack of understanding and the disconnect from manual operations. In collaboration with industrial partners, a mechatronic based data capturing device was developed to accurately capture and analyze operational variables such as force, torque, vibration, polishing pattern, and feed rates. Also reported in this article is a set of experiments carried out to identify the polishing parameters that a manual operator controls through tactile and visual sensing. The captured data is interpreted to the operators' preferences and polishing methods and should then be included in the design of an automated polishing system. The research results reported in this article are fed back to an ongoing research project on developing an integrated robotic polishing system.

Keywords: Capturing Manual Operation, Automated Robotic Polishing, Force and Motion Capture

--***--

1. INTRODUCTION

In the manufacturing industry, mechanical finishing plays a vital role in the development of product surface quality and final geometry [1]. Mechanical finishing typically includes deburring, grinding, polishing, buffing, and final visual inspection of a workpiece. These processes are generally performed at the final stage of the manufacturing process of a component or product and may represent up to a third of production time in some industry [2].

One of the main reasons for polishing is to improve surface finish by removing minimal amounts of material and to smooth a particular surface until obtaining the desired surface finish (i.e. roughness or aesthetic aspect) without affecting the geometry of the workpiece [1–3].

Mechanical polishing, as common finishing methods, refers to the removal of fine layer of material by means of abrasive tools to reduce the surface roughness to the desire level (e.g. roughness average or Ra). Smoothing of surfaces generally involves removing scratches, machining marks, pits, and other defects or features to obtain a uniform surface roughness evenly distributed throughout the part surface [3].

The polishing process is very important and highly used in aeronautical industry, whether it is to meet mechanical properties and design specifications, such as friction, or to meet the desired visual aspect. For example, a hydraulic turbine produces electricity by turning energy from water into kinetic energy for an electric generator [4]. The main factor that affects the efficiency of these hydraulic turbines is the friction between the water and turbine blades. The level of fiction will depend on the quality of the surface finish. Thus, improving the surface roughness of a turbine blade will significantly decrease the friction and increase the efficiency of the turbine. In addition, by meeting design specifications and surface quality, polishing processes can improve the service life of a component. Therefore, additional processes such as polishing are required after initial machining processes [5].

Despite the growth of automated technologies used in modern industry, polishing processes are still mainly carried out manually. Manual polishing typically involves a highly skilled worker holding a workpiece or a polishing tool in order to: remove a layer of material; remove scratches or machining marks; shape curves or radii; or deburr and break sharp edges. Skilled human operators have the advantages of adapting quickly to changes, to be flexible, and ability to learn from their mistakes. However, it can take many months to train a new operator. In addition, the working environment is unhealthy for the operators, due to exposure to dust, vibration and noise. In many cases, lengthy manual polishing processes lead to "vibration white finger" or other musculoskeletal diseases (MSD). Current regulations stipulate that operators must wear safety glasses, respiratory-protective equipment and take regular breaks.

-155-

Development of an intelligent automated polishing system

E. Kalt[1], Dr R.P. Monfared[1], Prof. M.R. Jackson[1]

[1]*EPSRC Centre for Innovative Manufacturing in Intelligent Automation, Loughborough University*

e.kalt@lboro.ac.uk

Abstract

In high-value manufacturing sectors, many manufacturing processes are still performed manually, such as polishing operations for small metallic parts. Increasing volume, the need for consistency in quality, and health and safety issues are some of the reasons for industry to search urgently for alternative solutions for manual polishing processes. This article reports the development of an intelligent automated polishing system to achieve consistent surface quality and removal of superficial defects from high-value components, such as those used in aerospace industry. The article reports an innovative method to capture manual polishing processes by skilled operators. The captured polishing parameters are then used to develop and control a robotic polishing system that can adopt various polishing patterns. A brief summary of existing fully and semi-automated polishing systems and their inadequacy for industrial applications are discussed. The need for building automation system based on manual operations are explained and a systematic data capturing process for a specific aerospace-based component is defined. The development of the process capturing device is explained, the data analysis and interpretations are discussed and the migration from manual operation to an automated polishing system is reported. Further detailed information is given in relation with combining data from various sensors and building of an automated system based on learning from manual operations. The research results are also briefly discussed and conclusions are drawn regarding applicability of automated systems for highly skilled manual operations.

Type the keywords here   Automated Polishing, Robotic grinding, manual operation, data capture through mechatronic devices

1. Introduction

In the manufacturing industry, mechanical polishing plays a vital role in the development of a product's surface quality and final geometry. Despite the current growth of automated technologies in industry and in research, mechanical polishing is still mainly carried out manually. Manual polishing typically involves a highly skilled and trained worker in an un-healthy environment due to exposure to dusts, vibrations, and noises. For example, lengthy manual polishing processes could lead to musculoskeletal diseases (MSD) such as vibration white finger, or other severe injuries [1].

These processes are usually performed at the final stage of the manufacturing process of a component or product and could represent up to a third of production time in some industries [2]. Therefore, industry is strongly motivated to implement automation in polishing processes to improve the working environment and to drive cost down, whilst keeping the same level of quality or better [2-5].

Many industries already benefit from the advancement of multi-axis machining to produce parts to precise tolerances and specifications [4-5]. Industrial robots have also been widely used to perform well-defined, repetitive tasks in carefully controlled environments, but fully autonomous operation of the robot may not be cost effective for polishing [6]. However, none of the existing technologies are offering flexibility and the autonomous provided by skilled operators. For instance, one of the main challenges in automated polishing is to maintain a constant contact force between the tool and the workpiece in relation with the geometrical profile of the part. If the force is too high or uneven the part can be over polished [2].

Investigating the existing research and industrial efforts in automated polishing, it is understood that a key element missing in developing automated polishing is the understanding and capturing of manual operations, and building the automated system accordingly.

Mechanical polishing includes a wide range of technologies and processes, such as abrasive blasting, mass finishing, chemical mechanical polishing, and ultrasonic polishing. Review of the literature has shown three main technologies: robotic arm [2-3], commercial and designed computer numerical control (CNC) [5, 7], and mass finishing [4, 8] are all currently used in industry or are in development [9].

The main focus of these works are driven by cost, removing humans from unsafe/unhealthy processes, and interest in specific components (e.g. mold die or turbine blade). It was also noted that the study or capture of manual operations, in order to build an automated system, was neglected. In this research, the development of an intelligent automated system is based on the study of manual operation is investigated. Section 2 describes the development of a fixture to capture forces and motions of human operators during manual polishing operations. In Section 3, the capture and analysis of data with the fixture is reported. Finally, in Section 4, the development of the automated system based on the results in Section 2 is discussed.

2. Capture of Forces & Motions

The polishing approach proposed in this article is initially based on capturing and understanding the manual polishing operation. By understanding how manual operators adjust the process parameters to improve the surface quality and remove defects, the manual processes are interpreted to develop an automated robotic polishing system which is controlled flexibly and adapt to the surface profile intelligently. To achieve this, it was necessary to monitor the motion, the force, and the speed of the operators during the polishing processes. The other variables derived from captured parameters include time,

An Intelligent Automated Polishing System

Eugene KALT[1*], Radmehr P. Monfared[1], and Michael Jacskon[1]

[1] EPSRC Centre for Innovative Manufacturing in Intelligent Automation, Wolfson School of Mechanical & Manufacturing Engineering, Loughborough University, Loughborough, UK

*e.kalt@lboro.ac.uk

Abstract

The recent work carried out at the EPSRC Centre for Innovative Manufacturing in Intelligent Automation on automated finishing is reported by this article. The main focus is to investigate and develop appropriate level of automation to the existing manual finishing operations of small metallic workpieces to achieve required surface quality and to remove superficial defects.

In the manufacturing industries, finishing processes (such as polishing) plays a vital role in the development of high precision product, to give a desired surface finish, remove defects, break sharp edges and extend the working life cycle. The finishing operation is generally done at the final stage of the manufacturing process and traditionally carried out manually. It also can represent up to 37% of the production time, and [1]

The successful implementation of an automated polishing system requires a deep understanding of the polishing process and their parameters. [2] [3] To this end, a research framework have been created to systematically understand and capture the manual processes (through smart sensors), assess the challenges that an automated solution may be facing, and finally develop a novel solution to replicate and improve the manual processes through the use of right level of automation.

This article include a case study illustrating a method developed to capture the manual polishing operations through a set of sensors mounted on a workpiece holder. The sensors record in real-time the position (6DoF), accelerations, forces, and torques applied to the workpiece by the operator during a polishing process. These data are then compared with the pre-measurement of the workpiece to understand and quantify the polishing pattern based on the experience and habitual behaviour of a manual operator. These data are consequently analysed and reverse engineered to develop a robotic manipulation of the workpieces based on (almost) the same polishing pattern.

The article also illustrates some of the findings to this stage of the research based on the production and laboratory experiments carried out. The overall results are found encouraging to deploy further automation in a robotic polishing application.

Significance Statement

The significance of this work is to develop a novel automated finishing system through the study of manual operation. The authors believe that the framework mentioned early will help to understand manual operation and develop the right level automation for finishing.

[1] L. Liao and F. J. Xi, "A linearized model for control of automated polishing process," *Proc. 2005 IEEE Conf. Control Appl. 2005. CCA 2005.*, pp. 986–991, 2005.

[2] A. Rachmat and A. Besari, "Computer Vision Approach for Robotic Polishing Application using Artificial Neural Networks," no. SCOReD, pp. 13–14, 2010.

[3] S. Nakajima, S. Terashima, and M. Shirakawa, "Development of an Operating Robot System for Die and Mold Polishing," 2004.

1

References

Adhikarla, V.K., Barsi, A., Singhal, D., Kovács, P.T., Technology, I., 2014. FREEHAND INTERACTION WITH LARGE-SCALE 3D MAP DATA 1–4.

Ahn, J.., Lee, M.., Jeong, H.., Kim, S.., Cho, K.., 2002. Intelligently automated polishing for high quality surface formation of sculptured die. Journal of Materials Processing Technology 130-131, 339–344. doi:10.1016/S0924-0136(02)00821-X

Ahn, J.., Shen, Y.., Kim, H.., Jeong, H.., Cho, K.., 2001. Development of a sensor information integrated expert system for optimizing die polishing. Robotics and Computer-Integrated Manufacturing 17, 269–276. doi:10.1016/S0736-5845(00)00057-0

Akbari, A., Higuchi, S., 2002. Autonomous tool adjustment in robotic grinding. Journal of materials processing technology.

Annarumma, M., Pappalardo, M., Naddeo, A., 2008. Methodology development of human task simulation as PLM solution related to OCRA ergonomic analysis. Computer-Aided Innovation.

Arcos, 2013. ARCOS System for Surface Finishing. achossrlcom.

Automation, A.I., 2013. Multi-Axis Force / Torque Sensor [WWW Document]. ATI Industrial Automation. URL http://www.ati-ia.com/products/ft/sensors.aspx?campaign=ims

Axinte, D. a., Kwong, J., Kong, M.C., 2009. Workpiece surface integrity of Ti-6-4 heat-resistant alloy when employing different polishing methods. Journal of Materials Processing Technology 209, 1843–1852. doi:10.1016/j.jmatprotec.2008.04.046

Bassily, D., Georgoulas, C., Güttler, J., Linner, T., Bock, T., München, T.U., 2014. Intuitive and Adaptive Robotic Arm Manipulation using the Leap Motion Controller. International Symposium on Robotics 78–84.

Bauchau, O.A., Craig, J.I. (Eds.), 2009. Structural Analysis, Solid Mechanics and Its Applications. Springer Netherlands, Dordrecht.

Beaucamp, A., Namba, Y., Inasaki, I., Combrinck, H., Freeman, R., 2011. Finishing of optical moulds to λ/20 by automated corrective polishing. CIRP Annals - Manufacturing Technology 60, 375–378.

Beléndez, T., Neipp, C., Beléndez, A., 2002. Large and small deflections of a cantilever beam. European Journal of Physics 23, 371–379. doi:10.1088/0143-0807/23/3/317

Benjarungroj, P., Harrison, P., Vaughan, S., Ren, X.J., Morgan, M.N., 2011. Investigation of Thermally Treated Recyled Glass as a Vibratory Mass Finishing Media. Key Engineering Materials 496, 104–109. doi:10.4028/www.scientific.net/KEM.496.104

Besari, A.R.A., Prabuwono, A.S., Zamri, R., Palil, M.D.M., 2010. Computer vision approach for robotic polishing application using artificial neural networks, in: 2010 IEEE Student Conference on Research and Development (SCOReD). IEEE, pp. 281–286.

Borrego, M., Douglas, E.P., Amelink, C.T., 2009. Quantitative, Qualitative, and Mixed Research Methods in Engineering Education [WWW Document]. Journal of Engineering Education. URL http://crlte.engin.umich.edu/wp-content/uploads/sites/7/2013/06/Borrego-Douglas-Amelink-Quantitative-Qualitative-and-Mixed-Research-Methods-in-Engineering-Education.pdf (accessed 3.11.16).

Brydon-Miller, M., Greenwood, D., Maguire, P., 2003. Why Action Research? Action Research 1, 9–28.

Bryman, A., 2003. Quantity and quality in social research.

Capone, B.R., Kelly, E., Gianino, P.D., Masters, J.I., 1960. Technique for Polishing Single Crystal Yttrium-Iron-Garnet Spheres (Correspondence). IEEE Transactions on Microwave Theory and Techniques 8, 569–569. doi:10.1109/TMTT.1960.1124790

Cariapa, V., Park, H., Kim, J., 2008. Development of a metal removal model using spherical ceramic media in a centrifugal disk mass finishing machine. The International Journal of Advanced Manufacturing Technology 39, 92–106. doi:10.1007/s00170-007-1195-5

Chang, S., Wang, M., 2007. Digital human modeling and workplace evaluation: Using an automobile assembly task as an example. Human Factors and Ergonomics in.

Chen, X., Gong, Z., Huang, H., 2000. Development of robotic system for 3D profile grinding and polishing. SIMTech, Singapore, Tech Rep AT/00/012/AMP.

Chen, X., Gong, Z., Huang, H., Zhou, L., 1999. An automated 3D polishing robotic system for repairing turbine airfoils. Industrial Automation Journal 6–11.

Chen, X., Wang, D., Bai, S., Lin, W., 2004. Hybrid linear compensation and improved Hermite interpolation for optical measurement of 3D airfoil surface. Robotics, Automation and Mechatronics, 2004 IEE Conference 1, 197–201. doi:10.1109/RAMECH.2004.1438916

Chotiprayanakul, P., Liu, D.K., Dissanayake, G., 2012. Automation in Construction Human – robot – environment interaction interface for robotic grit-blasting of complex steel bridges. Automation in Construction 27, 11–23. doi:10.1016/j.autcon.2012.04.014

Cym Materiales, 2013. General Introduction to Shot Blasting [WWW Document]. DirectIndustry. URL http://pdf.directindustry.com/pdf/cym-materiales/general-introduction-to-shot-blasting/61241-631117.html (accessed 2.5.16).

Davidson, D., 2005. Surface finishing reaches new heights: Mass media finishing techniques can improve aircraft part performance and service life. Metal finishing.

Davidson, D.A., 2001. Mass finishing processes. Metal Finishing 99, 110–124. doi:10.1016/s0026-0576(01)85268-5

Dickman, A., 2007. The science of scratches—Polishing and buffing mechanical surface preparation. Metal Finishing.

Du, H., Sun, Y., Feng, D., Xu, J., 2015. Automatic robotic polishing on titanium alloy parts with compliant force/position control. Proceedings of the Institution of Mechanical Engineers, Part B: Journal of Engineering Manufacture 229, 1180–1192. doi:10.1177/0954405414567518

Dutta, T., 2012. Evaluation of the Kinect™ sensor for 3-D kinematic measurement in the workplace. Applied ergonomics 43, 645–649. doi:10.1016/j.apergo.2011.09.011

El-fatatry, A., 2003. Inertial Measurement Units – IMU [WWW Document]. BAE SYSTEMS.

Euler, L., 2013. Euler – Bernoulli beam theory 1–11.

Fern'ndez-Baena, A., Susin, A., Lligadas, X., 2012. Biomechanical Validation of Upper-Body and Lower-Body Joint Movements of Kinect Motion Capture Data for Rehabilitation Treatments, in: 2012 Fourth International Conference on Intelligent Networking and Collaborative Systems. IEEE, pp. 656–661.

Feynman, R.P., Leighton, R.B., Sands, M., 2011. Feynman Lectures on Physics, Volume II - The New Millennium Edition: Mainly Electromagnetism and Matter. Basic Books (New York).

Feynman, R.P., Leighton, R.B., Sands, M., 1963. The Feynman Lectures on Physics. Vol. 1.

Filieri, A., Melchiotti, R., 2012. Position Recovery from Accelerometric Sensors Algorithms analysis and implementation issues. Milan.

Fischer, C., Talkad Sukumar, P., Hazas, M., 2013. Tutorial: Implementing a Pedestrian Tracker Using Inertial Sensors. IEEE CS 12, 17–27. doi:10.1109/MPRV.2012.16

Fraunhofer, 2013. poliMATIC: AUTOMATED POLISHING FOR THE EUROPEAN TOOL INDUSTRY [WWW Document]. automated-polishingeu. URL http://www.automated-polishing.eu/

Georgiades, F., Warminski, J., Cartmell, M.P., 2013. Linear modal analysis of L-shaped beam structures. Mechanical Systems and Signal Processing 38, 312–332. doi:10.1016/j.ymssp.2012.12.006

Gillespie, L.K., 2007. Mass Finishing Handbook. Industrial Press, New York.

Glanzer, G., Bernoulli, T., Wiessflecker, T., Walder, U., 2009. Semi-autonomous indoor positioning using MEMS-based inertial measurement units and building information, in: Positioning, Navigation and Communication, 2009. WPNC 2009. 6th Workshop on. pp. 135–139.

Gong, Z., Chen, X., Huang, H., 2000. Optimal profile generation in distorted surface finishing. Robotics and Automation, 2000 ….

Guiot, A., Pattofatto, S., Tournier, C., Mathieu, L., 2011. Modeling of a Polishing Tool to Simulate Material Removal. Advanced Materials Research 223, 754–763. doi:10.4028/www.scientific.net/AMR.223.754

Guyson, 2013. Guyson Robotic Blasting Systems [WWW Document]. guysoncouk. URL http://www.guyson.co.uk/finishing-equipment/blast/blast-equipment/robotic-blasting-systems

Hang, B.T., Tan, T.D., Trinh, C.D., 2012. THREE-AXIS PIEZORESISTIVE ACCELEROMETER 34, 45–54.

Hansel, D., 2002. Abrasive blasting systems. Metal Finishing Guidebook-directory 100, 51–66.

Harders, M., Barlit, A., Akahane, K., Sato, M., 2006. Comparing 6dof haptic interfaces for application in 3d assembly tasks. Proc of EuroHaptics' 3–6.

Health Safety Executive, 2000. Safety in the use of abrasive wheels, HSE Books. ed.

Health Safety Executive, 1999. Health and safety in engineering workshops.

Hsu, M.H., Shih, T.K., Chiang, J.S., 2014. Real-Time Finger Tracking for Virtual Instruments. 2014 7th International Conference on Ubi-Media Computing and Workshops 133–138. doi:10.1109/U-MEDIA.2014.53

Huang, H., Gong, Z.., Chen, X.., Zhou, L., 2002. Robotic grinding and polishing for turbine-vane overhaul. Journal of Materials Processing Technology 127, 140–145. doi:10.1016/S0924-0136(02)00114-0

Huang, H., Gong, Z.M., Chen, X.Q., Zhou, L., 2003. SMART Robotic System for 3D Profile Turbine Vane Airfoil Repair Repair Process. International Journal of Advanced Manufacturing Technology 21, 275–283.

Huang, N., Liu, Y., Chen, S., Zhang, Y., 2014. Control of human welder's arm movement in manual gas tungsten arc welding (GTAW) process. 2014 IEEE/ASME International Conference on Advanced Intelligent Mechatronics 824–829. doi:10.1109/AIM.2014.6878181

Hughes, C., 2005. QUALITATIVE AND QUANTITATIVE APPROACHES. Warwick.

Ilangovan, B., Monfared, R., Jackson, M., 2016. An automated solution for fixtureless sheet metal forming. The International Journal of Advanced Manufacturing Technology 82, 315–326. doi:10.1007/s00170-015-7366-x

Ito, T., Morishige, K., 2009. Polishing process automation by industrial robots with polished surface quality judged based on imaging processing. Int J of Automation Technology 3, 130–135.

Jones, H.R., 1979. Magnetic Position and Orientation Tracking System. IEEE TRANSACTIONS ON AEROSPACE AND ELECTRONIC SYSTEMS AES-15, 709–718.

Kalt, E.J.B., 1886. Recherches anatomiques et physiologiques sur les opérations de strabisme. Faculte de medecine de Paris.

Kenton, A., 2008. Exploring options and alternatives for material removal and surface finishing. Metal finishing 106, 16–29. doi:10.1016/s0026-0576(08)80122-5

Kenton, T., 2009. The future of mechanical surface finishing. Metal Finishing.

Khakpour, H., Birglenl, L., 2014. Experimental Study on Abrasive Waterjet Polishing of Hydraulic Turbine Blades. IOP Conference Series: ….

Khan, M.I., 2013. Design and Development of Indoor Positioning System for Portable Devices. Luleå University of Technology.

Kowalczyk, D., 2015. Research Methodologies: Quantitative, Qualitative & Mixed Method [WWW Document]. studycom. URL http://study.com/academy/lesson/research-methodologies-quantitative-qualitative-mixed-method.html (accessed 3.11.16).

KUKA Gmb, 2014. Grinding and polishing of implants with KUKA robot [WWW Document]. YouTubecom. URL https://www.youtube.com/watch?v=gO_8spCu29M (accessed 4.9.15).

Liang Liao, Fengfeng Xi, 2005. A linearized model for control of automated polishing process, in: Proceedings of 2005 IEEE Conference on Control Applications, 2005. CCA 2005. IEEE, pp. 986–991.

Liao, L., Xi, F. (Jeff), Liu, K., 2008. Modeling and control of automated polishing/deburring process using a dual-purpose compliant toolhead. International Journal of Machine Tools and Manufacture 48, 1454–1463. doi:10.1016/j.ijmachtools.2008.04.009

Ma, L., Bennis, F., Chablat, D., Zhang, W., 2008. Framework for dynamic evaluation of muscle fatigue in manual handling work, in: 2008 IEEE International Conference on Industrial Technology. IEEE, pp. 1–6.

Määttä, T., 2007. Virtual environments in machinery safety analysis and participatory ergonomics. Human Factors and Ergonomics in Manufacturing &.

Min, S., Kim, J., Parnianpour, M., 2011. Effects of construction worker's experience, the presence of safety handrail and height of movable scaffold on postural and spinal stability, in: 1st Middle East Conference on Biomedical Engineering. Sharjah, pp. 146–149. doi:10.1109/MECBME.2011.5752086

Mohandes, M., Aliyu, S., Deriche, M., 2014. Arabic sign language recognition using the leap motion controller. 2014 IEEE 23rd International Symposium on Industrial Electronics (ISIE) 960–965. doi:10.1109/ISIE.2014.6864742

Nagata, F., Watanabe, K., Kiguchi, K., Tsuda, K., Kawaguchi, S., Noda, Y., Komino, M., 2001. Joystick Teaching System for Polishing Robots Using Fuzzy Compliance Control, in: Proceedings of 2001 IEE International Symposium on Computational Intelligence in Robotics and Automation. Alberta, Canada, pp. 362–368.

Nakajima, S., Terashima, S., Shirakawa, M., 2004. Development of an Operating Robot System for Die and Mold Polishing.

Ng, B., Lin, W., Chen, X., 2004. Intelligent system for turbine blade overhaul using robust profile re-construction algorithm, in: ICARCV 2004 8th Control, Automation, Robotics and Vision Conference. pp. 178–183. doi:doi: 10.1109/ICARCV.2004.1468819

Nur, N., Dawal, S., 2010. Muscles activities at two different work area boundaries during sedentary work. Biomedical Engineering and Sciences (….

Okamoto, K., Morishige, K., 2012. Polishing Process Automation by Industrial Robot with Polished Surface Quality Judgment Based on Image Processing-Visual Inspection Based on Pattern Matching. Key Engineering Materials.

Ortiz, F.J., Iborra, A., n.d. GOYA : A Teleoperated System for blasting applied to ships maintenance 1–12.

Pessoles, X., Tournier, C., 2009. Automatic polishing process of plastic injection molds on a 5-axis milling center. Journal of materials processing technology.

Pfister, A., West, A.M., Bronner, S., Noah, J.A., 2014. Comparative abilities of Microsoft Kinect and Vicon 3D motion capture for gait analysis. Journal of medical engineering & technology 1902, 1–7. doi:10.3109/03091902.2014.909540

Ramaswamy, B., 2011. KALMAN FILTER BASED ESTIMATION OF INERTIAL MEASURMENT UNIT PARAMTERS IN A PORTABLE BIOMECHANICAL ASSESSMENT SUITE (PBAS). The Pennsylvania State University.

Richter, L., Bruder, R., 2013. Design, implementation and evaluation of an independent real-time safety layer for medical robotic systems using a force-torque-acceleration (FTA) sensor. International Journal of Computer Assisted Radiology and Surgery 8, 429–436. doi:10.1007/s11548-012-0791-5

Richter, L., Bruder, R., Schlaefer, A., 2010. Proper force-torque sensor system for robotized TMS: Automatic coil calibration. Proceedings of CARS.

Richter, L., Bruder, R., Schweikard, A., 2012. Calibration of force/torque and acceleration for an independent safety layer in medical robotic systems. Cureus. doi:10.7759/cureus.59

RJH, 2014. Semi-Automatic Rise & Fall Grinder Wallaby - WAL Series [WWW Document]. rjhfinishingcouk. URL http://www.rjhfinishing.co.uk/finishing-machines/machines/power-grinders/wallaby

Rogers, R.M., 2003. Applied Mathematics in Integrated Navigation System, Second Edition, AIAA-Educa. ed. American Institute of Aeronautics and Astronautics, Inc.

Roswell, A., 2004. Modeling for contact stress control in automated polishing. Master of Applied Science Thesis, Ryerson University.

Roviaire, F.E.R., Nasseh, J., 2009. ACCELEROMETER DATA PROCESSING TOOL.

Sasaki, T., Miyoshi, T., Saito, K., Katohgi, O., 1991a. Knowledge Acquisition and Automation of Polishing Operations for Injection Mold (1st Report, Hand Polishing Properties of a Skilled Machinist). Journal of the Japan Society for Precision Engineering 53, 497–503.

Sasaki, T., Miyoshi, T., Saito, K., Katohgi, O., 1991b. Knowledge Acquisition and Automation of Polishing Operations for Injection Mold (2nd Report, Expert System for Mold and Die Polishing Operation). Journal of the Japan Society for Precision Engineering 53, 497–503.

Sasaki, T., Miyoshi, T., Saitoh, K., Okada, S., 1992. Knowledge acquisition and automation polishing operation for injection mold (3rd Report): development and construction of automatic polishing apparatus. Journal of the Japan Society for Precision Engineering 58, 2037–2043. doi:http://doi.org/10.2493/jjspe.58.2037

Schenk, M., Berndt, D., Warnmunde, R., 2011. AUTOMATIC TIME RECORDING FOR MANUAL ASSEMBLY [WWW Document]. ifffraunhoferde. URL http://www.iff.fraunhofer.de/content/dam/iff/en/documents/publications/automatic-time-recording-for-manual-assembly-processes-fraunhofer-iff.pdf

Schlette, C., Rossmann, J., 2009. Robotics enable the Simulation and Animation of the Virtual Human. Advanced Robotics, 2009 ICAR ….

SHL-Automatisierungstechnik, 2015. Core expertise – the perfect surface : automated polishing. SHL-Automatisierungstechnikde.

Siemieniuch, C., Sinclair, M., 1995a. Information technology and global developments in manufacturing: the implications for human factors input. International Journal of Industrial Ergonomics 16, 245–262. doi:10.1016/0169-8141(95)00011-5

Siemieniuch, C., Sinclair, M., 1995b. Information technology and global developments in manufacturing: the implications for human factors input. International Journal of Industrial ….

Siemieniuch, C.E., Sinclair, M. a., 1995. Information technology and global developments in manufacturing: The implications for human factors input. International Journal of Industrial Ergonomics 16, 245–262. doi:10.1016/0169-8141(95)00011-5

Slifka, L.D., 2004. AN ACCELEROMETER BASED APPROACH TO MEASURING DISPLACEMENT APPROACH TO MEASURING DISPLACEMENT by.

Tsai, M.J., Chang, J.-L., Haung, J.-F., 2005. Development of an Automatic Mold Polishing System. IEEE Transactions on Automation Science and Engineering 2, 393–397.

Varghese, P., Hagan, J., McNamee, R., 2015. Robotic Polishing of Turbine Engine Blades: Testing explores an airfoil finishing alternative to loose-abrasive polishing [WWW Document]. Modern

Machining Shop. URL http://www.mmsonline.com/articles/robotic-polishing-of-turbine-engine-blades (accessed 2.26.16).

Villani, L., Federico, N., 2007. Handbook of Robotics Chapter 7 : Force Control.

Vulcan Engineering, 2015. VTS - VULCAN TACTILE SYSTEM [WWW Document]. vulcangroupcom. URL http://www.vulcangroup.com/products-2/robotics/metal-removal-robots/vts-vulcan-tactile-system/

Wang, Q., Xu, Y.-R., Bai, X., Xu, D., Chen, Y.-L., Wu, X., 2014. Dynamic gesture recognition using 3D trajectory. 2014 4th IEEE International Conference on Information Science and Technology 598–601. doi:10.1109/ICIST.2014.6920549

Web, E., Project, P., 2013. Autonomous Indoor Positioning and Navigation with an Inertial Measurement Unit - Xsens Autonomous Indoor Positioning and Navigation with an Inertial 12–14.

Welch, G., 2002. Motion Tracking : No Silver Bullet , but a Respectable Arsenal. IEE Computer Graphics and Applications 24 – 38.

Welch, G.F., 1995. Hybrid Self-Tracker : An Inertial / Optical Hybrid Three-Dimensional Tracking System.

Wen-Jong Lin, Bryan Tsong-Jye Ng, Xiaoqi Chen, Zhiming Gong, Jingbing Zhang, Kiew Choon Meng, 2004. Self-compensating closed loop real-time robotic polishing system, in: ICARCV 2004 8th Control, Automation, Robotics and Vision Conference, 2004. IEEE, pp. 199–204. doi:10.1109/ICARCV.2004.1468822

Will, K., 2012. Deflection of L Shaped Cantilever Beam [WWW Document]. Physics Forums - The Fusion of Science and Community. URL https://www.physicsforums.com/threads/deflection-of-l-shaped-cantilever-beam.599635/

Xsens, 2013. MTw Development Kit Wireless Motion Trackers [WWW Document]. Xsens Technology BV. URL www.xsens.com

Xsens, n.d. MTw Development Kit Wireless Motion Trackers [WWW Document]. Xsens Technology BV. URL www.xsens.com

Zhang, J., Lim, Y., 2002. Burnishing of ultrathin carbon overcoat-towards further low glide height [hard disks], in: Magnetic Recording Conference, 2002. Digest of the Asia-Pacific. Singapore. doi:doi: 10.1109/APMRC.2002.1037681

Zhang, W., Ghogho, M., Yuan, B., 2012. Mathematical Model and Matlab Simulation of Strapdown Inertial Navigation System. Modelling and Simulation in Engineering 2012, 1–25. doi:10.1155/2012/264537

Appendix

All appendices and related videos can be found on the CD attached to this thesis.

Contents

List of Figure

List of Table

Appendix A. Sensor Calibration Experiment

This appendix is divided into two main parts. The first part concerns the sensor calibration experiments for the multi-axial force and torque sensor. The second part relates to the benchmarking and calibration experiments for motion capture systems.

Both sensor calibration experiments focus on observing and collecting data, in order to calibrate sensors for the fixture. The first set of experiments focused on collecting data output from the multi-axial force and torque sensor. The second set of experiments focused on benchmarking and selecting a motion sensor to capture the operator's movements.

A.1   Calibration of Multi-Axial Force and Torque Sensor

The aim of the calibration of the multi-axial force and torque sensor was to test the sensor precision under a single axial load; select an appropriate frame rate for further experiments; and observe the sensor behaviour when the single-axial load is applied at different points on the profile of the workpiece.

A.1.1.   Single Axial Load and Sample Rate

Figure A.1 illustrates the setup of the first experiment with the multi-axial force and torque sensor. The sensor captured a single axial force applied with the weighted load (250 g), and data were recorded using different sample rates, as shown in Figure A.2.

In this experiment, the force output of the weighted load and the number of frames were recorded for each sample rate. Each sample rate was tested for 10 seconds. Table A.1 and Figure A.3 shows the force output and measurement error for each sample rate, as well as the number of frames. A range of sample rate was tested (304Hz, 250Hz, 200Hz, 152Hz, 73Hz, 35Hz, and 18Hz). As expected (see Figure A.2), the force measured with the sensor was equivalent to the weight of the peg load (250 g = 2.5 N). It was also observed that the number of frames changes depending on the sample rate, where a lower sample rate value would provide less quantity of data than a higher sample rate.
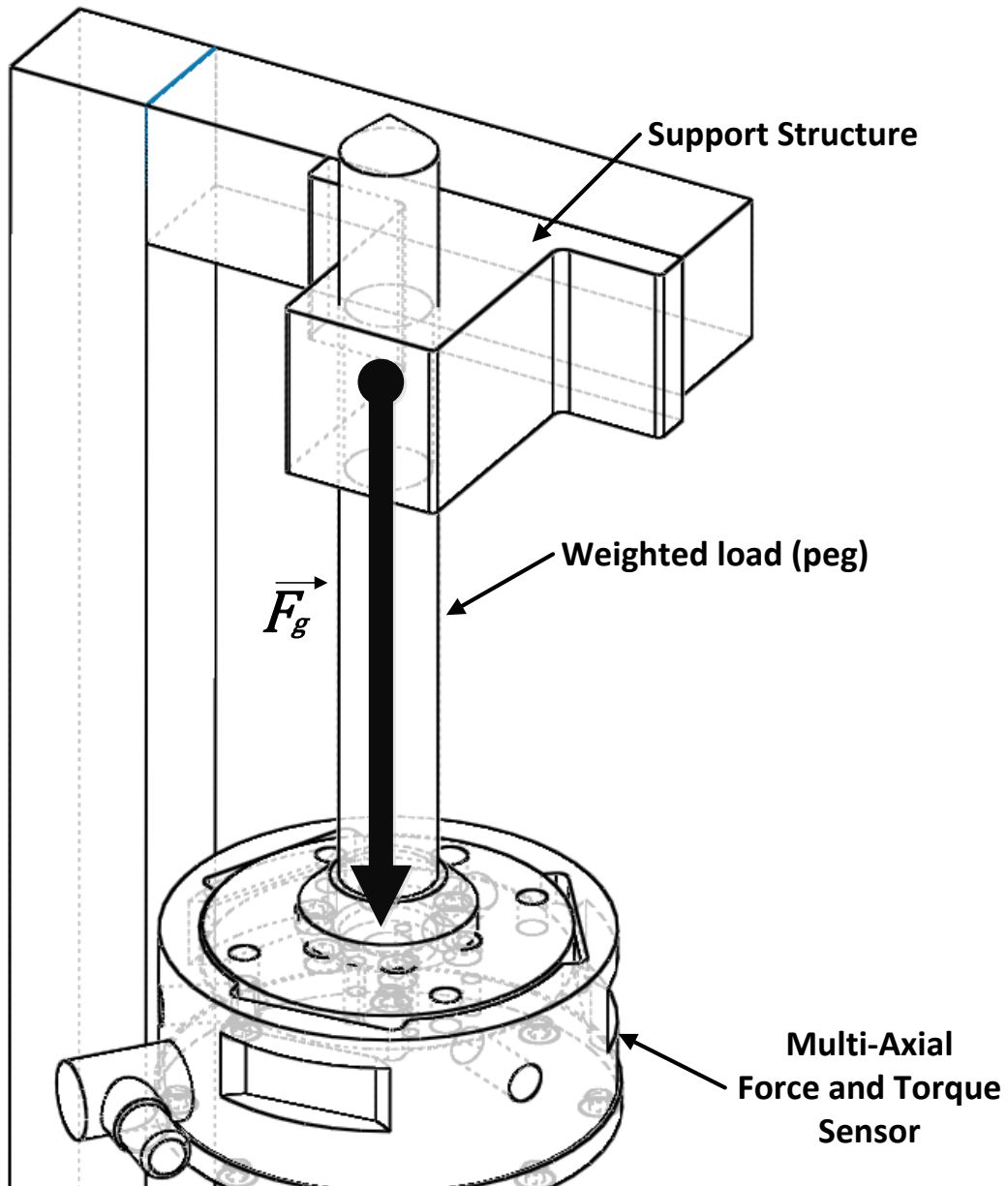
Figure A.1: Experiment setup for the pre-calibration experiment of the multi-axial force and torque sensor

Labels in figure: Support Structure; Weighted load (peg); Multi-Axial Force and Torque Sensor; $\vec{F_g}$
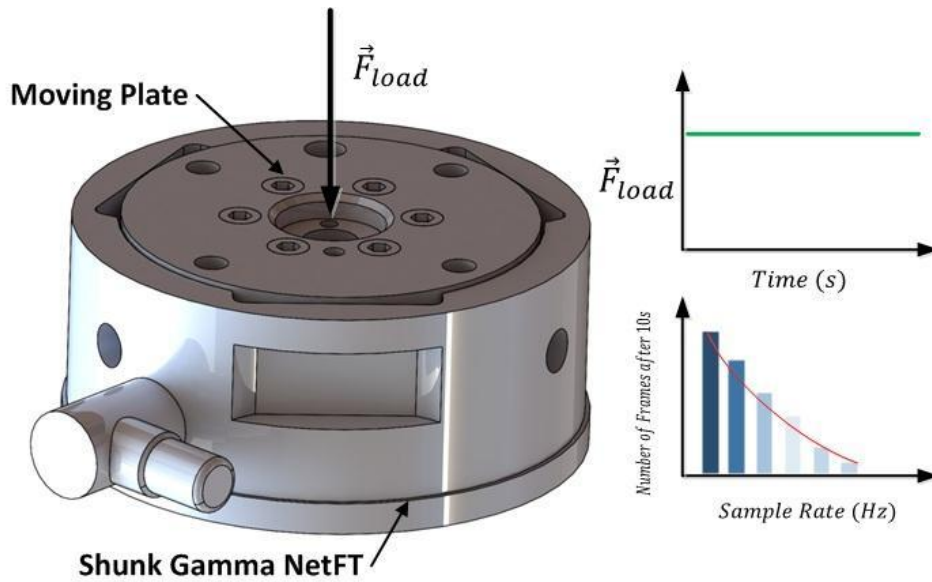
Figure A.2: Expected result for a single load applied on the multi-axial force and torque sensor

Table A.1: Data recorded using different sample rate

Sample Rate (Hz)	Number of Frame	*min*	*Max*	Average	Error
18	178	2.51	2.58	2.55	+0.05
35	333	2.55	2.49	2.52	+0.02
73	691	2.48	2.53	2.51	+0.01
152	1415	2.45	2.51	2.48	-0.02
200	1850	2.53	2.59	2.56	+0.06
250	2349	2.51	2.59	2.55	+0.05
304	2881	2.53	2.6	2.56	+0.06

Sample Rate for Single Axial Load
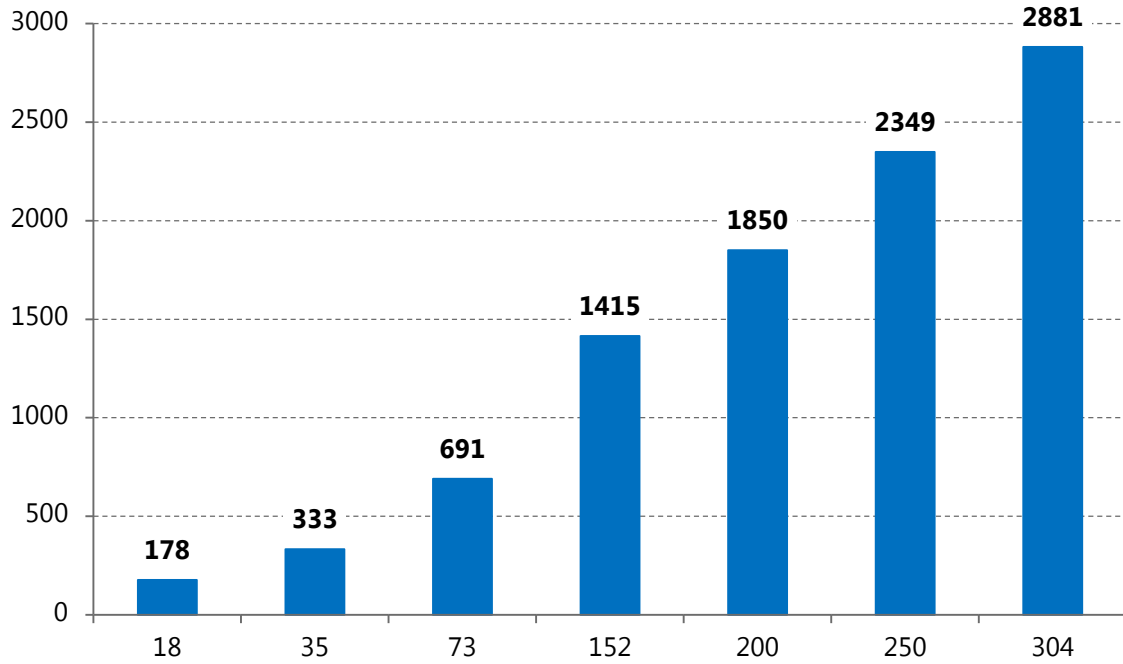
Figure A.3: Histogram of number of frames captured after 10s of measurement using different frame rate

A.1.2. Understanding of the Sensor Output for Manual Polishing Processes

The second calibration experiment with the multi-axial force and torque sensor focused on observing and understanding the change in force and torque at various points on a complex surface, such as the sample workpiece, as illustrated in Figure A.4 and A.5. As in the previous experiment, a weighted load was used with a range of additional weights. This was to simulate a range of force applied to the workpiece at different locations. The additional weights provided with a range of forces from 2.45 N to 6.59N, as shown in Table A.2.

Table A.2: Range of weight used for the calibration experiment

Items	Mass (kg)	Force (N)
Peg	0.25	2.45
Additional weight	0.312	3.06
Additional weight	0.376	3.69
Additional weight	0.672	6.59

The multi-axial force and torque sensor was mounted on a 6DoF robotic arm (ABB R120) using a plate specifically designed to accommodate the sensor and the sample workpiece, as illustrated in Figure A.4.
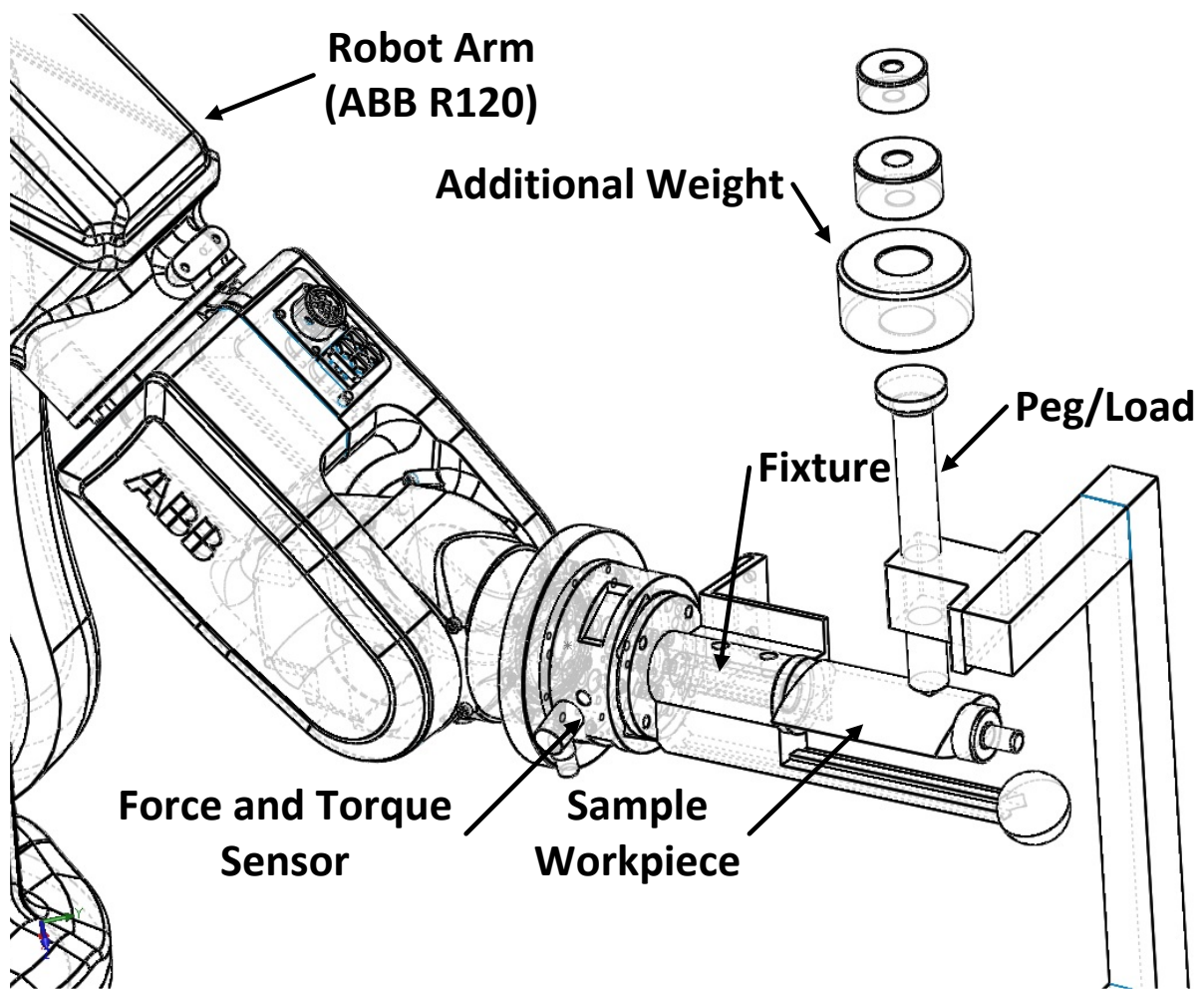
Figure A.4: Pre-calibration experiment setup for the multi-axial force and torque sensor
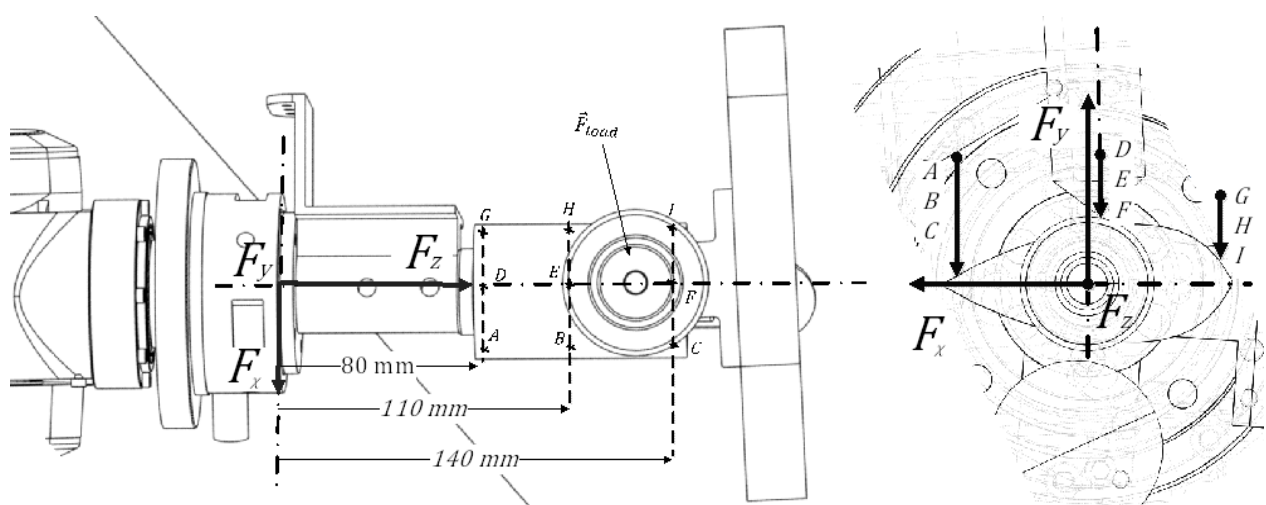
Figure A.5: Applied forces at different location

Figure A.5 shows where the different loads were applied onto the surface (Point A, B, C, D, E, F, G, H, I), 3 points aligned with the centre of the workpiece and the *z-axis* of the multi-axial force and torque sensor (Points D, E, F), and 6 points at each edge of the workpiece, small and thick edge respectively. Following newton's second laws, the force and torque applied at each point could be calculated using Equations 5.1 and 5.2, respectively.

$$\vec{F} = m\vec{g} \qquad\qquad \text{Eq.(A.1)}$$

Where $\vec{F}$ is the force applied on the surface (*N*), m is the mass of the load (*kg*), and $\vec{g}$ is the gravity $(9.81 ms^2)$.

$$T = \vec{F}L \qquad\qquad \text{Eq.(A.2)}$$

Where T is the torque (*Nm*), $\vec{F}$ is the load applied (*N*), and L is the distance (*m*) between the sensor and the point where the load is applied.

As the locations and values of the loads were known, it was assumed that the force value observed would be in a single axis and that the torque would be dependent on the location of the load, i.e. the distance from the sensor to the load, as illustrated in Figure A.6.
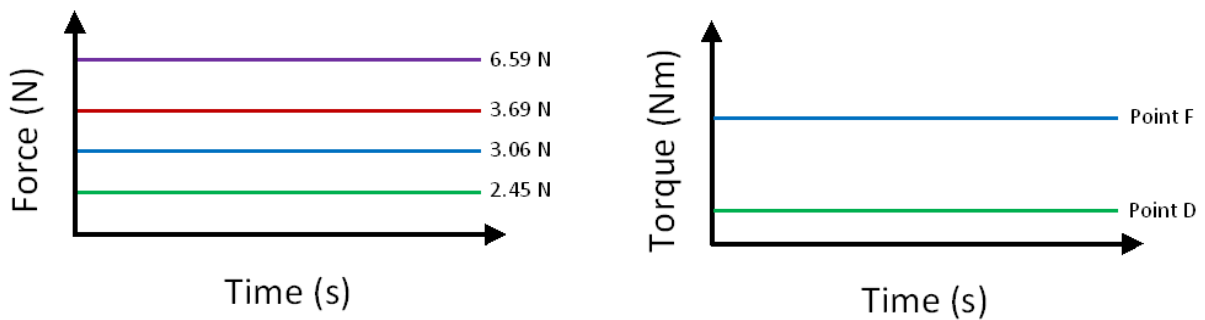
Figure A.6: Force and torque output assumption

Figure A.7 to A.14 and Table A.3 to A.6 present the results of this experiments. The multi-axial force and torque sensor showed increasing torque output when the load was applied further away from the sensor, as expected (see Equation A.2 and Figure A.6). However, the force output also changed in axis depending on the location of the load.

For example, at points D, E, and F, the applied force was detected mainly in the *y-axis* by the sensor. This is because these points were aligned with the origin of the sensor along *Fz (Z-axis)*, as seen in Figure A.5.

However, at points A to C and G to I, the force output was distributed around the *Fx* and *Fy (X-Y-axis)*, especially at points G to I (see Figures A.7 to A.14). Moreover, the combination of each axis (i.e. the force vector) shows the actual value for the load at each point.

As expected the torque increased for the same force load, due to the distance between the multi-axial force and torque sensor and the point where the load is applied. The above behaviours have been observed for each iteration (or weighted load).

Table A.3: Experiment result with a load of 250g (2.45 N)

Ref	Pt	l	$\overrightarrow{F_{nomial}}$	$\overrightarrow{T_{nomial}}$	F_x	F_y	F_z	T_x	T_y	T_z	$F_{recorded}$	$T_{recorded}$	F_{error}	T_{error}
FT_A_250	A	0.08	2.45	0.2	-0.77	4.322	-0.484	-0.343	-0.085	-0.094	3.069	-0.522		
FT_B_250	B	0.11	2.45	0.275	-0.366	1.996	0.389	-0.211	-0.039	-0.045	2.019	-0.295		
FT_C_250	C	0.14	2.45	0.35	-0.442	1.821	0.149	-0.243	-0.057	-0.041	1.528	-0.341		
FT_D_250	D	0.08	2.45	0.2	0.047	2.266	-0.047	-0.191	0.01	-0.005	2.266	-0.185	9.36	4.5
FT_E_250	E	0.11	2.45	0.275	-0.055	2.267	0.286	-0.25	-0.005	-0.001	2.498	-0.257	9.32	9.09
FT_F_250	F	0.14	2.45	0.35	0.086	2.351	0.117	-0.341	0.014	-0.002	2.554	-0.329	5.96	2.57
FT_G_250	G	0.08	2.45	0.2	1.099	0.863	0.139	-0.077	0.086	0.018	2.023	0.027		
FT_H_250	H	0.11	2.45	0.275	1.216	1.015	0.274	-0.112	0.126	0.021	2.505	0.034		
FT_I_250	I	0.14	2.45	0.35	1.042	1.28	0.111	-0.167	0.133	0.025	2.433	-0.009		
Average											2.322	-0.209		

Force output under 2.45N load

	A	B	C	D	E	F	G	H	I
Fz	-0.484	0.389	0.149	-0.047	0.286	0.117	0.139	0.274	0.111
Fy	4.322	1.996	1.821	2.266	2.267	2.351	0.863	1.015	1.28
Fx	-0.77	-0.366	-0.442	0.047	-0.055	0.086	1.099	1.216	1.042
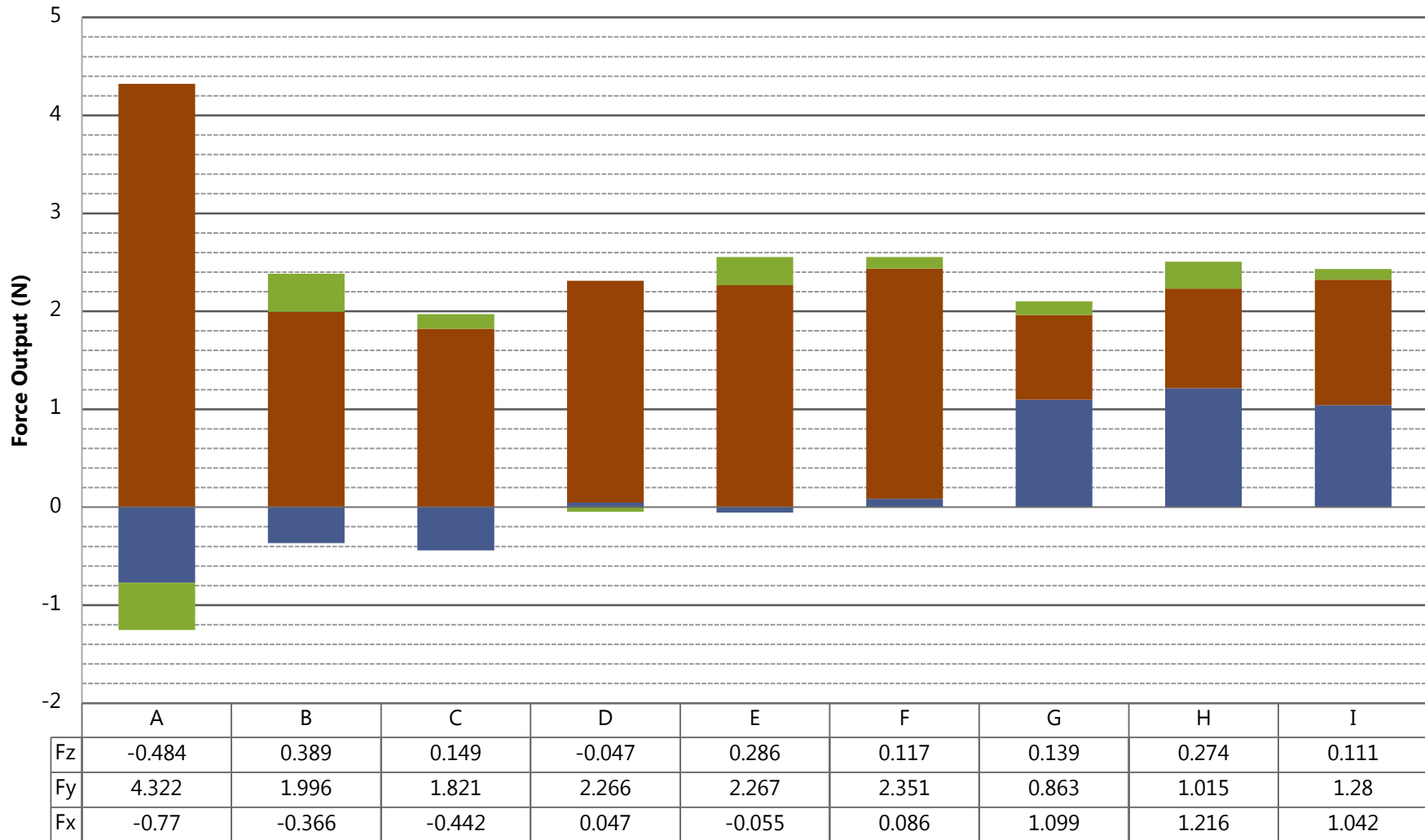
Figure A.7: Force result with a load of 250g (2.45 N)
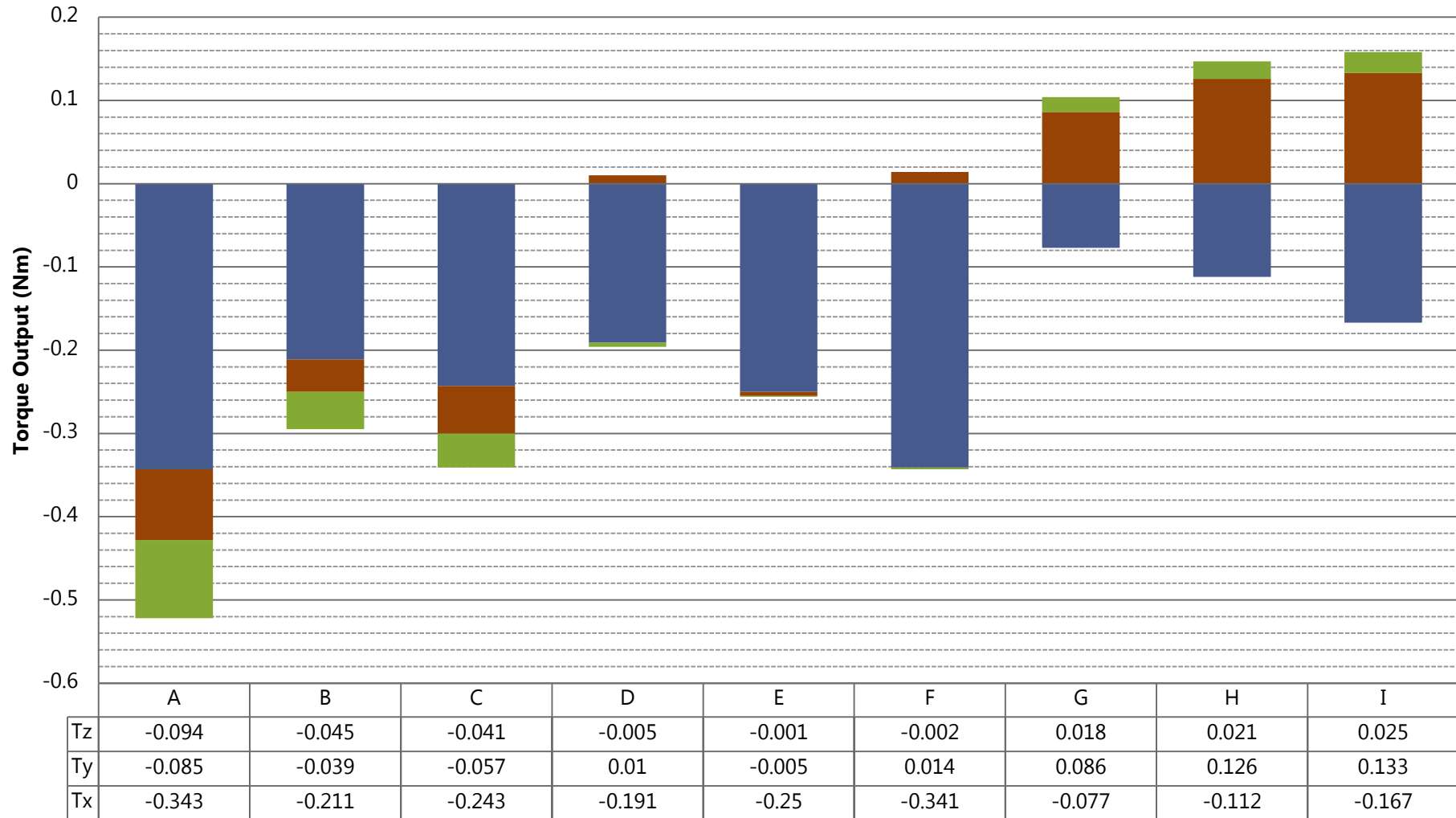
Figure A.8: Torque result with a load of 250g (2.45 N)

	A	B	C	D	E	F	G	H	I
Tz	-0.094	-0.045	-0.041	-0.005	-0.001	-0.002	0.018	0.021	0.025
Ty	-0.085	-0.039	-0.057	0.01	-0.005	0.014	0.086	0.126	0.133
Tx	-0.343	-0.211	-0.243	-0.191	-0.25	-0.341	-0.077	-0.112	-0.167

Table A.4: Experiment result with a load of 312g (3.06 N)

Ref	Pt	l	$\overrightarrow{F_{nomial}}$	$\overrightarrow{T_{nomial}}$	F_x	F_y	F_z	T_x	T_y	T_z	$F_{recorded}$	$T_{recorded}$	F_{error}	T_{error}
FT_A_312	A	0.08	3.06	0.2496	-0.239	2.9	-0.167	-0.224	-0.031	-0.06	2.494	-0.315		
FT_B_312	B	0.11	3.06	0.3432	-0.581	2.695	-0.066	-0.291	-0.068	-0.061	2.048	-0.421		
FT_C_312	C	0.14	3.06	0.4368	-0.477	2.497	0.268	-0.33	-0.066	-0.056	2.288	-0.453		
FT_D_312	D	0.08	3.06	0.2496	-0.211	3.07	-0.08	-0.256	-0.013	0.007	2.779	-0.262	1.60	-2.56
FT_E_312	E	0.11	3.06	0.3432	-0.261	2.876	0.051	-0.337	-0.021	-0.004	2.667	-0.363	7.82	1.80
FT_F_312	F	0.14	3.06	0.4368	0.001	2.959	0.08	-0.427	0.006	0.001	3.04	-0.42	5.16	2.24
FT_G_312	G	0.08	3.06	0.2496	1.527	1.035	0.041	-0.097	0.122	0.026	2.603	0.051		
FT_H_312	H	0.11	3.06	0.3432	1.67	1.455	0.054	-0.162	0.175	0.034	3.18	0.047		
FT_I_312	I	0.14	3.06	0.4368	1.347	1.532	-0.003	-0.207	0.177	0.028	2.876	-0.002		
Average											2.664	-0.238		

Force output under 3.06 N load

	A	B	C	D	E	F	G	H	I
Fz	-0.167	-0.066	0.268	-0.08	0.051	0.08	0.041	0.054	-0.003
Fy	2.9	2.695	2.497	3.07	2.876	2.959	1.035	1.455	1.532
Fx	-0.239	-0.581	-0.477	-0.211	-0.261	0.001	1.527	1.67	1.347
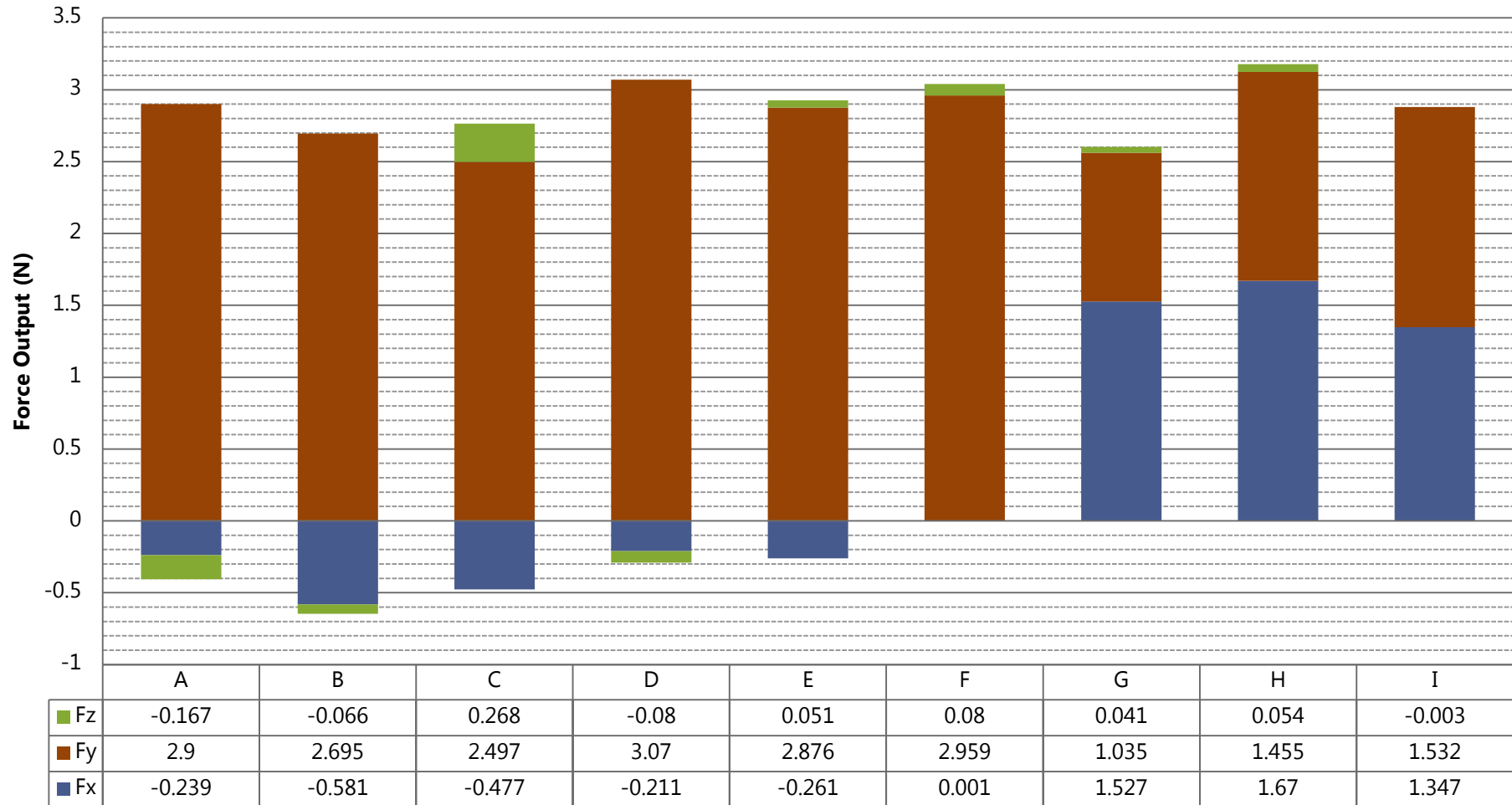
Figure A.9: Force result with a load of 312g (3.06 N)

Torque output under 3.06 N load

	A	B	C	D	E	F	G	H	I
■ Tz	-0.06	-0.061	-0.056	0.007	-0.004	0.001	0.026	0.034	0.028
■ Ty	-0.031	-0.068	-0.066	-0.013	-0.021	0.006	0.122	0.175	0.177
■ Tx	-0.224	-0.291	-0.33	-0.256	-0.337	-0.427	-0.097	-0.162	-0.207
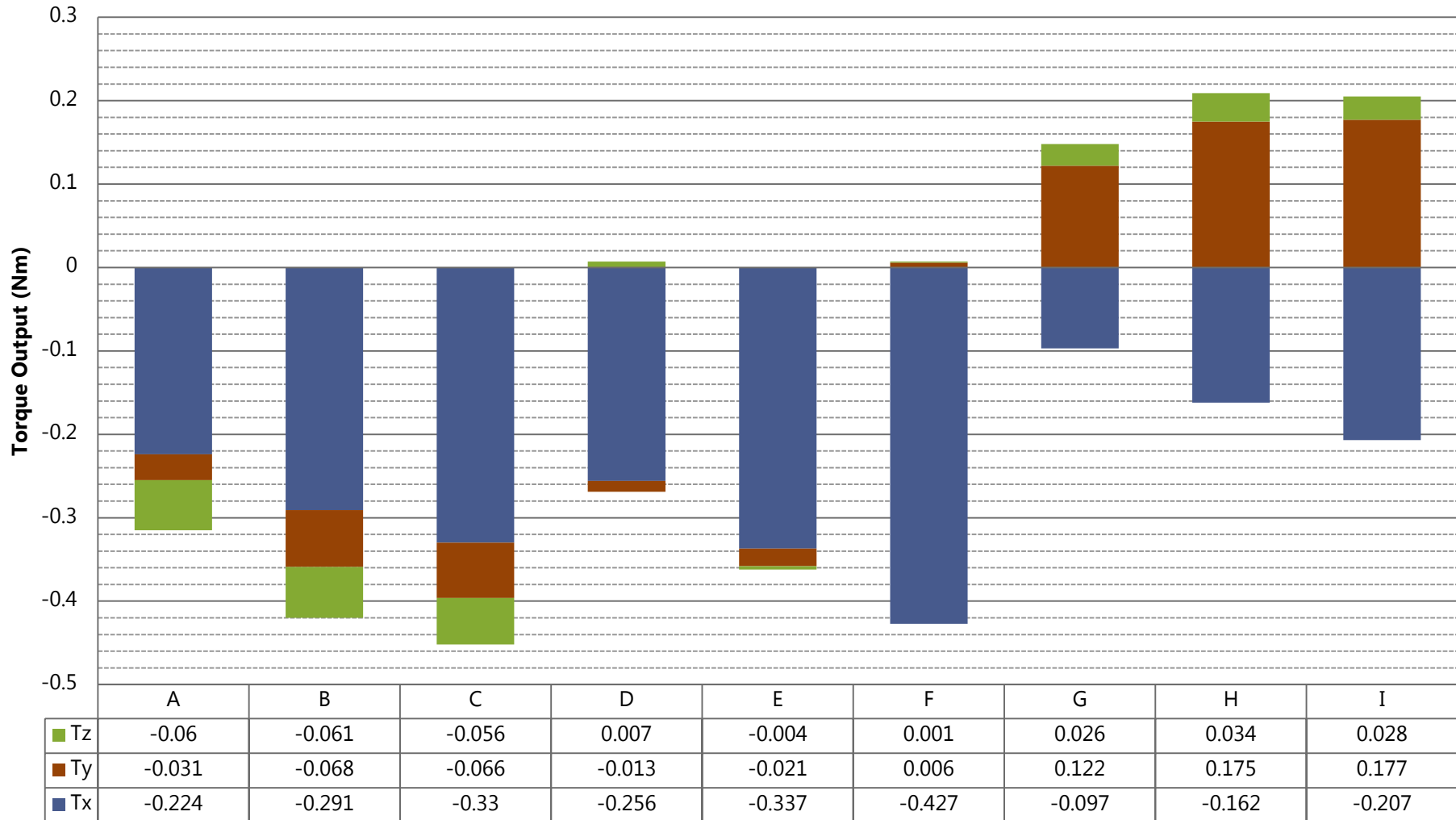
Figure A.10: Torque result with a load of 312g (3.06 N)

Table A.5: Experiment result with a load of 376g (3.69 N)

Ref	Pt	l	$\overrightarrow{F_{nomial}}$	$\overrightarrow{T_{nomial}}$	F_x	F_y	F_z	T_x	T_y	T_z	$F_{recorded}$	$T_{recorded}$	F_{error}	T_{error}
FT_A_376	A	0.08	3.69	0.3008	-0.108	3.688	0.427	-0.29	-0.01	-0.082	4.007	-0.382		
FT_B_376	B	0.11	3.69	0.4136	-0.696	2.685	-0.022	-0.292	-0.078	-0.062	1.966	-0.432		
FT_C_376	C	0.14	3.69	0.5264	-0.6	3.046	-0.032	-0.446	-0.07	-0.082	2.414	-0.598		
FT_D_376	D	0.08	3.69	0.3008	0.374	3.588	0.066	-0.282	0.026	0.006	4.028	-0.25	4.57	6.25
FT_E_376	E	0.11	3.69	0.4136	-0.305	3.218	0.002	-0.368	-0.029	-0.004	2.914	-0.402	14.41	11.025
FT_F_376	F	0.14	3.69	0.5264	0.083	3.718	0.121	-0.516	0.011	0.005	3.922	-0.5	1.11	1.97
FT_G_376	G	0.08	3.69	0.3008	1.814	1.366	0.219	-0.104	0.134	0.035	3.399	0.065		
FT_H_376	H	0.11	3.69	0.4136	1.704	1.171	-0.059	-0.145	0.182	0.029	2.817	0.066		
FT_I_376	I	0.14	3.69	0.5264	1.38	1.787	0.262	-0.263	0.186	0.031	3.429	-0.047		
Average											3.211	-0.276		

Force output under 3.69 N load

	A	B	C	D	E	F	G	H	I
■ Fz	0.427	-0.022	-0.032	0.066	0.002	0.121	0.219	-0.059	0.262
■ Fy	3.688	2.685	3.046	3.588	3.218	3.718	1.366	1.171	1.787
■ Fx	-0.108	-0.696	-0.6	0.374	-0.305	0.083	1.814	1.704	1.38
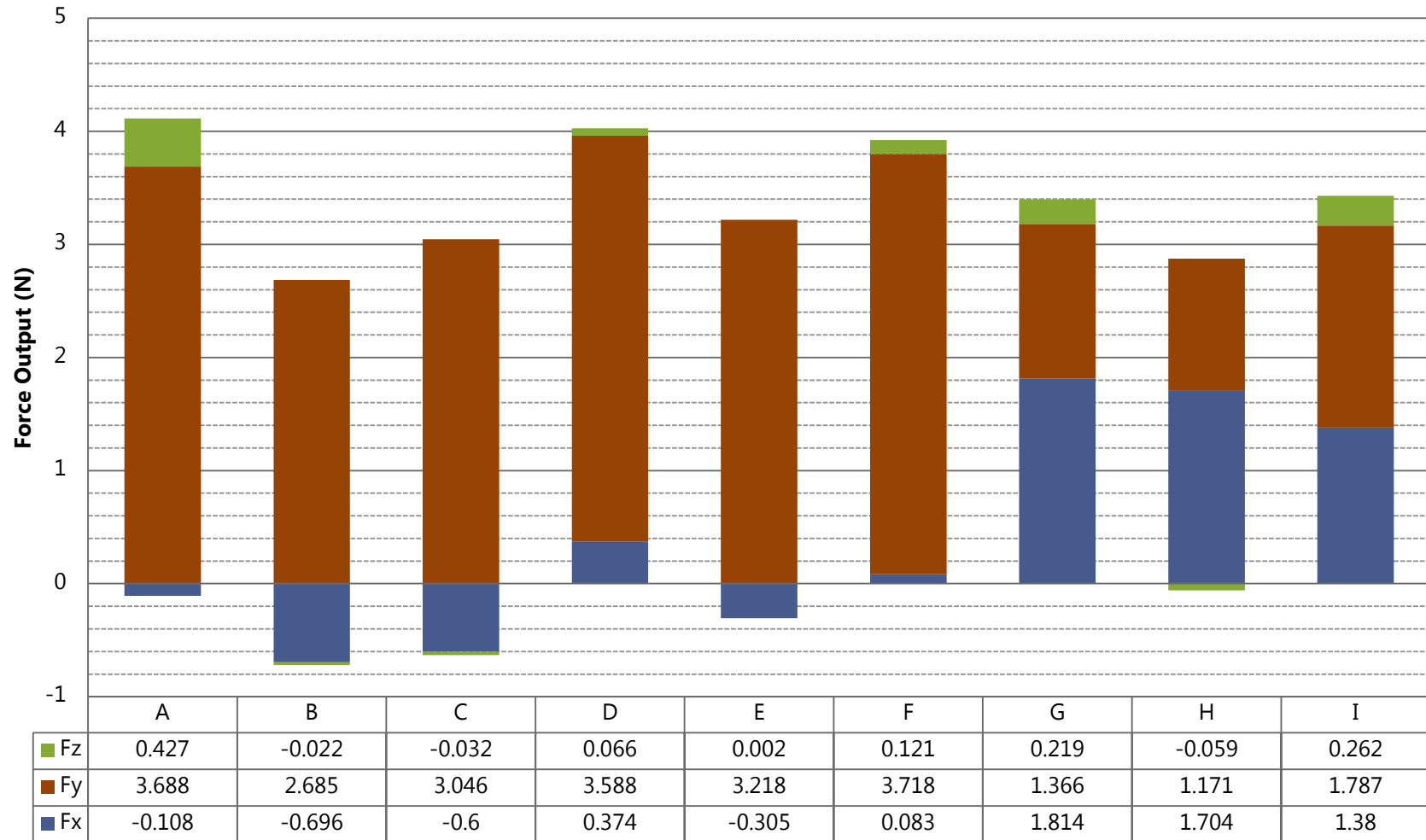
Figure A.11: Force result with a load of 376g (3.69 N)

Torque output under 3.69 N load

	A	B	C	D	E	F	G	H	I
Tz	-0.082	-0.062	-0.082	0.006	-0.004	0.005	0.035	0.029	0.031
Ty	-0.01	-0.078	-0.07	0.026	-0.029	0.011	0.134	0.182	0.186
Tx	-0.29	-0.292	-0.446	-0.282	-0.368	-0.516	-0.104	-0.145	-0.263
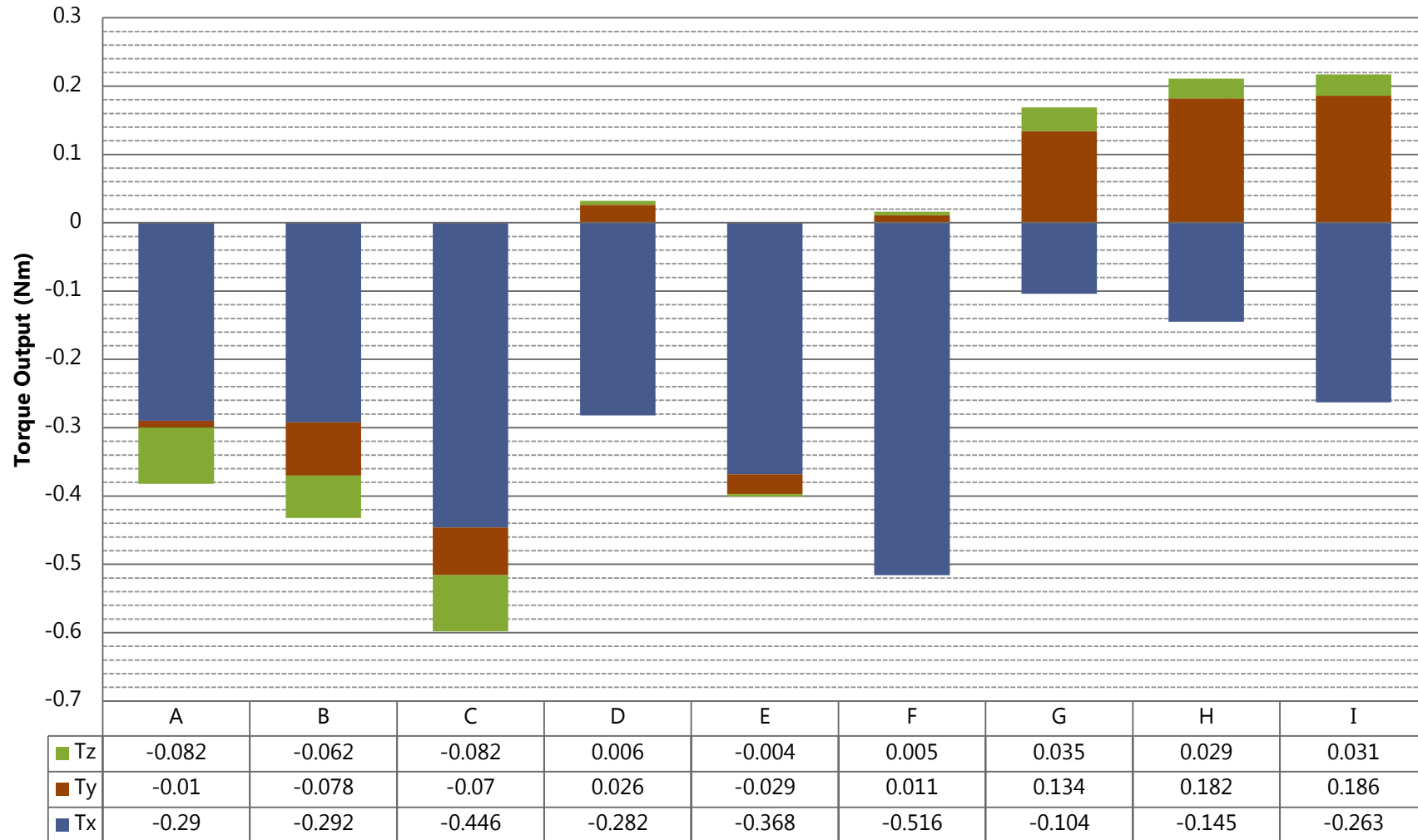
Figure A.12: Torque result with a load of 376g (3.69 N)

Table A.6: Experiment result with a load of 672g (6.59 N)

Ref	Pt	l	$\overrightarrow{F_{nomial}}$	$\overrightarrow{T_{nomial}}$	F_x	F_y	F_z	T_x	T_y	T_z	$F_{recorded}$	$T_{recorded}$	F_{error}	T_{error}
FT_A_672	A	0.08	6.59	0.5376	-0.398	5.284	0.224	-0.425	-0.026	-0.12	5.11	-0.571		
FT_B_672	B	0.11	6.59	0.7392	-1.395	6.186	0.449	-0.682	-0.145	-0.148	5.24	-0.974		
FT_C_672	C	0.14	6.59	0.9408	-0.696	5.494	0.324	-0.756	-0.093	-0.136	5.122	-0.984		
FT_D_672	D	0.08	6.59	0.5376	-0.308	5.757	-0.571	-0.48	-0.018	0.004	4.878	-0.493	14.33	10.71
FT_E_672	E	0.11	6.59	0.7392	-0.238	6.541	0.246	-0.711	-0.03	-0.004	6.549	-0.745	2.66	3.814
FT_F_672	F	0.14	6.59	0.9408	0.502	6.697	0.072	-0.936	0.067	-0.01	7.27	-0.879	0.342	0.510
FT_G_672	G	0.08	6.59	0.5376	2.564	3.243	0.302	-0.26	0.194	0.063	6.108	-0.004		
FT_H_672	H	0.11	6.59	0.7392	2.782	3.089	0.456	-0.343	0.288	0.051	6.327	-0.004		
FT_I_672	I	0.14	6.59	0.9408	1.718	4.818	0.311	-0.685	0.228	0.053	6.846	-0.404		
Average											5.939	-0.562		

Force output under 6.59 N load

	A	B	C	D	E	F	G	H	I
Fz	0.224	0.449	0.324	-0.571	0.246	0.072	0.302	0.456	0.311
Fy	5.284	6.186	5.494	5.757	6.541	6.697	3.243	3.089	4.818
Fx	-0.398	-1.395	-0.696	-0.308	-0.238	0.502	2.564	2.782	1.718
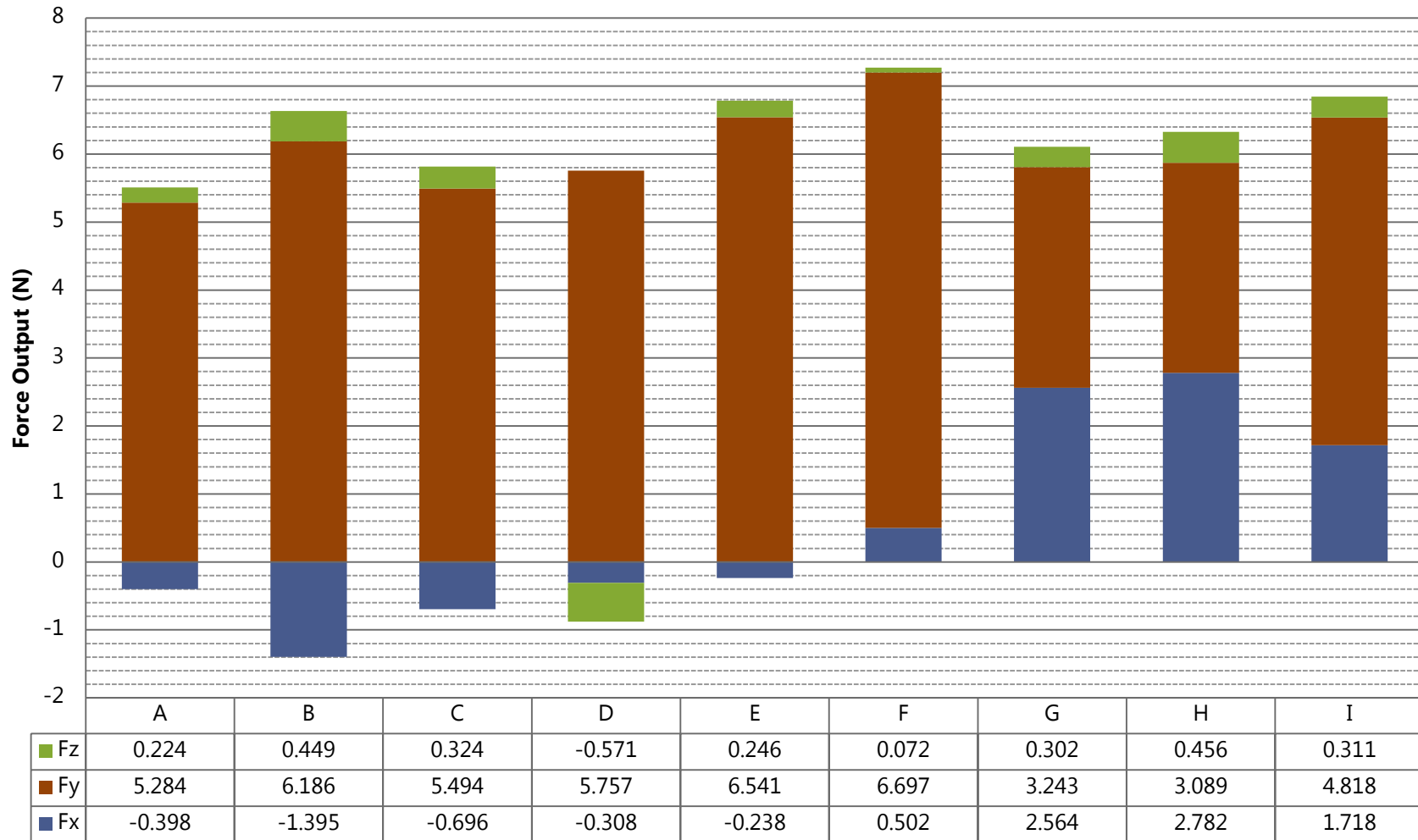
Figure A.13: Force result with a load of 672g (6.59 N)

Torque output under 6.59 N load

	A	B	C	D	E	F	G	H	I
Tz	-0.12	-0.148	-0.136	0.004	-0.004	-0.01	0.063	0.051	0.053
Ty	-0.026	-0.145	-0.093	-0.018	-0.03	0.067	0.194	0.288	0.228
Tx	-0.425	-0.682	-0.756	-0.48	-0.711	-0.936	-0.26	-0.343	-0.685
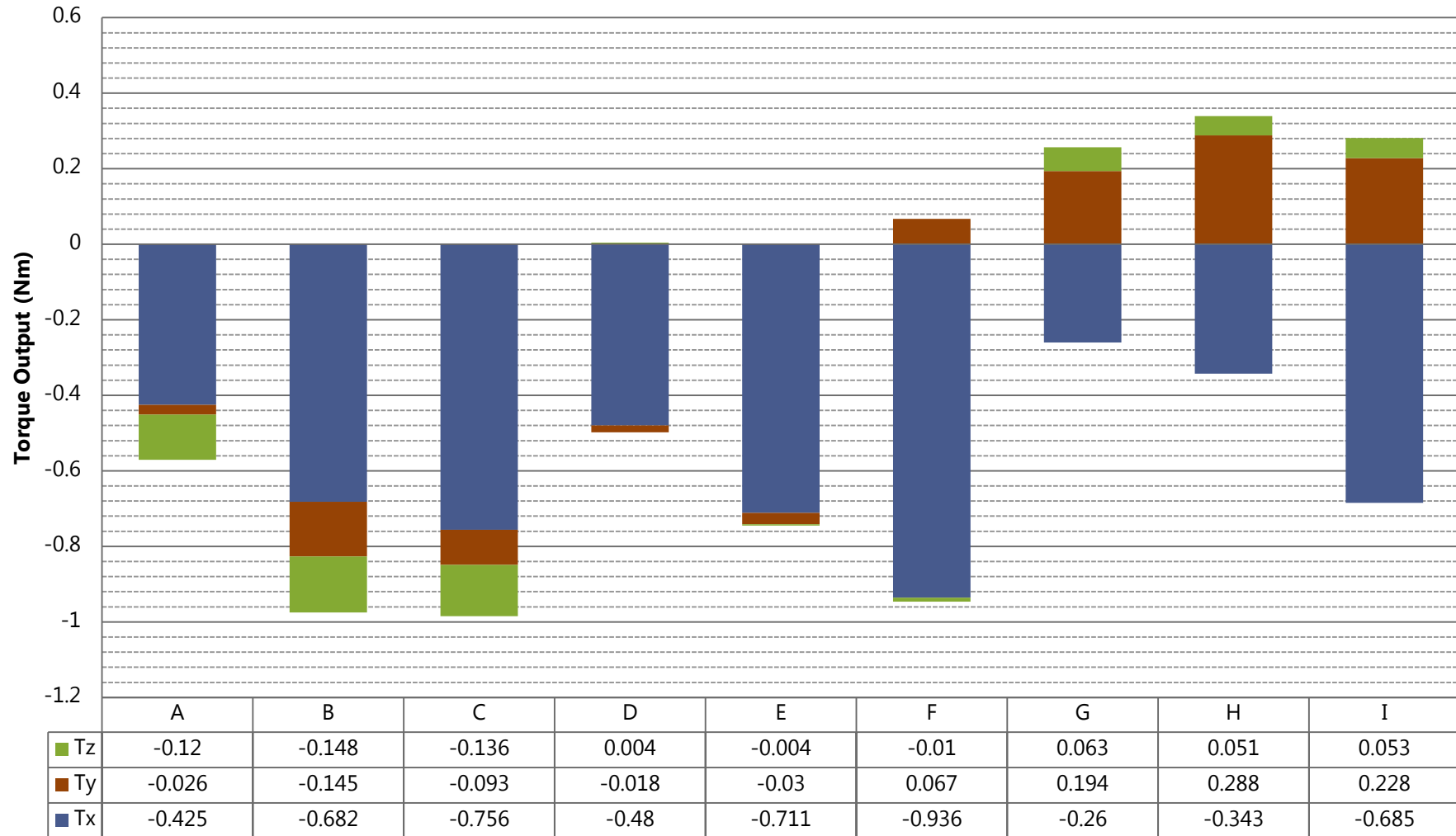
Figure A.14: Torque result with a load of 672g (6.59 N)

A.1.1.1. Discussion of the Sensor Calibration (multi-axial force and torque)

Both experiments with the multi-axial force and torque sensor provided with a better understanding of data output expected during the capture of the forces and torques in subsequence to manual polishing experiments (see Chapter 6).

In the first experiment, the precision of the sensor using different sample rate was observed. The data collected (Figure A.1 to A.3 and Table A.1) showed how the sample rate value have an impact on the processing power and the quality of data captured. For example, a high sample rate will obtain more precise data but require more processing power when capturing or analysing the data. However, the force and torque values collected for a constant load were not affected by the sample rate.

The minimum and maximum error recorded with the sensor was 0.02N and 0.06N respectively. This represents less than 5% at any sample rate, which is an acceptable accuracy.

The second calibration experiment (Section A.1.2) of the multi-axial force and torque sensor elucidated to understand how the forces are distributed under a perpendicular load applied on a complex surface. From the experimental results, it was noted that the force was distributed differently along the *x-y-z-axes* depending on the location of the contact point. However, the combination (or vector) of all 3 forces remained the same. As expected the torque output increased, the further away the load was to the sensor.

From these results, it can be assumed that during the capture of manual polishing parameters (see Chapter 6), the force contact between the sample workpiece and the abrasive tool will be observed around all 3-axis (*Fx*, *Fy*, and *Fz*).

These experiments had shown good capabilities of the multi-axial force and torque to capture forces and torques for the fixture.

A.2   Benchmark and Calibration of the Motion Sensor

The following section focuses on motion capture technology. These experiments aim to demonstrate the capabilities of selected technologies to track operator's motion with the fixture. At the end of these experiments, a motion capture system would be chosen to capture operator motions (see Section A.3).

A.2.1.   Inertial Measurement Unit (Xsens MTw)

The aim of this experiment was to evaluate the capability of the Xsens MTw (Xsens, n.d.) to track human movements within a small workspace (such as in manual polishing) and investigate the processing of acceleration data to position using different algorithms.

Different studies have shown the capabilities of inertial measurement unit sensors (or IMU) for motion tracking in 3D environment using a single (Fischer et al., 2013a; Glanzer et al., 2009; Walder and Bernoulli, 2010) or multiple sensors (Roetenberg et al., 2009) in real-time or with offline processing.

The conventional way to calculate the position from the acceleration is to use a double integration of the acceleration data, as shown on Figure A.15. Following this method, different researches were carried out to develop solutions for indoor positioning system using an inertial measurement systems (El-fatatry, 2003; Filieri and Melchiotti, 2012; Fischer et al., 2013b; Glanzer et al., 2009; Hang et al., 2012; Jones, 1979; Khan, 2013; Ramaswamy, 2011; Rogers, 2003; Roviaire and Nasseh, 2009; Slifka, 2004; Web and Project, 2013; Welch, 1995; Zhang et al., 2012).
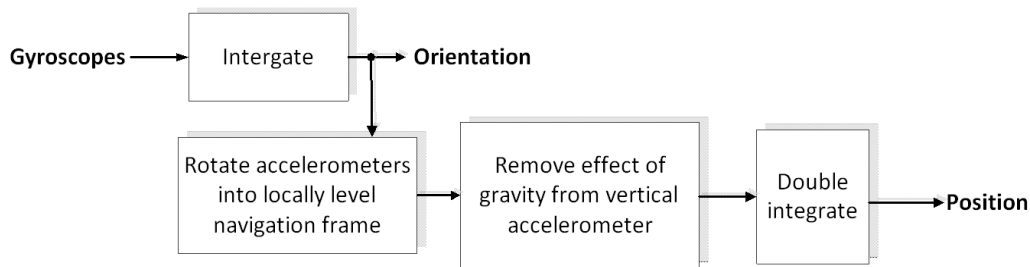
Figure A.15: Block diagram to compute/calculate the position from acceleration data (Fischer et al., 2013b)

In this experiment, data output from the accelerometer was processed offline using the same methodology. A rectangular path (*19 cm x 20 cm*) was drawn on an A4 paper for the operator to follow. The IMU was wirelessly connected to a PC host and recorded the acceleration, orientation and magnetic field from the operator's movements. The recorded data was then processed using Ulrich (Glanzer et al., 2009) and Fischer (Fischer et al., 2013b) algorithms, as illustrated in Figures A.17 and A.18 respectively, to compute the position and path followed.

Different research studies have shown successful development of solutions for motion tracking using a single or several sensors (El-fatatry, 2003; Eskin, 2006; Filieri and Melchiotti, 2012; Fischer et al., 2013b; Jones, 1979; Khan, 2013; Ramaswamy, 2011; Rogers, 2003; Slifka, 2004; Zhang et al., 2012). Commercial solutions also exist such as a CAD plug-in (Roetenberg et al., 2013) which can record and display in real-time the position of the sensor (or object) in 3D environment, but with a small latency.

However, the results of this calibration experiment were not convincing, as shown in Figures A.17 and A.18. This may be due to the tracking environment being too small (rectangular figure of *19 cm x 20 cm*), compare to the different case studies that used the same sensor and algorithm in a larger environment, such as pedestrian positioning (Fischer et al., 2013a).

In overall, the IMU showed promising results for measuring accelerations and orientations. Therefore, this sensor was used with the fixture to measure and compute the fixture orientation (through gyroscope), and speed and vibration (through accelerometer).
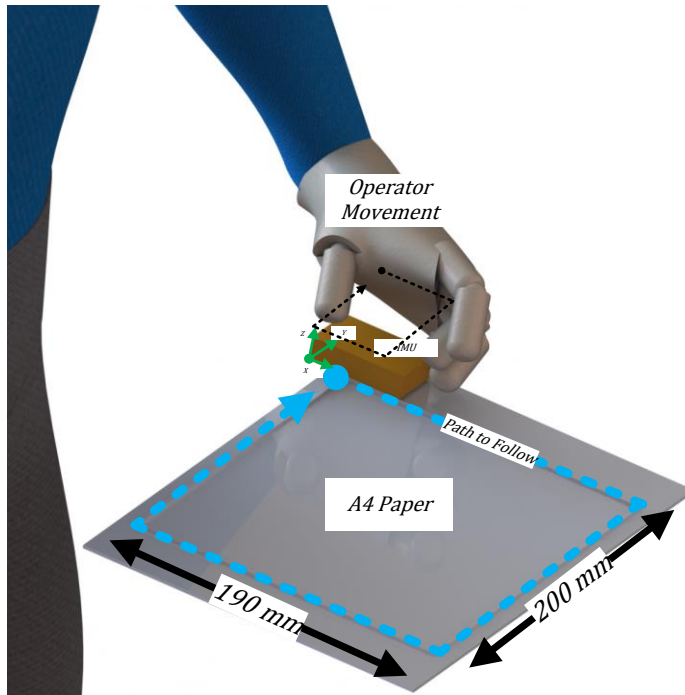
Figure A.16: Inertial measurement unit benchmark experiment setup and procedure

Algorithm 1: Gait Tracking Algorithm
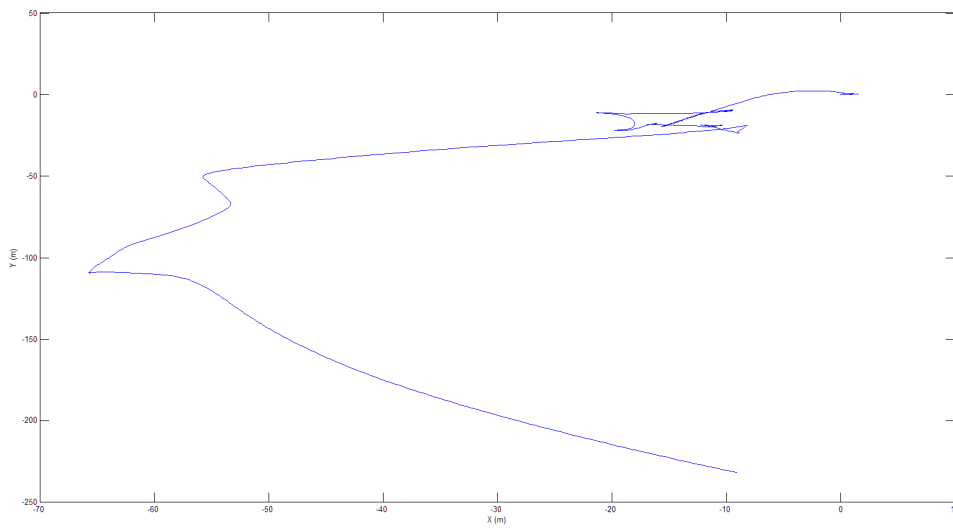
Figure A.17: XY axis position result computed with Ulrich et al. algorithm (Glanzer et al., 2009)

Algorithm 2: Implementing a Pedestrian Tracker Using Inertial Sensor (Fischer et al., 2013a)
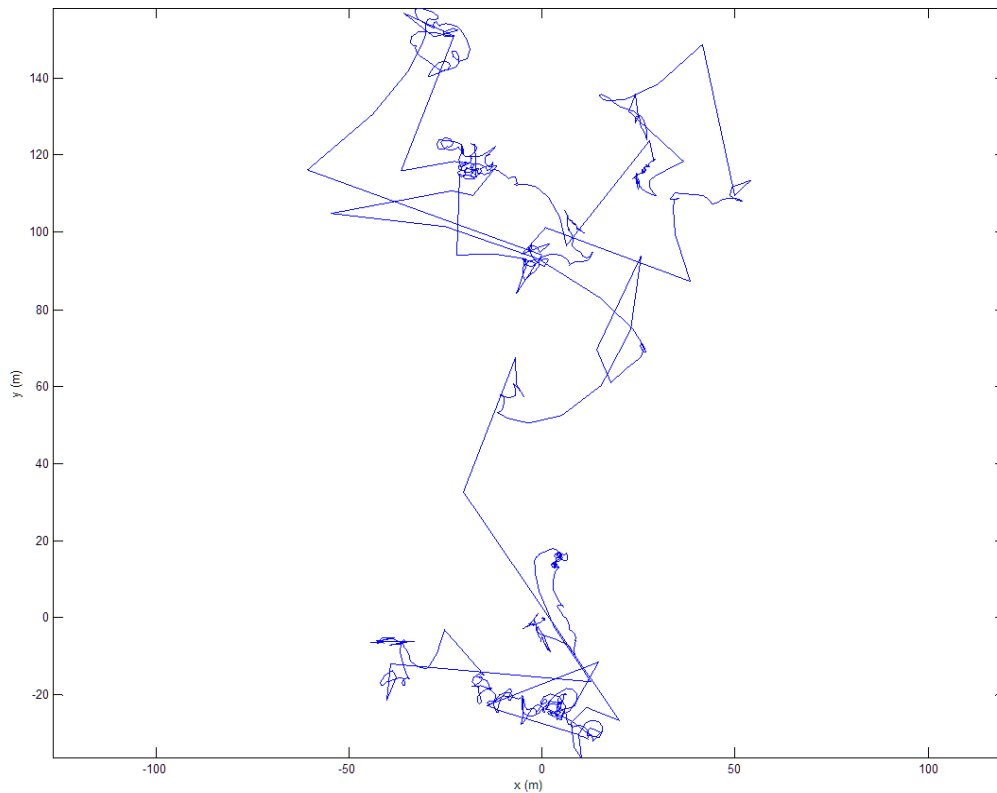
Figure A.18: XY axis position computed with Fischer algorithm (Fischer et al., 2013a)

A.2.2. Motion Controller (Leap Motion)

The following section focuses on the assessment and capture of data, using a commercial motion controller (Leap Motion). In this experiment, the capability of the sensor to track hands or fingers in 3D space and small environment was evaluated.

The Leap Motion controller has been primarily developed for hand and finger(s) tracking for computing and video games applications (Adhikarla et al., 2014; Bassily et al., 2014; Hsu et al., 2014; Huang et al., 2014; Mohandes et al., 2014; Wang et al., 2014). These applications have shown good capabilities of this sensor for gesture tracking and recognitions.

As for the IMU (Section A.2.1), the sensor tracked the operator movement when following a rectangular path, as illustrated in Figure A.19 and A.20. Three set of experiments were carried out with the sensor at different positions. This was to try different configurations (as seen in Figure A.20 and Table 5A.7) that may be optimum for the capture of human movement with the fixture.

All data shown in Figure A.21 to A.23 were captured in real-time with the sensor at different positions (see Figure 0A20). Overall, the sensor did not provide adequate results for this experiment, despite having shown good capabilities in other applications (Adhikarla et al., 2014; Bassily et al., 2014; Hsu

et al., 2014; Huang et al., 2014; Mohandes et al., 2014; Wang et al., 2014). However, the sensor was adequate at tracking gestures when in a horizontal position.
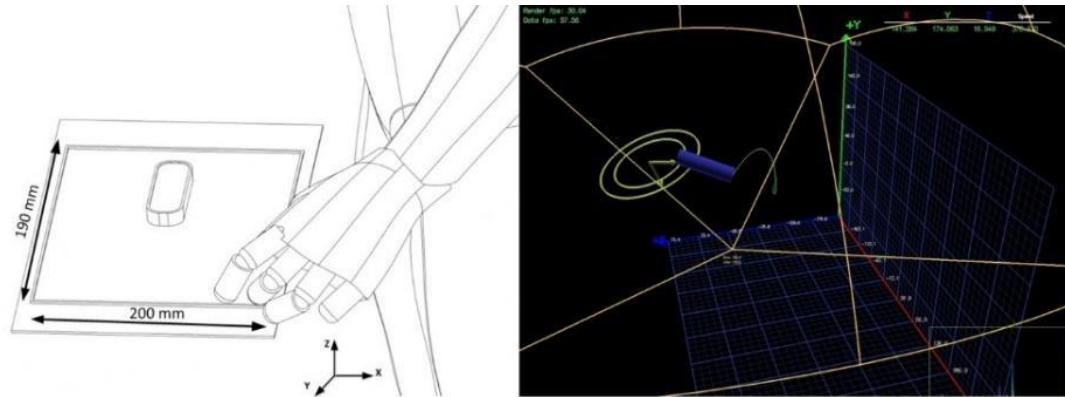
Figure A.19: Leap motion capture environment (left) and software environment (right)

Table A.7: Leap motion orientation for pre-calibration experiment

Iteration Number	Sensor Orientation
110	Horizontal
120	Reversed
130	Vertical
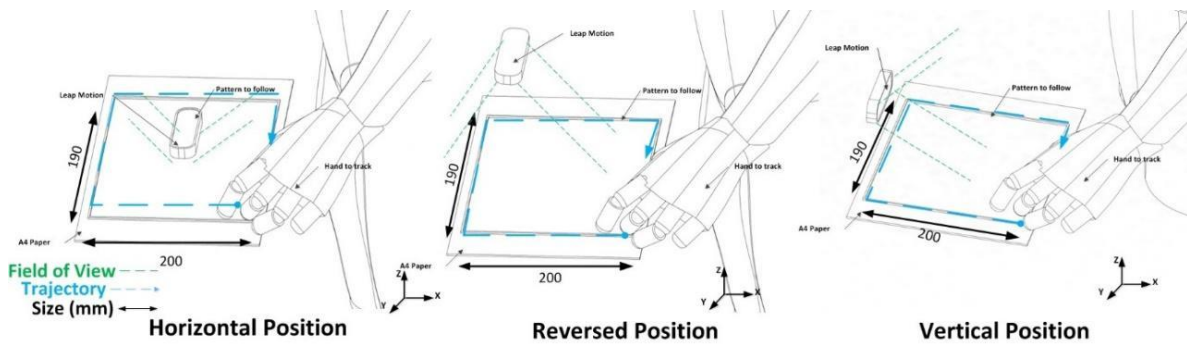
Figure A.20: Leap motion experimental setup

Iteration 110 Horizontal Position
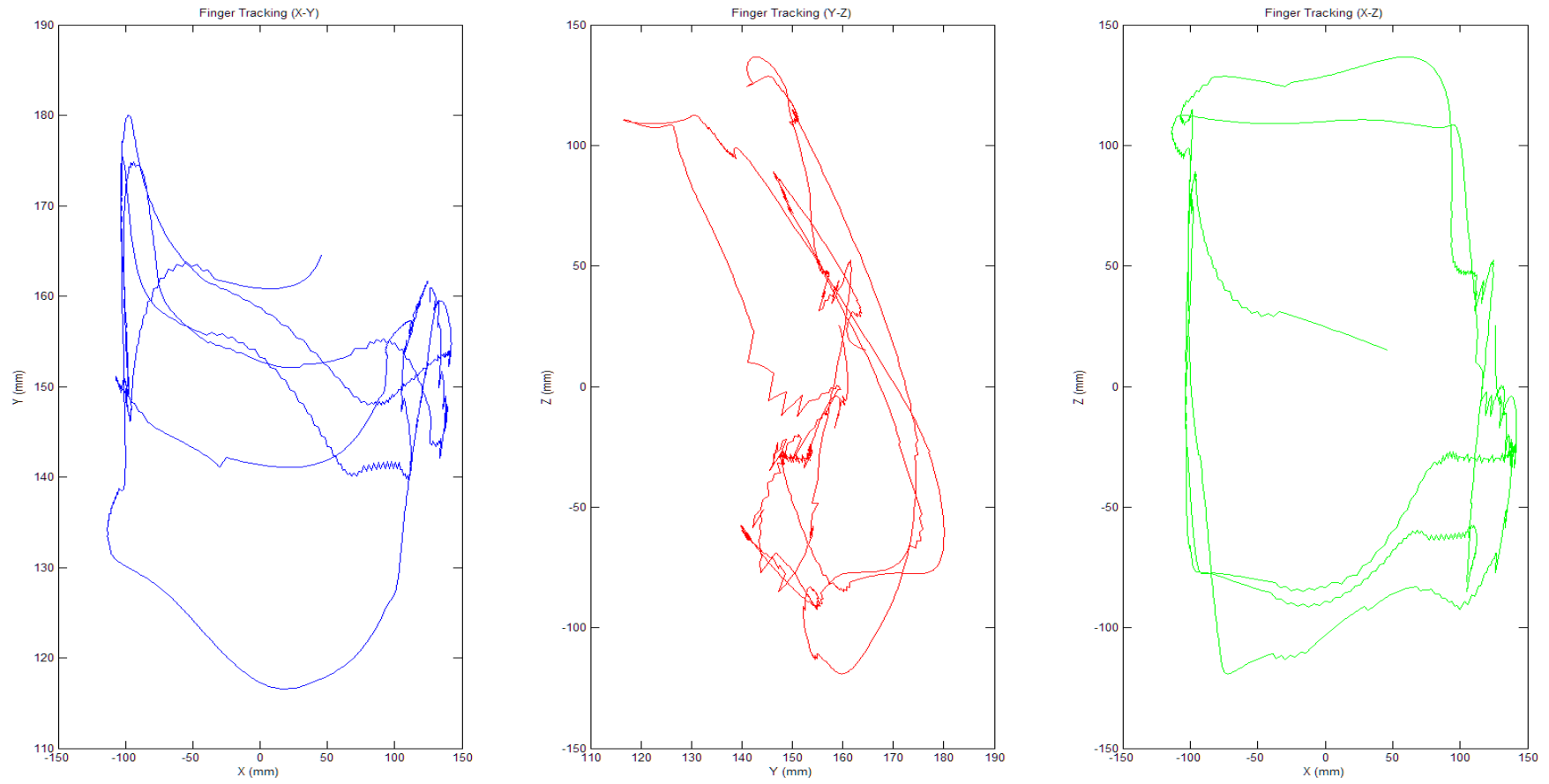
Figure A.21: Leap motion experiment – vertical position – Iteration 110

Figure A.22: Leap motion experiment – reversed position – Iteration 120

Iteration 130: Vertical Position
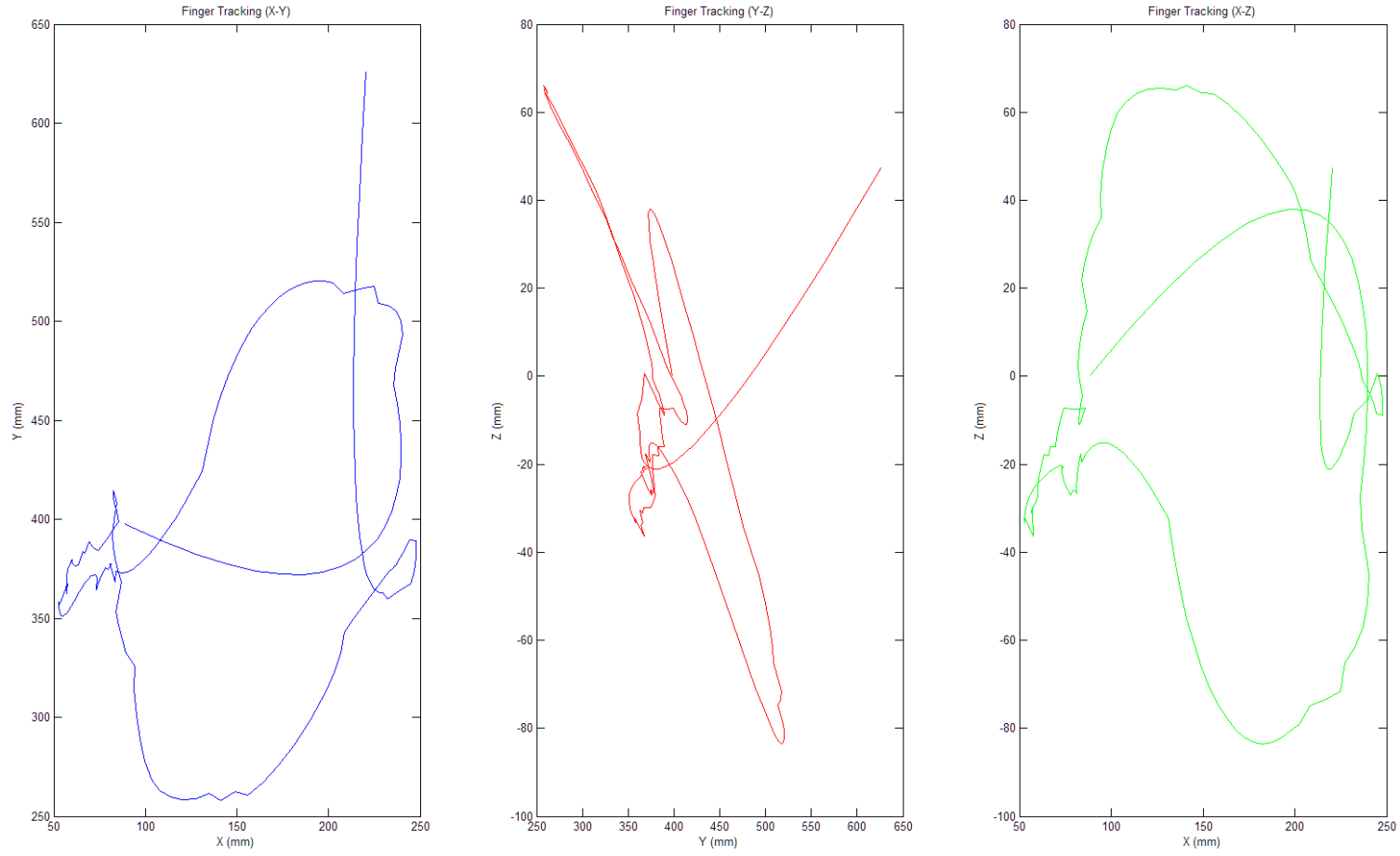
Figure A.23: Leap motion experiment – vertical position – Iteration 130

A.2.3.   3D Motion Capture System

The following section focuses on the capture of data using a high-performance motion capture system. Vicon is a professional motion capture system (MoCap) used in sports science, ergonomics, cinemas, and video games. Two set of experiments were carried out to 1) assess the positional accuracy, and 2) evaluate the sensor integration and capability to capture human movements.

Vicon MoCap uses reflective markers and infrared cameras. The two cameras are tracking the reflective markers in real-time within a 3D space. A virtual object was created based on the position of the markers to map and capture orientation data. Both cameras were placed with a 90 degrees' angle for the reflective markers to be within the field of view of both cameras.

A.2.3.1. *Experiment 1: Positional Accuracy*

This experiment focuses on assessing the positional accuracy of the Vicon MoCap. In this experiment, the tracking markers were mounted onto a robotic arm. The positional accuracy of the sensor was evaluated based on the values (x, y, z coordinate) provided by the robot controller and the Vicon system, as illustrated in Figure A.24. Then both coordinates were compared to each other using Equation A.3 and Equation A.4.
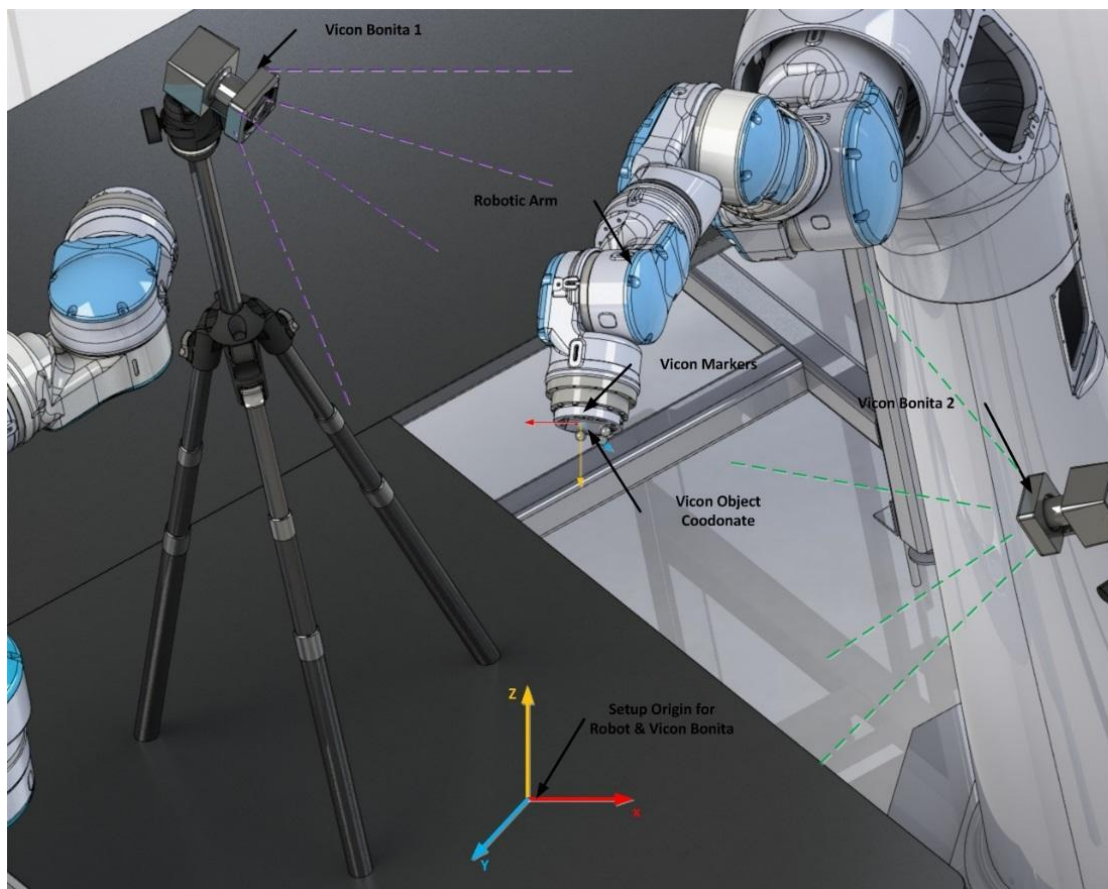
Figure A.24: Experiment setup on the accuracy evaluation of the Vicon Bonita motion capture system

This experiment was divided into three iterations. Each iteration corresponds to a movement of the end-effector in a single or multiple axes. After recording the x, y, z coordinate of the end-effector with both Vicon MoCap and the robot controller, the distance ($D_{(x,y,z)}$) between the starting point (P_{start}) and finishing point (P_{end}) was calculated. Position readings in x, y, z $axis$ at each iteration was taken from both robot and sensor, then these values were subtracted to each other to calculate the displacement of the movement in each axis, using Equation A.3. Finally, the positional accuracy was determined using Equation A.4

$$D_{(x,y,z)} = P_{start}\,(x, y, z) - P_{end}(x, y, z)$$ **Eq.(A.3)**

Where $D_{(x,y,z)}$ is the distance calculated form P_{start} starting position to P_{end} ending position in mm and that in x, y, z-$axes$.

$$P_{diff}(x, y, z) = P_{vicon}\,(x, y, z) - P_{robot}(x, y, z)$$ **Eq.(A.4)**

Where P_{diff} is the positional accuracy between the Vicon markers and the robot end-effector coordinate; P_{vicon} is the distance calculated between starting and ending point of the Vicon reading in x, y, z $axes$; P_{robot} is the distance calculated between starting and ending point of the robot reading in x, y, z $axes$.

From this experiment, encouraging results for motion tracking and position accuracy has been shown, as seen in Table A.8. The results presented in Table A.8 shows a close agreement in x, y, z position data between the robot and Vicon system. The position differentials calculated between both systems were also very close. The maximum P_{diff} value calculated was 3.75 mm, but average the P_{diff} value calculated was less than 1 mm, which is acceptable accuracy for further experiments.

Table A.8: Experiment results

Iteration 1			Iteration 2			Iteration 3		
Starting Point	Robot	Vicon	Starting Point	Robot	Vicon	Starting Point	Robot	Vicon
X (mm)	413.46	426	X (mm)	405	418	X (mm)	228.7	238
Y (mm)	-17.851	-24	Y (mm)	-106.6	-112.6	Y (mm)	-218	-218
Z (mm)	-441.109	-485	Z (mm)	-303.8	-347.2	Z (mm)	-757	795
End Point	Robot	Vicon	End Point	Robot	Vicon	End Point	Robot	Vicon
X (mm)	405	418	X (mm)	222.79	232	X (mm)	344.5	356
Y (mm)	-106.6	-112.6	Y (mm)	-218.58	-228	Y (mm)	-219.9	-228
Z (mm)	-303.8	-347.2	Z (mm)	-751.58	795	Z (mm)	-315.4	357
Displacement	Robot	Vicon	Pdiff	Displacement	Robot	Vicon	Pdiff	Displacement	Robot	Vicon	Pdiff
D(x)	8.46	8	0.46	D(x)	182.25	186	3.75	D(x)	115.8	118	3
D(y)	88.749	88.6	0.149	D(y)	11.98	11.54	0.44	D(y)	1.9	1	0.9
D(z)	137.309	137.8	0.491	D(z)	447.78	448	0.22	D(z)	441.6	438	3.6

A.2.3.2. Experiment 2: Motion and Pattern Capture

In the second set of experiments, the Vicon MoCap had to track the hand movement following a rectangular path (as in the Xsens MTw and Leap Motion experiments). The aim of this experiment was to evaluate the capability of the Vicon system to track motion and pattern of an operator's movement within a small volume.

Figure A.25 illustrates the setup of the experiment. As in the previous experiments with the Vicon system, two cameras were tracking the position and orientation of the reflective markers in real-time. Then, the data were processed offline.
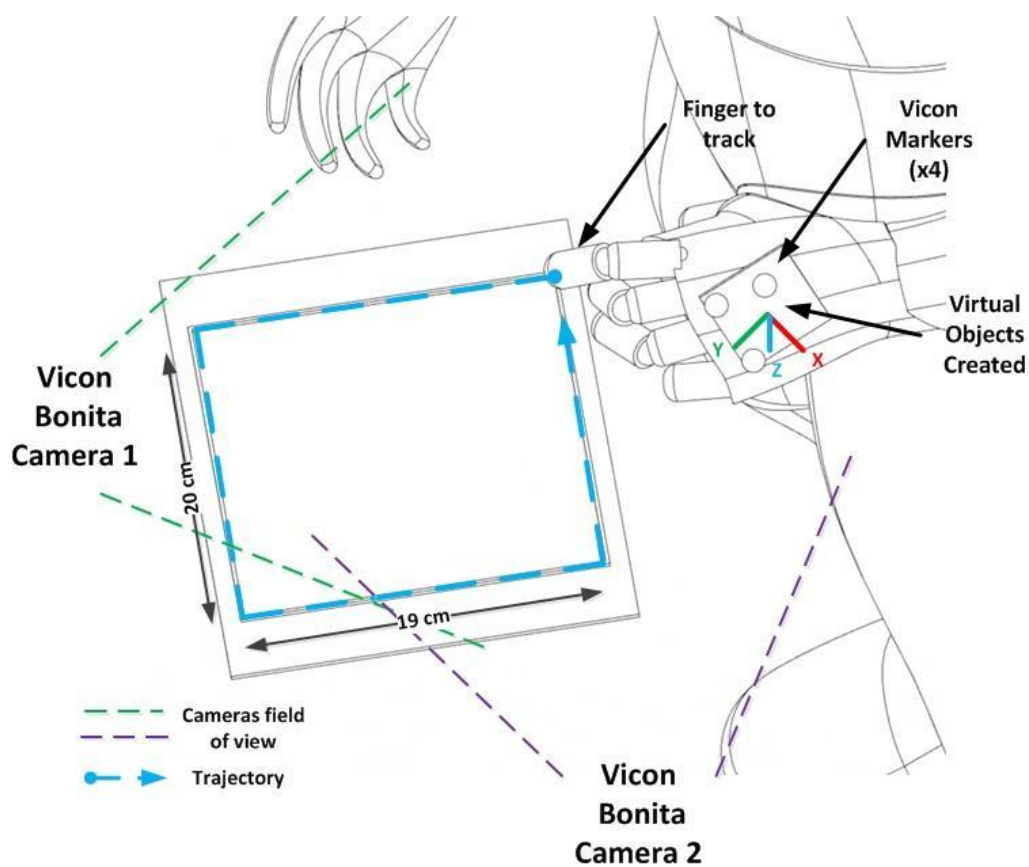
Figure A.25: Vicon motion capture system pre-calibration experiment

Figure A.26 and A.27 illustrate the results of the data captured with the Vicon system. Figure A.26 shows the rectangular path followed by the operator (a rectangular figure of *19 cm x 20 cm*). Figure A.27 reveals the operator's pattern when following the rectangular path (e.g. how many time the path has been followed). From this figure, it can be noted that the operator followed the rectangular path twice.

The performance showed by the Vicon MoCap system was very encouraging. Therefore, this sensor would be used to track the motions and patterns of the skilled operator using the fixture.

Overall Trajectory of the Hand
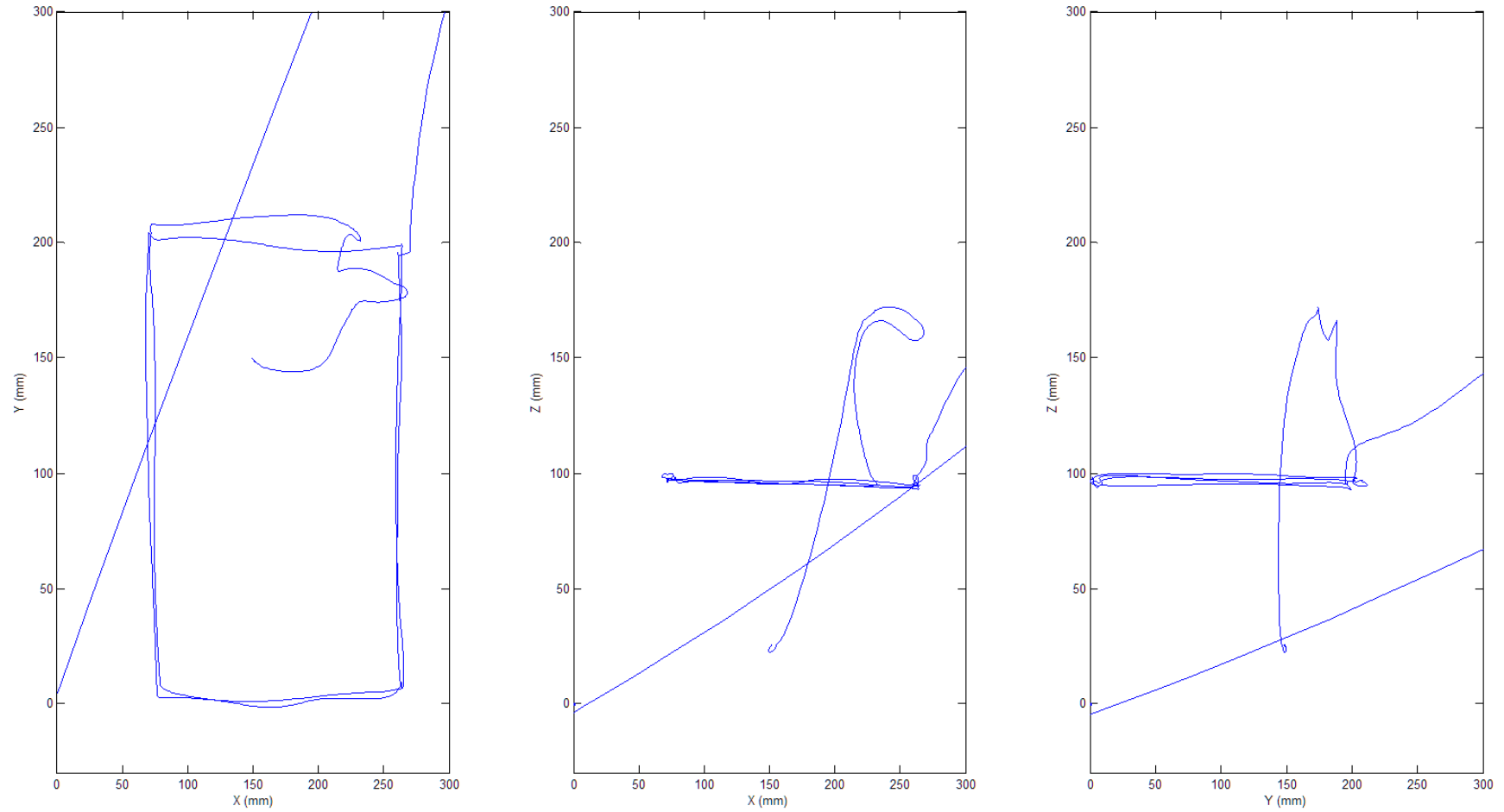
Figure A.26: Pre-calibration Vicon experiment 2: from left to right, X-Y axis view, X-Z axis view, Y-Z axis view

Captured Pattern of the Hand Motion:
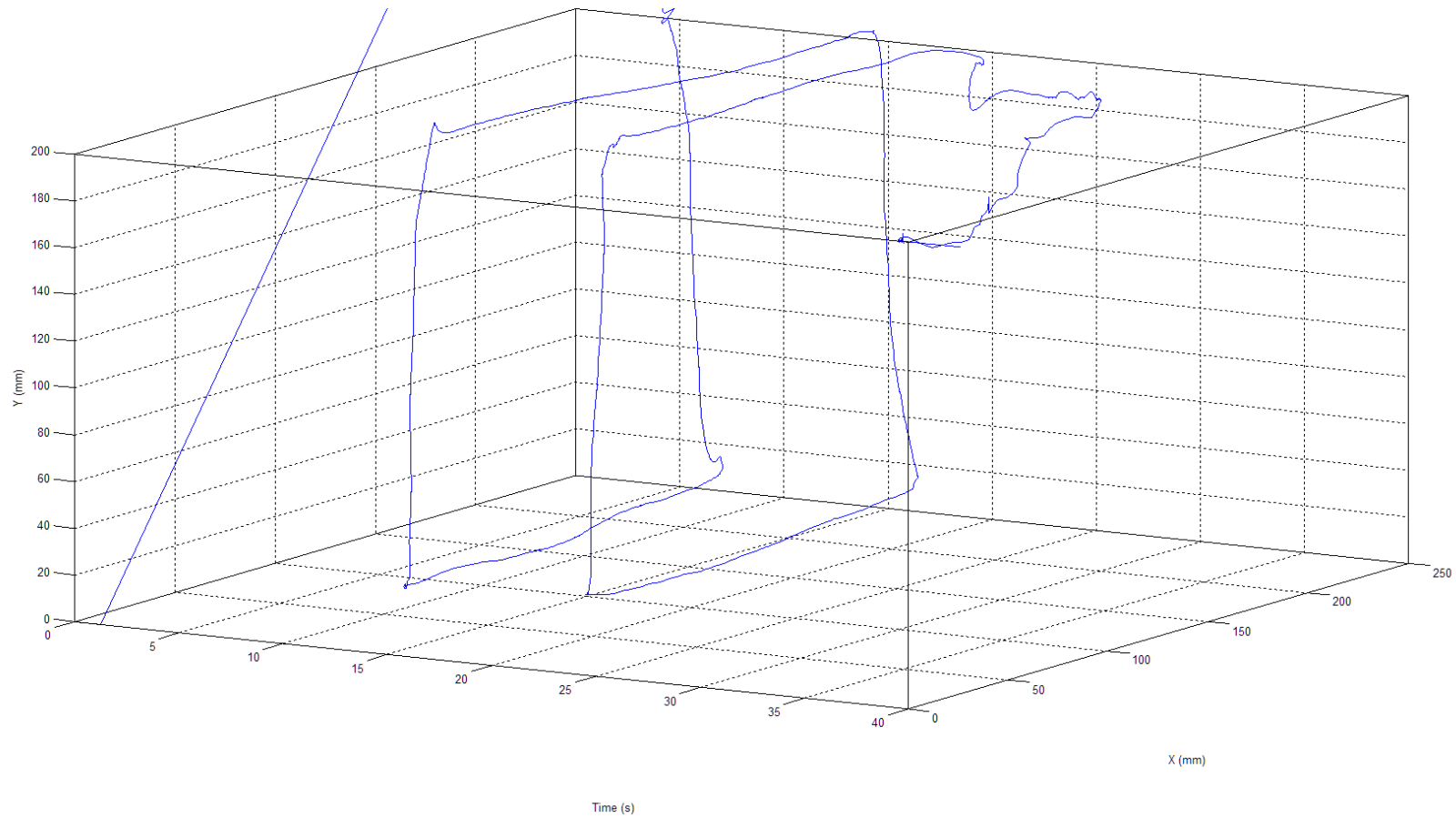
Figure A.27: Captured pattern during the pre-calibration experiment of the Vicon system

A.3 Discussion and Conclusion of Sensor Calibration Experiment

As mentioned in Section 5.3, a set of sensor calibration experiments were carried out for each sensor, to evaluate their precisions and choose the sensors to be integrated within the fixture. Some sensor evaluated performed well; other did not.

The experiments with the multi-axial force and torque sensor showed good accuracy for this sensor. As mentioned in Section 5.3.1, the minimum and maximum error recorded with the sensor was 0.02N and 0.06N respectively, representing less than 5% of measured values. In addition, a distribution of the forces output has been observed when an external load was applied on a complex profile (such as the sample workpiece). Therefore, this must be taken into account during the data processing and analysis of the polishing experiments.

A benchmark of three motion capture system was carried out in Section A.2. The Vicon MoCap has shown great performance in capturing the movements and patterns of a human operator. Despite some research carried out with the motion controller and inertial measurement unit, these sensors did not perform well in providing accurate values for capturing and processing position data. However, the inertial measurement unit performed well when providing acceleration and orientation data.

From the results of these experiments, the design of the fixture should integrate the multi-axial force and torque sensor (Shunk Gamma) to measure forces and torques; the 3D motion capture system (Vicon) to track the motion of the operator; and the inertial measurement unit (Xsens MTw) to measure speed and vibration during the process.

The next stages of this research were to develop the fixture (Section 5.4) and test it with the sensors to capture manual polishing process parameters (Section 5.5).

Appendix B. Fixture Calibration Experiment

The following appendix focuses, on a set of calibration experiments for the fixture embedding the smart sensors. The first part of the calibration process focused on collecting and synchronising data with and without external forces (Section B.1). The second calibration experiment focused on initial investigation on force gravity compensation for the multi-axial force and torque sensor (Section B.2). The third and last part of the calibration focused on collecting and understanding data for manual polishing operation (Section B.3).

B.1   Calibration Experiment 1: Capture Data from Sensors

The aim of this calibration experiment was to integrate and collect data from the different sensors. Due to the setup and specification of the sensors (e.g. sample rate), the decision was made to carry out the synchronisation and data analysis offline. Figure B.1 show the data collected during the experiment.

Matching and synchronising data from the different sensors was a complex task. Due to the sensors being triggered manually and individually. Therefore, a small time delay was created. During the experiment the Vicon system was triggered first, then the inertial measurement unit and the multi-axial force and torque sensor were calibrated and triggered respectively.

Using the different data plot in Figure B.1, the time delay was calculated between all of the sensors at a specific point. A delay of 20 seconds was calculated. This delay was needed in order to calibrate and triggered the inertial measurement unit and force torque sensor. In Figure B.1, common data were easily identified. The synchronisation line shows points of data captured at a specific time.

The time delay, to synchronise the data (therefore create the synchronisation line), was calculated based on a common pattern at a specific time during the experiment. The synchronisation line indicates the set of parameters used when the operator applied a simple pressure onto the workpiece surface.

Synchronisation Line

Inertial Measurement Unit

Multi-Axial Force and Torque Sensor

Vicon Motion Capture System
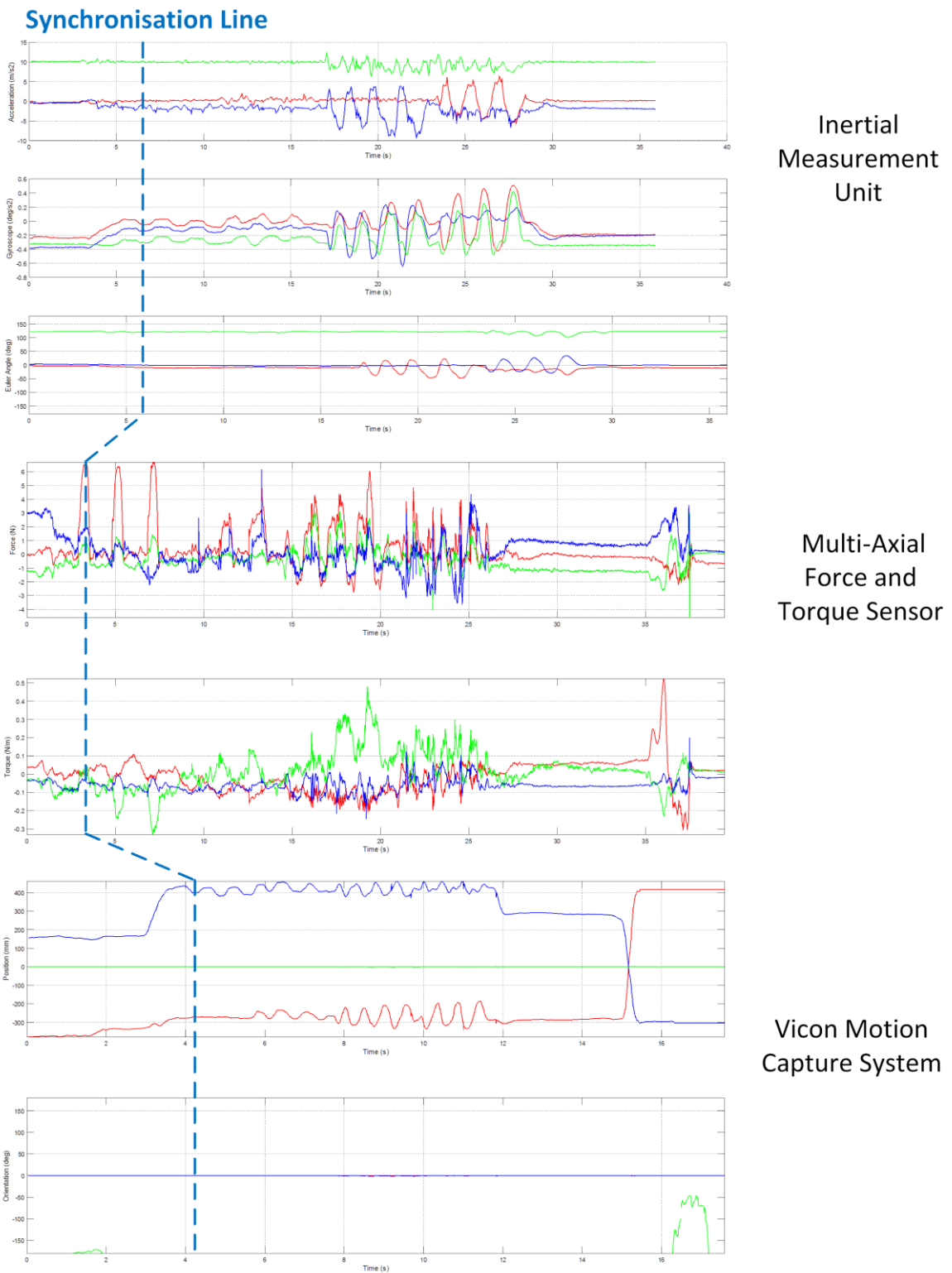
Figure B.1: Data synchronisation

B.2 Calibration Experiment 2: Initial Investigation of Force Gravity Compensation

Due to some similarities observed between the acceleration and force output during the previous calibration experiment (see Section B.1), the decision was made to investigate the correlation between the multi-axial force and torque output and inertial measurement unit output.

In the first test, it was found that the multi-axial force and torque sensor showed forces and torques values under the operator movement without external forces. The sensor outputted values due to the weight of the fixture attached to it and the effect of the gravity. Further investigation towards gravity compensation was carried out in Section 7.5.

At this stage of this research project, the main objective of this experiment was to record the force value output at different orientations. These values would be used to remove forces output due to rotation of the fixture to compute the force only applied by the operator, in offline data processing and analysis.

For this experiment, the multi-axial force and torque sensor was mounted onto the fixture with the inertial measurement unit, as seen in Figure B.2. Both sensors were then calibrated at the same position. Then the operator rotated and moved the fixture in different directions.

From the experimental results, the inertial measurement unit output matched the force reading. The graph plot shown in Figure B.3 shows a similarity between the acceleration, orientation, and force. The maximum force output observed was 15 N for a rotation of over 90 degrees. Any forces generated under 45 degrees were too small to be relevant.

Therefore, the inertia output should also, in addition to capturing speed and vibration, be used to compensate forces output due to the operator movements.
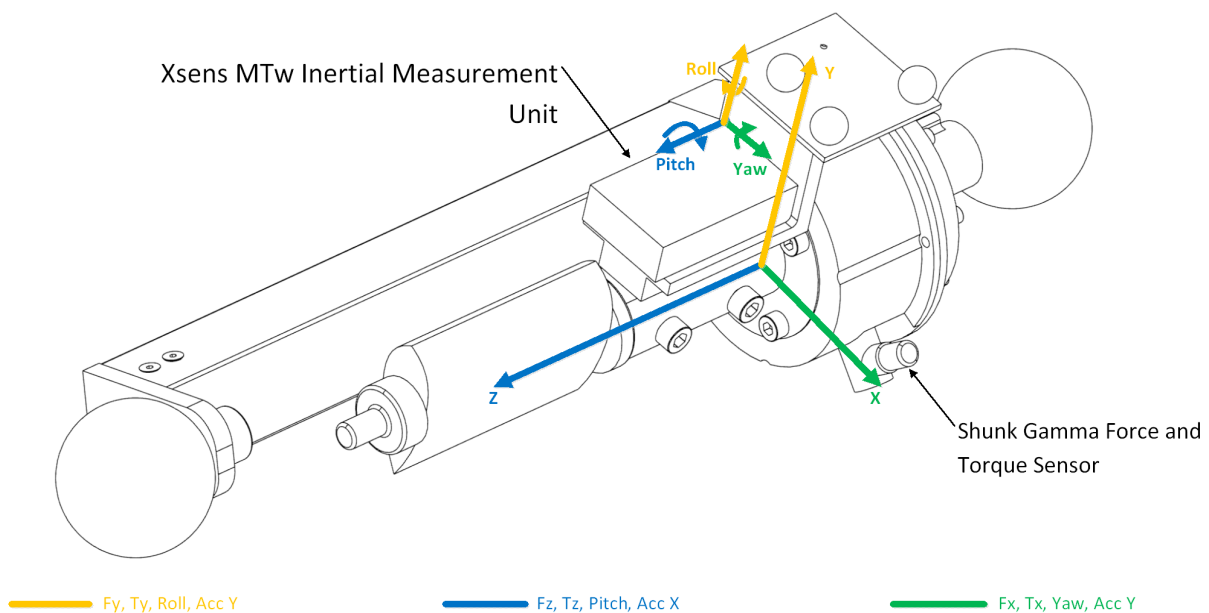
Figure B.2: Fixture with force and torque sensor and inertial measurement unit
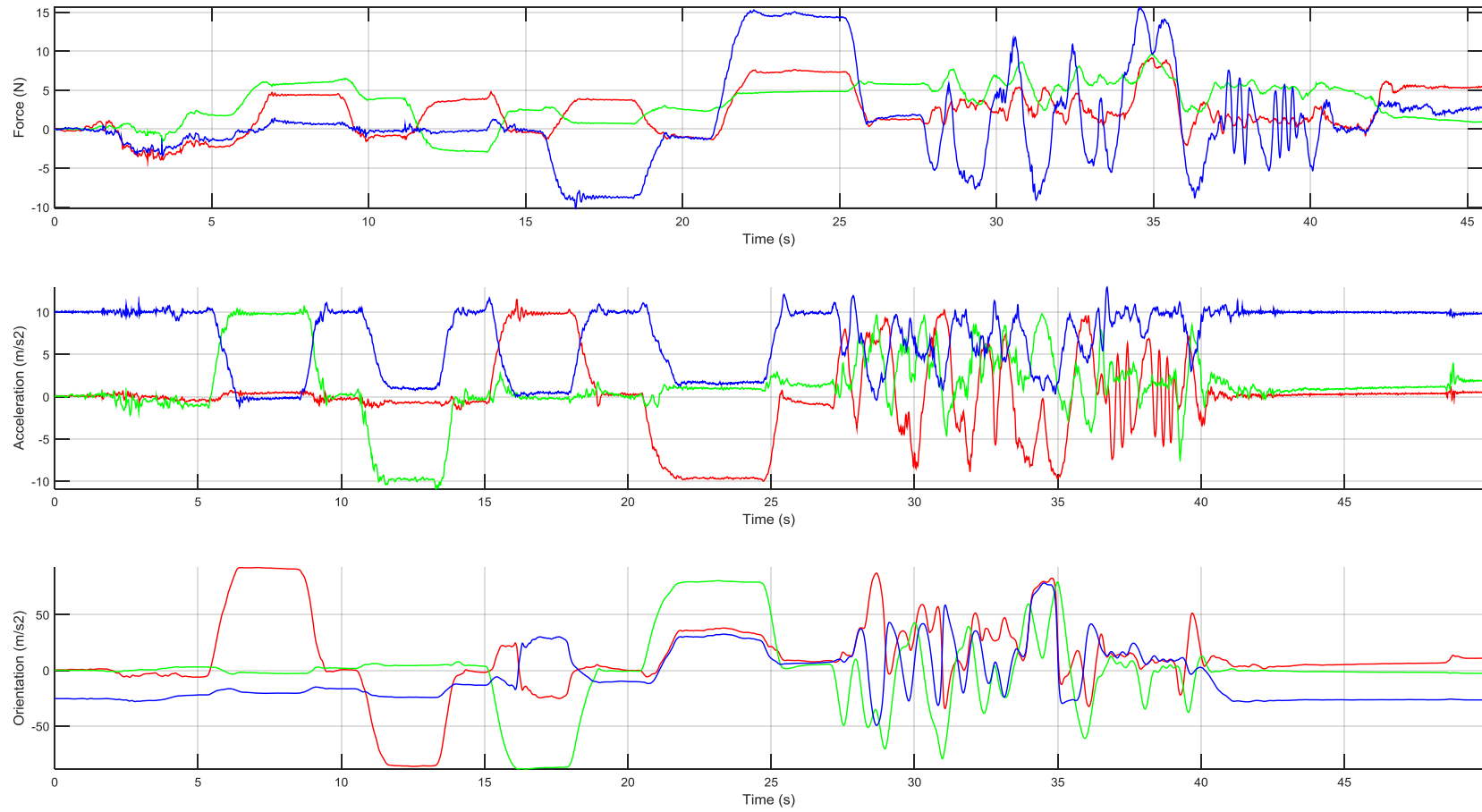
Figure B.3: Force vs inertia. Top to bottom, forces (*Fx, Fy, Fz*), Acceleration (*x, y, z*), and Euler orientation (*pitch, yaw, roll*).

B.3   Calibration Experiment 3: Understand Data Output for Manual Polishing

This set of experiments aims at capturing and understanding data output with the fixture during the manual polishing operation of a sample workpiece. The sample workpiece being polished was a replica of an industrial component used in the industrial collaboration (see Chapter 4).

The objectives of the experiment were to capture data from different sensors, validate the capturing and analysis procedure while imitating the technique of a skilled operator, and learn to interpret the data provided by the fixture. The scope of the experiment was to use and identify different patterns or techniques that may be used by a skilled worker during standard operation procedure of manual polishing process.

In this experiment, four iterations (1 to 4) were captured to obtain and understand the data output form the various sensors under known conditions.

B.3.1.   Experiment Setup and Procedure

Figure B.4 illustrates the setup and parameters captured by the fixture during this experiment. The operator's task was to carry out the polishing operation with the fixture using four patterns, as seen in Figure B.5. The experiment was carried out with a traditional linisher belt (for grinding, polishing, and deburring). The two Vicon MoCap cameras were set up at each side of the linisher belt to record the operator's movements. And the fixture recorded the accelerations and vibrations with the inertial measurement unit, and forces and torques with the multi-axial force and torque sensor.
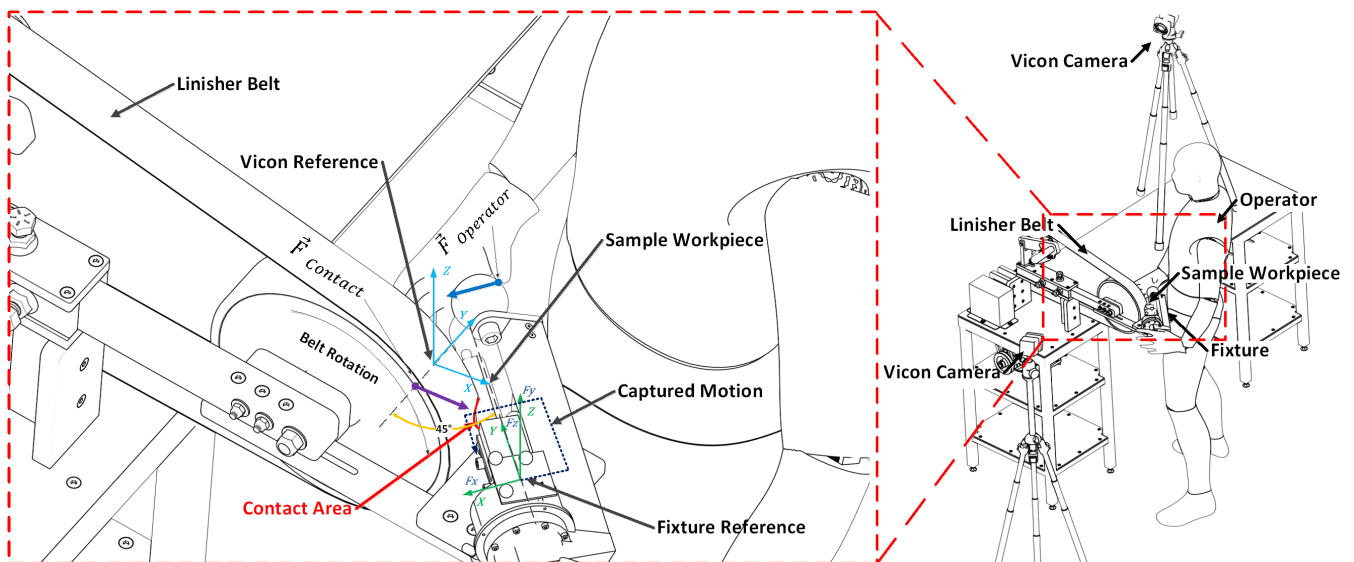
Figure B.4: Setup for calibration experiment

B.3.2. Techniques and Patterns

As mentioned, four iterations were carried out a skilled operator, as illustrated in Figure B.5. In Iteration 1, the operator used different patterns to identify multiple techniques within the same iteration. In Iteration 2, the operator applied a single pressure of the sample workpiece against the abrasive belt for 1 second and at three different locations. In Iteration 3, the operator had to execute a horizontal movement starting from one side of the workpiece to finish to the opposite side (from left to right, and right to left, repeated three times). Finally, in Iteration 4, the operator followed the profile of workpiece (surface profiling), as it is a technique commonly used by skilled worker in industry (see Section 4.4).

These techniques were chosen as references for further experiment (see Chapter 6). As each technique used by the operator are known. Therefore, it should be possible to identify the different parameters captured in Chapter 6. In other words, it was by learning from this that it will be possible to identify the different techniques used by the operator in Chapter 6 and understand how manual polishing operation is carried out.
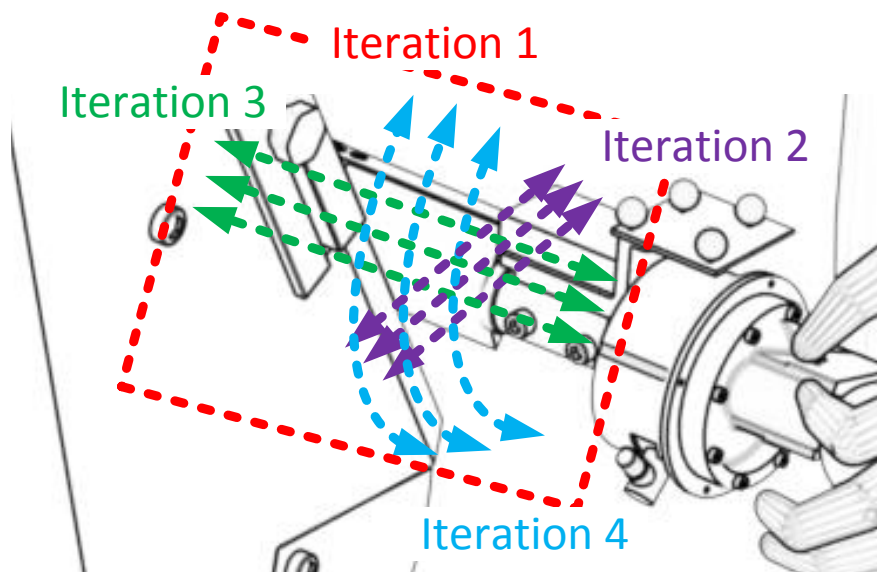
Figure B.5: Techniques used during Iterations 1 to 4

B.3.3. Experimental Results

The following section shows the data captured from each sensor during this experiment, and that for each iteration. Figure B.6 to B.11 shows the data captured for iteration 1, where several patterns can be identified. Figure B.12 to B.17 shows the data captured for iteration 2, where a singular pressure was applied at different locations on the workpiece surface. Figure B.18 to B.23 shows the data captured for iteration 3 where a singular linear motion was carried out. Finally, Figure B.24 to B.29 shows the data captured for iteration 4 where the profile of the surface has been followed.

B.3.3.1. *Iteration 1: Technique and Pattern Identification*

As mentioned, this iteration focused on identifying several techniques that may be used by skilled operators in industry. The operator was tasked with using four patterns (simple pressure, linear movement, surface profiling). From the data collected (Figure B.6 to B.11) the change of pattern and technique was observed.

It can be noted that the operator started the experiment by applying a simple pressure at different locations on the surface, then moved the fixture horizontally while keeping the contact between the surface and the abrasive belt constant and perpendicular. Finally, the operator followed the profile of the workpiece. Figure B.10 and B.11 shows the three different movements used by the operator and the overall trajectory used during this iteration, respectively.

In addition, the timing indicators of the multi-axial force and torque sensor and inertial measurement unit are synchronised, therefore each technique were easily identified.

B.3.3.2. *Iteration 2: Simple Pressure Motion*

In this iteration, the operator had the task of applying a simple pressure against the abrasive belt for 1 second at four different locations on the surface. From the data collected (Figure B.12 to B.17), it can be noted that when applying a static pressure, the multi-axial force and torque sensor capture data around Fx and Ty axes (see Figure B.15). Fx shows the force applied by the operator on the workpiece and Ty shows the torque generated by the contact with the abrasive belt. The inertial measurement unit (Figure B.12), shows some small data peaks which are caused by the vibration when the part was in contact with the abrasive belt.

B.3.3.3. *Iteration 3: Singular Linear Motion*

In iteration 3, the operator had the task to polish the sample workpiece from one end to the other end while moving horizontally. From the data collected it can be observed that, when the operator moved the fixture in one direction while keeping a constant force, the data showed a clear change of the motion direction from the Vicon MoCap system (Figures B.18 to B.23), and a data output from the multi-axial force and torque sensor in Fx, Fz, and Ty axes.

Fx and *Fz* output were due to the contact with the abrasive tool and the movement of the operator respectively. As in the previous iteration, a torque in *Ty* axis was generated from the contact with the abrasive tool. In addition, a small change in torque value was observed. This is due to the location of the contact point from the multi-axial force and torque sensor.

The inertial measurement unit also showed the direction and speed of the movement in *x-axis* Figure B.18 to B.20, which collaborates the data collected with the Vicon MoCap and pattern used by the operator.

B.3.3.4. Iteration 4: Surface Profiling

In iteration 4, the operator had the task to polish the sample workpiece by following the profile of the surface. In Section A.1.2, a distribution of the force output along *x-y-axis* was observed when a contact force was applied at different locations on the curve surface of the sample workpiece. When following the profile of the surface in manual polishing operation, similar data were provided by the multi-axial force and torque sensor.

The Vicon MoCap results shown in Figure B.29 shows the path and pattern followed by the operator. The path drawn by the operator movement shows similarity with the profile of the surface.

The multi-axial force and torque sensor shows data in *Fx*, *Fy*, *Fz*, *Tx*, *Ty* axes, due to the complex movement of the operator. The change of the fixture orientation, and of the location of the contact point were distributed along *Fx* and *Fy* axes, as seen in Section A.1.2. As in the previous iteration (iteration 3), *Fz* data are generated from the horizontal movement of the operator. As for the forces, *Fx* and *Fy* , and the Torques, *Tx* and *Ty*, were generated from the change of the orientation of the fixture.
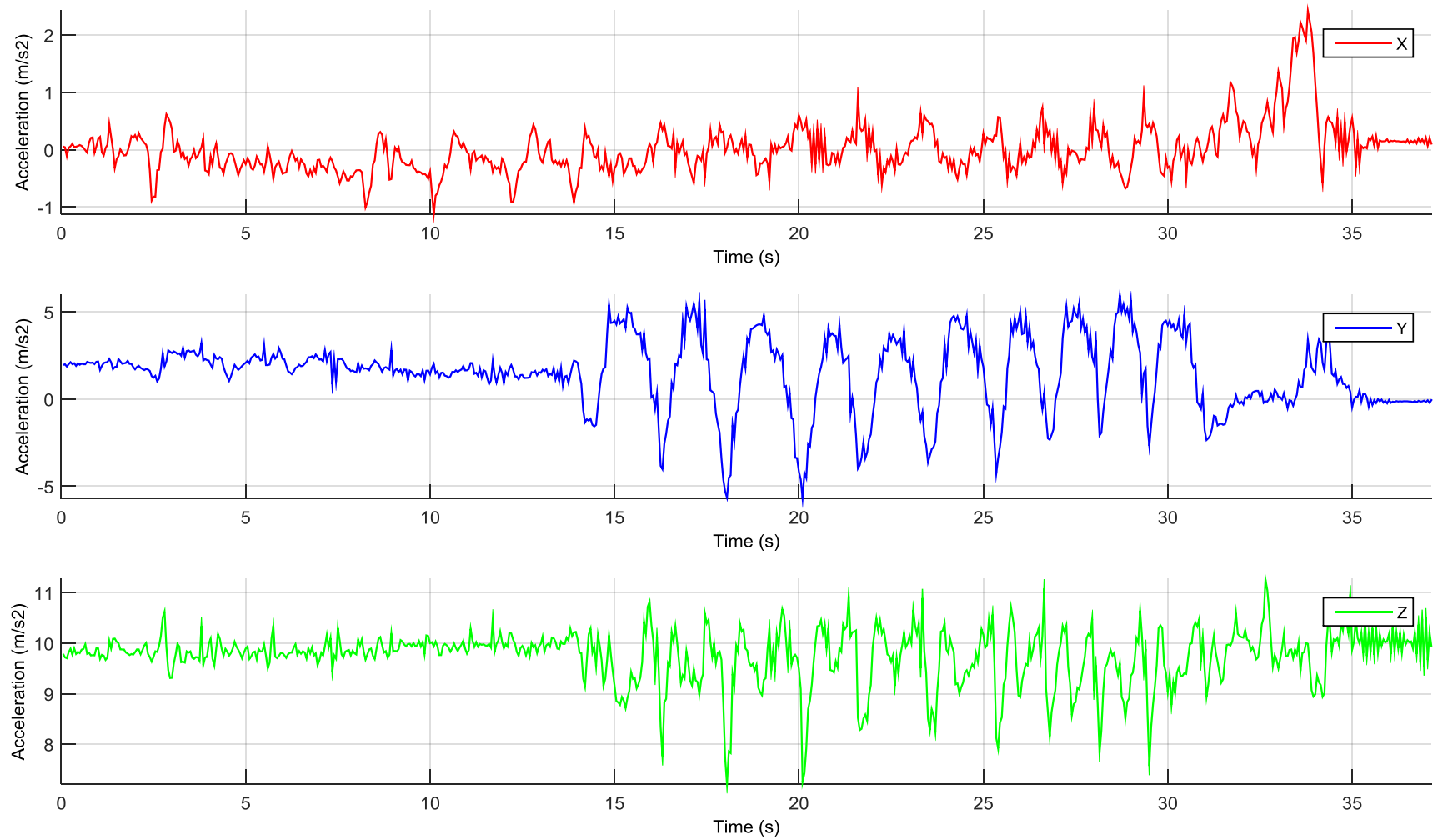
Figure B.6: Acceleration data captured in Iteration 1
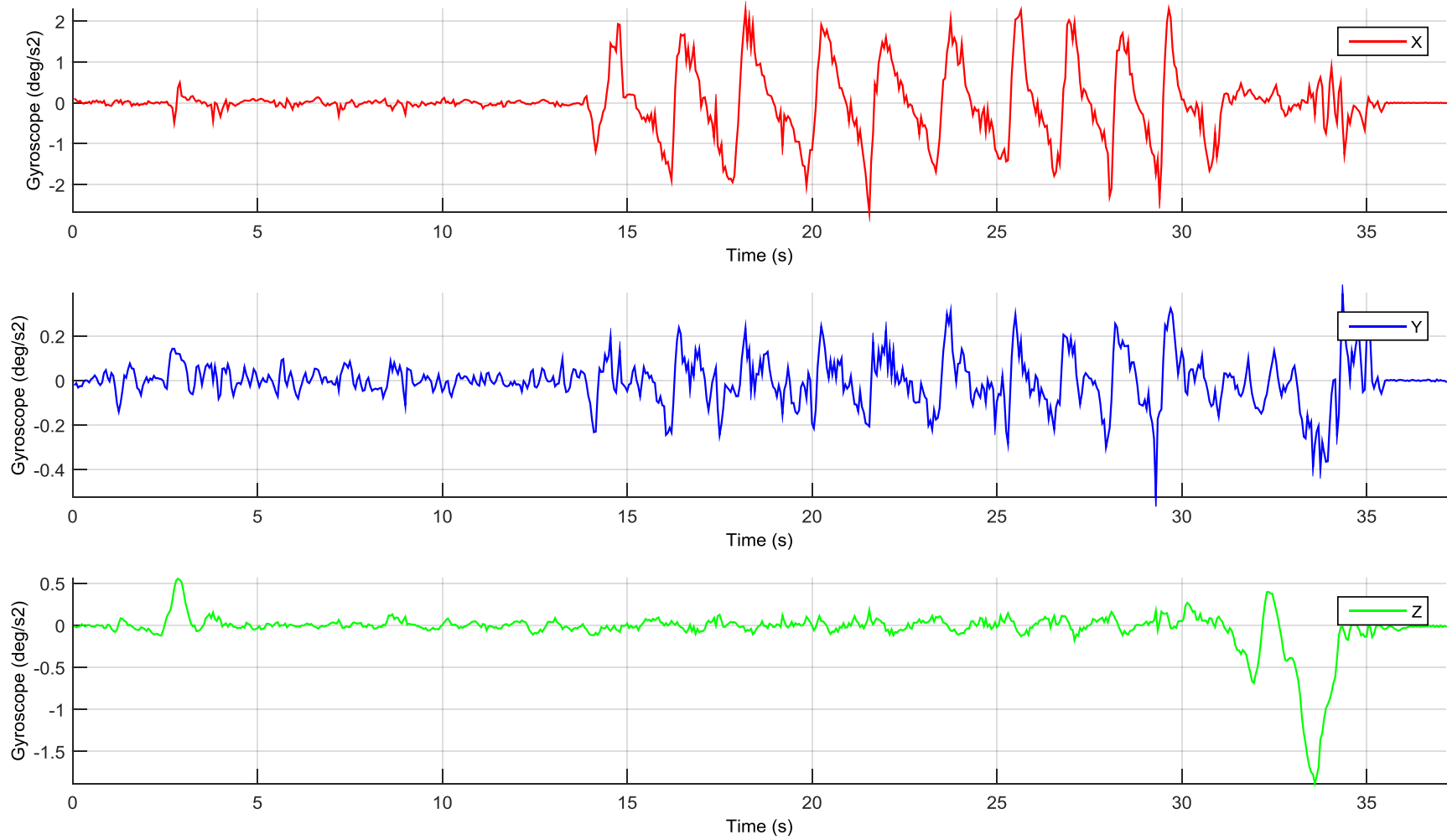
Figure B.7: Gyroscopic data captured in Iteration 1

Iteration 1: Technique and Pattern Identification
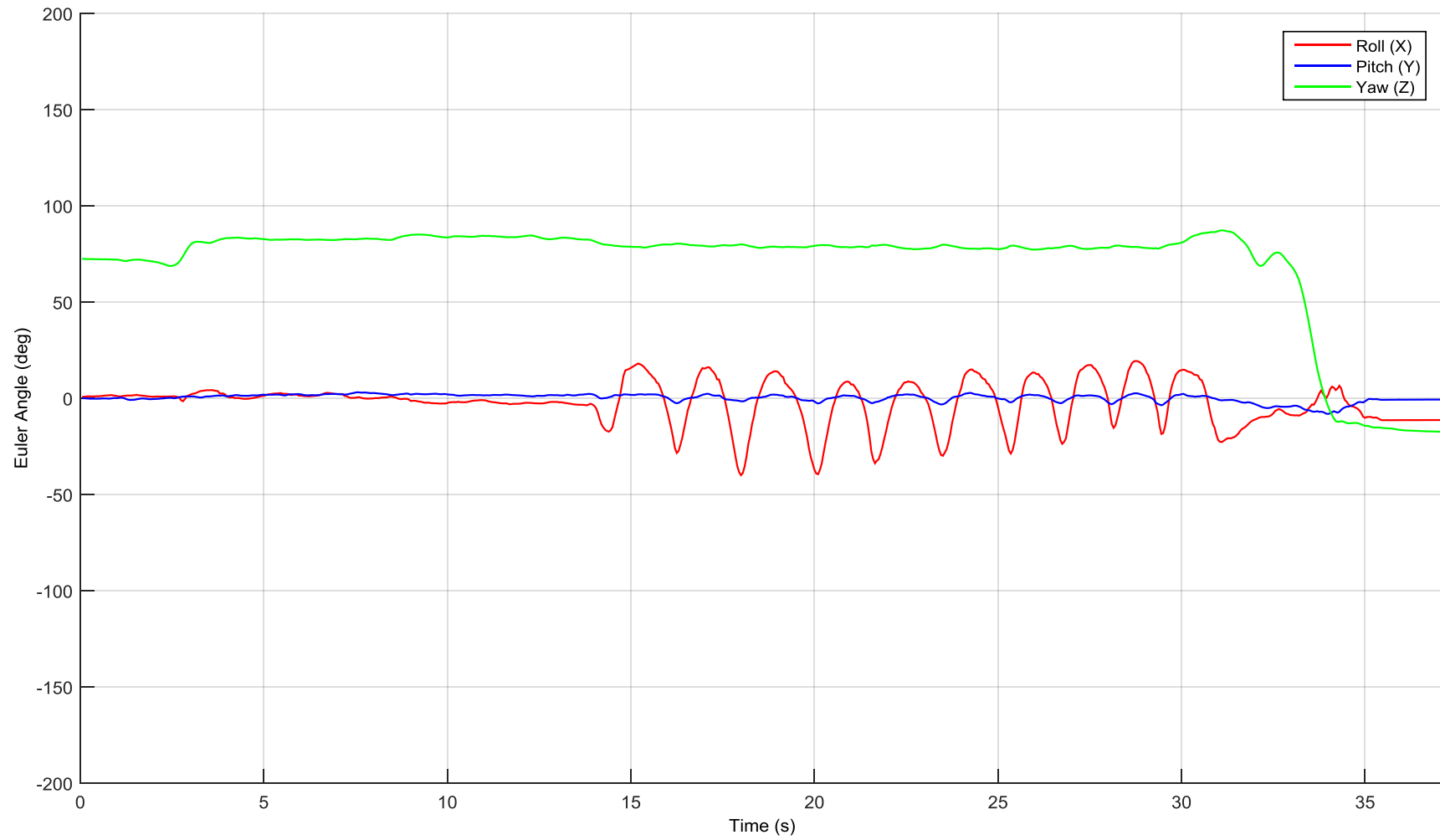
Figure B.8: Euler orientation data captured in Iteration 1

Iteration 1: Technique and Pattern Identification
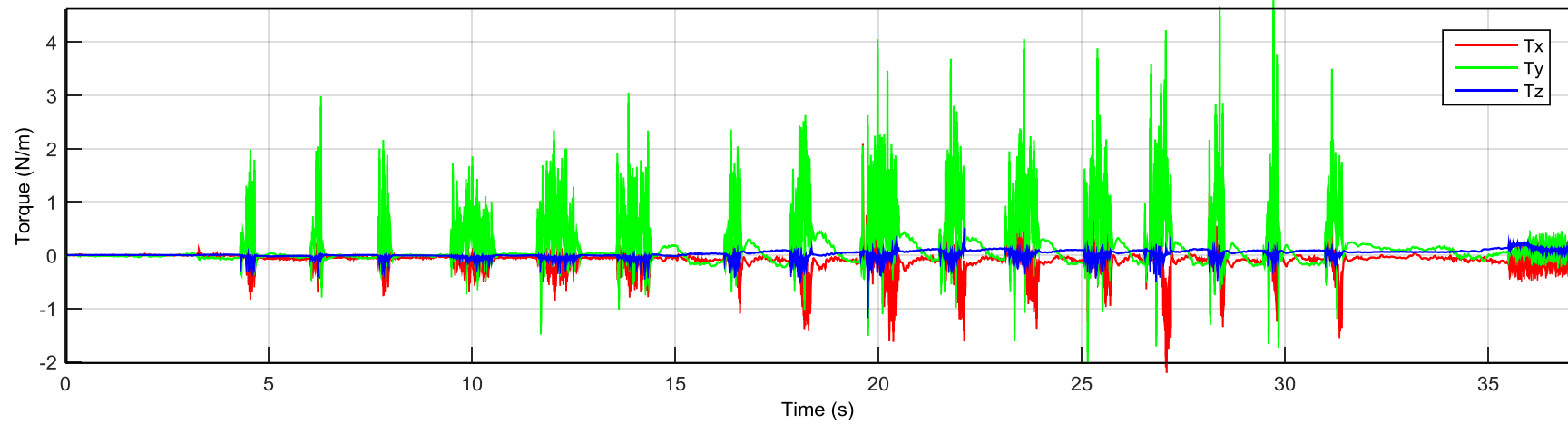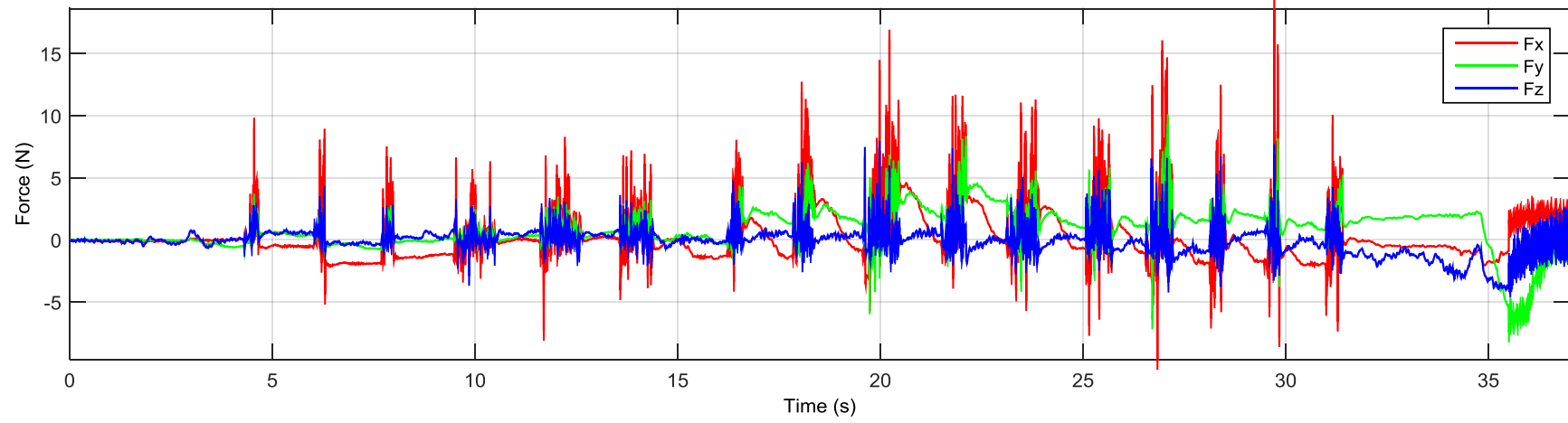
Figure B.9: Forces and torques data captured in Iteration 1

Iteration 1: Technique and Pattern Identification
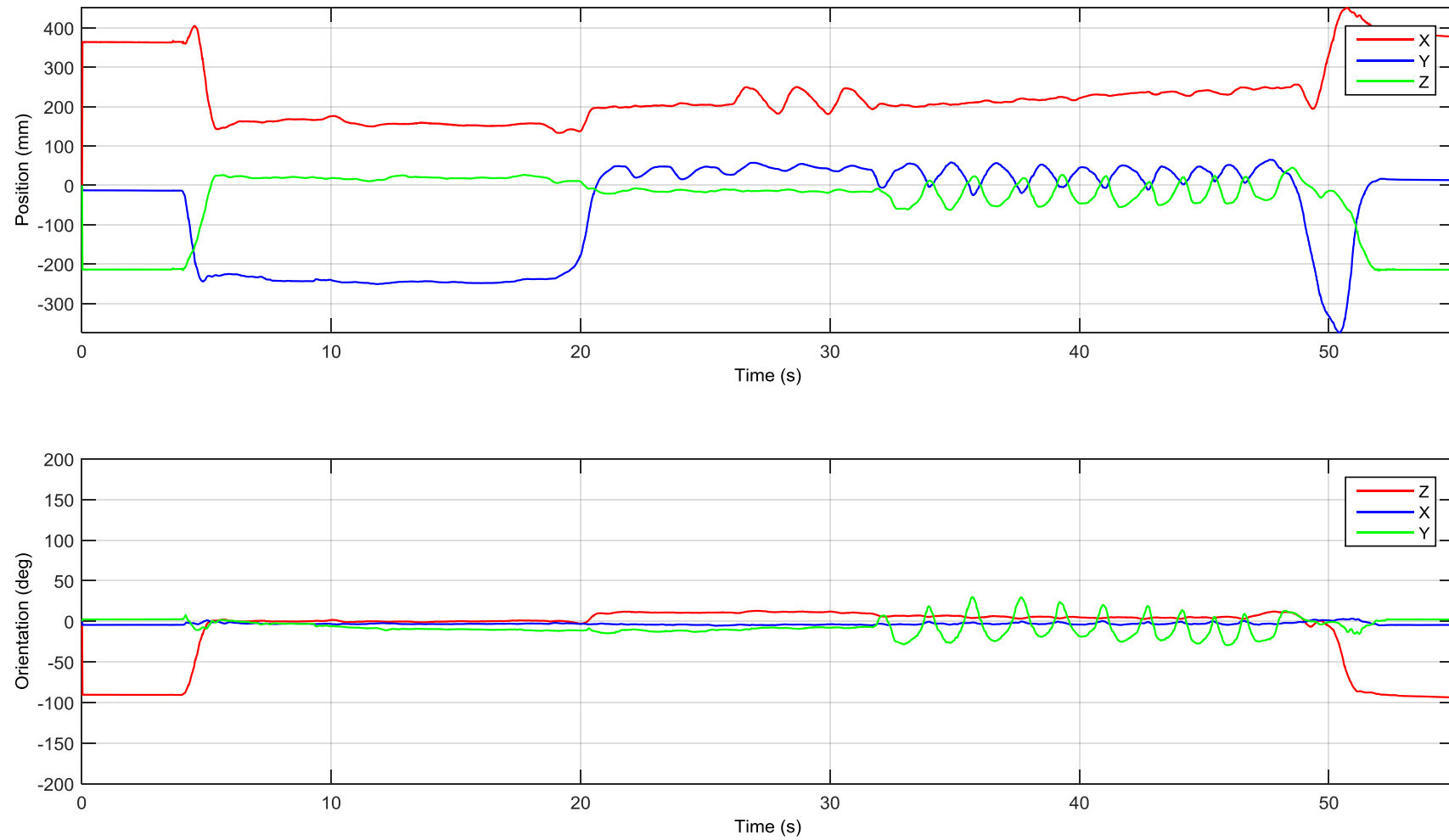
Figure B.10: Position and orientation data captured in Iteration 1

Iteration 1: Technique and Pattern Identification
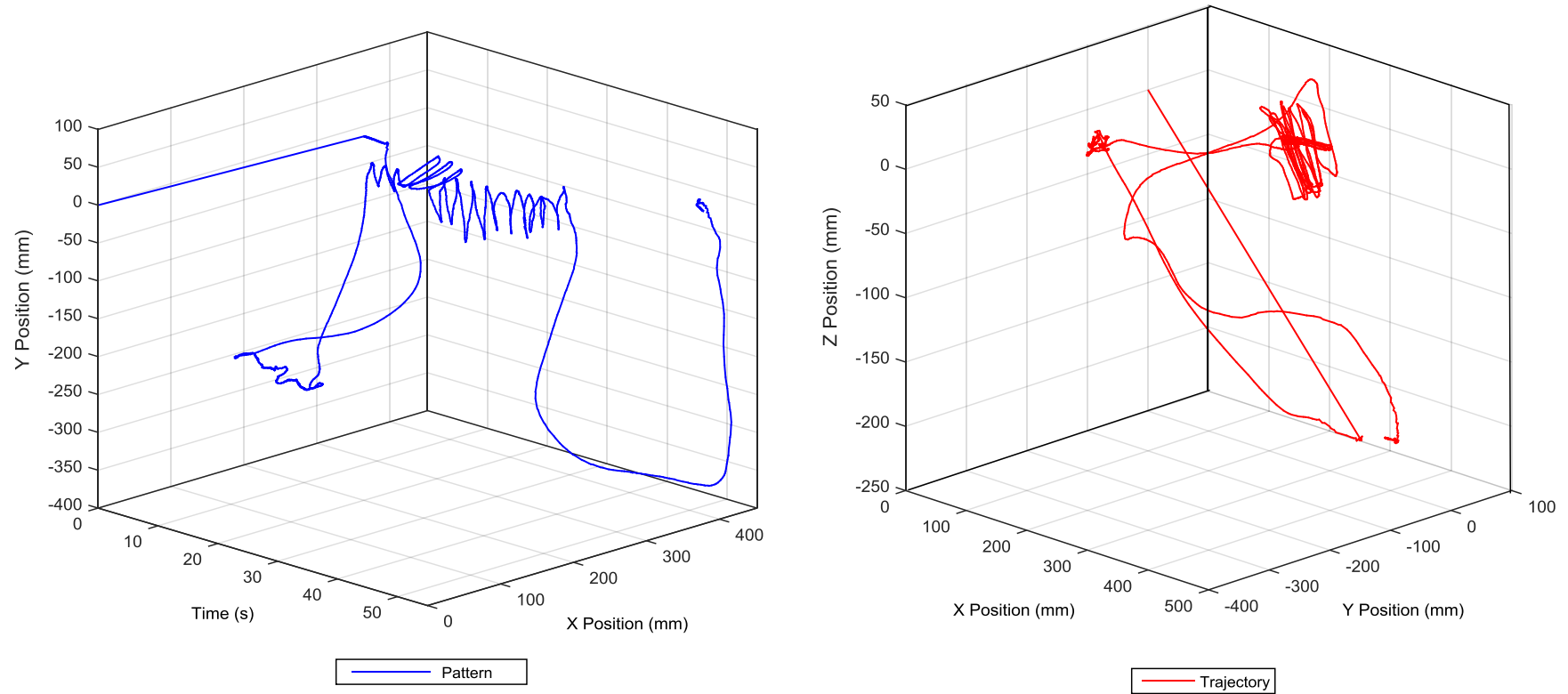
Figure B.11: 3D path and 3D pattern data captured in Iteration 1
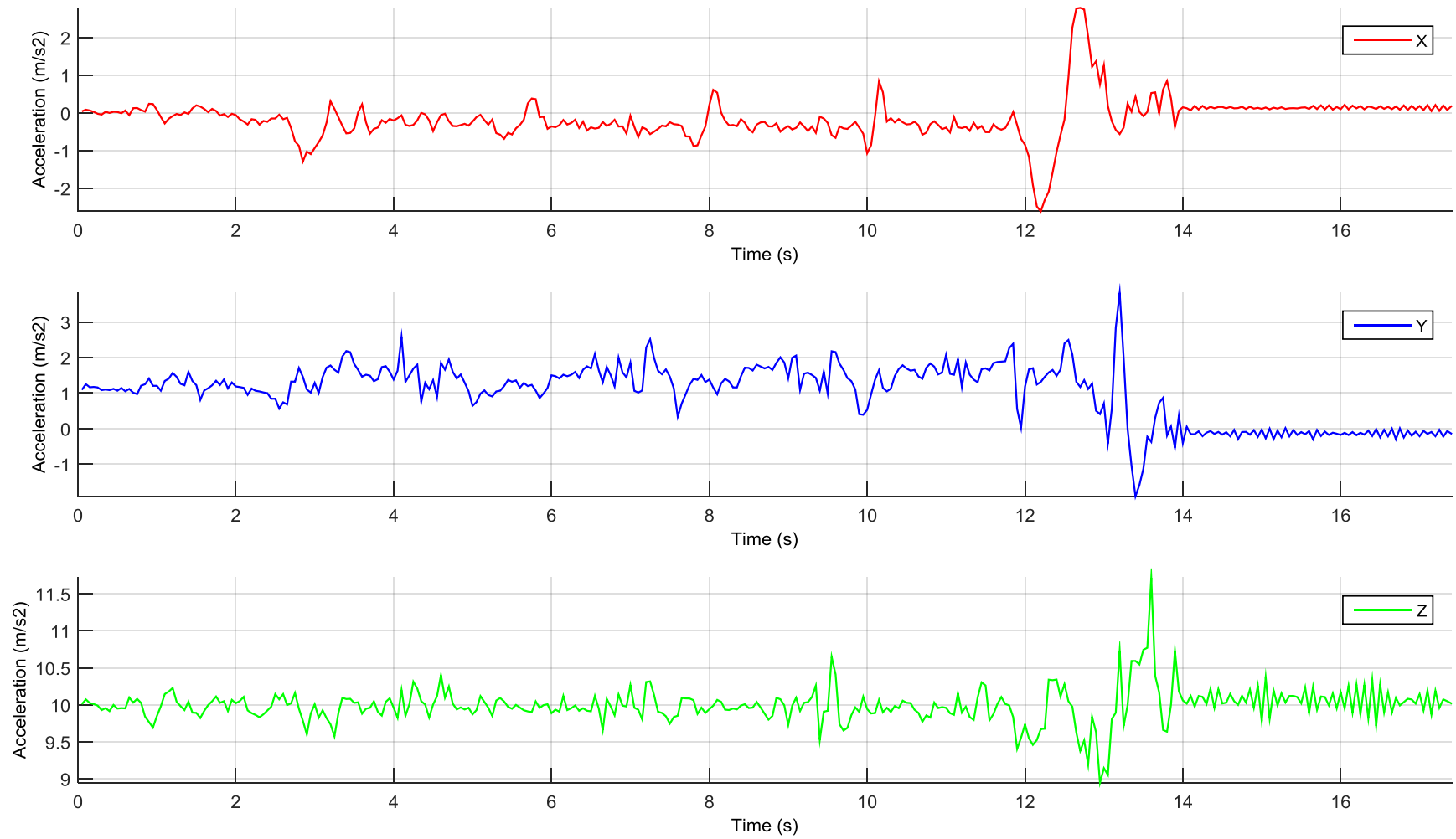
Figure B.12: Acceleration data captured in Iteration 2

Figure B.13: Gyroscopic data captured in Iteration 2

Figure B.14: Euler orientation data captured in Iteration 2

Figure B.15: Force and torque data captured in Iteration 2

Figure B.16: Position and orientation data captured in Iteration 2

Iteration 2: Simple Pressure Motion
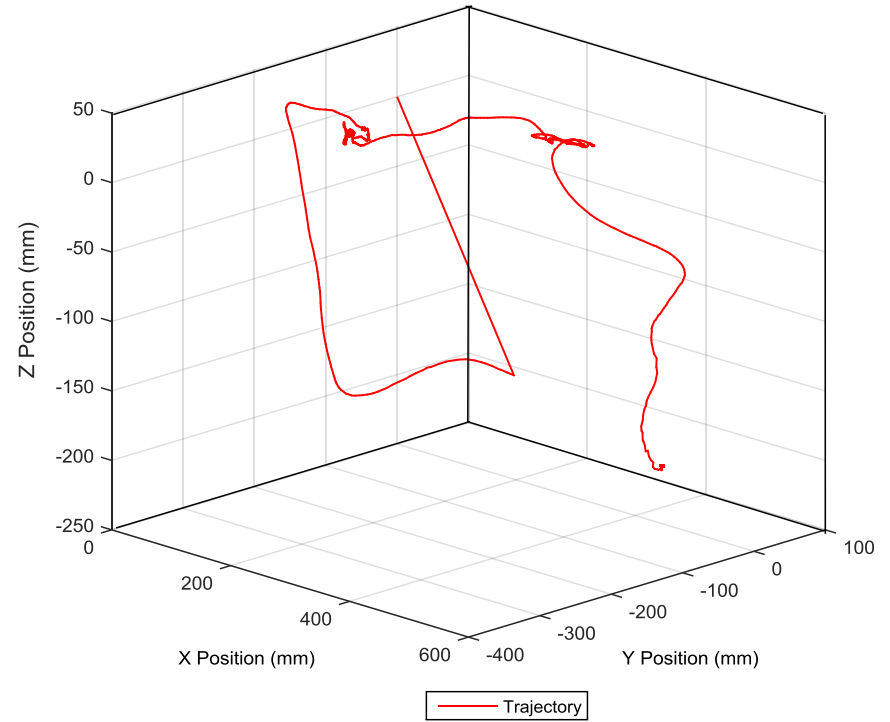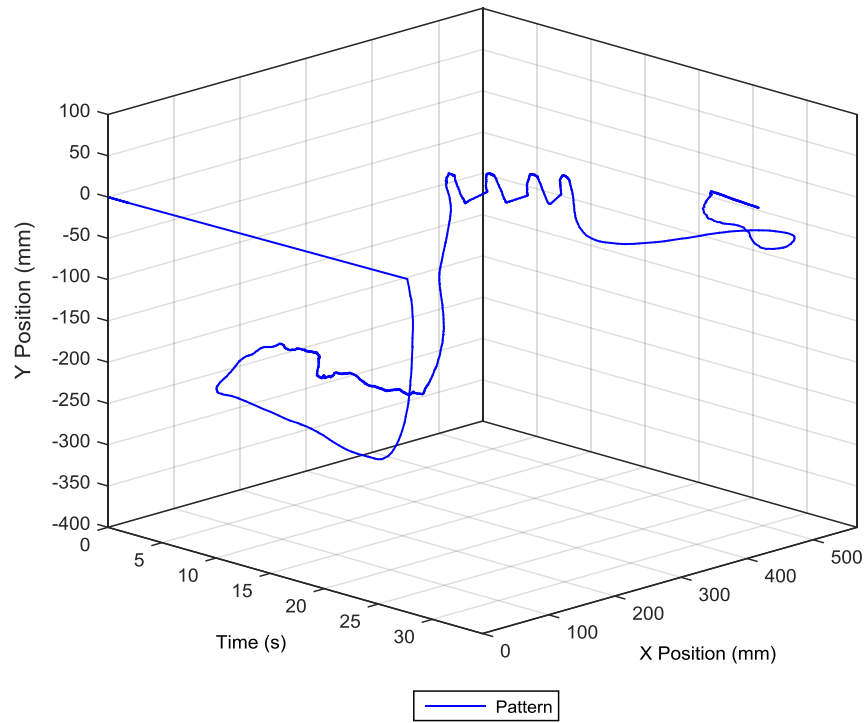
Figure B.17: 3D pattern and 3D path data captured in Iteration 2
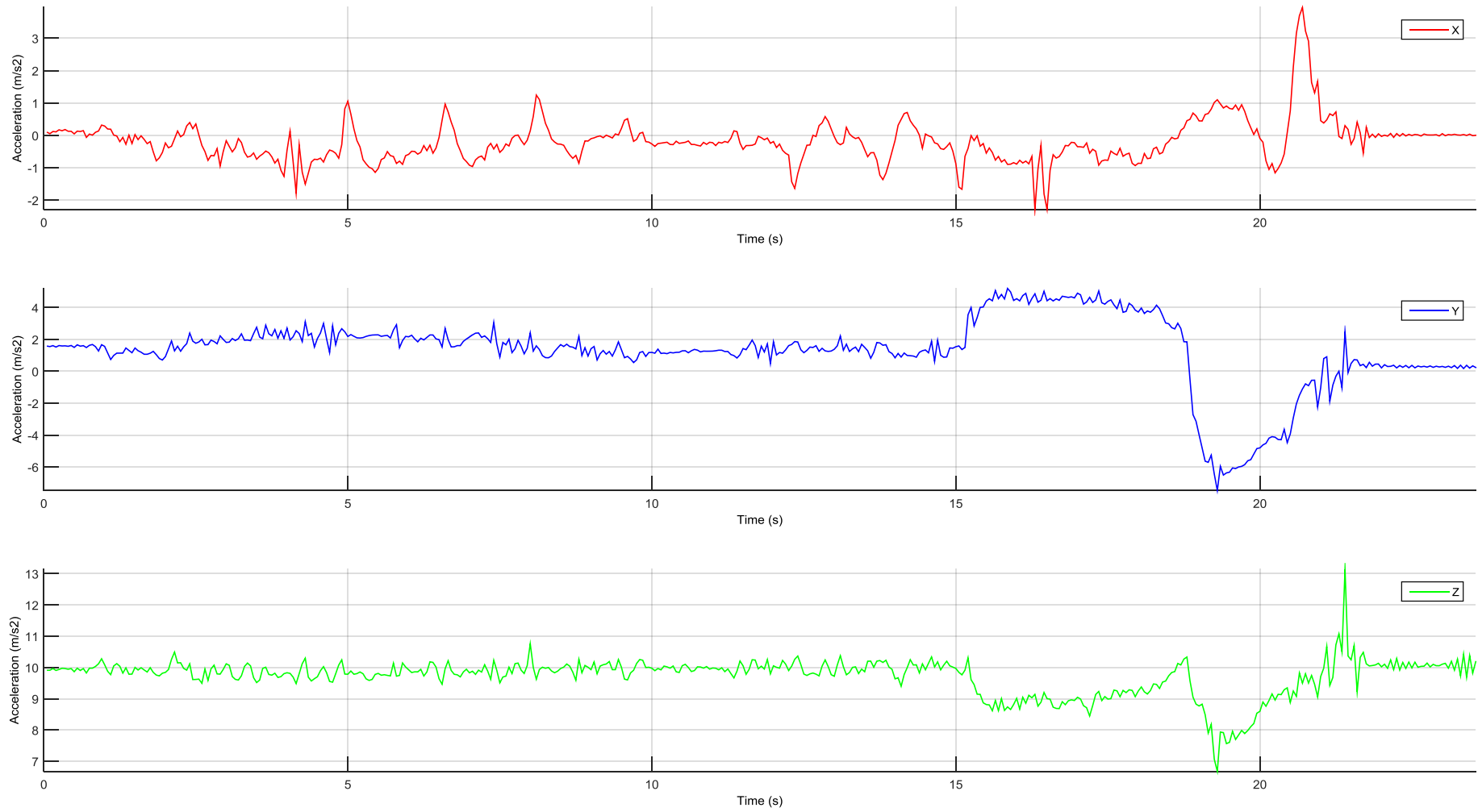
Figure B.18: Acceleration data captured in Iteration 3
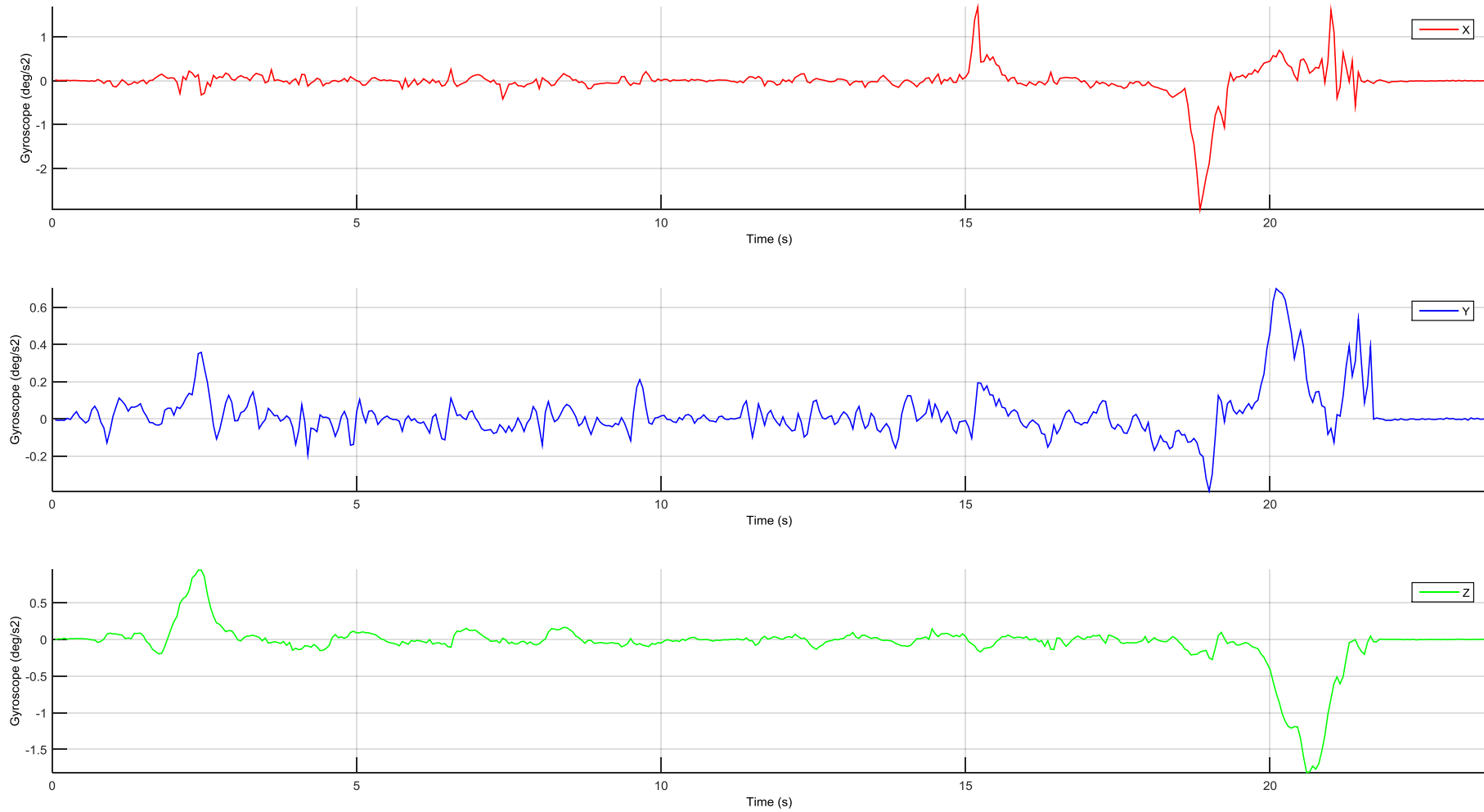
Figure B.19: Gyroscopic data captured in Iteration 3

Iteration 3: Singular Linear Motion
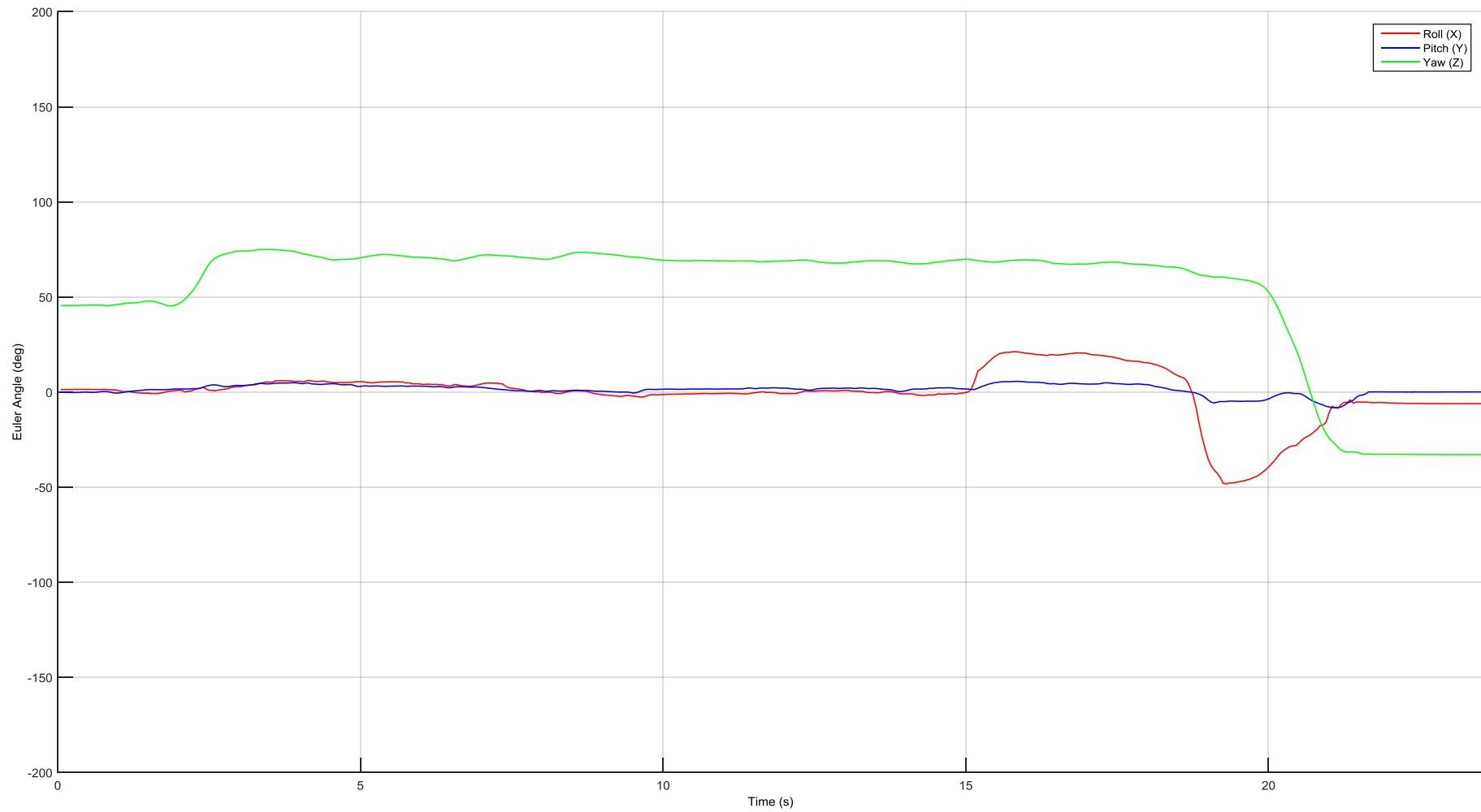
Figure B.20: Euler orientation data captured in Iteration 3

Iteration 3: Singular Linear Motion
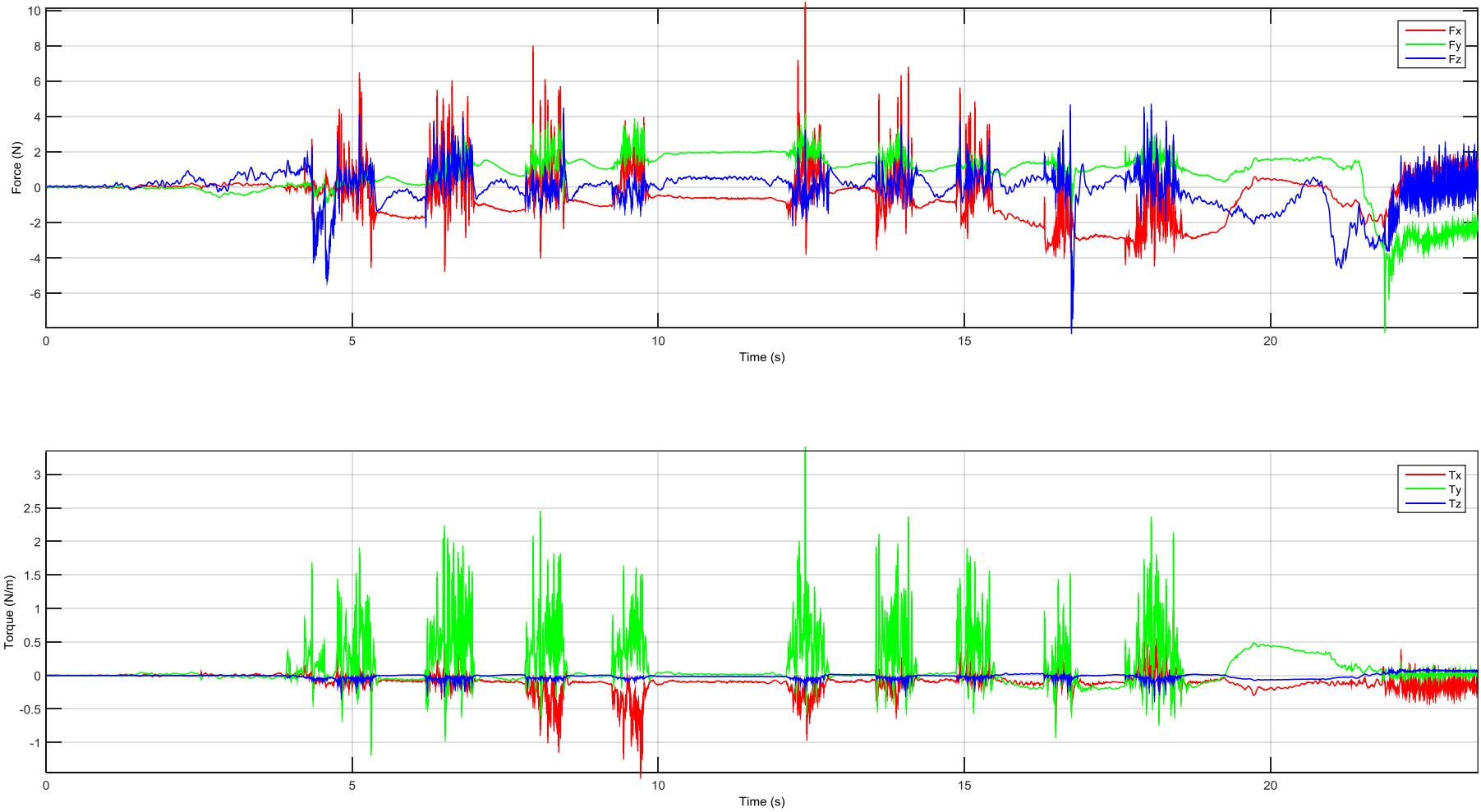
Figure B.21: Force and torque data captured in Iteration 3

Iteration 3: Singular Linear Motion
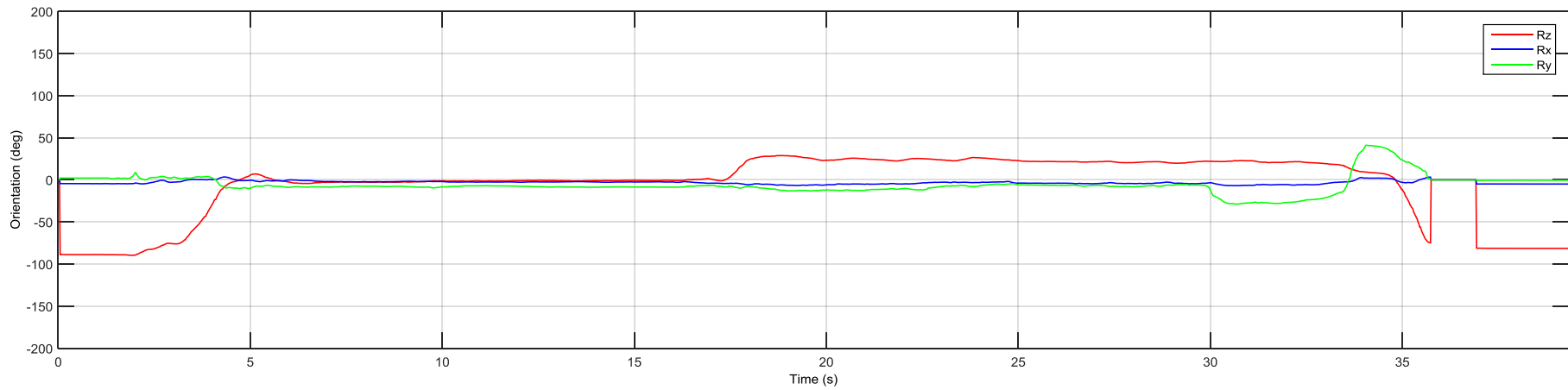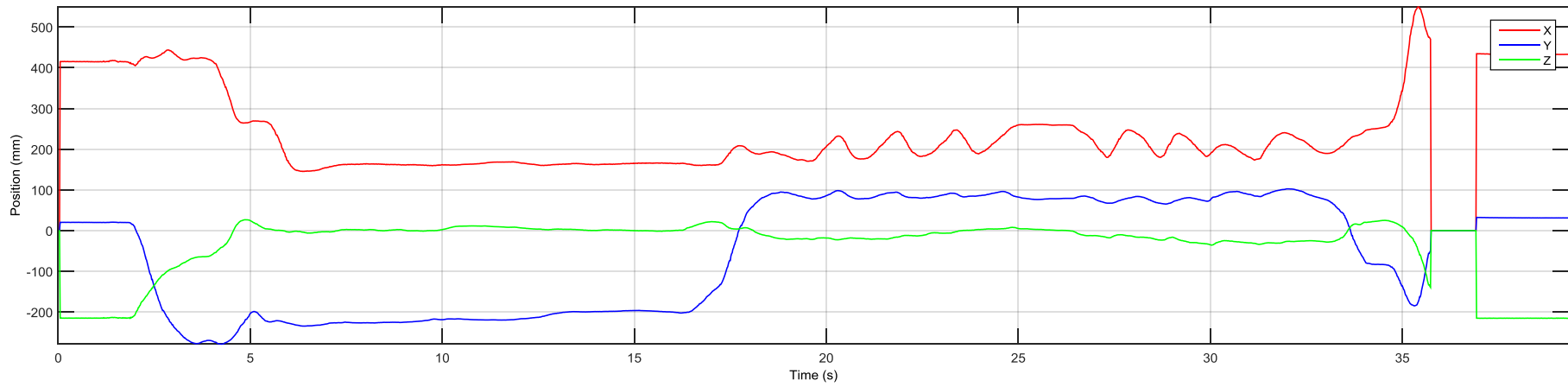
Figure B.22: Position and orientation data captured in Iteration 3

Iteration 3: Singular Linear Motion
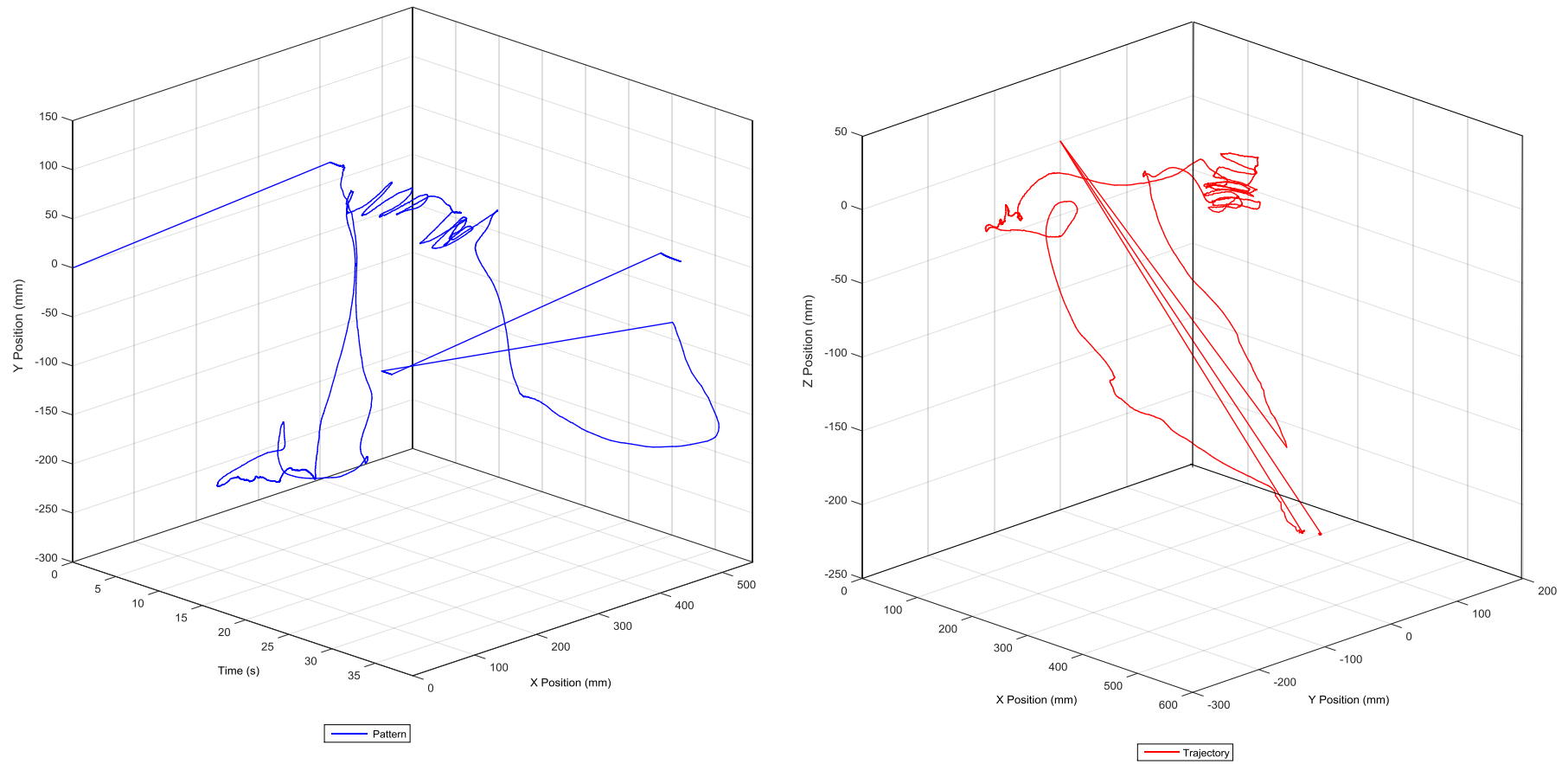
Figure B.23: 3D pattern and 3D path data captured in Iteration 3

Iteration 4: Surface Profiling
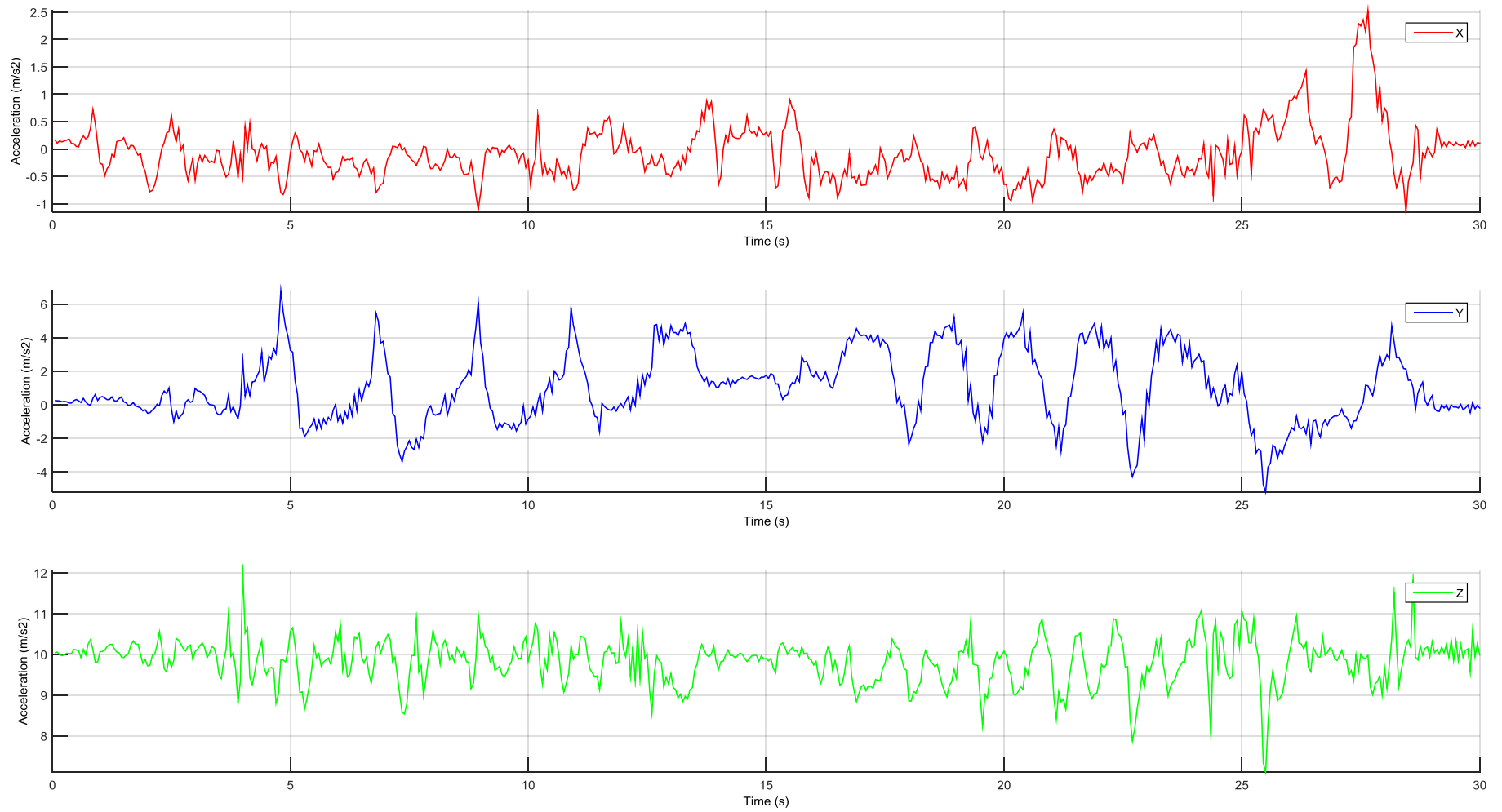
Figure B.24: Acceleration data captured in Iteration 4

Iteration 4: Surface Profiling
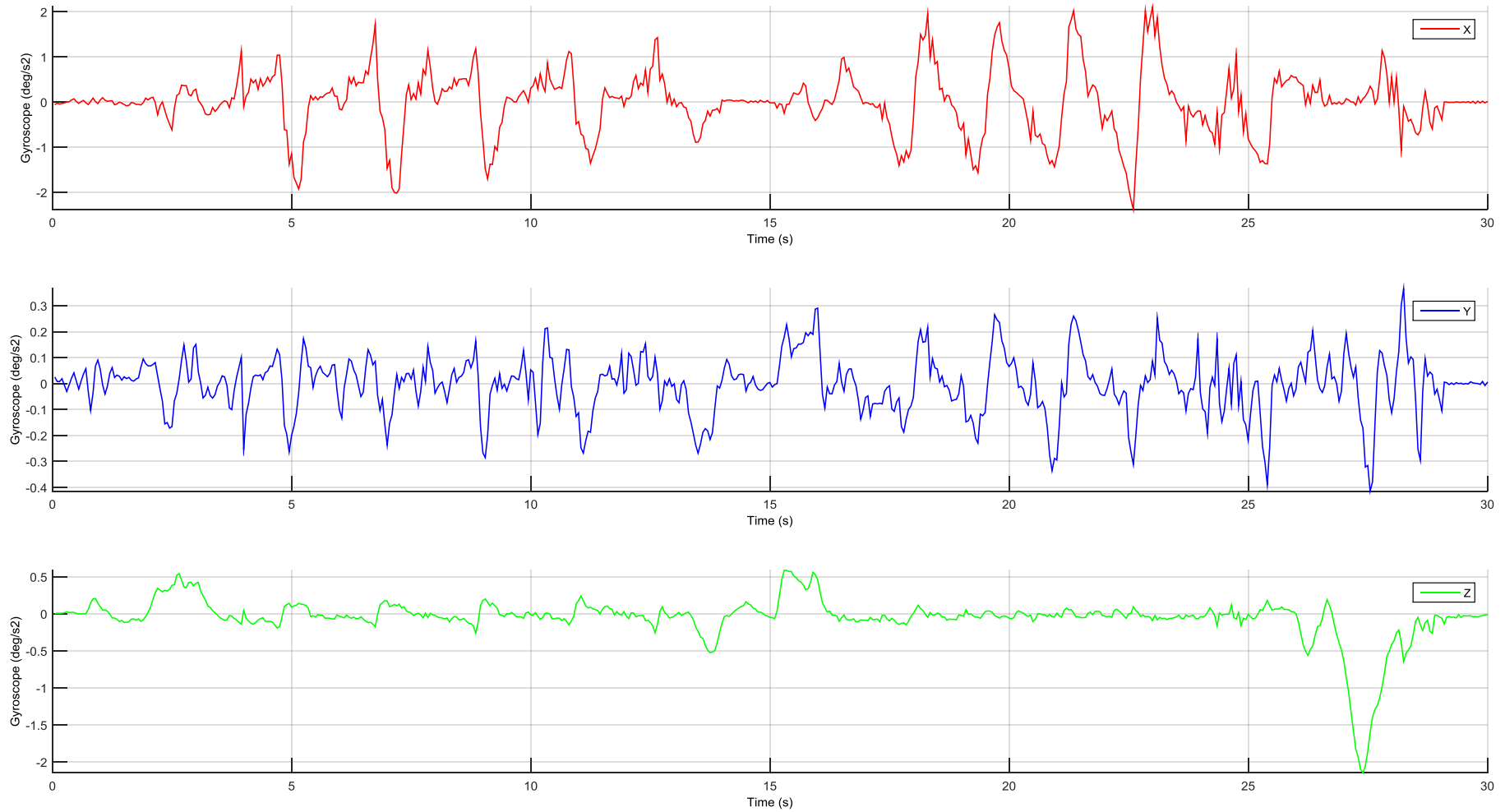
Figure B.25: Gyroscopic data captured in Iteration 4

Iteration 4: Surface Profiling
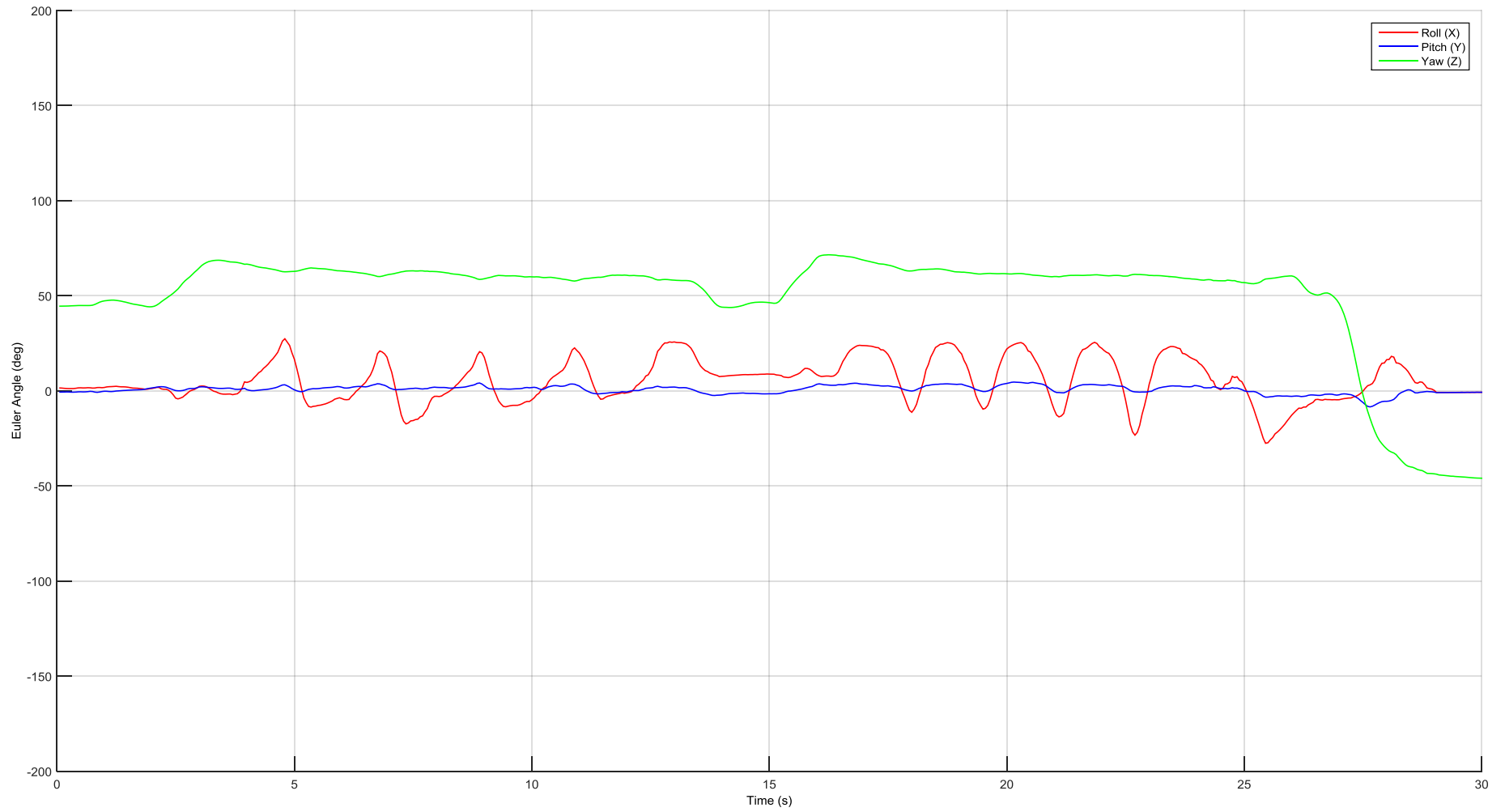
Figure B.26: Euler orientation data captured in Iteration 4

Iteration 4: Surface Profiling
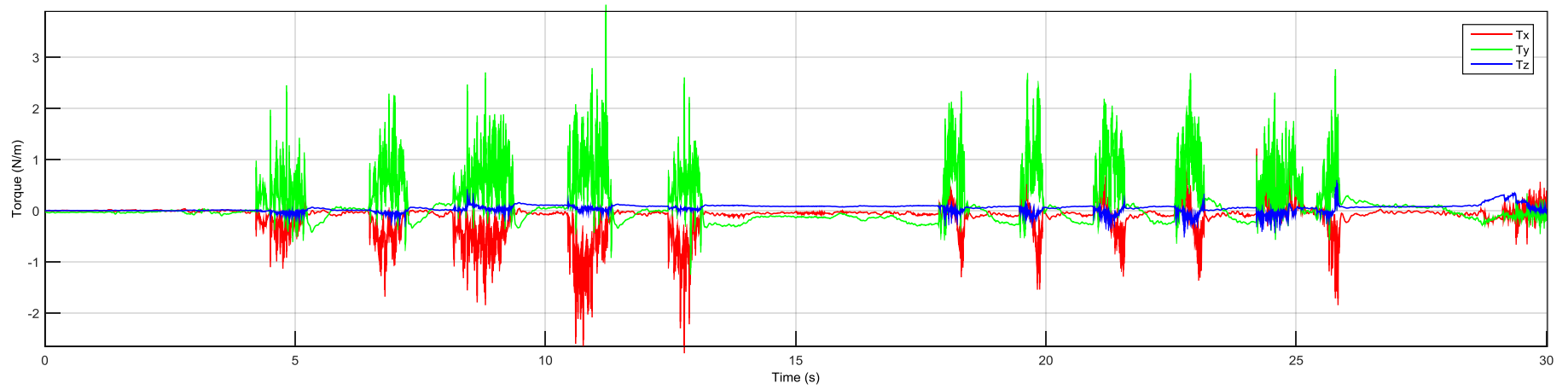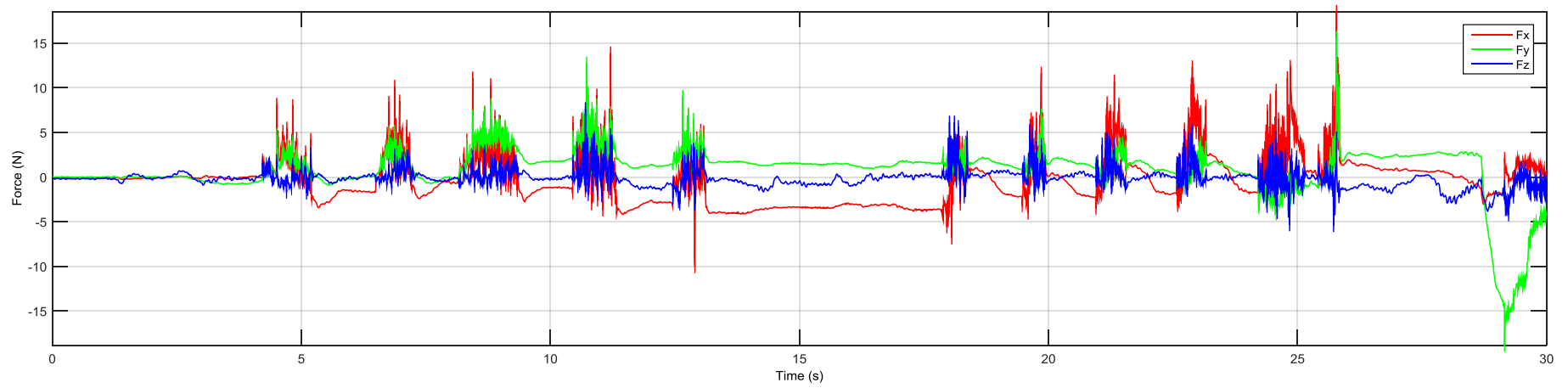
Figure B.27: Force and torque data captured in Iteration 4

Iteration 4: Surface Profiling
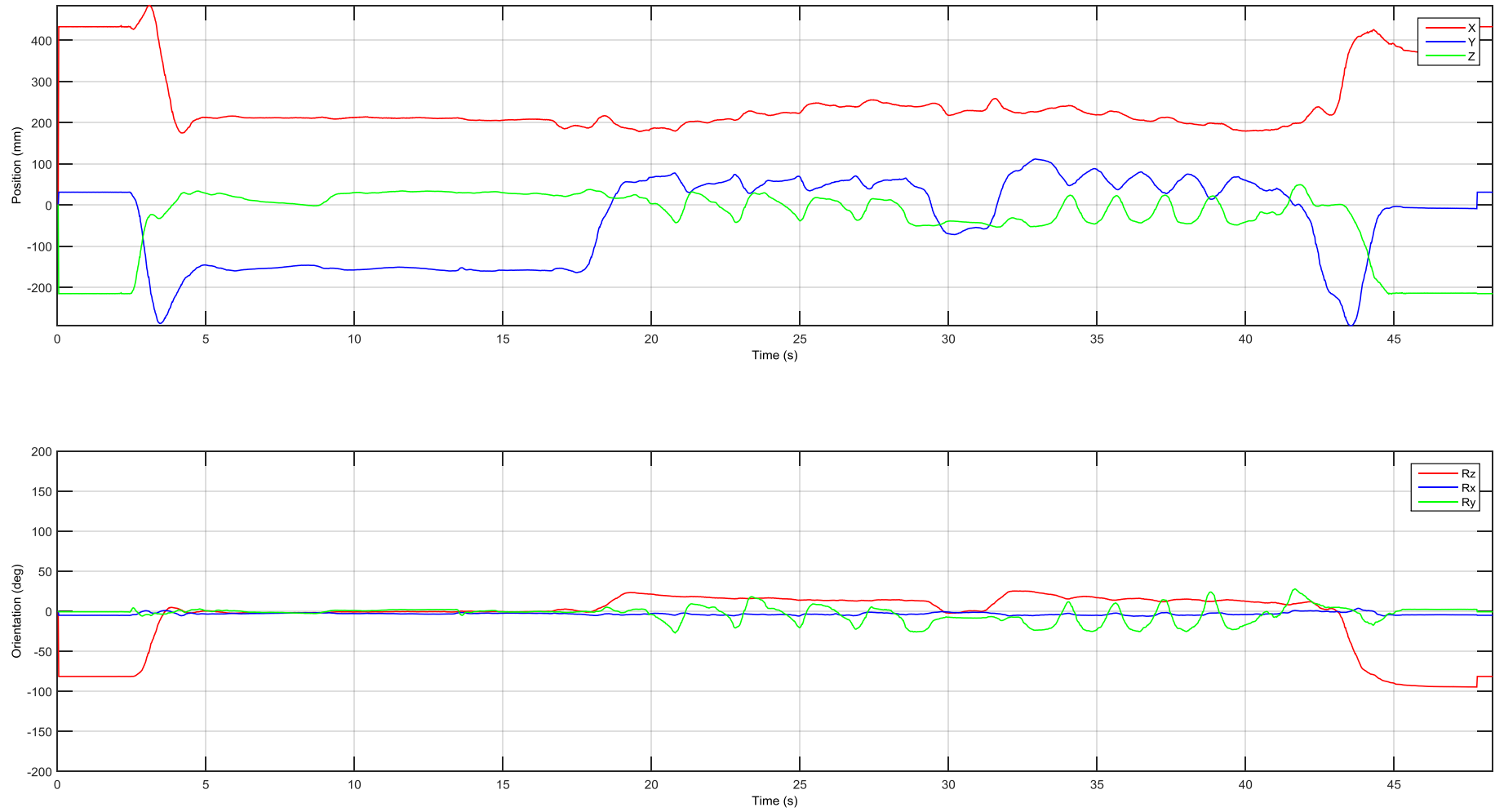
Figure B.28: Position and orientation data captured in Iteration 4

Iteration 4: Surface Profiling
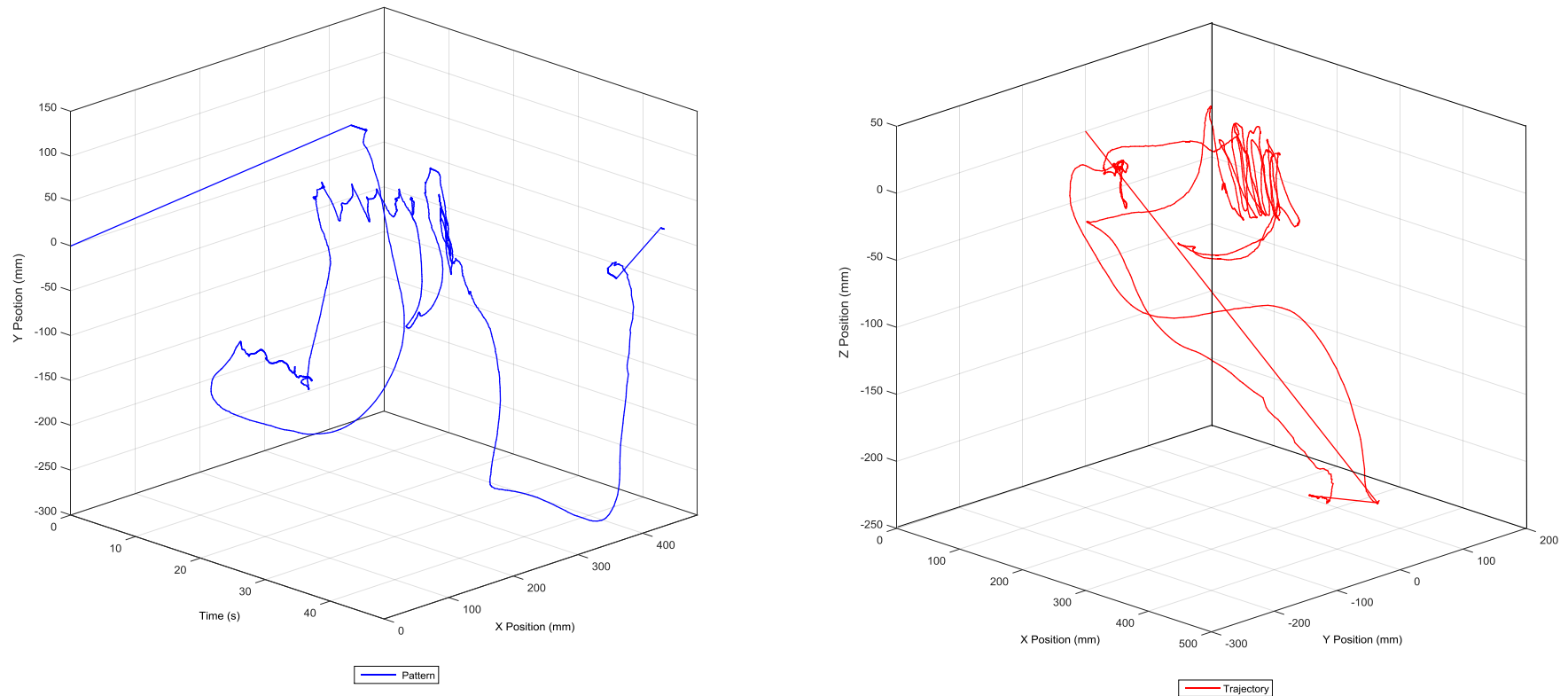
Figure B.29: 3D pattern and 3D path data captured in Iteration 4

B.3.4. Data Analysis and Discussion

The aim of these calibration experiments was to capture data from different sensors while validating the capturing and analysis procedure, while imitating the manual polishing operation and technique of a skilled operator. Overall, the current procedure shows good results in capturing and understanding of manual polishing operations. The results showed the patterns and forces used by the operator during the experiment, which helped to understand the data output of the different sensors during manual polishing operation.

B.3.4.1. Operator Experiment Feedback

The operator did find the fixture to be ergonomics and easy to handle. The weight did not affect the techniques used to complete the calibration experiments. However, the operator mentioned that vibration could not be felt during the experiment. This was due to the structure of fixture which acted as a damping device.

In addition, the operator did not feel close enough to the abrasive belt, due to the size of the fixture and the environment of the experiment. Therefore, the operator could not get good visual feedback and tactile feedback during the operation. Tactile feedback and visual feedback are important to the operator as skilled operators' uses them to monitor the polishing operation and to adapt their techniques accordingly (see Chapter 4).

B.3.4.2. Iteration Analysis

During the calibration experiment, the operator was aware of the different techniques used in each iteration. The current experimental procedure showed good results for capture and analysis of data in each iteration. Patterns and techniques were clearly identified. In iteration 1, three techniques were identified, then each technique was individually used in iterations 2 to 4. Each technique was identified by each sensor. For example, the Vicon MoCap system showed a clear path followed by the operator and the multi-axial force and torque sensor showed some pattern depending on the technique used.

B.3.4.3. Sensors Performance

The Vicon MoCap system showed good results for capturing the motion in previous experiments (see Section A.2.3). The data captured during this experiment showed the paths and patterns used by the operator. For example, in iteration 4, where the operator followed the profile of the part, the geometry of the curve plotted shows similarity with the real geometry of the sample workpiece being polished (Figure B.29). In addition, in Iteration 1 the Vicon data showed the three different patterns and techniques used by the operator. In other words, the Vicon MoCap system was particularly good at capturing the paths and patterns of the operator movements.

The multi-axial force and torque sensor (Shunk Gamma) was particularly good at providing data when the part was in contact with the abrasive belt. The sensor showed output values along the *x-y* axis depending on the

movement of the operator. This needs to be taken into consideration when computing the polishing force used by the operator. Moreover, the multi-axial force and torque sensor can provide with the duration of each polishing action, which can indicate the operator speed and the level of vibration.

The inertial measurement unit (Xsens MTw) provided acceleration, gyroscopic, and Euler orientation data. The IMU showed good result for recording the orientation of the fixture. Some patterns were also identified with the accelerometer and the gyroscope.

B.3.4.4. Data Matching and Analysis

Matching data from the various sensors was a complex task, as all sensors were triggered individually and at different times. The Vicon MoCap was triggered first, followed by the calibration and triggering of the multi-axial force and torque sensor and the inertial measurement unit, creating a 20 second the time delay with the Vicon MoCap. The synchronisation and analysis of data were carried out offline. The time delay for each sensor was calculated based on a specific point of each graph plot.

For example, the output data of the multi-axial force and torque sensor was matched with the position data, where every peak of force applied could be matched to the position. The same method was used to synchronise the Vicon MoCap data with the inertial measurement unit.

These data were then cross-referenced with each task specifications (Iterations 1 to 4). Each action of the operator was clearly identified. For example, in Iteration 2 the operator applied a static pressure on the workpiece surface, which was shown in the Vicon MoCap and multi-axial force and torque data as a linear movement in one axis.

B.3.5. Conclusion

The calibration experiments carried out showed good capabilities for the fixture and the sensors to capture the force, speed, and motion data, and to carry out the analysis into understanding and capturing patterns and techniques of skilled human operator during manual polishing procedure.

During the experiments, three known patterns were used (simple pressure, linear translation, and surface profiling). The main idea was to learn from these iterations, to identify and understand the data output from the fixture. These techniques were chosen as references for the capture of manual polishing parameters experiment (see Chapter 6), as these techniques may be used by the operator.

From the data captured by the sensors, the Vicon MoCap system and multi-axial force and torque sensor were found to be very useful during the experiment. The Vicon MoCap captured the position and orientation of the fixture, which provided the path and pattern used by the operator. In addition to the forces and torques, the multi-axial force and torque sensor could be used to monitor the operator speed (or feed rate) by looking at the length of each polishing action or pass. Even if the inertial measurement unit did not provide additional information to the Vicon MoCap and multi-axial force and torque sensor, it may be used to complete orientation data when the reflective markers are out of the field of view of one or both Vicon cameras.

The matching and analysis of data from the different sensors showed the forces and torques applied at any given point on the workpiece surface (based on the time frame). In addition, the motion data showed the different pattern(s) or technique(s) used by the operator. Therefore, patterns such as increasing or decreasing the speed to remove particular defect would be captured and identified.

The calibration experiment showed good results and provides a good understanding of the technique used by the human operator in the manual polishing process. This was made possible through research, where different techniques were captured and identified.

Therefore, the same configurations and procedure were followed in the capture of manual polishing parameters experiment, see Chapter 6.

Appendix C. Fixture Concepts and Designs

The following appendix is presenting the detail development method used to design the fixture to enable the capture of manual polishing parameters. Section C.1 is describing the design process for the fixture. The design process for the fixture includes engineering embodiment method and evaluation matrix. Section C.2 is presenting the prototype of the fixture chosen from Section C.1. In Section C.3, the improvement of the design and mechanical calculation are presented for a new design of the fixture. Sections C.4 and C.5 are presenting the final concept and design of the fixture based on the results of the previous sections.

C.1 Engineering Embodiment and Evaluation Matrix

Mechanical engineers often use various tools, such as engineering embodiment and evaluation matrices, to design and develop a product. These tools were used to develop the fixture to capture manual polishing parameters. Figure C.1shows the methodology used during the development of the fixture (Brezing, 2012; Derelöv, 2009; Langeveld, 2007). Figures C.2 and C.3 illustrates the various concept designed for the fixture.

As mentioned in Section 5.1, the fixture was designed to enable the capture of variables and parameters used by skilled operators during manual polishing operation of an industrial parts. To enable this, a set of sensors must be embedded within the fixture measure and capture the operator's forces and movements.

A prototype of the fixture was made (Section C.1.1) and some pre-test were also carried out. Improvements on the design were made based on the results of the pre-test with the prototype (Section C.1.2).
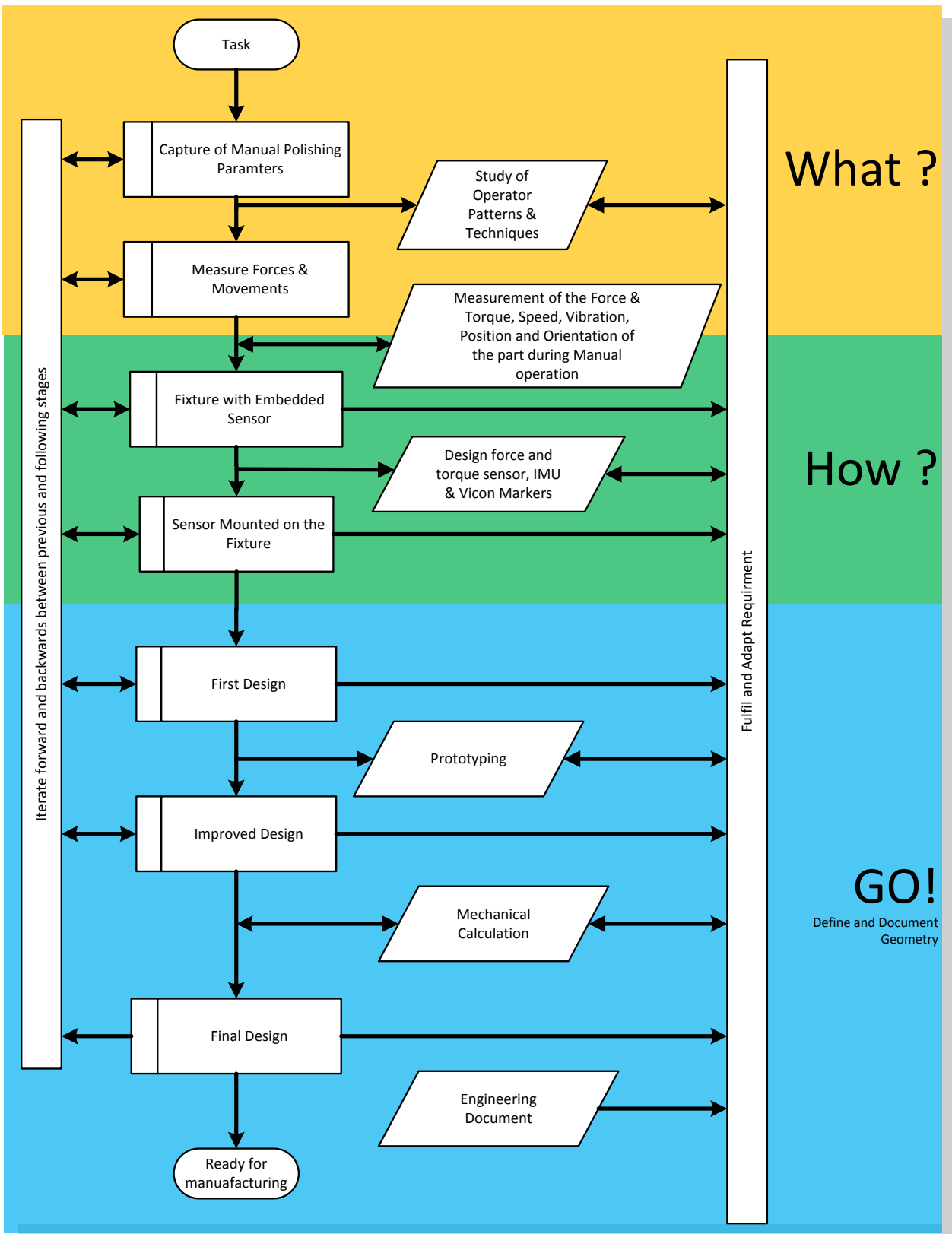
Figure C.1: Process diagram for fixture design

Fixture Design : Specifications, Part and Assembly

Spec & Requirement	The aim of the fixture is to capture data during manual operation of sample workpiece. The design of the fixture should to accommodate multiple sensors, such as a multi-axial force and torque sensor (shunk Gamma), an inertial measurement unit (Xsens MTw), or markers for Vicon MoCap. The Shunk Gamma is used to measure the contact force between the part and the abrasive tool. The Xsens MTw could measure the operator speeds and monitor the level of vibration. The Vicon MoCap could capture the operator movement and patterns. Note: the Xsens MTw could also be used to capture movements, depending on the benchmark results described in section 5.3.

Engineering Embodiment for Fixture Design 1 of 2

	Part	Assembly
Design 001		
Design 002		
Design 003		
Design 004		

Figure C.2: Engineering embodiment - fixture layout - 1 of 2

Engineering Embodiment for Fixture Design 2 of 2		
	Part	Assembly
Design 005		
Design 006		
Design 007		
Design 008		

Figure C.3: Engineering embodiment - fixture layout - 2 of 2

Figures C.2 and C.3 and Table C.1 show the design layout and specifications of various concepts for the fixture. Each concept integrates at least two sensors: one to capture the force, and one to capture the movement. However, multiple sensors maybe used to capture the movement depending on the results of the benchmark experiments (see Appendix A).

An evaluation matrix was generated, as seen in Table C.1, to compare the different design based on specific criteria. Some of the design criteria include the ergonomics and manipulation (how comfortable and easy the fixture is to use), number of sensors embedded, aesthetic aspect of the fixture, the portability, and number of components required for the fixture.

Table C.1: Evaluation matrix for fixture

Design	001	002	003	004	005	006	007	008
Datum	Yes	No	No	No	No	No	No	No
spec.								
Ergonomic	Datum	-	=	---	--	=	+	+++
Weight		--	-	++	+++	=	+	---
Num. Component	2	1	2	1	1	3	1	1
Num. Sensors	2	2	2	2	2	2	2	3
Assembly	Datum	=	+	+++	++	++	+++	+++
Manipulations		-	=	---	---	=	++	+++
Volume of Material	Datum	+	+	++	+++	=	--	--
Aesthetic		=	=	=	-	+	++	++
Size	Datum	=	=	+++	+++	=	=	=
Portability		=	=	+	+	=	+	+
Capture of data		=	=	--	--	=	++	+++
Σ=		4	6	1	0	7	1	1
Σ+		1	1	10	12	3	12	14
Σ-		4	1	8	8	0	2	2
Σ+ : higher than datum, Σ= : same as datum, Σ- :lower than datum								

Design 001 was chosen as datum (or reference) for the other designs. Each criterion was evaluated using a pros and cons marking system (+, -, =). From the total of Σ= Σ+ and Σ- (see Table C.1), Design 008 has obtained the highest of positive marks (14 Σ+). Therefore, this design has been chosen as final concept for the fixture.

C.2   Prototype Fixture to Capture Manual Polishing Parameters

Design 008 of the fixture has been chosen as final concept (see Figures C.3 and C.4). Due the complexity of the geometry and the short manufacturing time, a fixture prototype has been made from a single part using additive manufacturing processes. And ABS plastic material was chosen for its lightness.
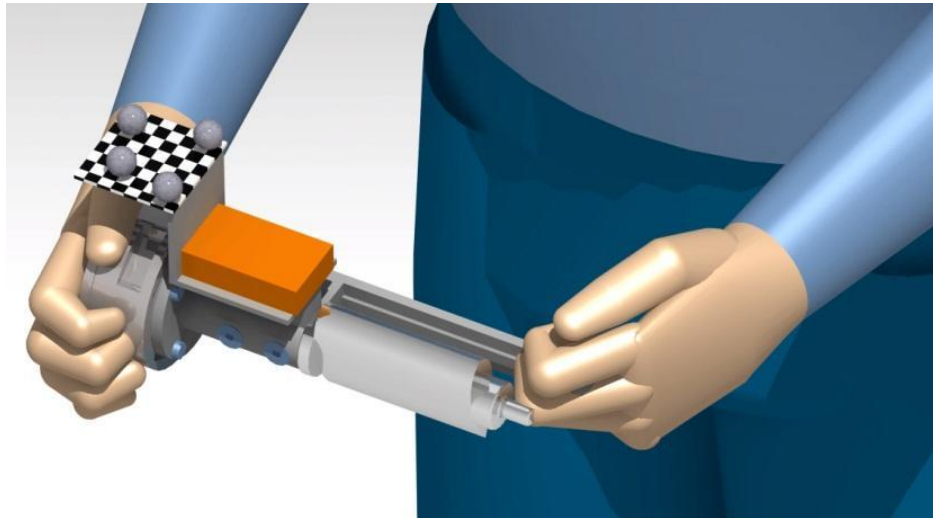
Figure C.4: Ergonomic analysis for the fixture to capture forces and movement

The next section of this appendix describes the first test with the prototype and the design improvement of a new concept for the fixture.

C.3   Design Improvement

C.3.1   Fixture Prototype

The first test with the fixture prototype showed that the design was a comfortable size, and easy for the operator to hold and manipulate (see Figure C.4). After further testing, it was noticed that this design would not accurately measure the forces and torques during the polishing operation.

The fixture prototype features a handle attached to the multi-axial force and torque sensor. This may create a null force output if the force applied on the sample workpiece surface ($F_{contact}$) and the force applied by the operator on the handle ($F_{operator}$) are of the same magnitude and opposite directions, as illustrated in Figure C.5. To resolve this issue, a new concept design has been proposed, in the following section.
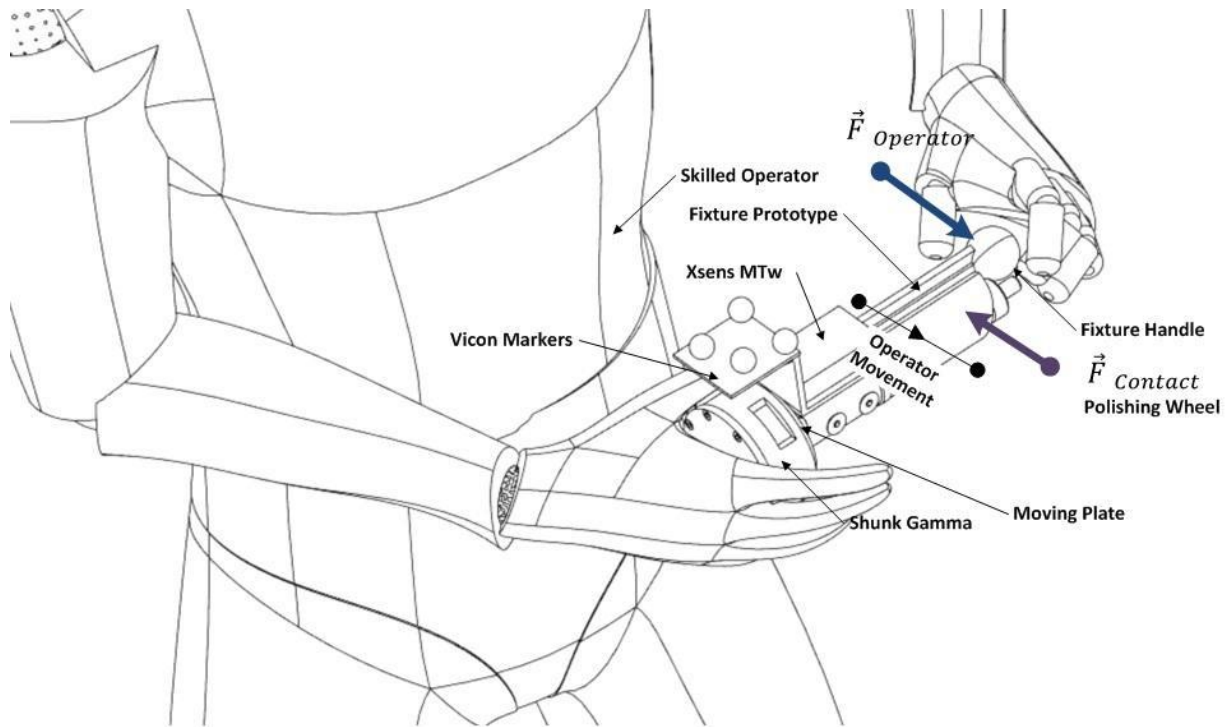
Figure C.5: Constraint of original fixture design

C.3.2 Improved Concept

Figure C.6 illustrates the new design of the fixture. In this design, the handle is attached to the back plate of the multi-axial force and torque sensor. This layout should not allow any false reading from the sensor as in the previous design (see section above). The new design also includes two handles: one handle with the multi-axial force and torque sensor on the left, and one handle on the right side. These handles were designed to be comfortable, allowing a good grip, and to mimic the way that the operator would hold the workpiece in standard manual polishing procedure.
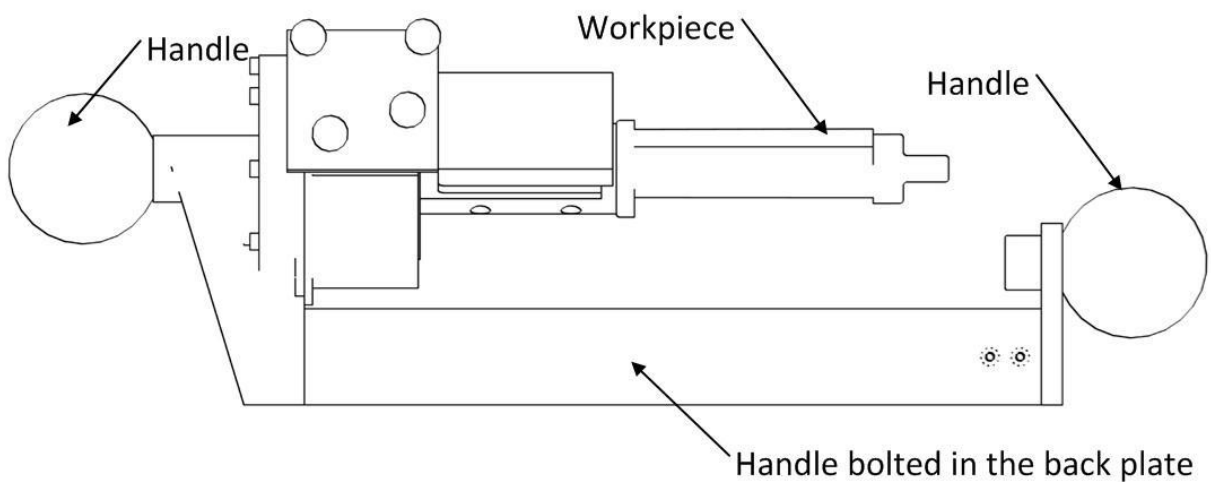
Figure C.6: Concept of the new fixture

C.3.3   Euler-Bernoulli Beam Theory

The Euler-Bernoulli theory was used to verify the mechanical strength of the new design of the fixture and calculate adequate dimensions. The geometry of the new concept was close to an L-shaped beam (see Figure C.7 and C.9). For the purpose of simplifying the calculation, the defection of two separates cantilever beam were carried out using Euler-Bernoulli Beam equations.

L-Shaped Cantilever Beam
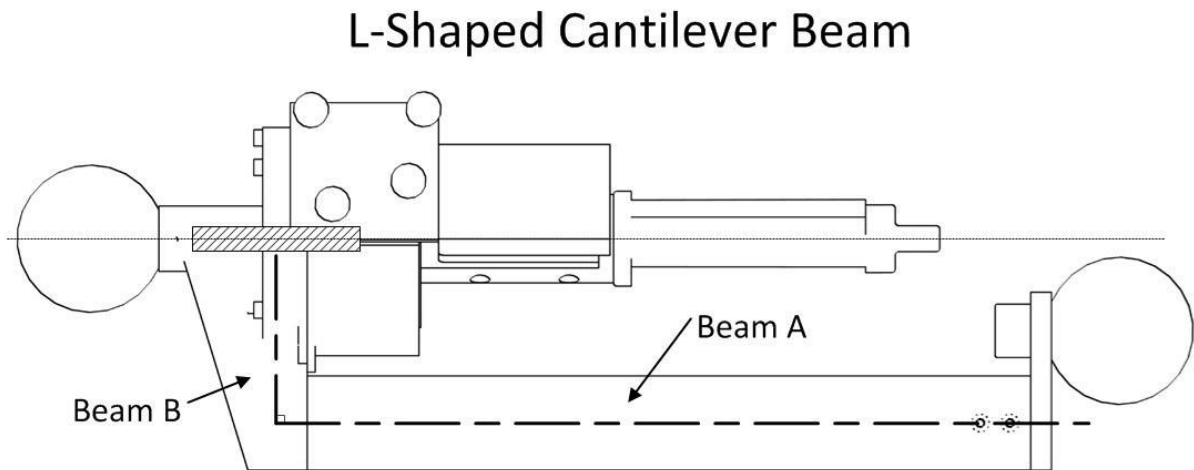
Figure C.7: Representation of the new fixture design as an L-Shaped Beam

The general approach to calculate displacements and bending moments using the Euler-Bernoulli beam theory is as follows (Beléndez et al., 2002; Euler, 2013; Feynman et al., 2011, n.d.; Forums, 2015; Georgiades et al., 2013; Kuo and Lin, 2000; Will, 2012):

Maximum Deflection:

$$\delta = \frac{F.L^3}{3EI}$$

<div align="right">

Eq.(C.1)
</div>

Where δ is the maximum deflection (*m*), F is the force applied on the beam (*N*), L is the beam length (*m*), E is the material young modulus (*Nm*), and I is the beam cross section (*m⁴*).

Distributed Deflection:

$$\delta_{(x)} = \frac{Fx^2(3L - x)}{6EI}$$

<div align="right">

Eq.(C.2)
</div>

Where $\delta_{(x)}$ is the deflection (m) at x a specific point (m), F is the force applied on the beam (*N*), L is the beam length (*m*), E is the material young modulus (*Nm*), I is the cross section (*m⁴*).

Maximum Bending moment:

$$M_b = F.L$$

Where M_b is the maximum bending moment (*Nm*), F is the force applied on the beam (*N*), L is the beam length (*m*).

Distributed Moment:

$$M_{(x)} = F(x - L)$$

Where $M_{(x)}$ is the bending moment (*Nm*) at x specific point (*m*), F is the force applied on the beam (*N*), and L is the beam length (*m*).

Maximum Deflection Angle:

$$\theta = \frac{F.L^2}{2EI}$$

Where θ is the maximum deflection angle (*degrees*), F is the force applied on the beam (N), L is the beam length (*m*), E is the material young modulus (*Nm*), and I is the beam cross section (*m⁴*).
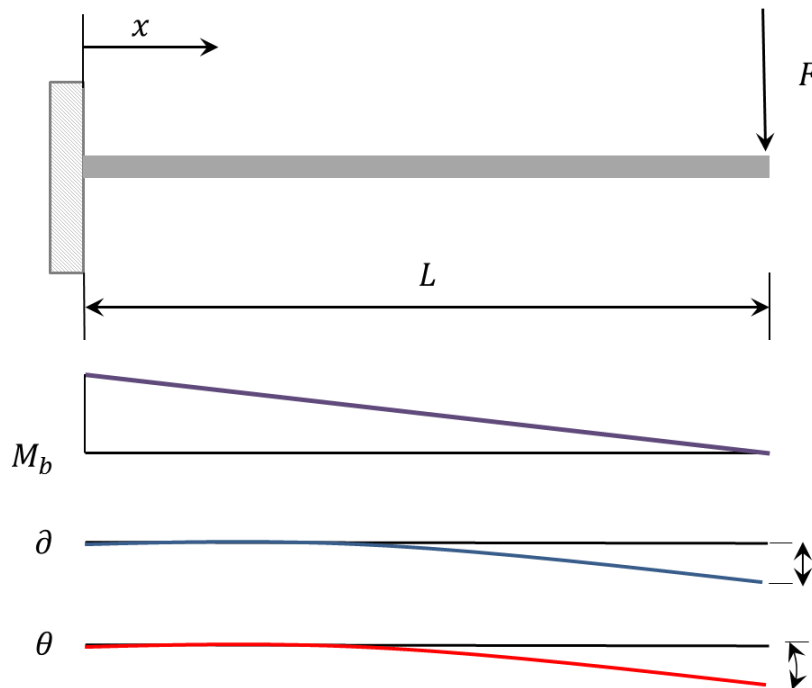
Figure C.8: Euler-Bernoulli beam theory for a cantilevered beam
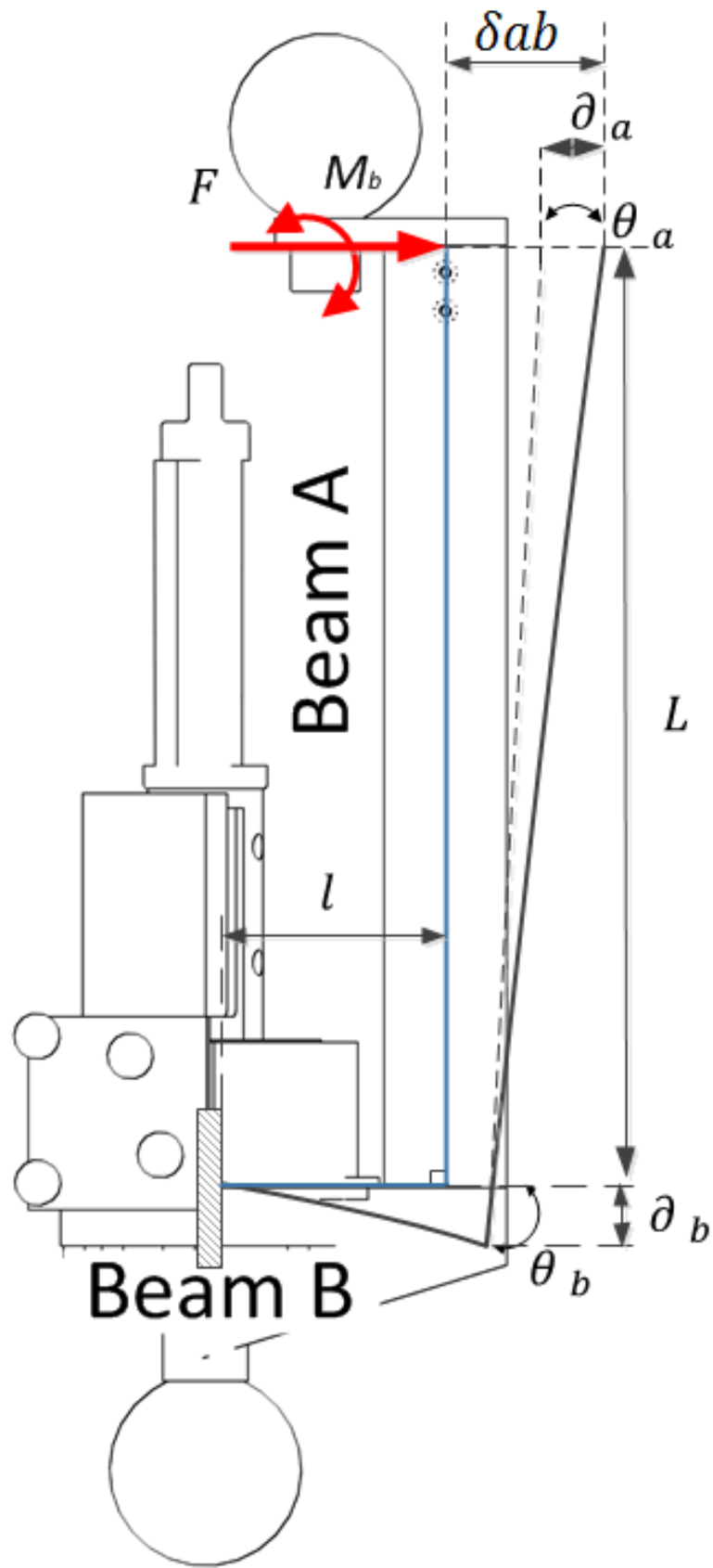
Figure C.9: Euler-Bernoulli solution for the fixture

C.3.4 Application of Euler-Bernoulli for the design of the new fixture

As mentioned earlier, for simplification it is was assumed that that the geometry of the new fixture is comparable to two perpendicular cantilevered beams forming an L-shape. As illustrated in Figure C.9 and C.10, the force applied on the fixture by the operator is perpendicular to *Beam A* and parallel to *Beam B*. In the following section, the maximum deflection and deflection angle was first calculated for *Beam A*, then for *Beam B*. Finally, the combination of the deflection for both beam was calculated.
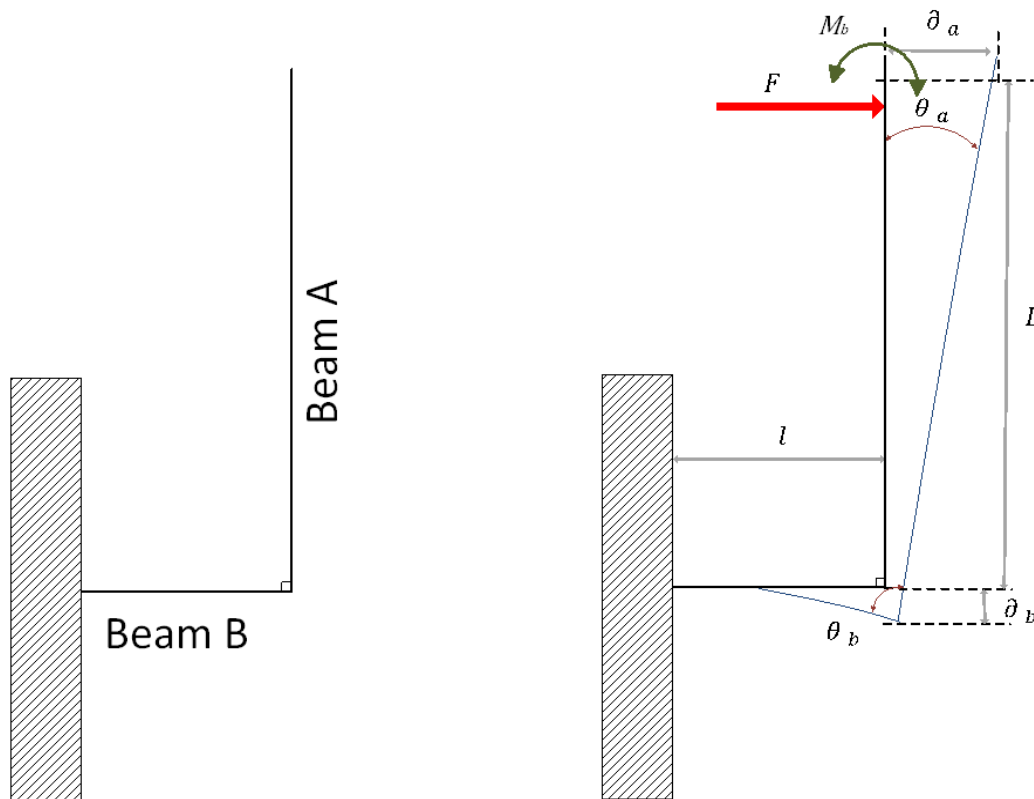
Figure C.10: Euler-Bernoulli theory for two perpendicular cantilever beam

Calculation for Beam A:

For *Beam A,* the displacement and displacement angle were calculated using Equations C.6 and C.7 as the force is perpendicular to the beam.

$$\delta_a = \frac{F.L^3}{3EI}$$

<div align="right">Eq.(C.6)</div>

Where δ_a is the maximum displacement of *Beam A* , L is length of the beam (*m*), E is the material young modulus, I is the cross section of the beam, and F is the applied force (*N*).

$$\theta_a = \frac{F.L^2}{2EI}$$

<div align="right">Eq.(C.7)</div>

Where θ_a is the maximum displacement angle of *Beam A*.

Calculation for Beam B:

As shown in Figure C.10, the force applied at *Beam A* is parallel to *Beam B*. To calculate the displacement and displacement angle, the choice was made to use the bending moment applied on *Beam B* instead of the force. Therefore, the maximum displacement and displacement angle at *Beam B* were calculated using Equations 5.12 and 5.13:

$$\delta_b = \frac{M_b . l^2}{2EI}$$

Eq.(C.8)

Where δ_b is the maximum displacement of *Beam B*, *L* length of the beam, *E* the material young modulus, *I* is cross section of the beam, and M_b the bending moment apply on *Beam B*.

$$\theta_b = \frac{M_b . l}{EI}$$

Eq.(C.9)

Where θ_b is the maximum displacement angle of *Beam B*.

Calculation of Displacement x-y direction :(Forums, 2015)

Using the equations for *Beam A* (Equations C.6 and C.7) and *Beam B* (Equations C.8 and C.9), the whole displacement of the fixture was calculated using Equation C.10, as follow:

$$\delta ab = \delta a \times cos\theta_a + \delta b \times sin\theta_b$$

Eq.(C.10)

Where δab is the total displacement calculated for the fixture.

Investigation and Calculation:

For the previous equations (Equations C.6 to C.10), the force applied is known ($\approx$100 N), the young modulus E is 6.9E+10 N for aluminium, and the cross section *I* of each beams would vary depending on the size and geometry. In addition, *Beam A* is a standard hollow beam. As the geometry and size of *Beam A* would not vary, the deflection of *Beam A* would stay constant during the calculation. Therefore, calculation and improvement were concentrated on the length and geometry of *Beam B*, as seen on Table C.2.

Table C.2 shows the deflections calculated with Equations C.8 to C.10, for various sizes and geometries for *Beam B*. The deflection in *Beam B* changes greatly (from 1.12E-02 mm to 7.20E-04 mm) depending on its size. However, a small change in the total displacement can be observed ($\approx$0.84 mm). As *Beam A* is a hollow beam of *20 mm x 20 mm*, and the results shown in Table C.2, the height of *Beam B* should be *20 mm x 20 mm*. Based on Table C.2, the smallest displacement calculated is 7.20E-04 mm for this size.

Table C.2: Application of Euler-Bernoulli beam theory

Height	Width	F(N)	L (m)	E (Nm)	I (m^4)	δ_b	A(deg)	$\delta ab(mm)$
20	8	100	0.02365	6.90E+10	8.53E-10	1.12E-02	0.054449	0.848506
22	8	100	0.02365	6.90E+10	9.38E-10	1.02E-02	0.049515	0.848401
24	8	100	0.02365	6.90E+10	1.024E-09	9.36E-03	0.045356	0.848319
25	8	100	0.02365	6.90E+10	1.06E-09	8.99E-03	0.043569	0.848286
30	8	100	0.02365	6.90E+10	1.28E-09	7.49E-03	0.036285	0.848166
35	8	100	0.02365	6.90E+10	1.49E-09	6.42E-03	0.031108	0.848095
40	8	100	0.02365	6.90E+10	1.7E-09	5.62E-03	0.027224	0.848048
50	8	100	0.02365	6.90E+10	2.13E-09	4.49E-03	0.021774	0.847993
20	10	100	0.02365	6.90E+10	1.66E-09	5.75E-03	0.02788	0.84806
20	14	100	0.02365	6.90E+10	4.57E-09	2.10E-03	0.010156	0.847916
22	14	100	0.02365	6.90E+10	5.03E-09	1.91E-03	0.009234	0.847912
24	14	100	0.02365	6.90E+10	5.48E-09	1.75E-03	0.008463	0.84791
25	14	100	0.02365	6.90E+10	5.71E-09	1.68E-03	0.008125	0.847908
30	14	100	0.02365	6.90E+10	6.86E-09	1.40E-03	0.00677	0.847904
35	14	100	0.02365	6.90E+10	8.00E-09	1.20E-03	0.005803	0.847902
40	14	100	0.02365	6.90E+10	9.146E-09	1.05E-03	0.005078	0.8479
50	14	100	0.02365	6.90E+10	1.14E-08	8.38E-04	0.004062	0.847898
20	20	100	0.02365	6.90E+10	1.33E-08	7.20E-04	0.00348	0.8479

C.4   Weight Check

The overall weight of the fixture was also an important parameter (see Section 5.1), as it might affect the operator technique. Table C.3 shows the weight of each component in the fixture (excluding the sample workpiece). The overall weight of the fixture is 0.976 kg, which is reasonable and should not impede the operator too much.

Table C.3: Fixture weight check

Item	Weight (g)	Item	Weight
Hollow Beam	214	FT Handle Plate	255
Spigot	3	Door Knob	150
Aluminium Body	20	Shunk FT	266
Xsens MTw	35	Vicon Plate	33
Total weight*	976	*total weight of the fixture excluding the part	

C.5   New Design

Figure C.11 illustrates the final design of the fixture. Small adjustments had to be made for machining purposes and to meet British Standards. After mounting all of the sensors into the fixture, it was noted that the fixture size and the way that it is held was comfortable and the overall weight felt right for the operator.

(10) Plate for Shunk Gamma

(3) Xsens MTw

(8) Long Beam

(9) Spigot

(6) Dust Protector

(7) Main Body

(2) Shunk Gamma

(1) Workpiece

(5) Fixture Handle
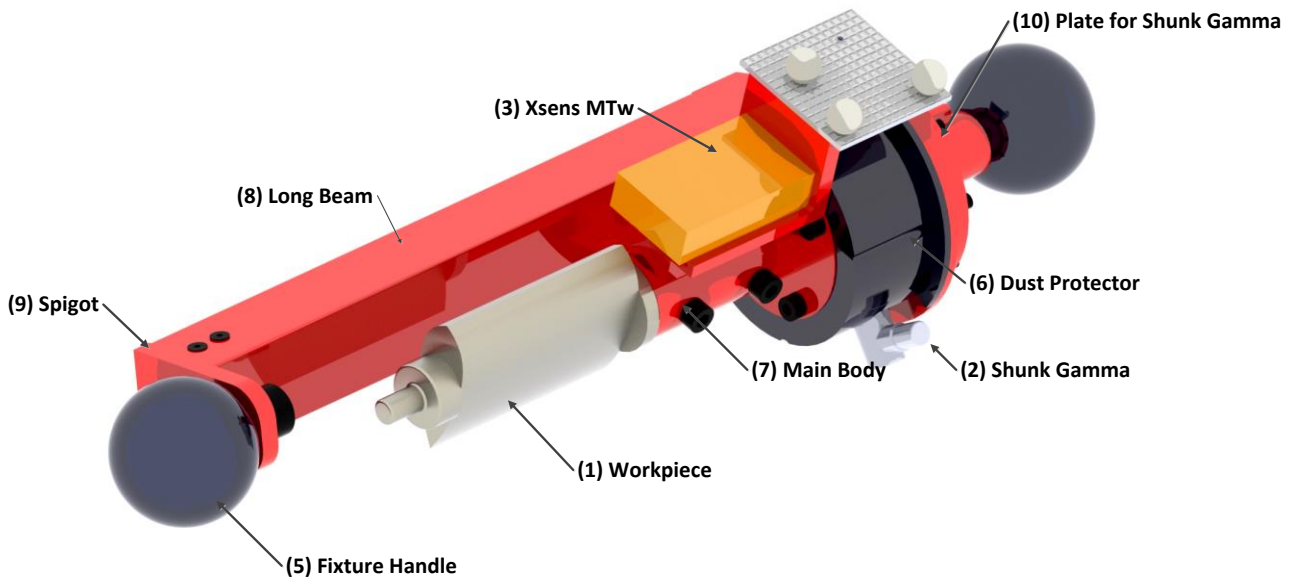
Figure C.11: Final fixture design with embedded sensors

Appendix D.Experiment 1: Removing a Thick Layer

The following appendix presents the detail data captured by the fixture for Experiment 1 (see Section 6.2). Figure D.1 to D.3 illustrate the data captured with the inertial measurement unit, showing the acceleration, gyroscope, and Euler-orientation respectively. Figure D.4 illustrates the forces and torques captured with the multi-axial force and torque sensor. Figure D.5 to D.7 illustrate the data captured by the Vicon MoCap system including the position and orientation, 3D path, and 3D pattern of the operator.
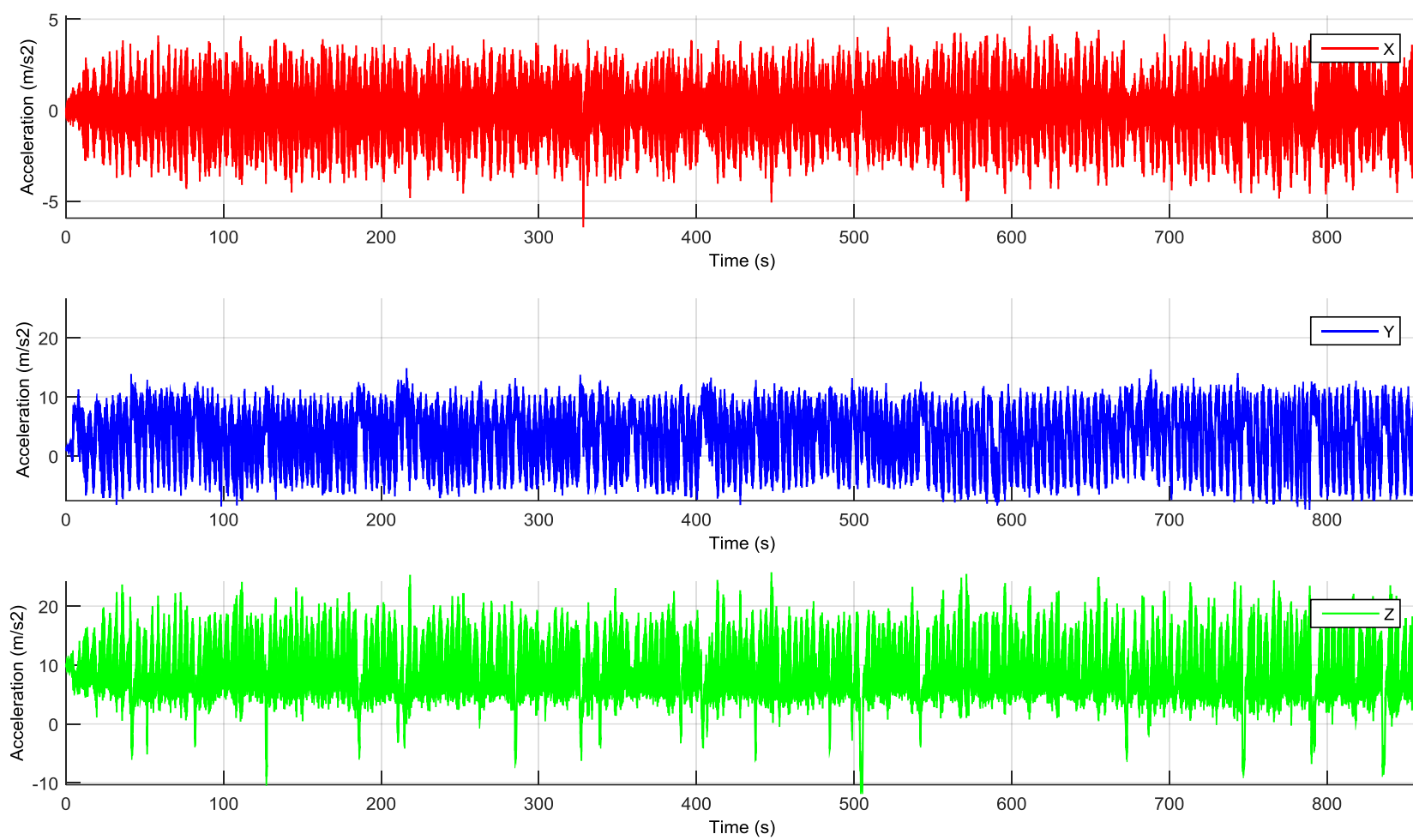
Experiment 1 - Acceleration
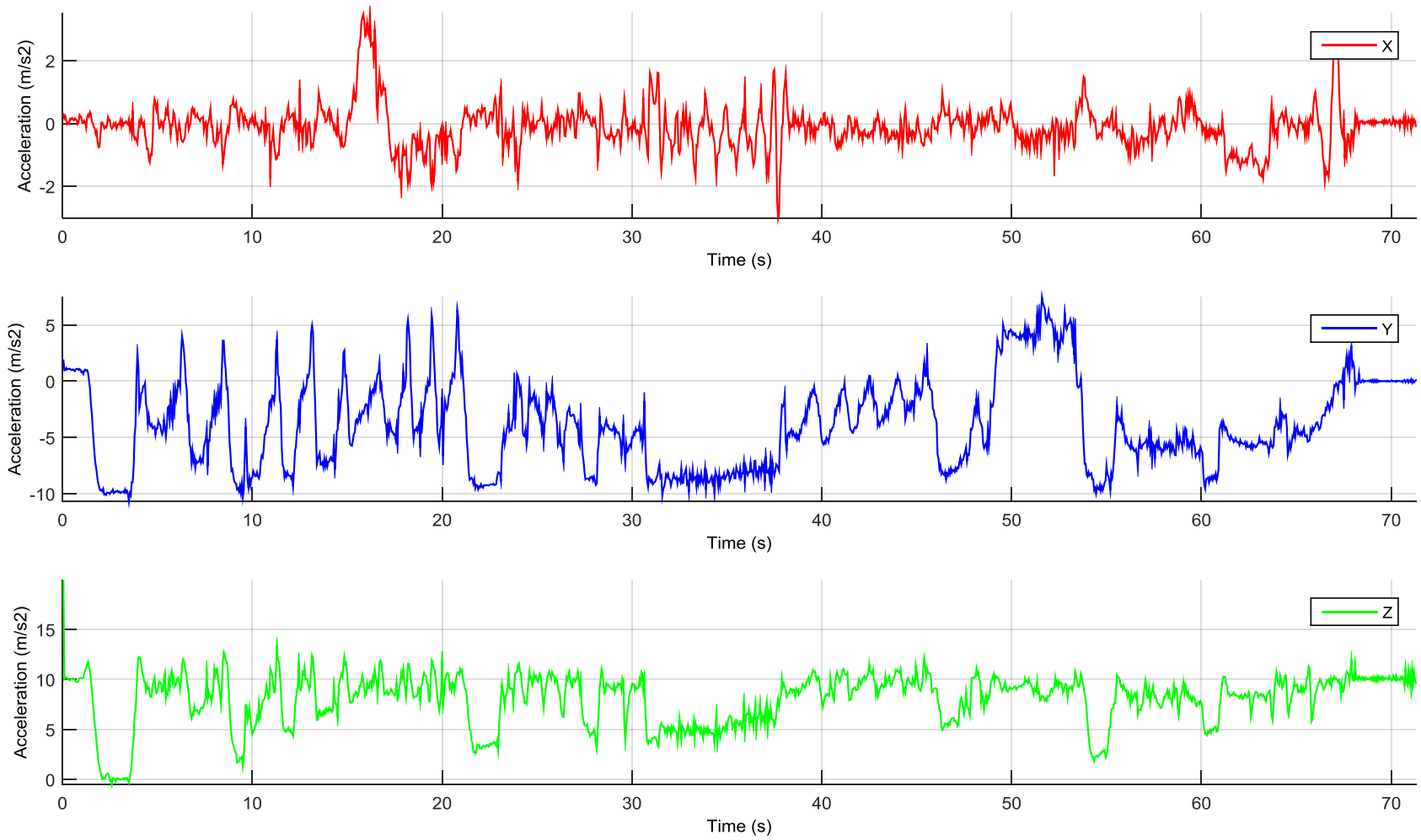
Figure D.1: Acceleration data (Xsens MTw) - Experiment 1: Removing a Thick Layer
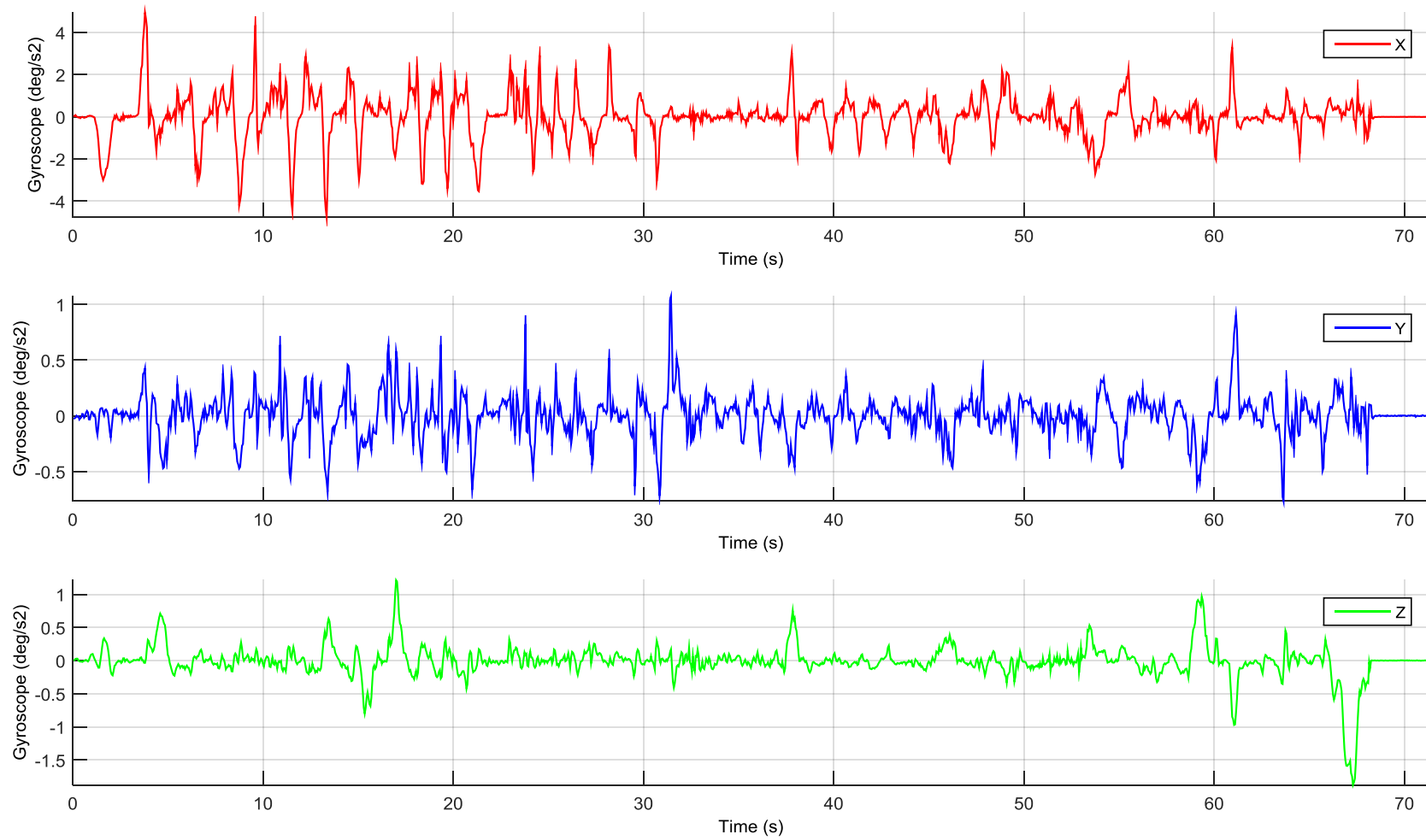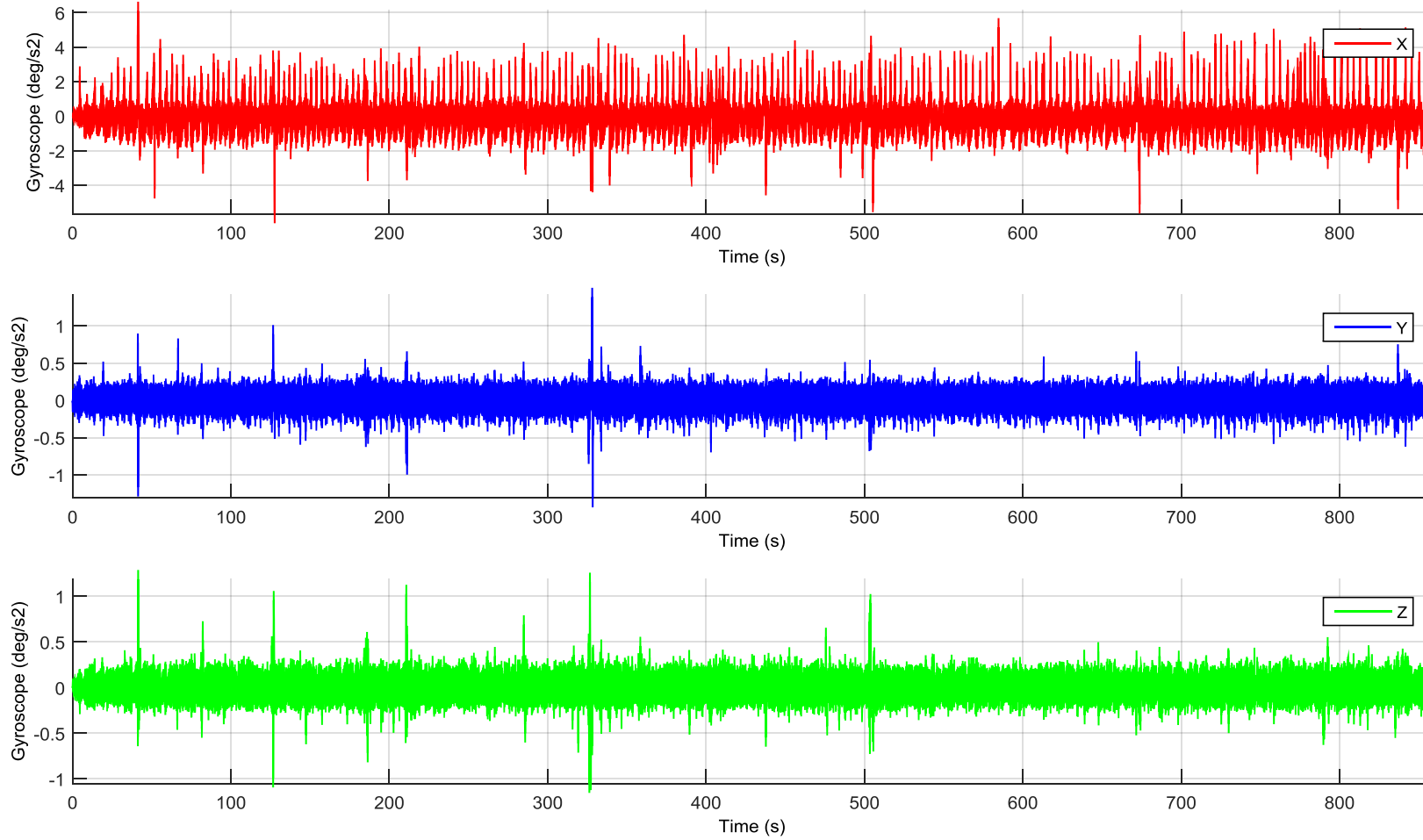
Figure D.2: Gyroscopic data (Xsens MTw) - Experiment 1: Removing a Thick Layer

# Experiment 1 – Euler-angle orientation
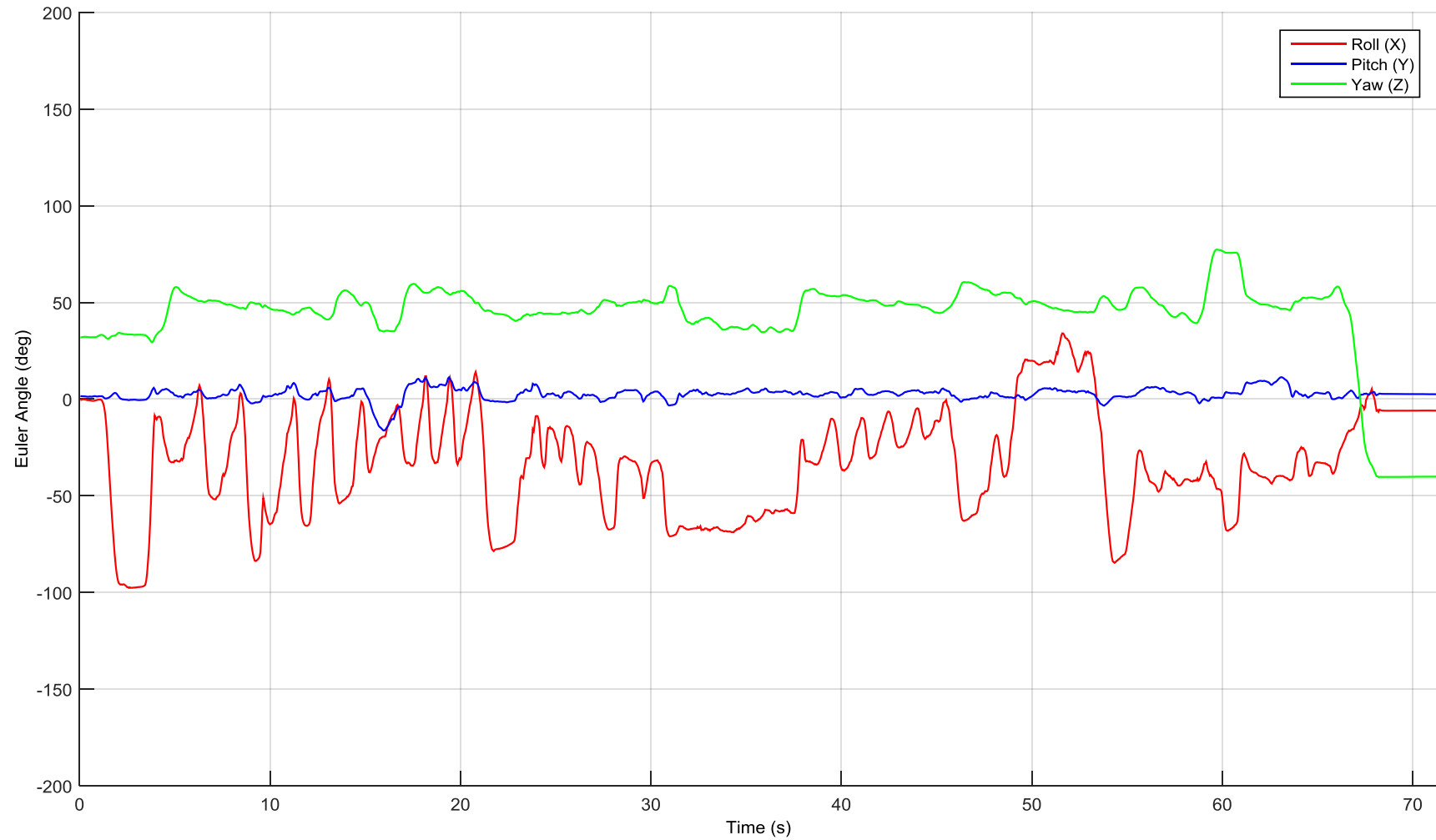
Figure D.3: Euler orientation data (Xsens MTw) - Experiment 1: Removing a Thick Layer
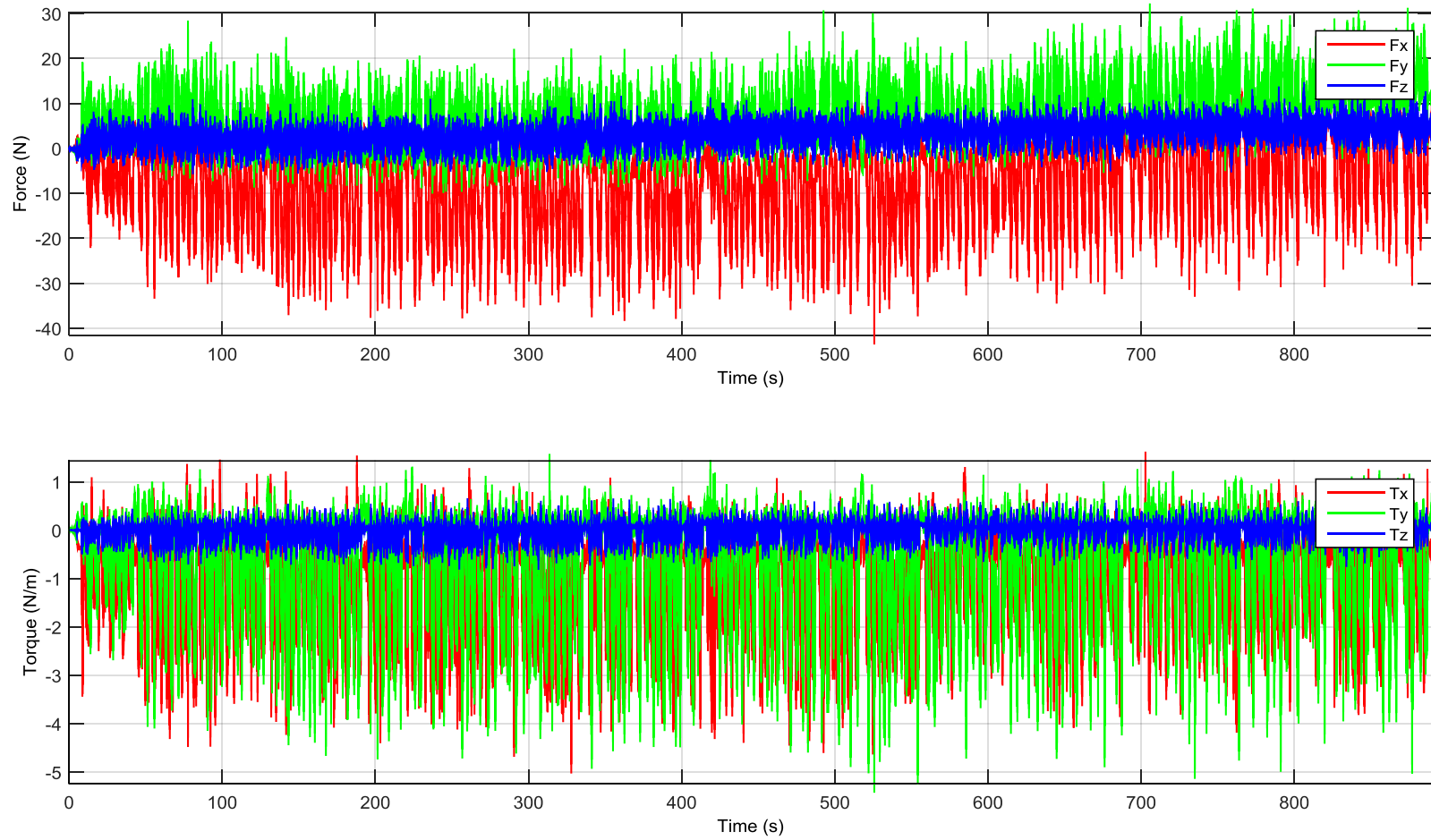
Experiment 1 – Forces and torques
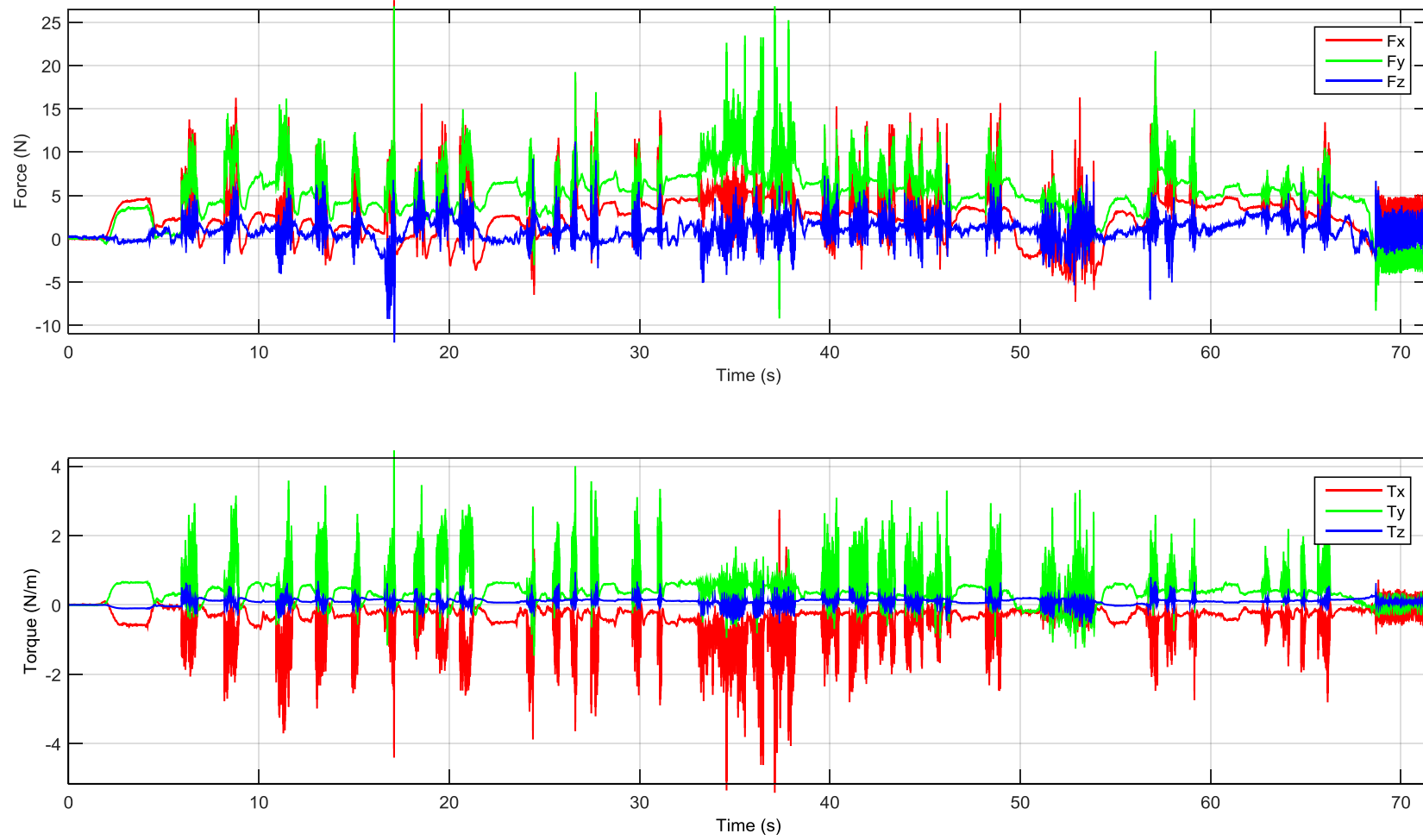
Figure D.4: Forces and torques data (Shunk Gamma) - Experiment 1: Removing a Thick Layer

Experiment 1 – Positions and orientations (2D)
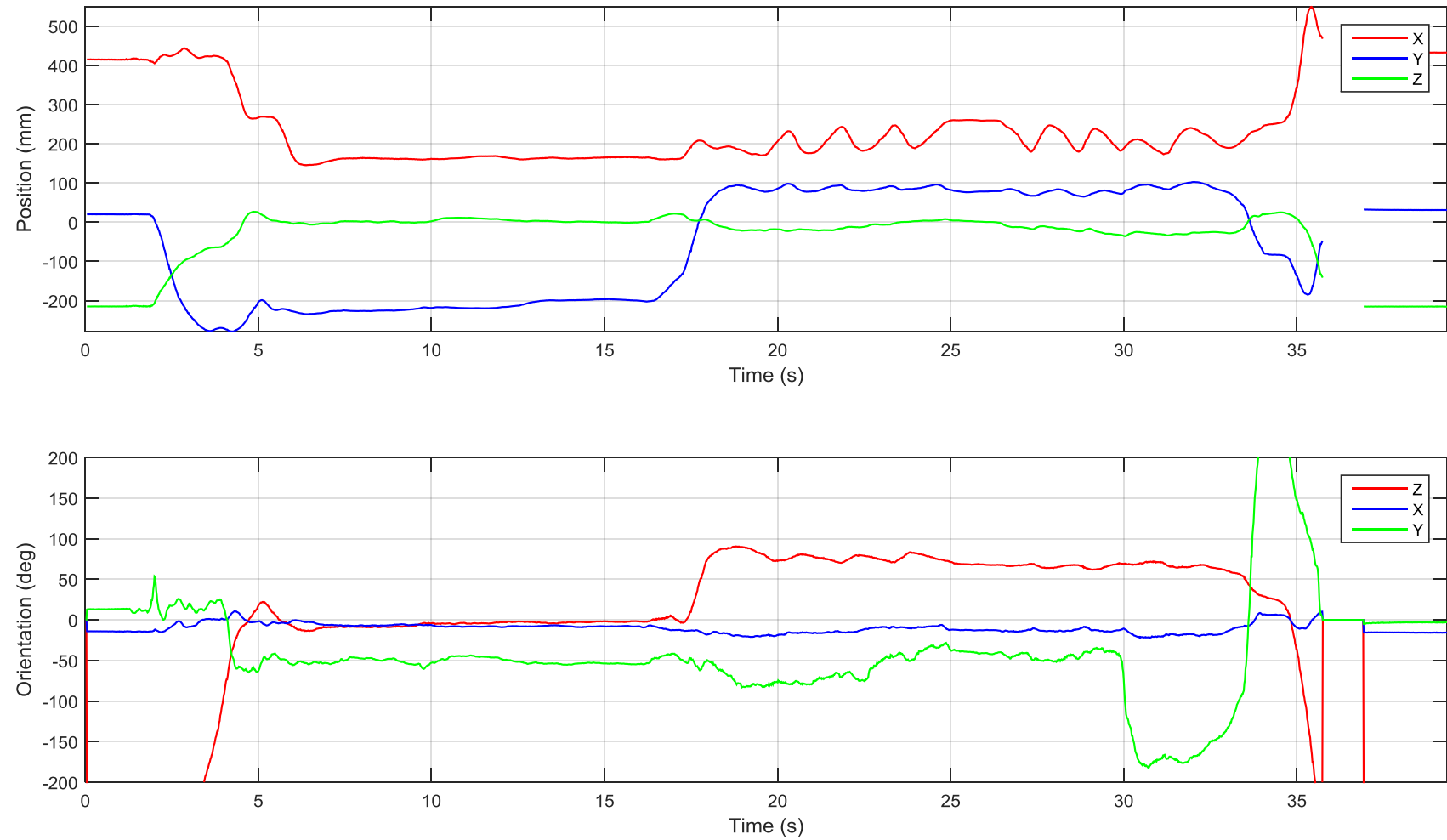
Figure D.5: Position and orientation data (Vicon) - Experiment 1: Removing a Thick Layer

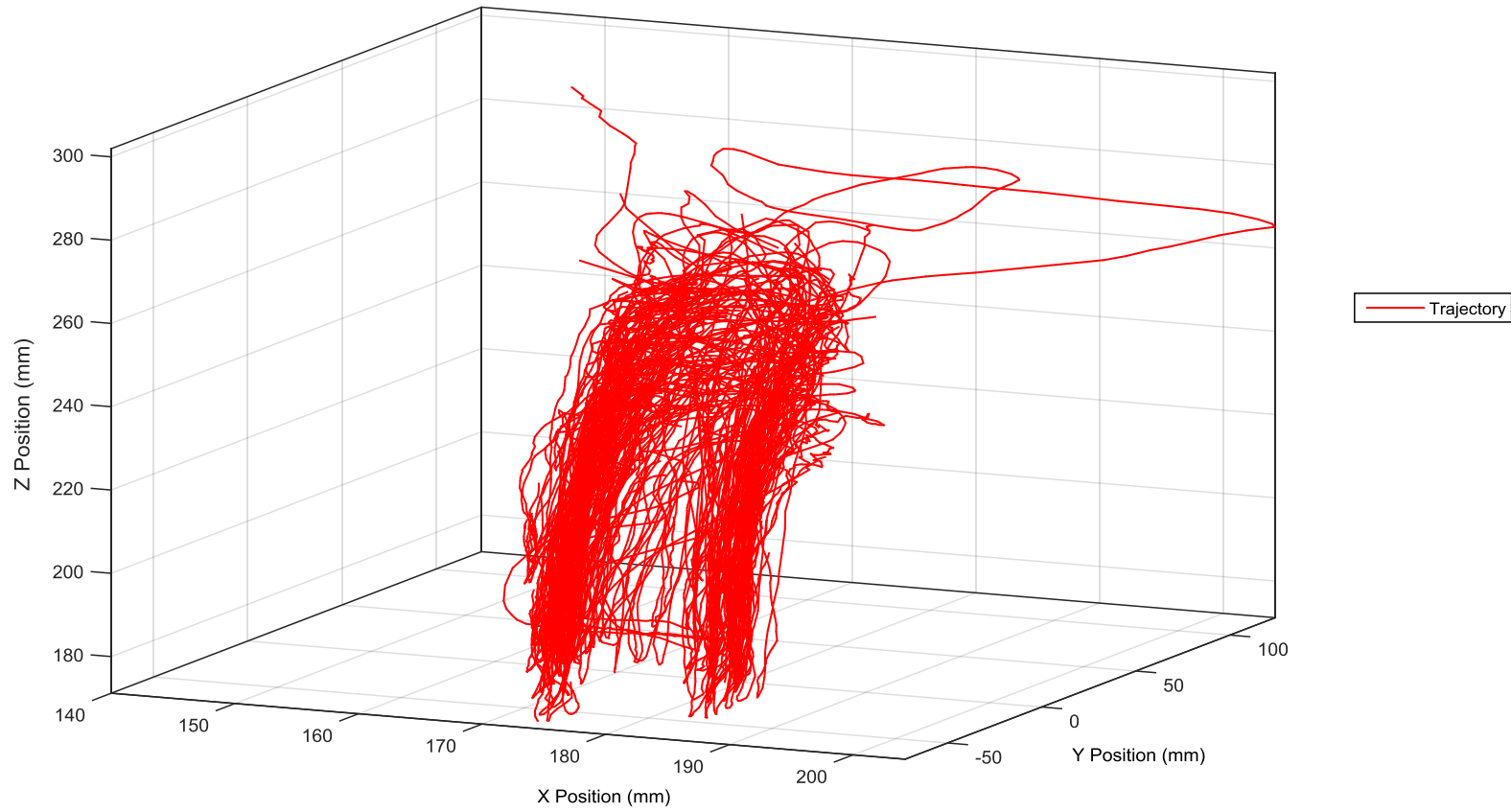**Experiment 1 – 3D Path**
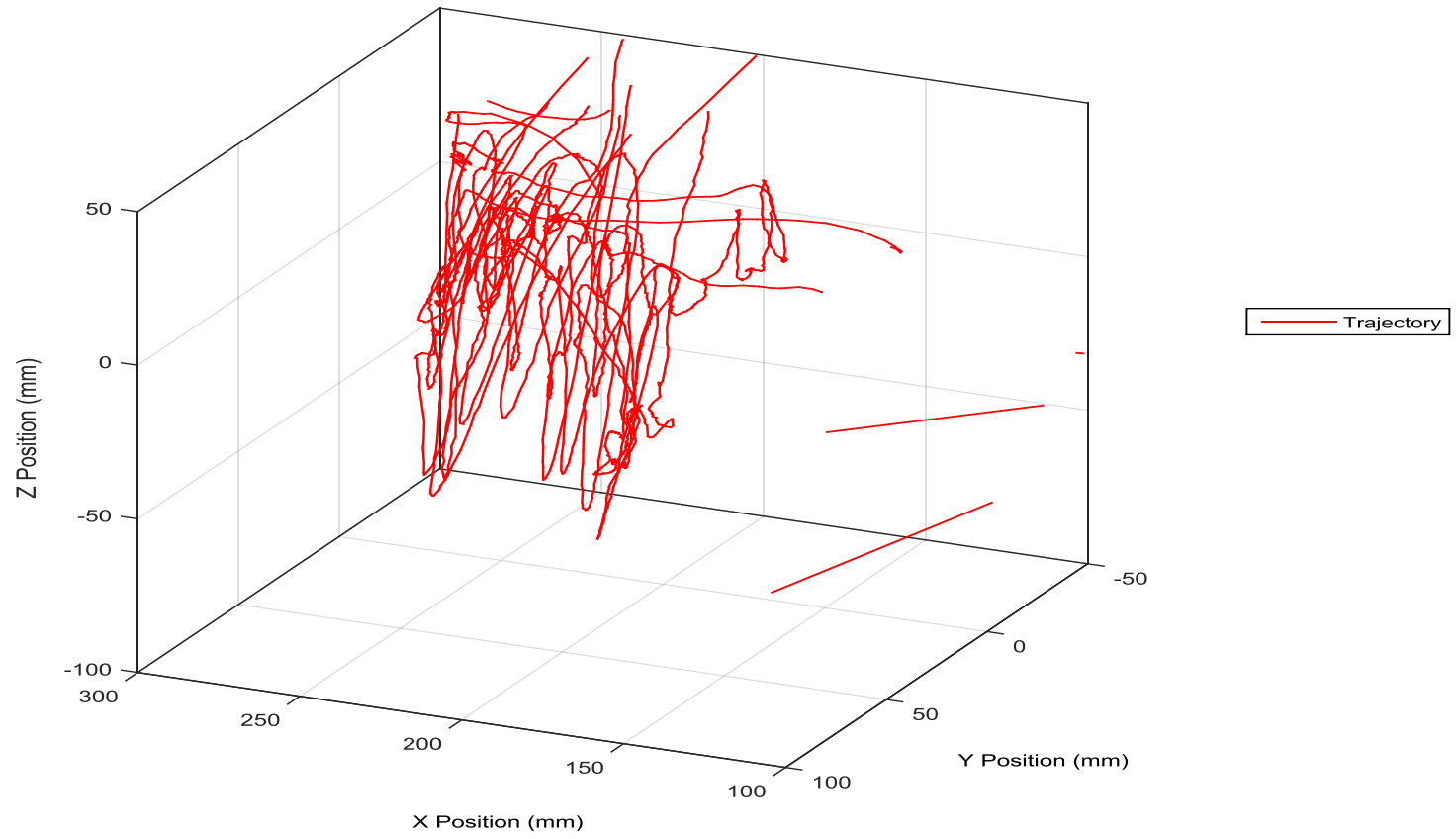
Figure D.6: Operator trajectory (Vicon) - Experiment 1: Removing a Thick Layer

Experiment 1 – 3D Pattern
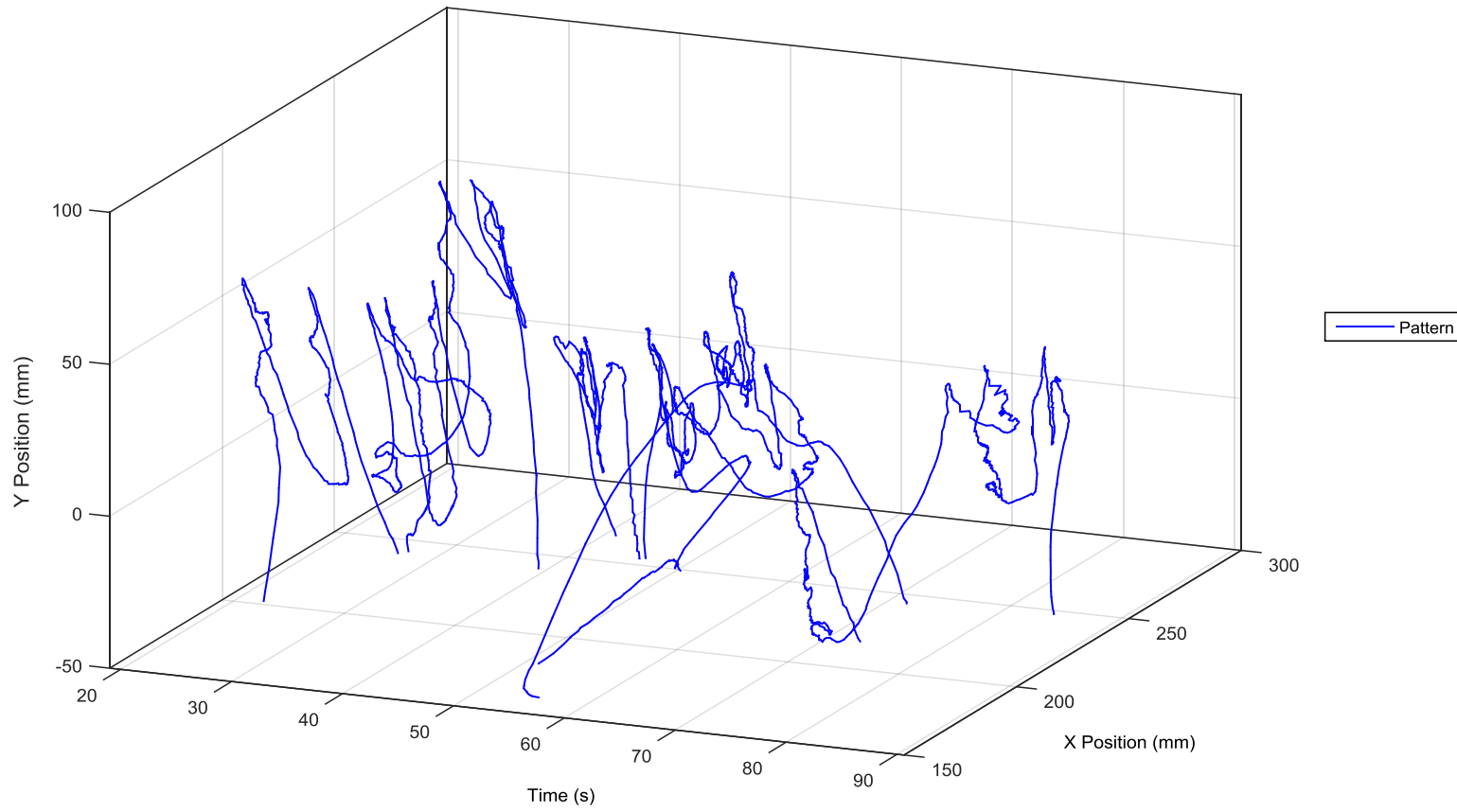
Figure D.7: Operator pattern (Vicon) - Experiment 1: Removing a Thick Layer

Appendix E. Experiment 2: Removing Machining Marks

The following appendix presents the detail data captured by the fixture for experiment 2 (see Section 6.3). Figures E.1 to E.3 illustrate the data captured with the inertial measurement unit, showing the acceleration, gyroscope, and Euler-orientation respectively. Figure E.4 illustrates the forces and torques captured with the multi-axial force and torque sensor. Figures E.5 to E.7 illustrate the data captured by the Vicon MoCap system including the position and orientation, 3D path, and 3D pattern of the operator.

Figure E.1: Acceleration data (Xsens MTw) - Experiment 2: Remove Grinding Marks
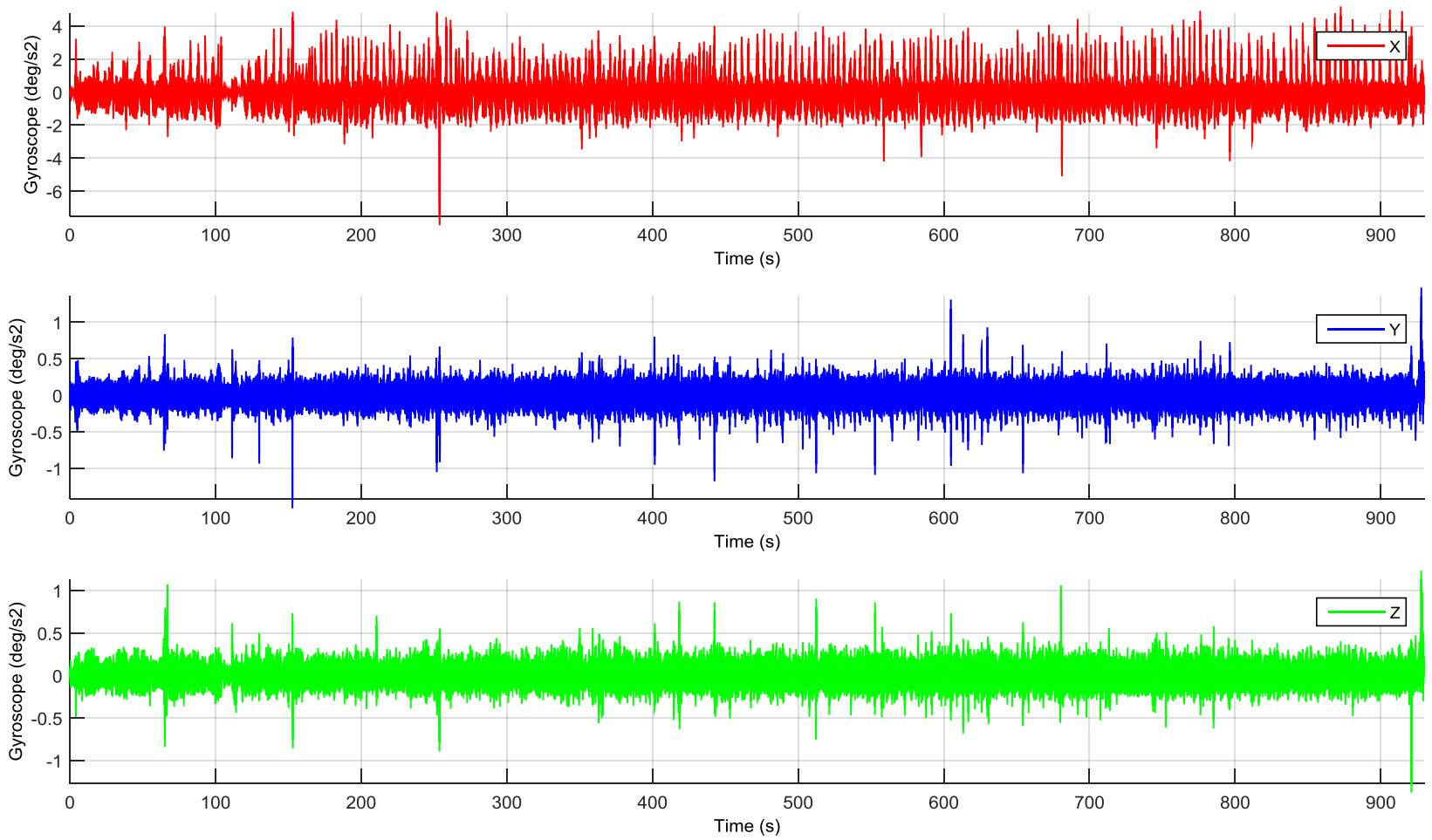
Figure E.2: Gyroscopic data (Xsens MTw) - Experiment 2: Remove Grinding Marks

Experiment 2 – Euler-angle orientation
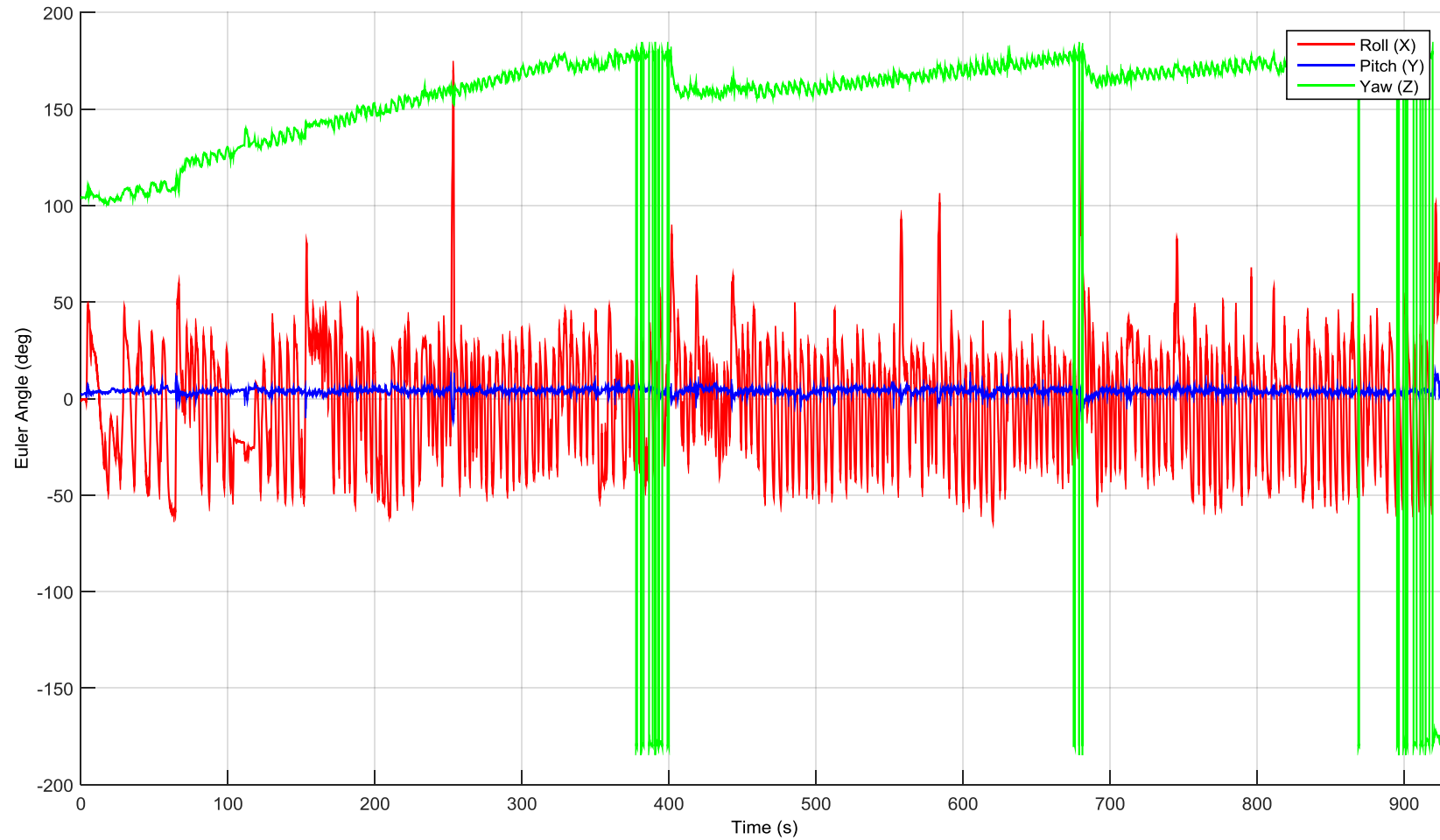
Figure E.3: Euler orientation data (Xsens MTw) - Experiment 2: Remove Grinding Marks

Experiment 2 – Forces and torques
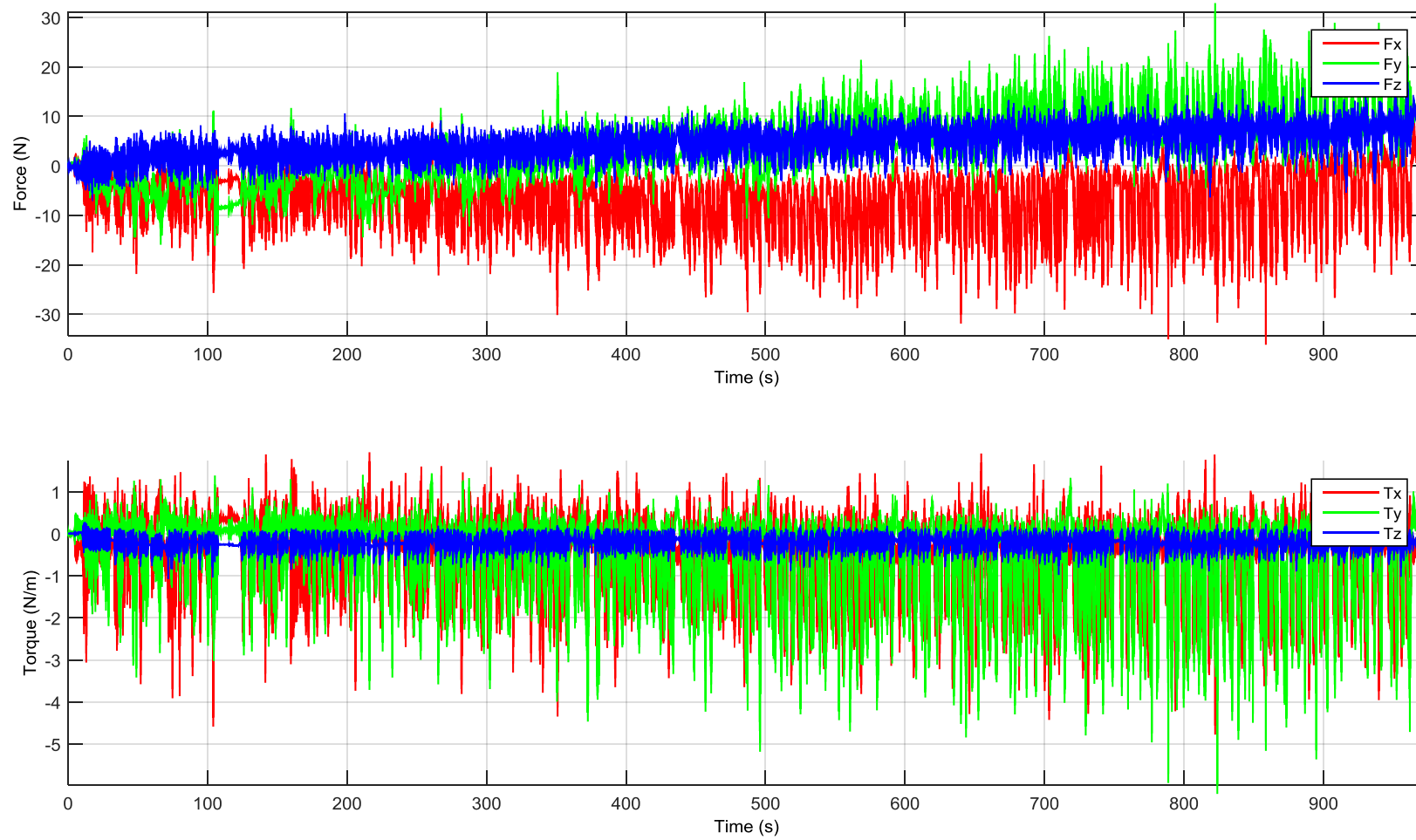
Figure E.4: Force and torque data (Shunk Gamma) - Experiment 2: Remove Grinding Marks

Experiment 2 – Positions and orientations (2D)
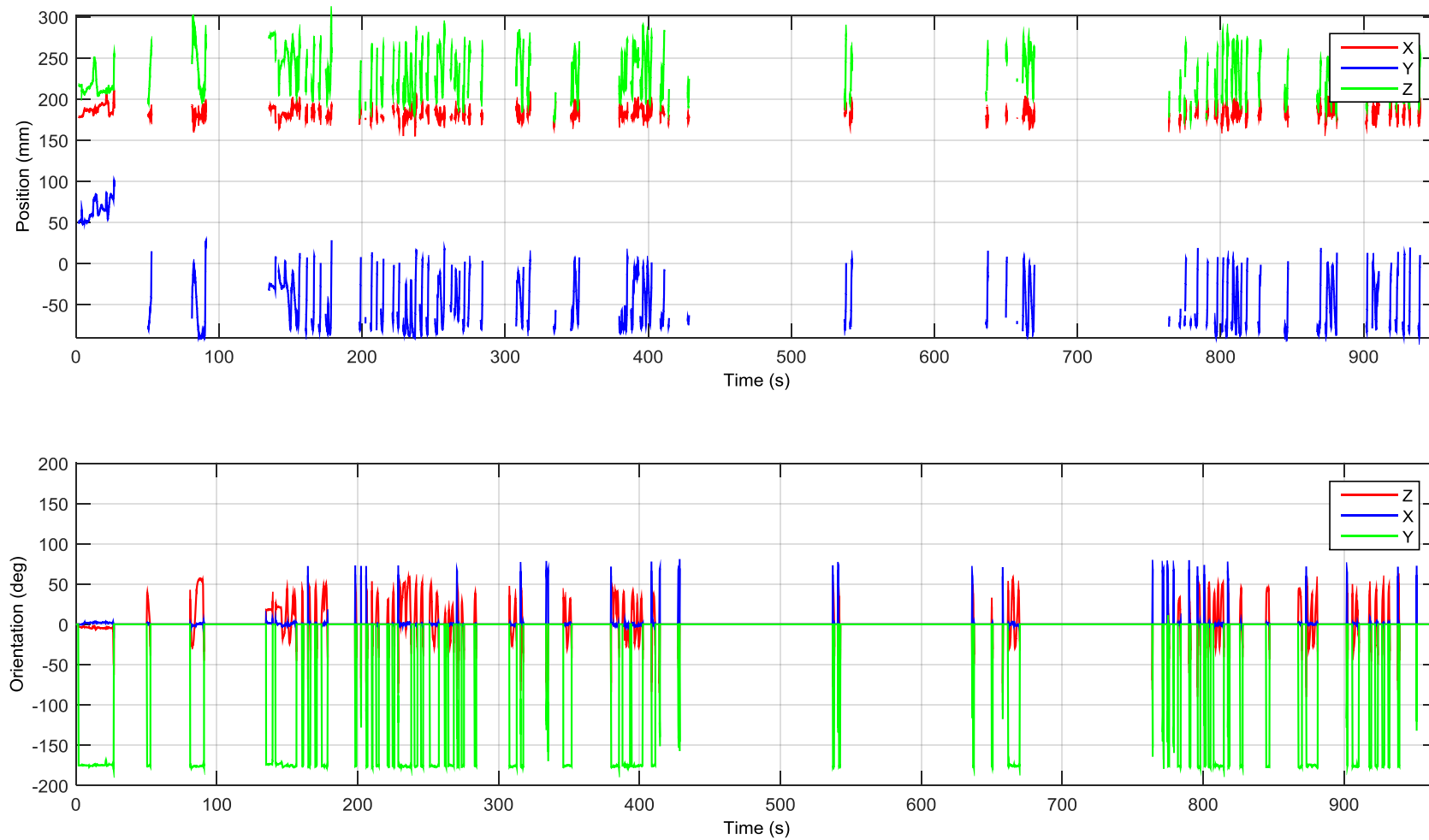
Figure E.5: Position and orientation data (Vicon) - Experiment 2: Remove Grinding Marks

Experiment 2 – 3D Path
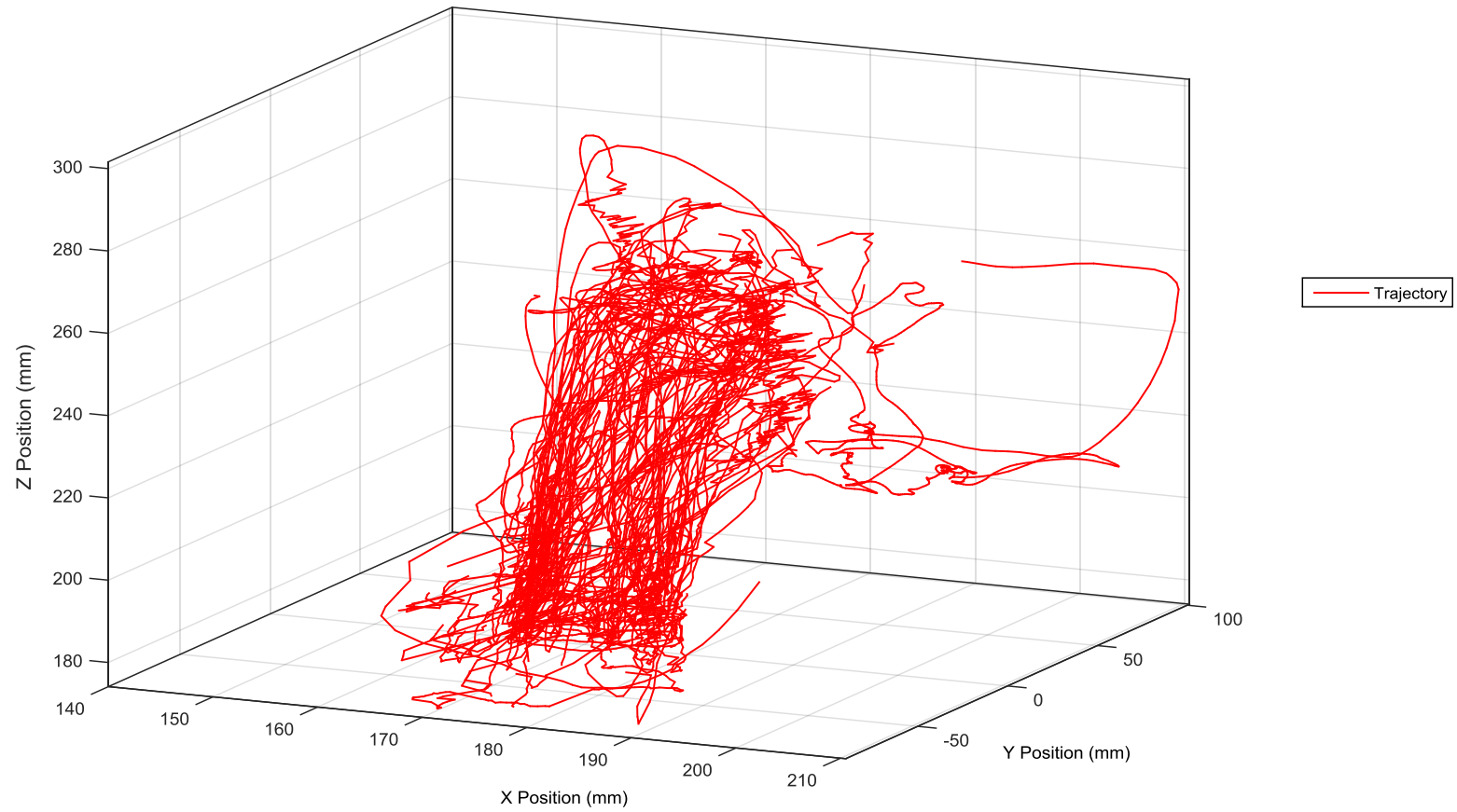
Figure E.6: Operator trajectory data (Vicon) - Experiment 2: Remove Grinding Marks

Experiment 2 – 3D Pattern
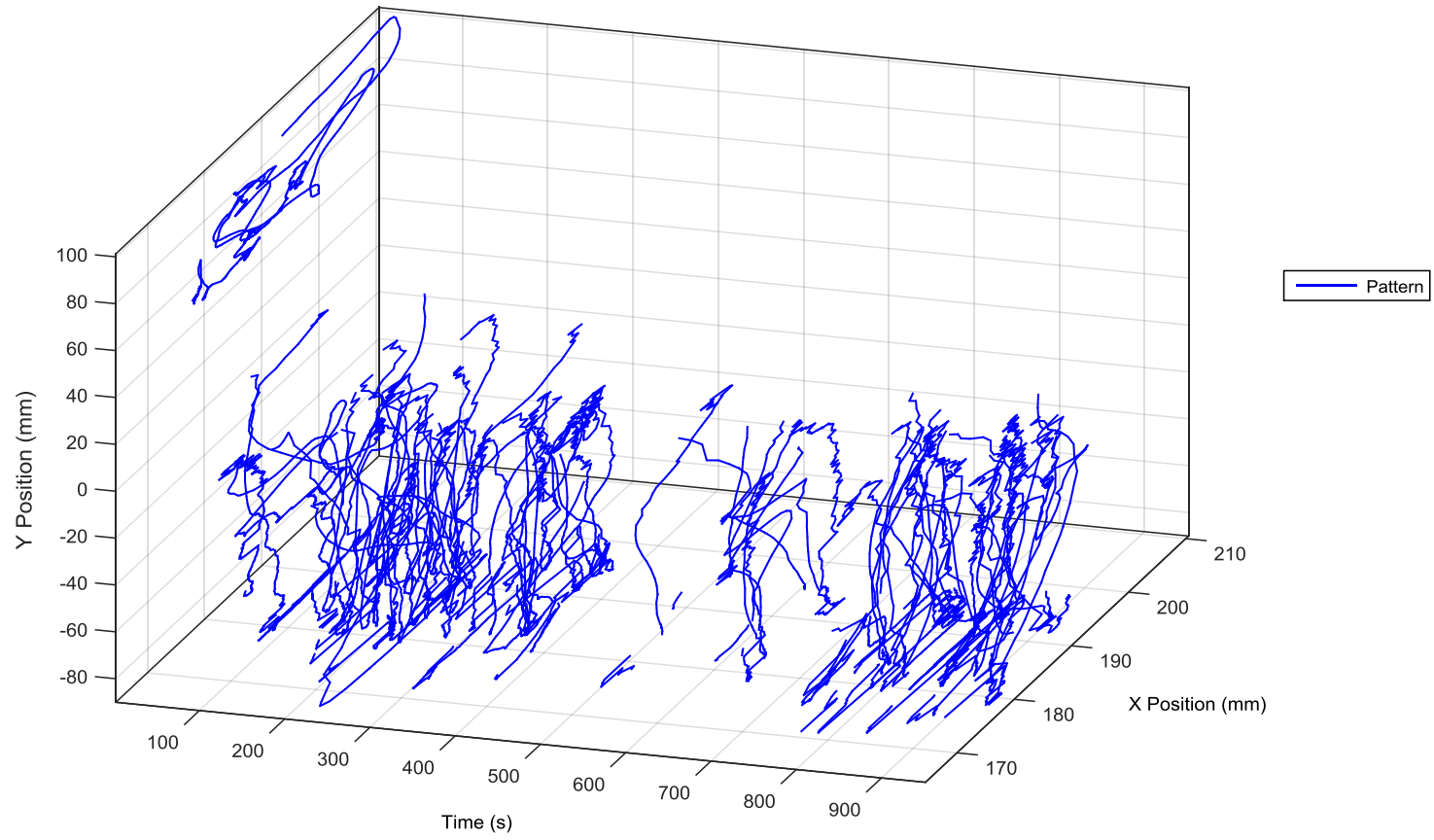
Figure E.7: Operator pattern data (Vicon) - Experiment 2: Remove Grinding Marks

Appendix F. Experiment 3: Removing Defects

The following appendix presents the detail data captured by the fixture for Experiment 3 (see Section 6.4). Figures F.1 to F.3 illustrate the data captured with the inertial measurement unit, showing the acceleration, gyroscope, and Euler-orientation respectively. Figure F.4 illustrates the forces and torques captured with the multi-axial force and torque sensor. Figures F.5 to F.7 illustrate the data captured by the Vicon MoCap system including the position and orientation, 3D path, and 3D pattern of the operator.

Figure F.1: Acceleration data (Xsens MTw) - Experiment 3: Removing Defects

Figure F.2: Gyroscopic data (Xsens MTw) - Experiment 3: Removing Defects

Experiment 3 – Euler-angle orientation
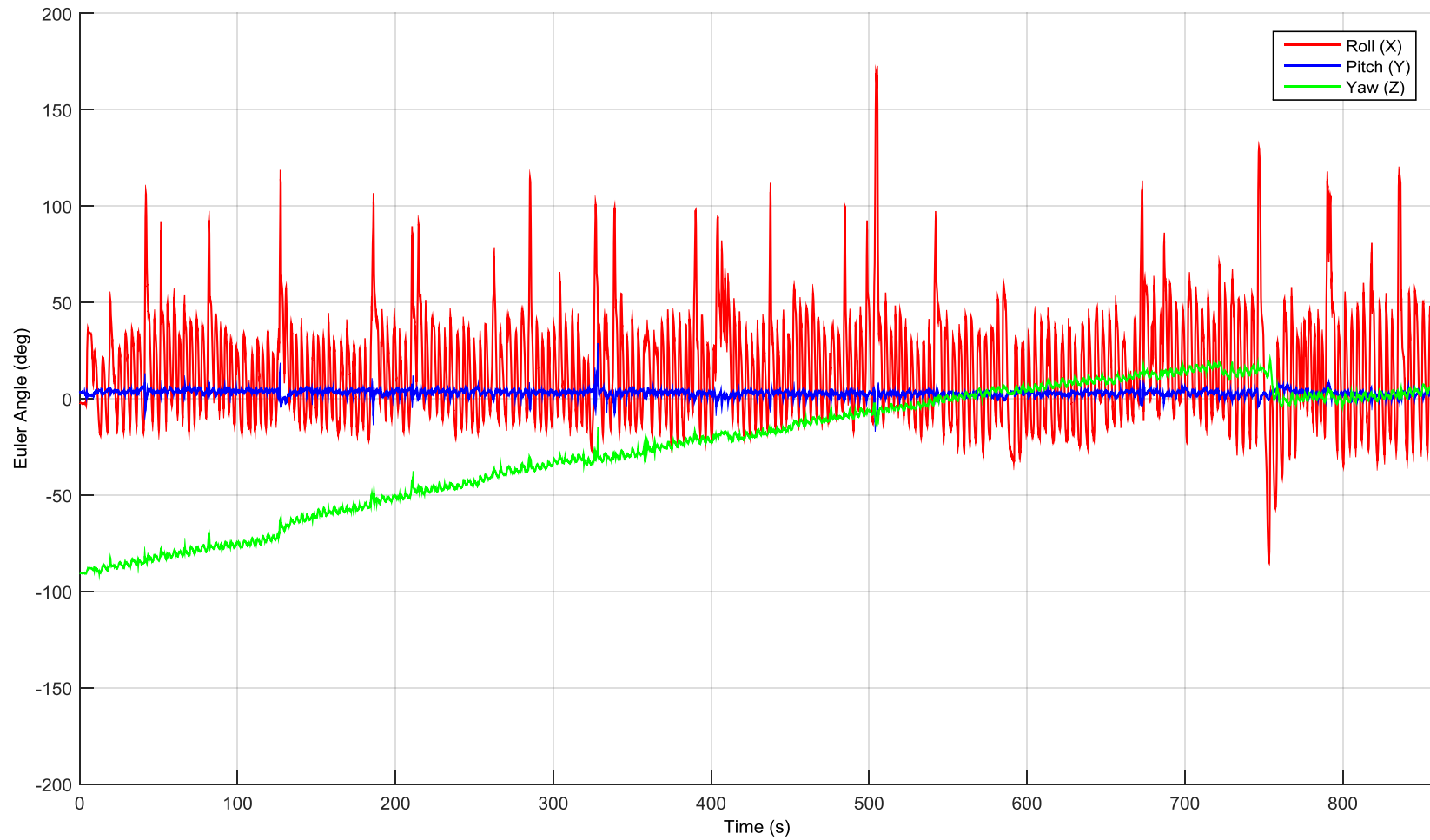
Figure F.3: Euler orientation data (Xsens MTw) - Experiment 3: Removing Defects

Experiment 3 – Forces and torques

Figure F.4: Force and torque data (Shunk Gamma) - Experiment 3: Removing Defects

Experiment 3 – Positions and orientations (2D)
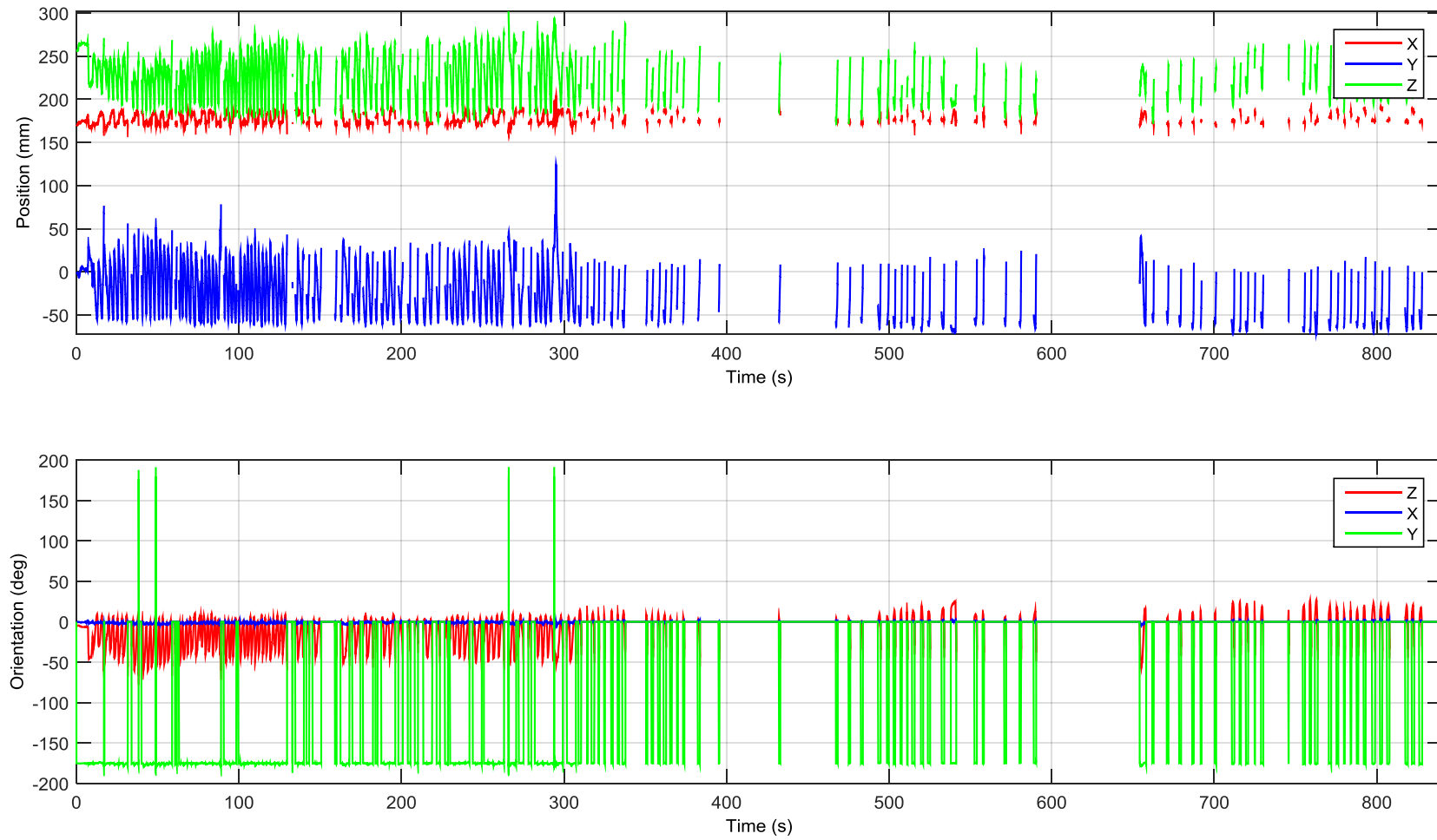
Figure F.5: Position and orientation data (Vicon) - Experiment 3: Removing Defects

Experiment 3 – 3D Path

Figure F.6: Operator trajectory data (Vicon) - Experiment 3: Removing Defects

Experiment 3 – 3D Pattern
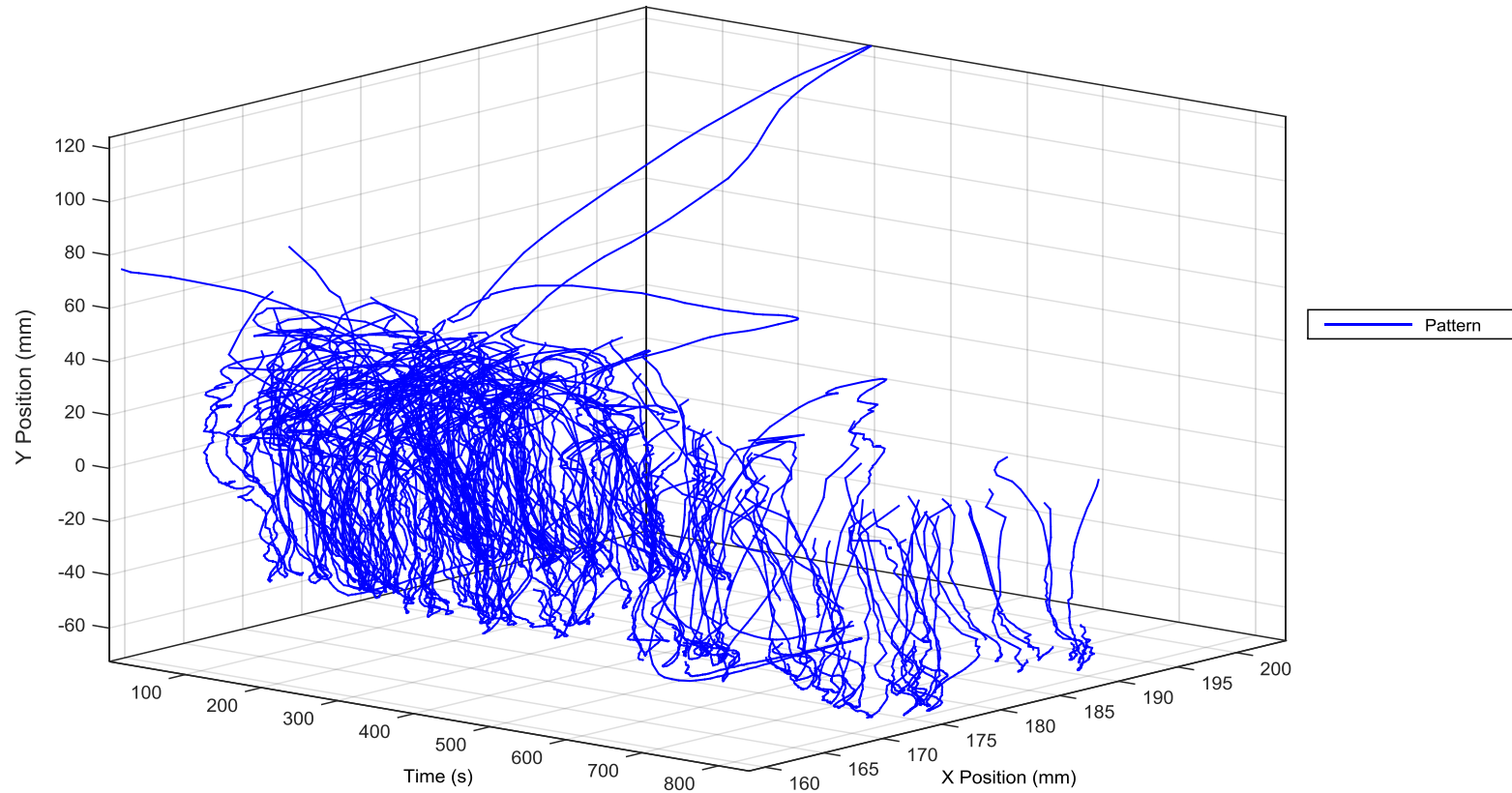
Figure F.7: Operator pattern data (Vicon) - Experiment 3: Removing Defects

Appendix G.Sensor Performance

The following appendix focuses on the performance of the sensors during the experiments. As in section 5.6, the fixture and the sensors performed well when capturing manual polishing parameters and variables. The following appendix is analysing some of the data collected and assess the performance of each sensor for each experiment.

G.1   Multi-Axial Force and Torque Sensor

The multi-axial force and torque sensor measured the force and torque involved during the operation. However, the data output of the sensor also included inertia and gravity effect due to the mass of the fixture and movement of the operator (avg. 5-10N in each axis), as describe in Section 5.6.

The sensor also provided with the timing of the operator actions (i.e. frequency and speed). It was possible to identify when the part was in contact with the abrasive belt and the duration of each polishing actions, as seen in Figure G.1. First data analysis is showing that each operator carried out a pass every 5 seconds. Further details on the frequency analysis is described in Appendix I.

Frequency of Polishing Actions
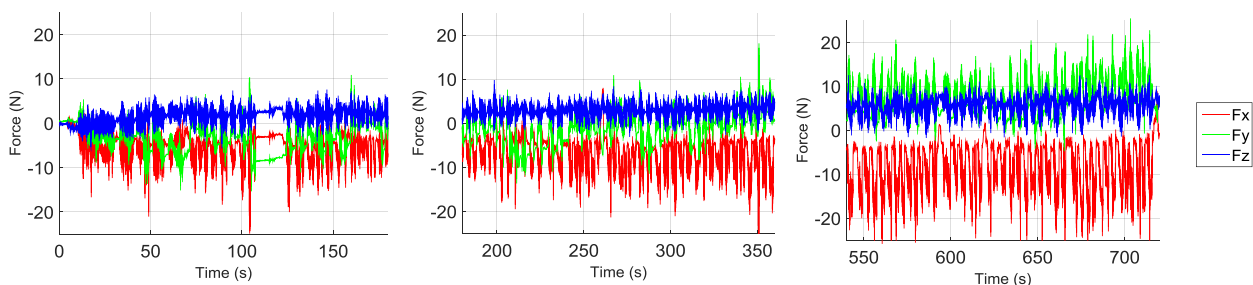
Figure G.1: Change of frequency of the force and torque indicating a change of speed of each polishing action

The polishing force captured mainly involved around *x-y axis* (*z-axis* vibration at each polishing action), as shown in Figure G.2. The overall force applied by both operators was around 10-20N, including inertia and gravity effect output. Further investigation towards gravity compensation should be carried out to compute the range of force used by the operators, and to calibrate the multi-axial force and torque sensor for the robotic system (as described in Section 7.4).
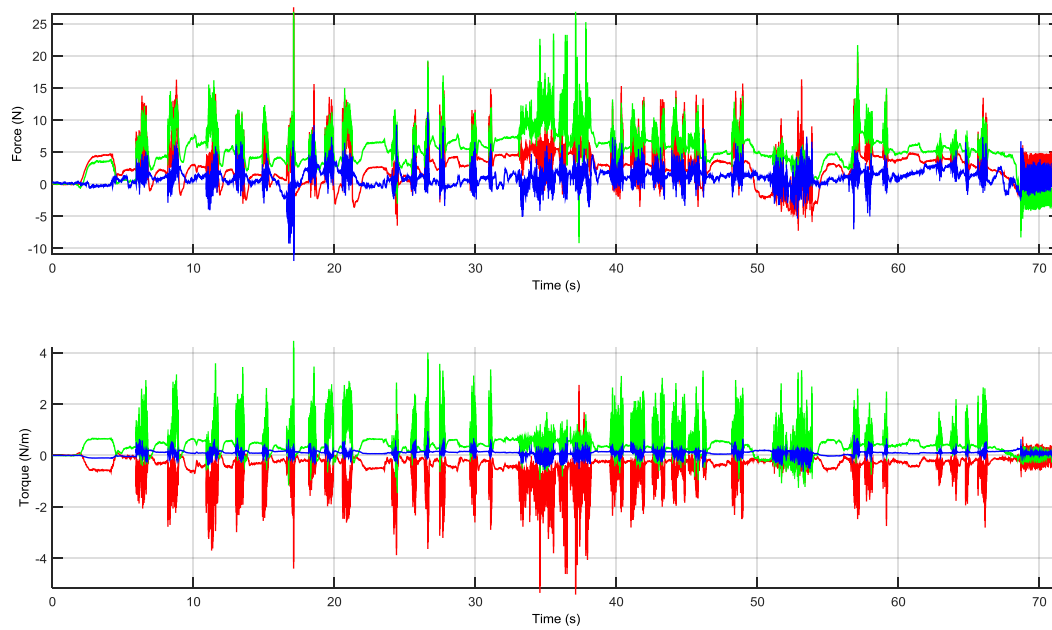
Figure G.2: Forces and torques captured in Section 6.2. Output include operator force, mass of the fixture, and inertia

G.2   Inertial Measurement Unit

As in the calibration experiment (section 5.6), the initial measurement unit was able to capture acceleration, gyroscope, magnetic earth, and Euler-angle orientation in 3-axies. The accelerometer provided with the speed, the direction and pattern of the movement, and the vibration generated at each polishing action.

As with the multi-axial force and torque sensor, each polishing action used by the operator (every time that the part was in contact with the belt), was identified by the inertial measurement unit as illustrated in Figure G.3. In Section 6.3 and 6.4, it was noticed that the operator was applying a longer contact at the start of the operation (see amplitude and length of contact) and then speed up the pace. This method allows the operator to remove most of the defects at the start of the operation and then improve the surface quality, where required without over-or-under polish the surface.
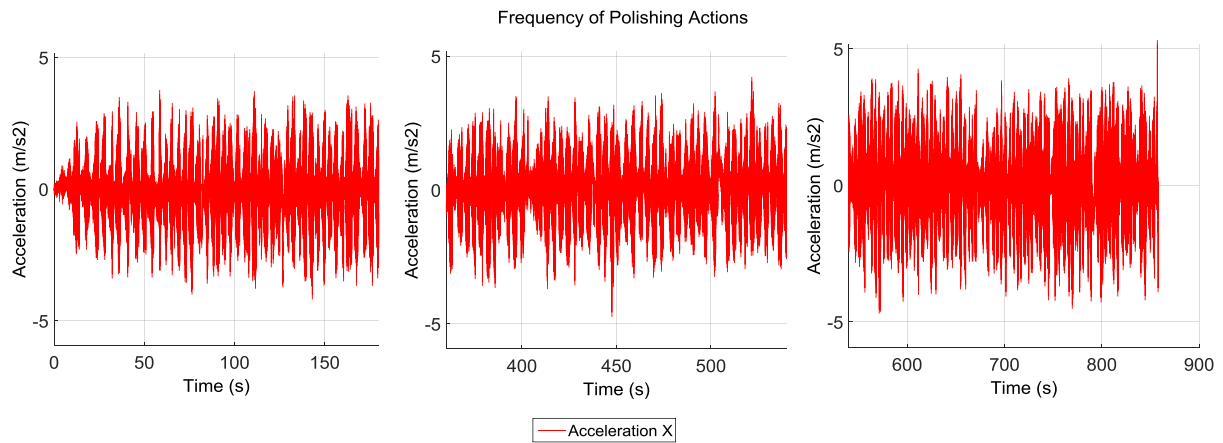
Figure G.3: Increase of the operator speed for each polishing action

The gyroscope indicates the change of orientation of the part when the operators carried out the polishing activity. The pattern in the change of the fixture orientation (Roll) showed that the operators followed the geometry of the surface while keeping a perpendicular contact to the abrasive belt (Pitch). Moreover, the data showed when the operators inspected the surface (Roll > 50 deg.). As this was not captured by the Vicon MoCap as the fixture was out of the field of view.

G.3 Vicon MoCap System

As in the calibration experiment (Section 5.5), the Vicon MoCap system captured the path followed by each operator. The data captured showed similarity with the surface geometry of the sample workpiece, which indicated that both operators mainly followed the profile of the surface.

However, due to the setup of the experiment and the complexity of movement captured, the Vicon MoCap system was not able to perform as well as expected (resulting in some plot holes). As explained early, the orientation data captured with the IMU can be used to complete the analysis of the operator movement.

For example, when the operators were inspecting the surface of the workpiece the markers on the fixture were outside of the field of view of the Vicon MoCap cameras but the fixture orientation was still recorded by the IMU.
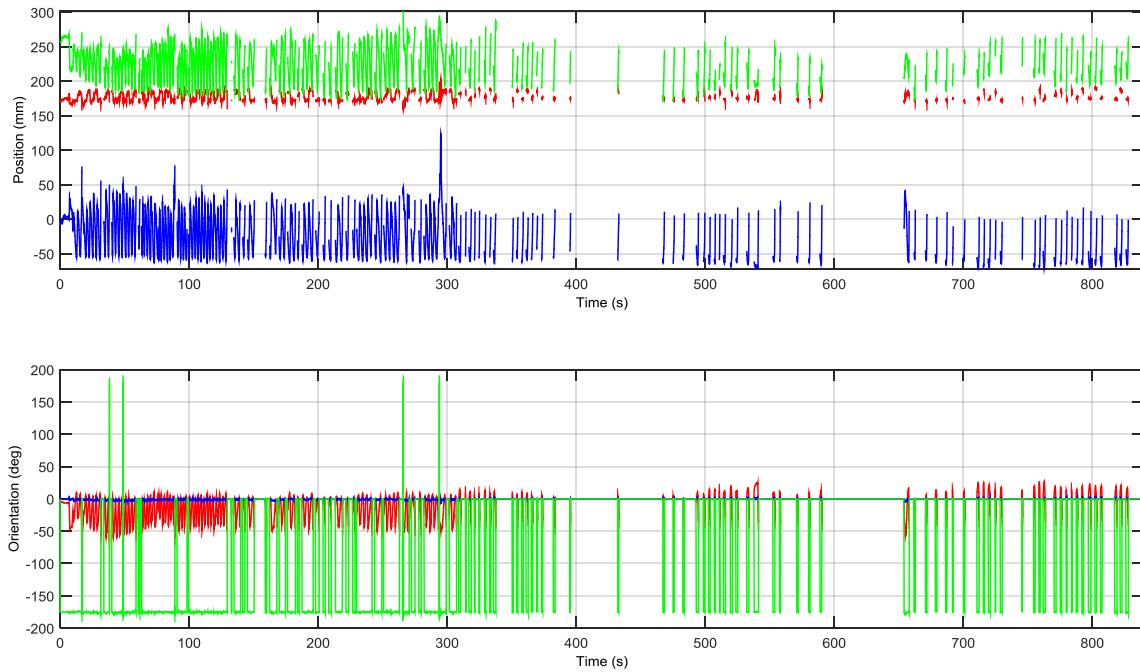
Figure G.4: Data from Vicon MoCap system with plot holes

However, the plot holes observed in Figure G.4 did not affect the analysis. For example, in Figure G.5 (representing a segment of the path and pattern captured in experiment 2), it is clearly showed that the profile of the surface (Pattern C) and trailing edge (Pattern B) was followed by the skilled operator during the experiment, and that until the surface quality was satisfactory.
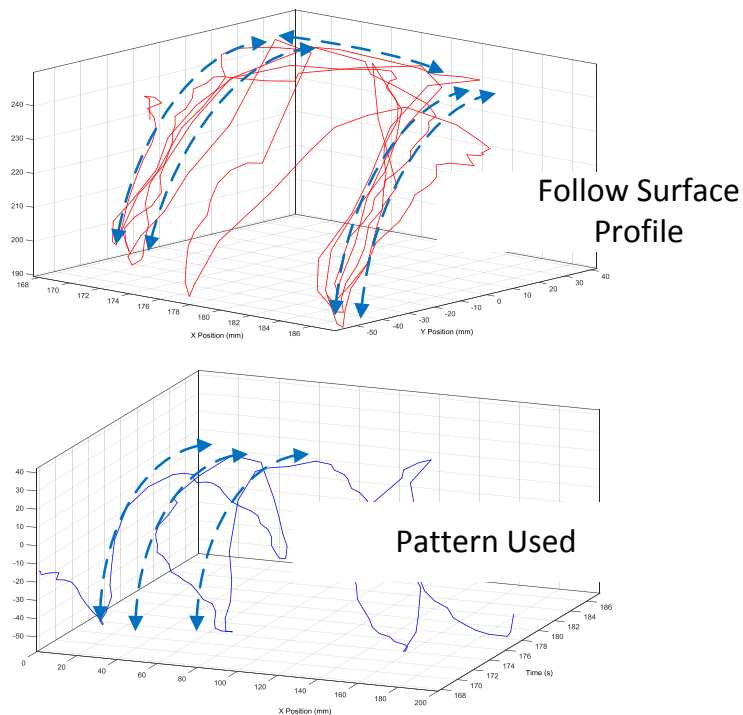

Figure G.5: Section diagram of the operator pattern and 3D trajectory

Appendix H. Material Removal Rate

In addition to the data captured with the fixture, the profile of the polished surface was measured. The measurement of the surface profile was carried out using a laboratory custom build blue laser scanner. The point cloud of data collected may help to determine the material removal rate (MRR) of the operators. Figure H.1 shows the surface aspect of the sample workpiece before and after experiment 2 (see Section 6.3).

Surface texture before removing grinding marks

Location of the defects to be removed

Surface texture before removing grinding marks under blue light

Depth of Material Removed

Marks left after polishing operation

Surface texture after removing grinding marks
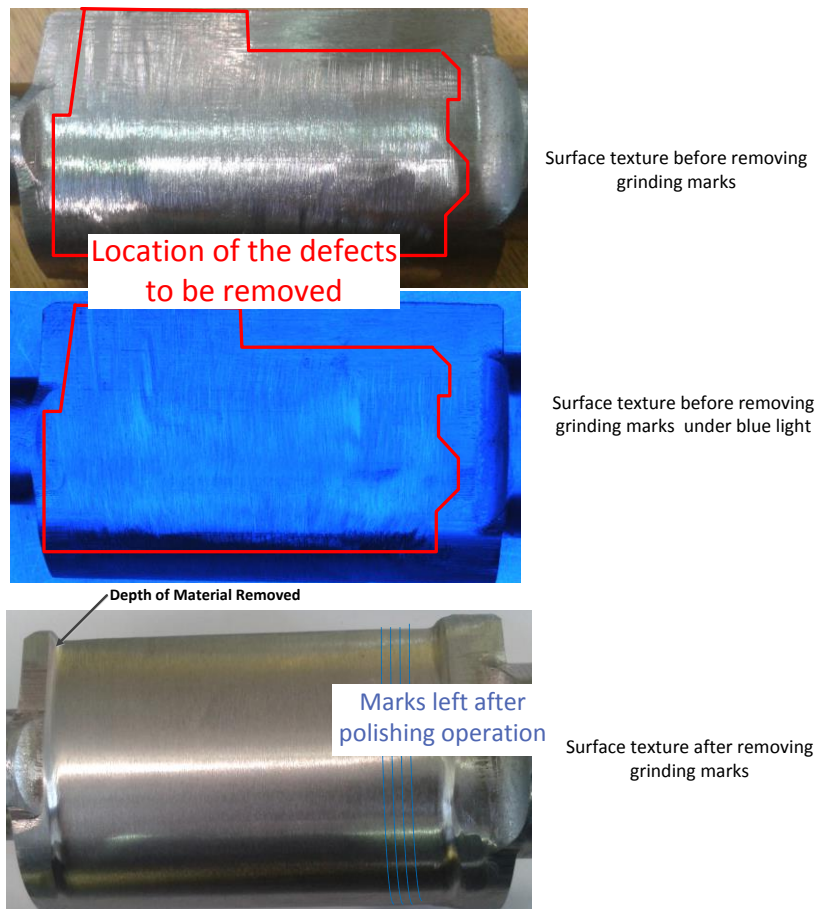
Figure H.1: Surface texture before and after polishing

The 3D point cloud of the surface measured (see Figure H.2) with the blue laser scanner shows the layer of material removed during the experiment. Using CAD software and some data processing to measure the volume of material removed by comparing the measured surface to the original CAD file.
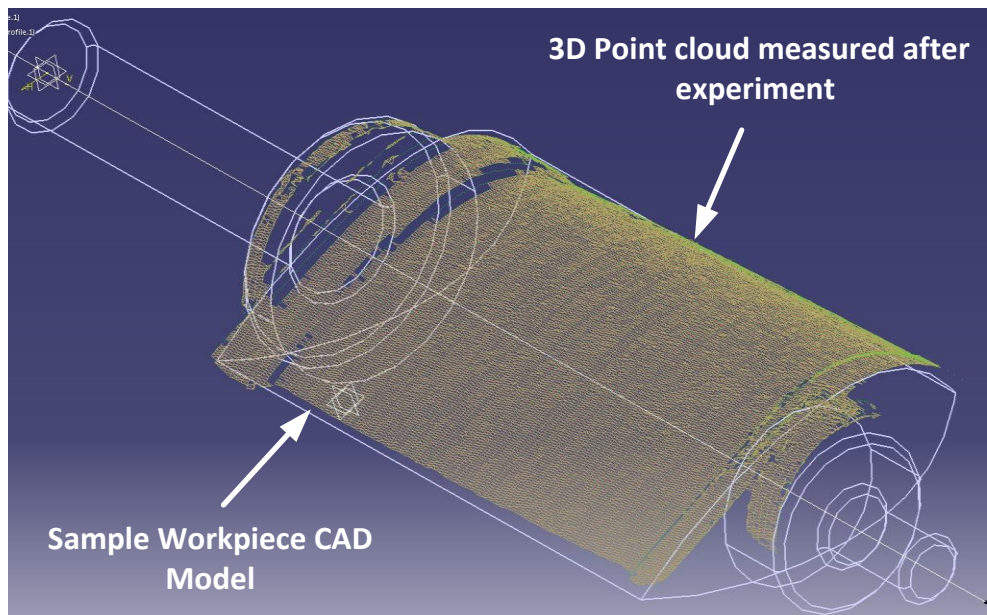
Figure H.2: 3D point cloud collected of the polished sample part using blue laser stripes
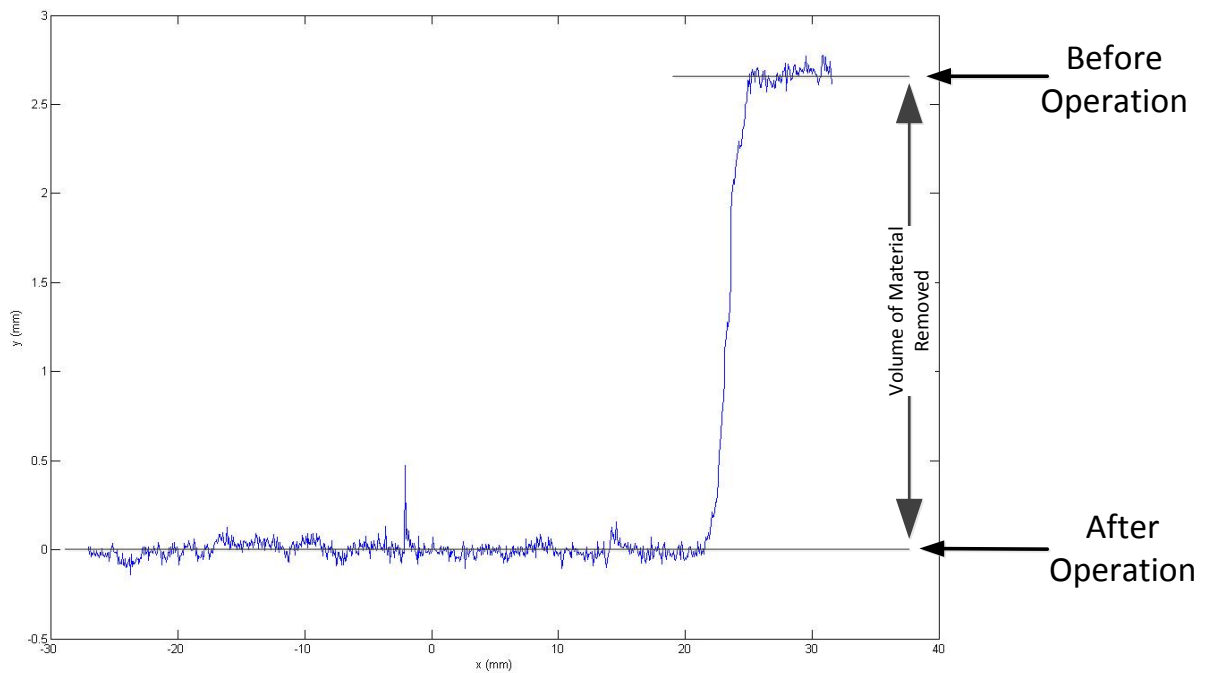
Figure H.3: Experiment 3 - Removing Defects - layer of material removed by the operator using the fixture

From the data showed in Figure H.3, it can be observed that the operator removed a significant layer of material (over 2.5 mm) on the whole surface during experiment 2. The operator was instructed to only remove the heavy grinding marks and to improve the surface roughness (Ra) until the quality of the surface was satisfactory.

Due to the operator's attention to detail, the polishing the sample workpiece took 15 min, including 2 minutes to remove the defect and 13 minutes to increase the surface quality. However, Operator 1 assured the author that in normal industrial environment, less time would have been spent per workpiece (e.g. 1 min), such as Operator 2. Therefore, less material would have been removed. Fortunately, this does not affect the understanding of manual polishing process carried out by Operator 1.

Appendix I. Frequency Analysis

This appendix focuses on the analysis frequency of polishing action carried out by the operators. To further the data analysis on the pattern used by the operators', a frequency analysis was carried out. Figure I.1 illustrates the forces and torques measured in section 6.3. As mentioned early, in addition to the force and torque output each polishing action can be observed with the multi-axial force and torque sensor. Therefore, the operator speed can be calculated.
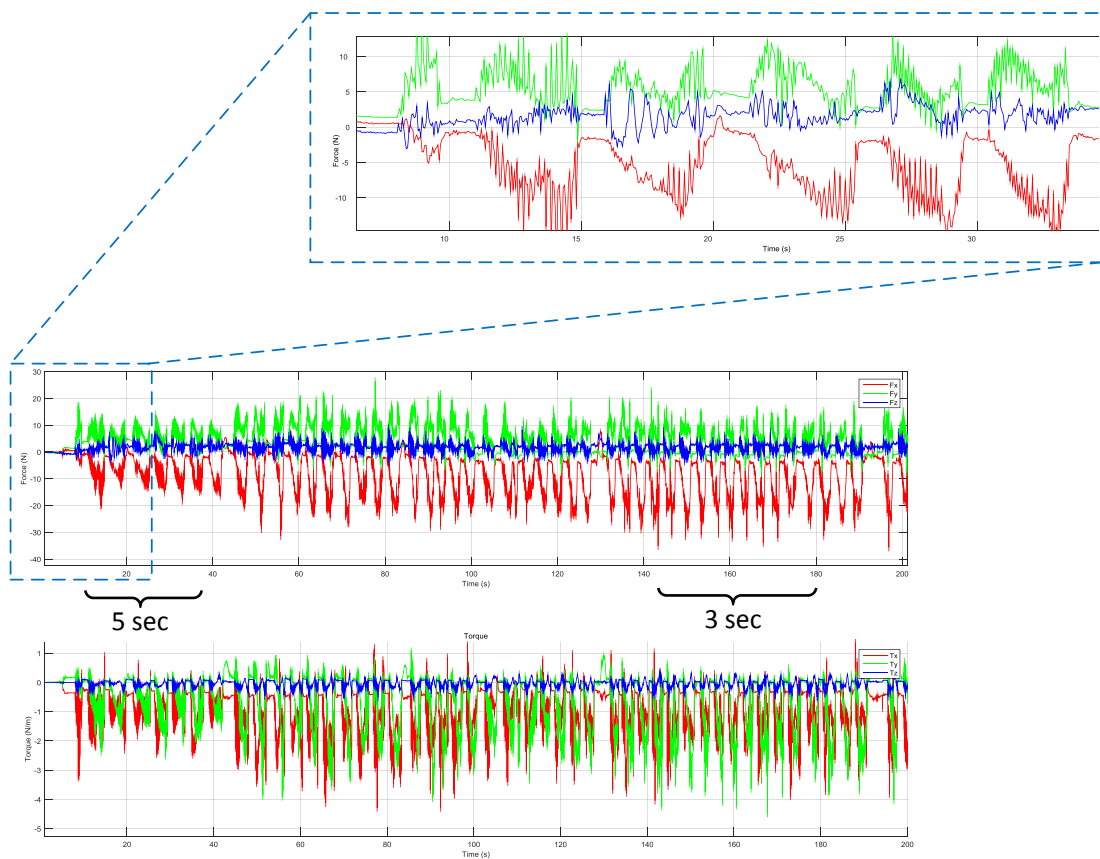
Figure I.1: Example of the frequency of the polishing action

In the example shown in Figure I.1, it can be observed that the operator completes a pass in 5 seconds at the start of the operation but then speed up to 3 seconds per pass at the end of the experiment. The Fast-Fournier Transformation (FFT) (Ninness, 2013) was used to calculate the frequency of the polishing action for each experiment. The FFT analysis is illustrated in Figures I.1 to I.3, representing each experiment carried out in Chapter 6. Moreover, equations I.1 and I.2 were used to calculate the operator speed.

Calculate period T (ms)

$$T = \frac{1}{f}$$

Eq.(I.1)

Calculate frequency f (Hz)

$$f = \frac{1}{T}$$

Eq.(I.2)

Table I.1: Frequency analysis – Operators' speed

Experiment	Frequency	Period (s)
1	0.024	4.1
2	0.020	4.8
3	0.029	3.4

From Table I.1, it can be observed that the operators are completing a pass every 4.1 seconds, 4.8 seconds, and 3.4 seconds for each experiment 1, 2, and 3, respectively.

Frequency Analysis – Experiment 6.1
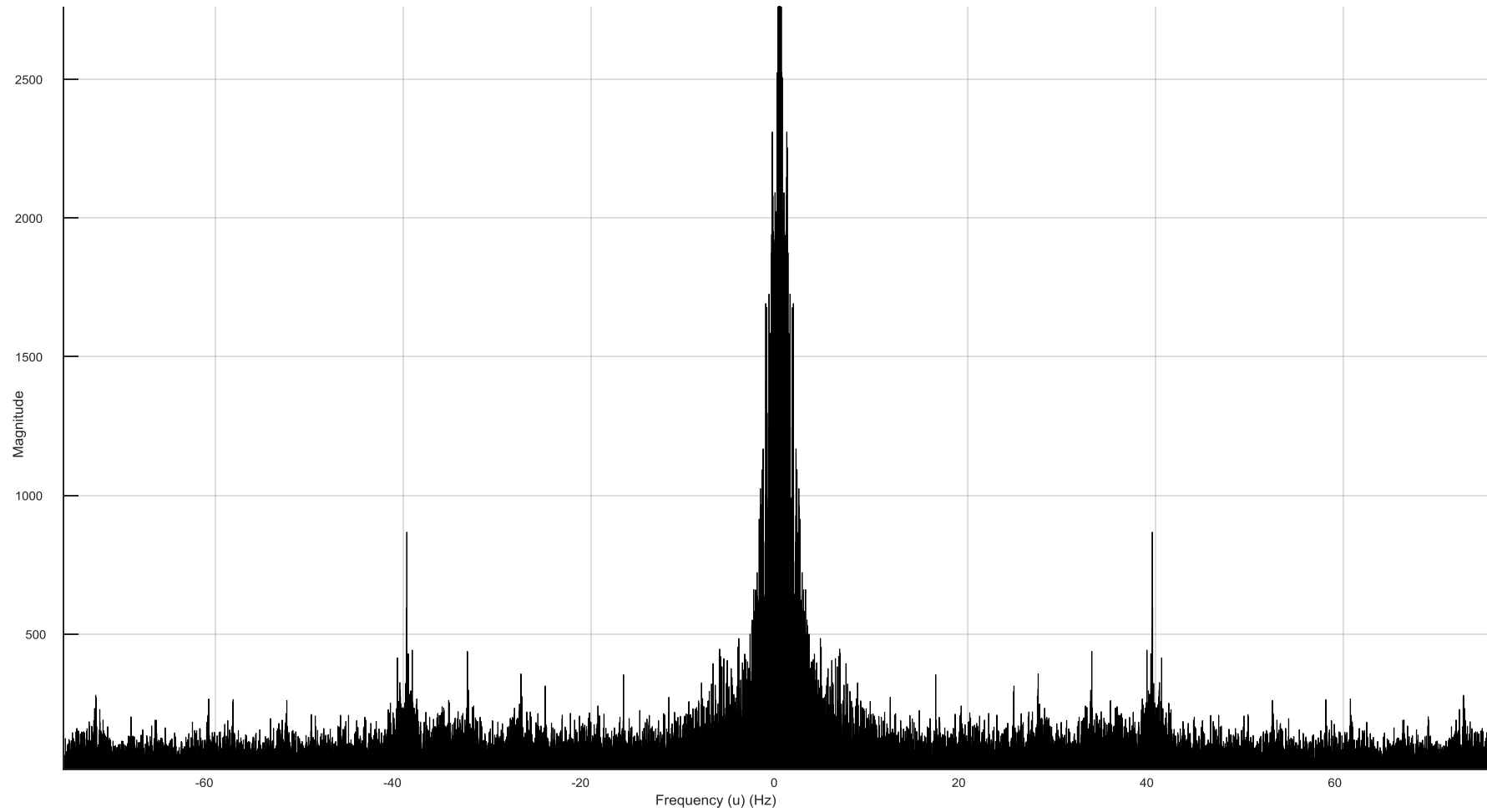
Figure I.2: Frequency analysis - Experiment 6.1

Figure I.3: Frequency analysis - Experiment 6.2

Frequency Analysis – Experiment 6.3
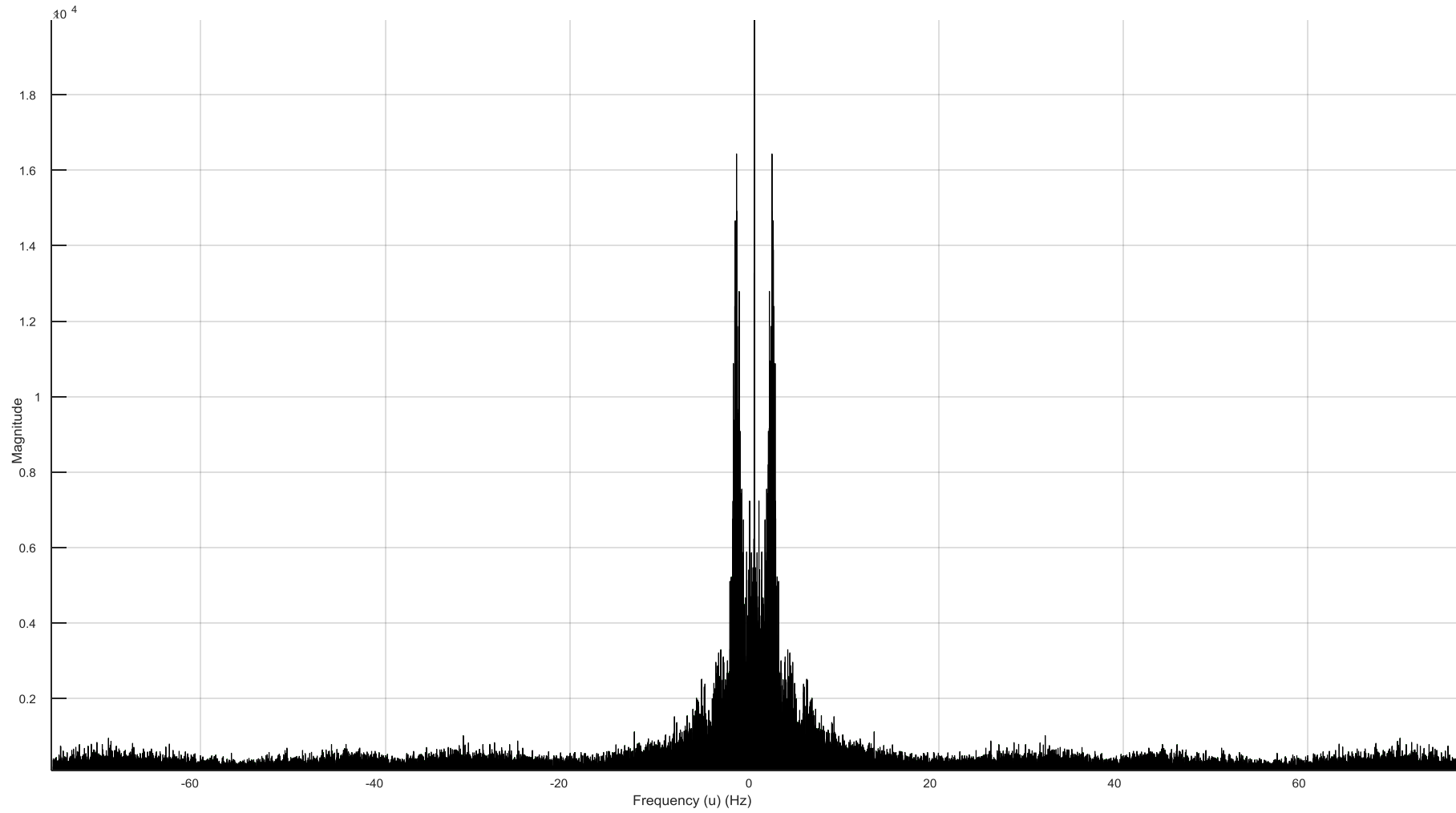
Figure I.4: Frequency analysis - Experiment 6.3

Appendix J. Multi-Axial Force and Torque Sensor Calibration

This appendix is focusing on the investigation and to better understand the gravity and inertia effect of the multi-axial force and torque sensor for robotic application.

The investigation presented in this section includes a study of the dynamic behaviour of the multi-axial force and torque sensor. As mentioned above, this would provide a better understanding of the relationship between inertia (acceleration and motion) and the force and torque output. In this study, data was collected using force and torque output relative to the inertia to develop an algorithm for gravity compensation.

As observed in Section 5.5, the multi-axial force and torque sensor output data in response to movement even without external force. This is caused by the inertia, gravity, and change of orientation of the sensor.

J.1   Force Gravity Compensation Investigation

The dynamic behaviour of force and torque sensors has rarely been investigated due to the complexity involved. In force control for robotic, the use of the Jacobian for the robot kinematic is necessary (Villani and Federico, 2007). Using the Jacobian to compute the dynamic behaviour of the force and torque sensor may be accurate but can be difficult. Researchers have explored different methods to do gravity compensation but there is still a need for further work.

From a control point of view, the use of the Jacobians' is necessary but simplified methods may be used. For example, some research demonstrates that the acceleration data can be used to compensate the dynamic behaviour of the force and torque sensor output during robot kinematic. L. Richer and R. Bruder (Richter and Bruder, 2013; Richter et al., 2012, 2010) developed a method based on acceleration and gravity to compensate force and torque error. In their research, the effect of the gravity is applied by the weight of the force and torque sensor and gripper attached at the end-effector.

In this section, a set of experiments were carried out where the sensors data (e.g. force, torque, acceleration, orientation) were captured during a known position (or kinematic) of the robot end-effector. Figure I.1 illustrates the variables and parameters at the initial position of the end-effector used in this study. Based on the methodology of Richter and Bruder (Richter and Bruder, 2013; Richter et al., 2012, 2010), the calibration of the multi-axial force and torque sensor was carried out.

In this study, the force of the gravity at the initial position was calculated based on the position of the fixture (see Sections I.1.1 and I.1.2). Then the transformations matrices for the end-effector and each joints axes were computed for the calculation to be with the same frame coordinate (see Section I.1.3). Finally, the force (and torque) due to inertia and gravity at different position for the end-effector can be calculated and removed from the multi-axial force and torque output (see Section I.1.4).
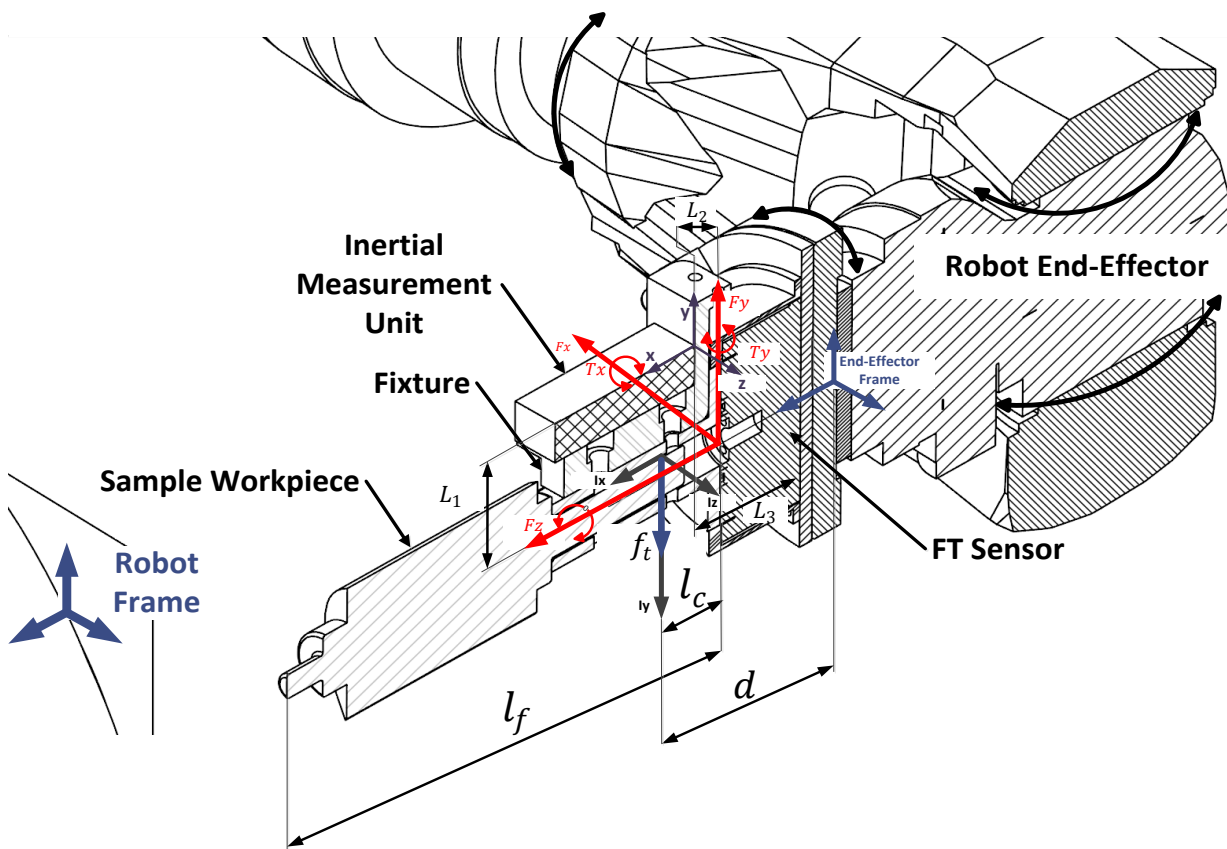
Figure J.1: Force gravity investigation

J.1.1 Calculate the Force Load at the Centroid of the Fixture

J.1.1 *Newton's Law*

$$\vec{F} = m \times g = 0.7 \times 9.81 = 6.867\ N$$

Eq.(J.1)

J.1.1.a *Torque/Moment Equation*

$$\vec{M} = F \times l$$

Eq.(J.2)

J.1.1.b *Calculate the Torque or Moment for the fixture attached on the FTC*

$$M_f = F \times l_f = 6.867 \times 0.185 = 1.27\ Nm$$

Eq.(J.3)

J.1.1.c Calculate the Force Load of the Tool at the Centroid of the Fixture, using Moment

$$f_t = \frac{M_f}{l_c} = \frac{1.27}{0.053} = 23.96 \, N \qquad \text{Eq.(J.4)}$$

J.1.2 Determine Forces Output at Initial Position

J.1.2.a Force at Initial Orientation with the Weight of the Object

$$F_0 = \begin{pmatrix} F_x^0 \\ F_y^0 \\ F_z^0 \end{pmatrix} = \begin{pmatrix} 0 \\ 0 \\ -f_t \end{pmatrix} \qquad \text{Eq.(J.5)}$$

In this case, the initial load before calibration is equal to *-f*, as the orientation of the end-effector points down along the Z-axis.

J.1.3 Compute Transformation Matrices for Robot Orientation and Tool/End-effector

J.1.3.a Transformation Matrix form Tool/End-effector

$$^E\zeta_{FT} = \begin{bmatrix} 1 & 0 & 0 & 0 \\ 0 & 1 & 0 & 0 \\ 0 & 0 & 1 & d \\ 0 & 0 & 0 & 1 \end{bmatrix} = \begin{bmatrix} 1 & 0 & 0 & 0 \\ 0 & 1 & 0 & 0 \\ 0 & 0 & 1 & .073 \\ 0 & 0 & 0 & 1 \end{bmatrix} \qquad \text{Eq.(J.6)}$$

Where d is the distance (*m*) between centroid of the tool (*Ix, Iy, Iz*) and end effector for KUKA KR16 6 DoF.

J.1.3.b Transformation Matrix for Robot

$$^R\zeta_E = {}^R\zeta_{A1.A2.A3} \cdot {}^R\zeta_{A4.A5.A6} \qquad \text{Eq.(J.7)}$$

Where A1 to A6 are the joints axes of the robot.

J.1.3.c Transformation Matrix for Joint Axes A1 to A3

$$^R\zeta_{A1.A2.A3}$$
$$= \begin{bmatrix} cos\theta_1 cos\theta_2 cos\theta_3 - cos\theta_1 sin\theta_2 sin\theta_3 & sin\theta_1 & cos\theta_1 cos\theta_2 sin\theta_3 & .15cos\theta_1 cos\theta_2 cos\theta_3 + .65cos\theta_1 cos\theta_2 + .3cos\theta_2 \\ sin\theta_1 cos\theta_2 cos\theta_3 - sin\theta_1 sin\theta_2 sin\theta_3 & -sin\theta_1 sin\theta_2 & 0 & .65\, sin\theta_1 cos\theta_2 + .3sin\theta_2 \\ sin\theta_2 & cos\theta_2 & 0 & .65sin\theta_2 - .675 \\ 0 & 0 & 0 & 1 \end{bmatrix} \qquad \text{Eq.(J.8)}$$

J.1.3.d Transformation Matrix for Joints Axes A4 to A6

$$
{}^{R}\zeta_{A4.A5.A6}
$$

$$
= \begin{bmatrix} cos\theta_4 cos\theta_5 cos\theta_6 - sin\theta_4 sin\theta_5 & -cos\theta_4 cos\theta_5 sin\theta_6 - sin\theta_4 cos\theta_6 & cos\theta_4 sin\theta_5 & .14cos\theta_4 sin\theta_5 \\ sin\theta_4 cos\theta_5 cos\theta_6 + cos\theta_4 sin\theta_6 & -sin\theta_4 cos\theta_5 cos\theta_6 + cos\theta_4 cos\theta_6 & sin\theta_4 sin\theta_5 & .14 sin\theta_4 sin\theta_5 \\ -sin\theta_5 cos\theta_6 & sin\theta_5 sin\theta_6 & cos\theta_5 & .14cos\theta_5 \\ 0 & 0 & 0 & 1 \end{bmatrix}
$$

Eq.(J.9)

J.1.3.e Rotation Matrix between Multi-Axial Force and Torque Sensor and the Inertial Measurement Unit Coordinates

$$
{}^{FT}\zeta_{imu} = \begin{bmatrix} 1 & 0 & 0 & L_3 \\ 0 & 1 & 0 & L_1 \\ 0 & 0 & 1 & L_2 \\ 0 & 0 & 0 & 1 \end{bmatrix} = \begin{bmatrix} 1 & 0 & 0 & 0.011 \\ 0 & 1 & 0 & 0.0275 \\ 0 & 0 & 1 & 0.01725 \\ 0 & 0 & 0 & 1 \end{bmatrix}
$$

Eq.(J.10)

Where L_3, L_1, L_2 are the distances between (rotation matrix)

J.1.3.f Gross Knowledge of the Force and Torque Sensor and Orientation

$$
\begin{aligned}
\vec{e}FT_x &\approx -\vec{e}A_z \\
\vec{e}FT_y &\approx \vec{e}A_y \\
\vec{e}FT_z &\approx \vec{e}A_x
\end{aligned}
$$

Eq.(J.11)

J.1.4 Compute and Remove Forces Resulting from Gravity and Acceleration

J.1.4.a Force due to Gravity

$$
F_g = \left({}^{E}\zeta_{FT} \right)^{-1} . \left({}^{R}\zeta_{E} \right)^{-1} . F_0
$$

Eq.(J.12)

J.1.4.b Remove Gravity Effect from Output

$$
\overline{F} = F_n - F_g
$$

Eq.(J.13)

Where F_n is the force (x, y, z) output form the sensor, and F_g is the calculated force (x, y, z) due to the gravity and weight of the tool.

J.1.4.c Force Output Based on Acceleration

$$
A_{FT} = {}^{FT}\zeta_{imu} . A_{IMU}
$$

Eq.(J.14)

$$
F_A = A_{FT} . f
$$

Eq.(J.15)

Where A(imu) is the acceleration output (Acc x, Acc y, Acc z), A_{FT} is the combination of acceleration and force and torque, and F_A is the force/acceleration compensation.

J.2   Calibration Experiment

In addition to the calculations shown above, a set of test were carried out with the robotic. In this experiment the end-effector was moved to different positions and the force and torque was collected, as seen on Table I.1. Figures I.2 to I.5 illustrate the forces, torques, and accelerations captured at different orientations. In Figures I.6 and I.7 the forces and torques were plotted against the orientation of the end-effector. From these results, a clear evolution of the force and torque output can be noted when the robot end-effector move at different positions. Finally, these data can be used in the IRPS to remove any "false" readings from the multi-axial force and torque sensor to measure the polishing force.

Table J.1: Robot joints position

Robot Axis	Joint Axes (degree)						Force (N) and Torque (Nm) Output					
	A1	A2	A3	A4	A5	A6	Fx	Fy	Fz	Tx	Ty	Tz
Starting Position	0	-133.7	133.7	0	0	0						
Calibration Position	0	-133.7	133.7	**90**	0	0	0	0	0	0	0	0
A	0	-133.7	133.7	90	0	**-90**	**-5**	**10**	**0.1**	**-0.7**	**-0.3**	**0.05**
B	0	-133.7	133.7	90	0	**0**	0	0	0	0	0	0
C	0	-133.7	133.7	90	0	**90**	**11.4**	**4.5**	**0**	**-0.3**	**0.7**	**0.02**
D	0	-133.7	133.7	90	0	**-90**	**-4.8**	**10.69**	**0**	**-0.7**	**-0.3**	**0.05**
E	0	-133.7	133.7	90	0	**90**	**11.2**	**4.6**	**0**	**-0.3**	**-0.7**	**0.03**
F	0	-133.7	133.7	90	**-90**	0	0	0	0	0	0	0
G	0	-133.7	133.7	90	**90**	0	0	0	0	0	0	0
H	0	-133.7	133.7	90	**-90**	0	0	0	0	0	0	0
I	0	-133.7	133.7	90	**-90**	**-90**	**-4.9**	**10.70**	**0**	**-0.7**	**-0.3**	**0.05**
J	0	-133.7	133.7	90	-90	**90**	**11.2**	**4.6**	**0**	**-0.3**	**-0.7**	**0.03**
K	0	-133.7	133.7	90	**0**	**0**	0	0	0	0	0	0
L	0	-133.7	133.7	90	**90**	0	0	0	0	0	0	0
M	0	-133.7	133.7	90	90	**-90**	**-4.9**	**10.63**	**0**	**-0.7**	**-0.3**	**0.05**
N	0	-133.7	133.7	90	90	**90**	**11.39**	**4.5**	**0**	**-0.3**	**-0.7**	**0.03**
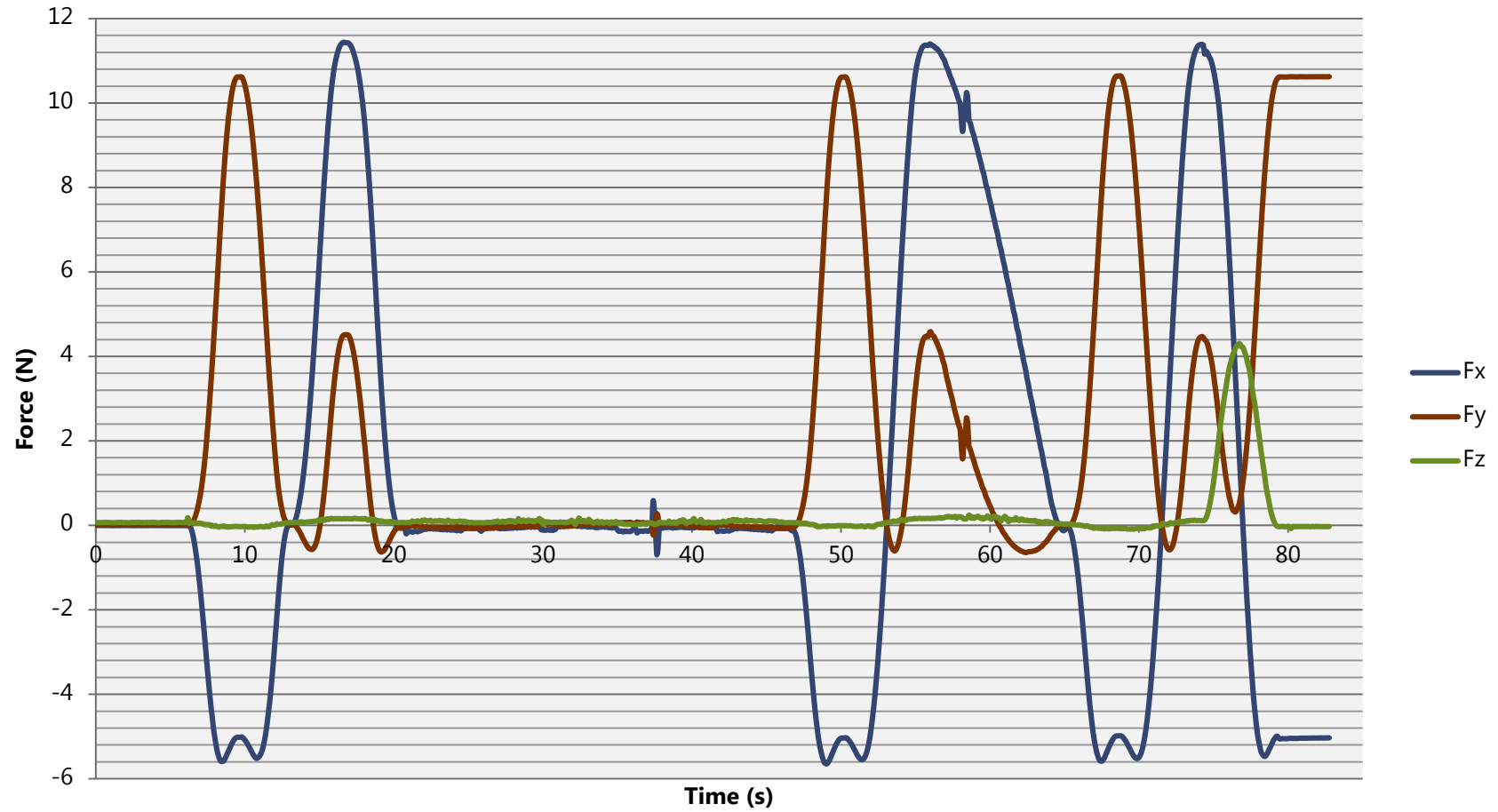
Figure J.2: Multi-axial force and torque sensor behaviour – force output

Figure J.3: Multi-axial force and torque sensor behaviour – torque output
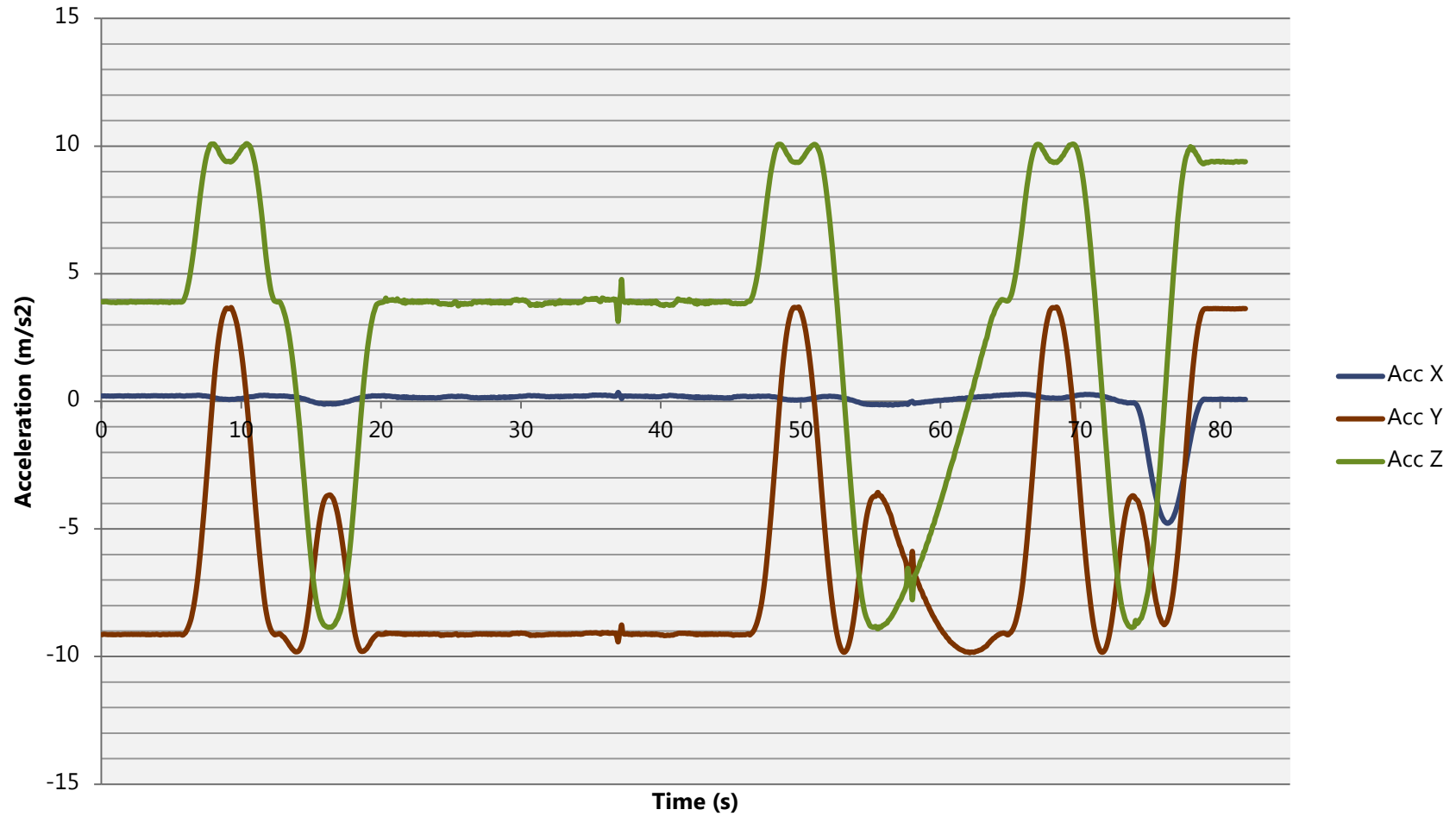
Figure J.4: Inertial measurement unit – acceleration output

Figure J.5: Inertial measurement unit – Euler-angle orientation output
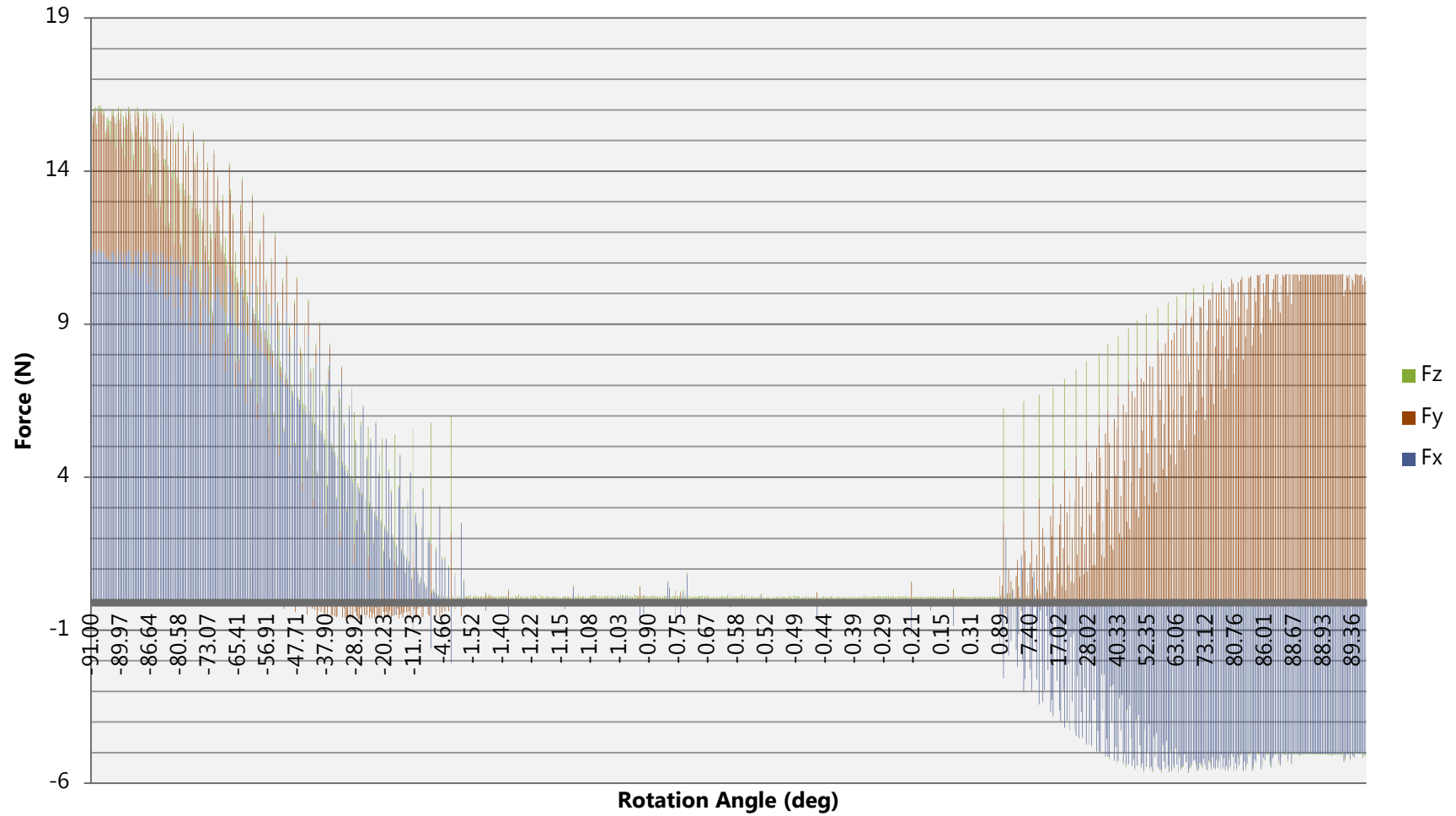
Dynamic behaviour - force vs orientation

Figure J.6: Sensor dynamic behaviour - force vs orientation

Figure J.7: Sensor dynamic behaviour - torque vs orientation

Appendix K.Development of an Integrated Robotic Polishing System

The following appendix is presenting the results related to the test of the Integrated Robotic Polishing System for the polishing operation of a cylindrical and triangular surface using force control only. Figures K.1 to K.3 present the results of the first trial for the cylindrical surface. Figures K.4 to K.6 illustrate the results of the second trial for the cylindrical surface. K.7 to K.9 present the results of the first trial for the triangular surface. K.10 to K.12 6 illustrate the results of the second trial for the triangular surface.
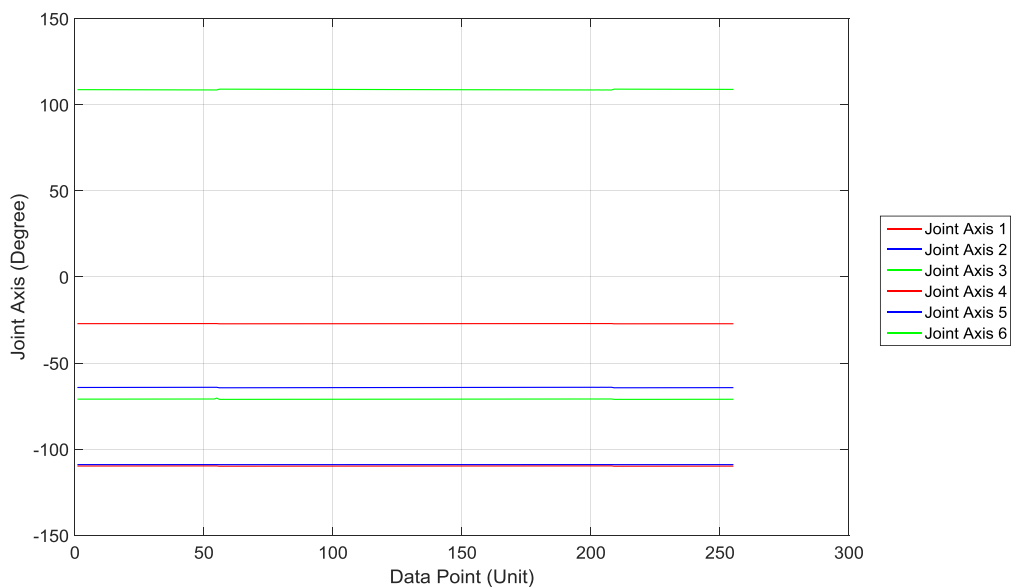
Figure K.1: Experiment 6 – cylindrical surface –test 1 – joint axis output
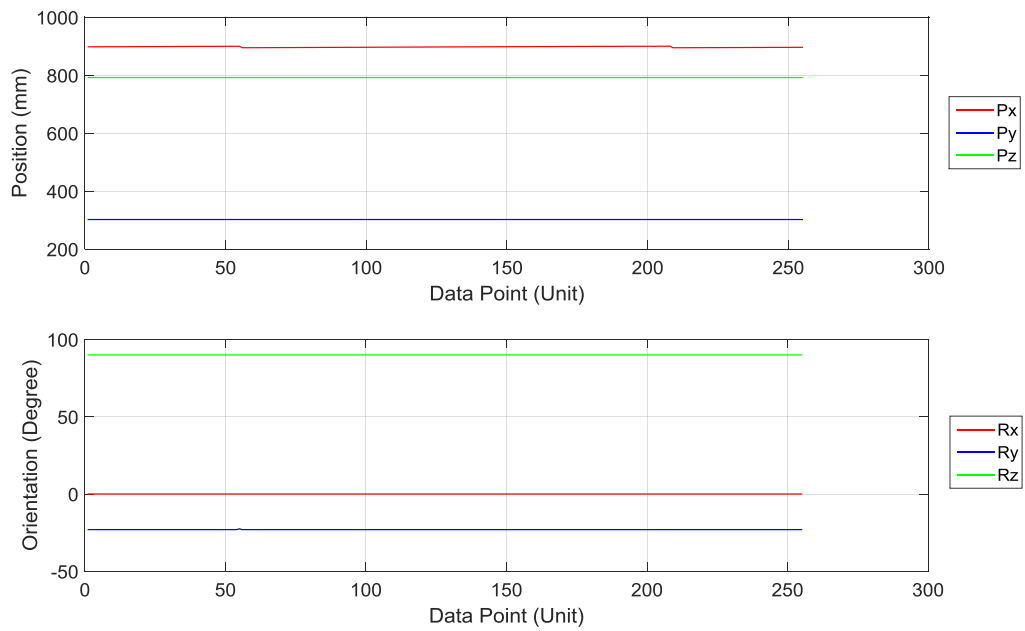
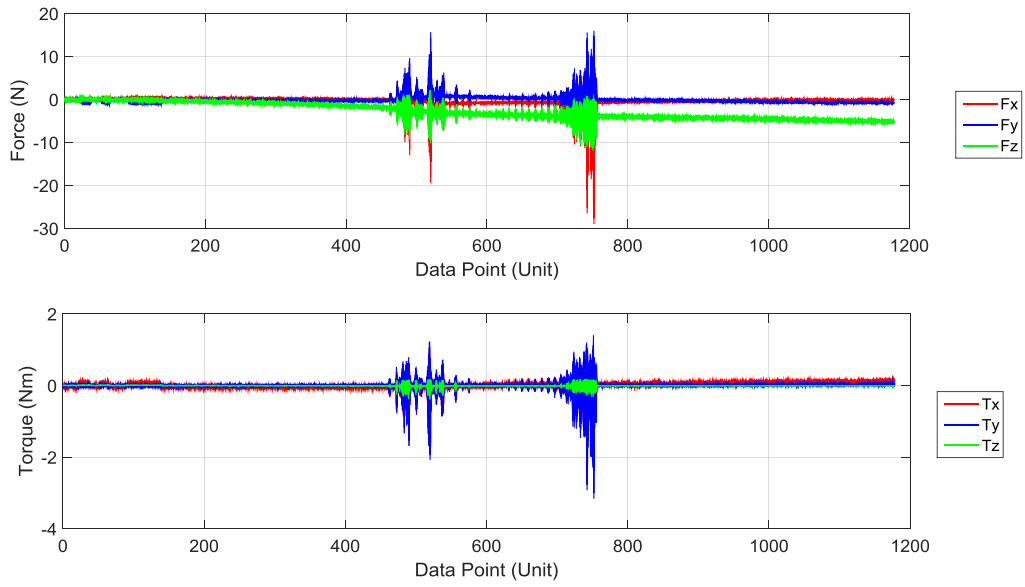**Figure K.2: Experiment 6 – cylindrical surface – test 1 – Cartesian position and orientation output**
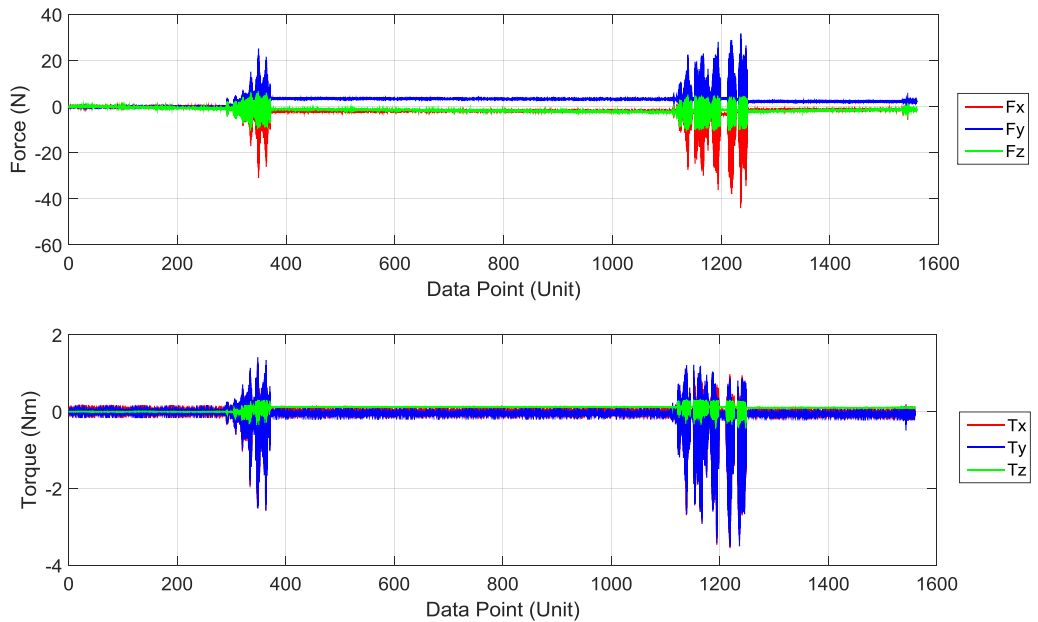
Figure K.3: Experiment 6 – cylindrical surface – test 1 – force and torque output
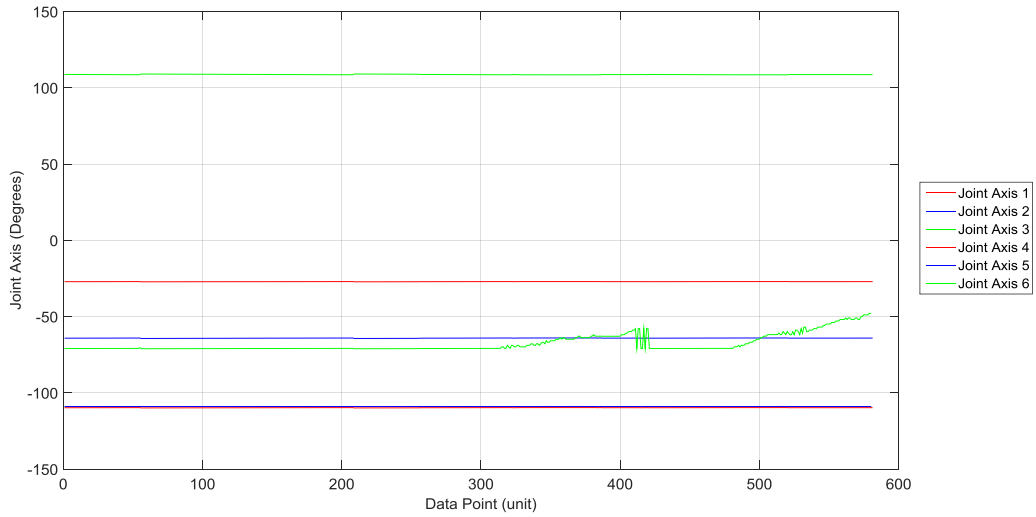
Figure K.4: Experiment 6 – cylindrical surface – test 2 – joint axis output
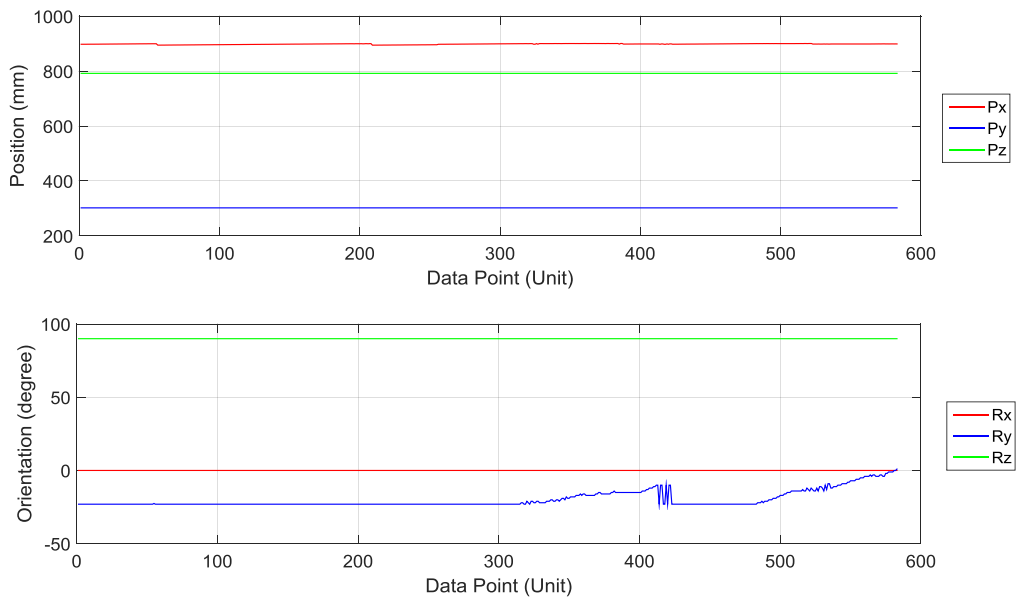
Figure K.5: Experiment 6 – cylindrical surface – test 2 – Cartesian output

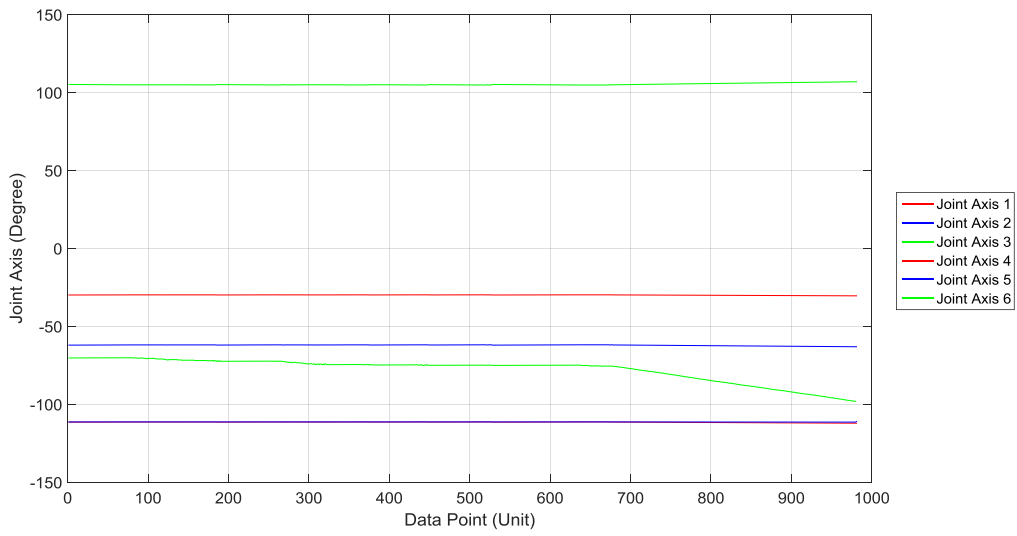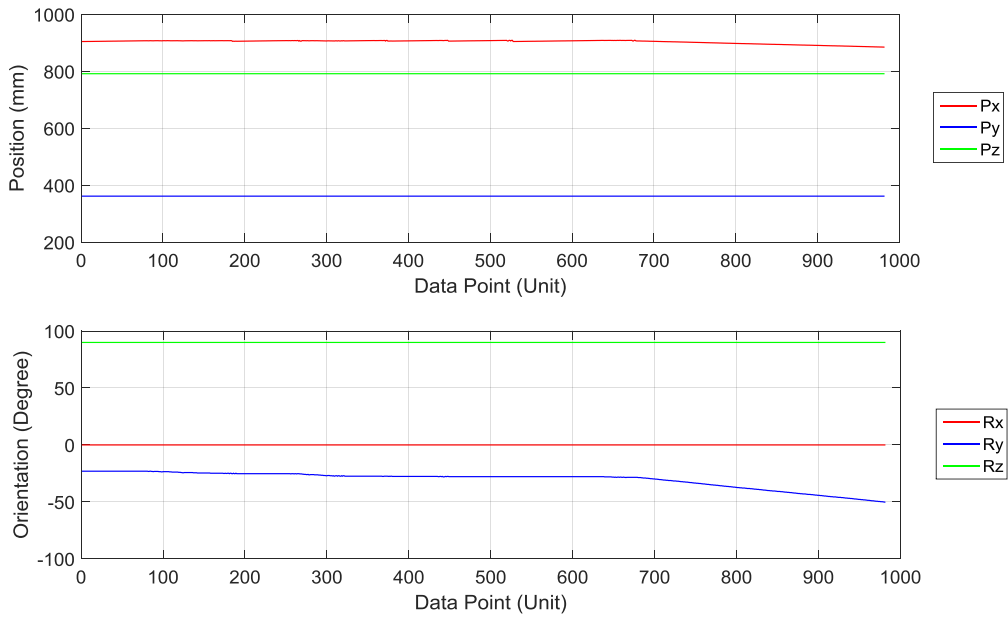**Figure K.6: Experiment 6 – cylindrical surface – test 2 – force and torque output**

Figure K.7: Experiment 6 – triangle surface – test 1 – joint axis output

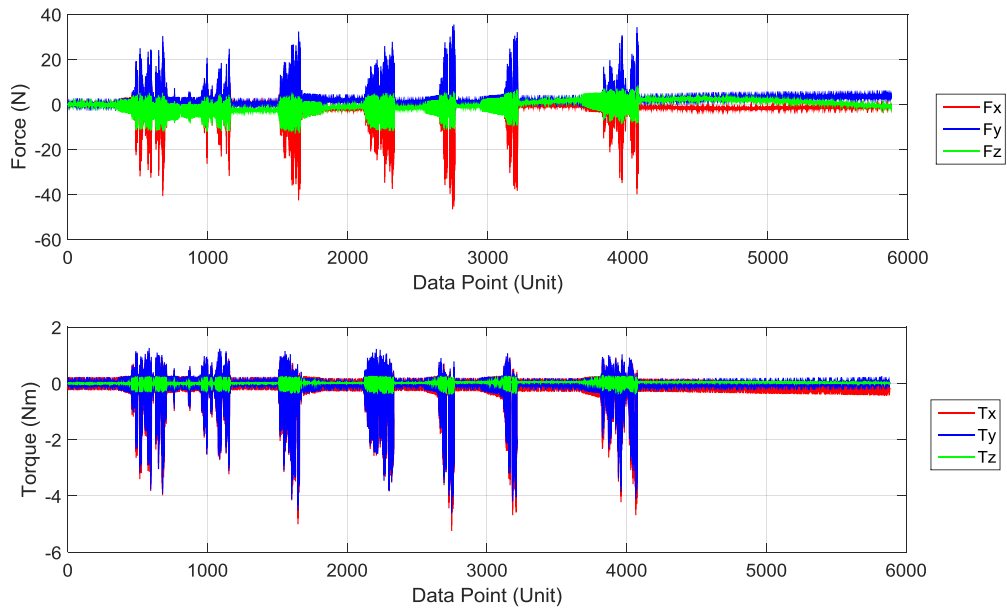**Figure K.8: Experiment 6 – triangle surface – test 1 – Cartesian output**

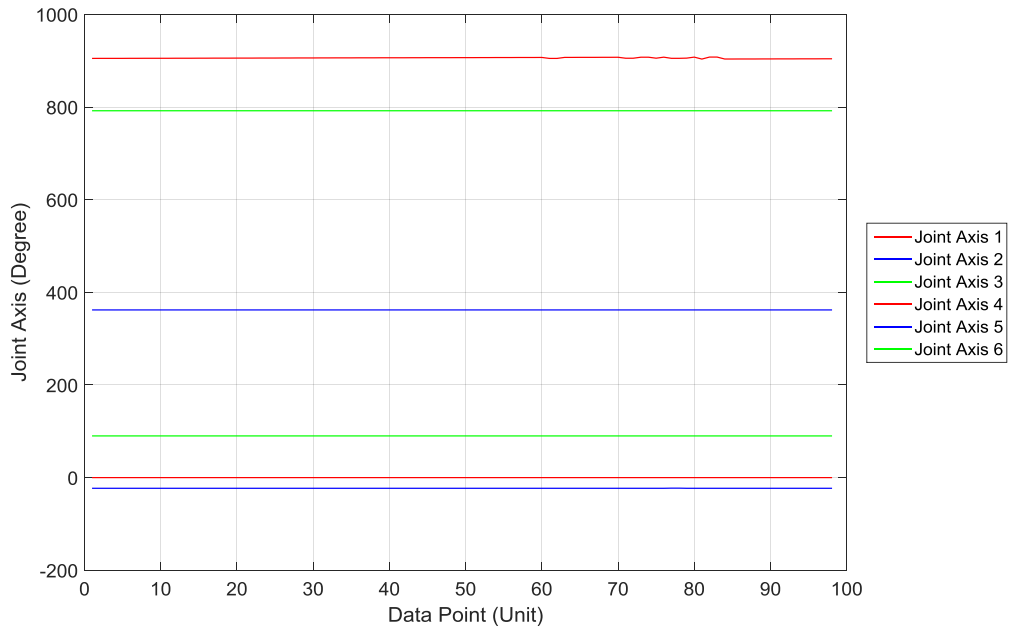**Figure K.9: Experiment 6 – triangle surface – test 1 – force and torque output**

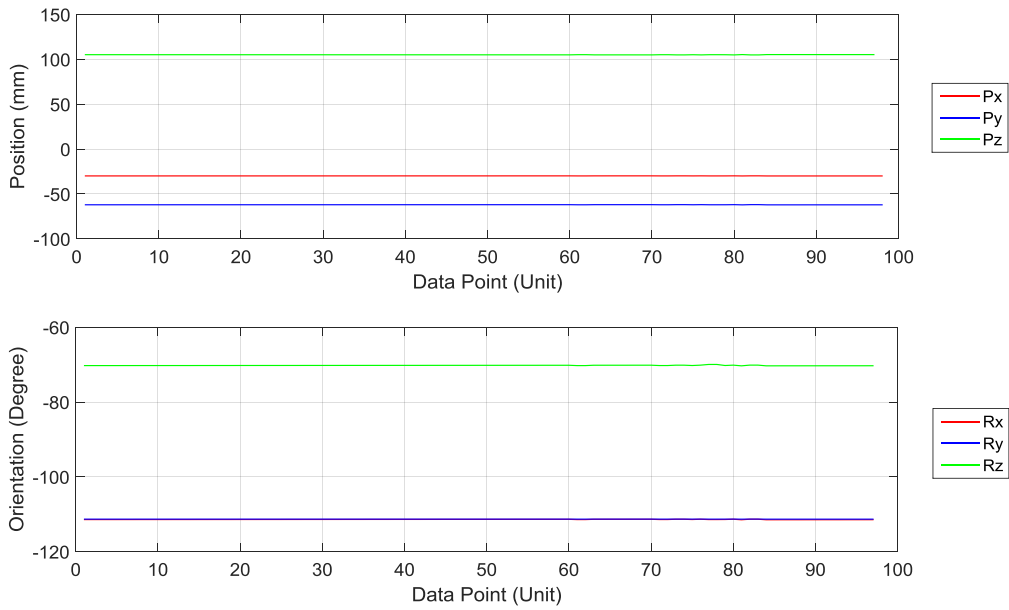**Figure K.10: Experiment 6 – triangle surface – test 2 – joint axis output**

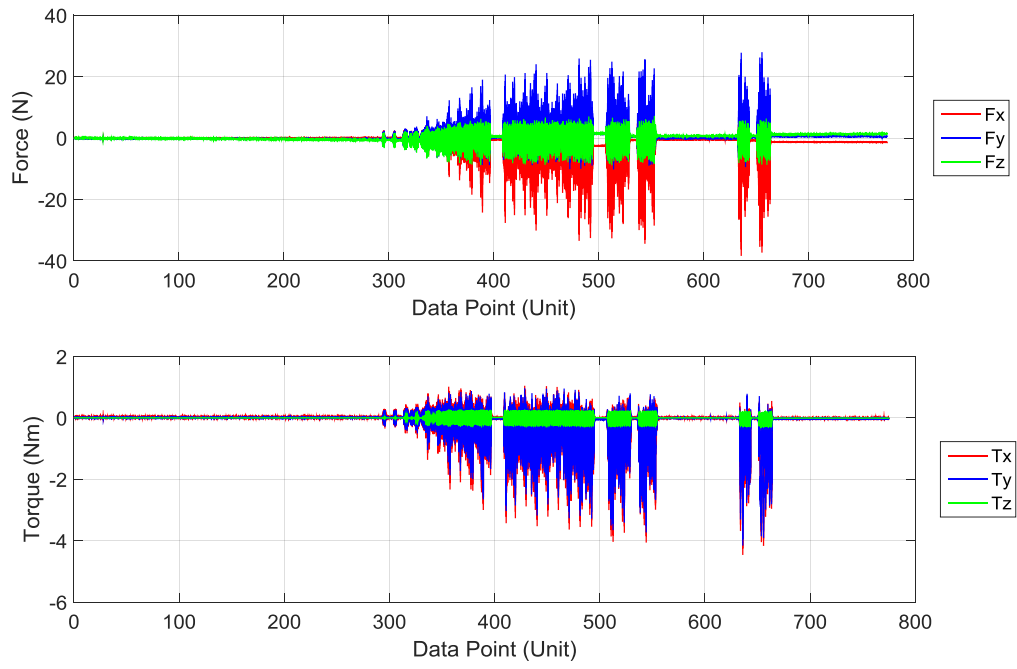**Figure K.11: Experiment 6 – triangle surface – test 2 – Cartesian output**

Figure K.12: Experiment 6 – triangle surface – test 2 – force and torque output